The interaction between the type 1 receptor tyrosine kinases and the oestrogen receptor in human breast cancer: The role of the Ras/Raf-1/MAPK pathway

Liane Marie McGlynn

Section of Surgical Sciences and Translational Research

Division of Cancer Sciences and Molecular Pathology

Submitted for the degree of PhD to the University of Glasgow

October 2006

The work presented in this thesis was performed entirely by the author except as acknowledged. This thesis has not been previously submitted for a degree or diploma at this or any other institution.

Liane McGlynn
July 2007

Dedication

This thesis is dedicated to James and Elizabeth McGlynn for all their love and support.

Acknowledgements

I would like to thank Dr. John Bartlett for his supervision during my time as a PhD student. Special thanks must go to Dr. Joanne Edwards, who gave up endless hours of her time to help and encourage me. I am much indebted for all her invaluable advice and support. I am also incredibly grateful to Pamela Traynor, without whose help I would probably still be in the lab trying to finish experiments. Thanks must also go to Dr. Tove Kirkegaard, Fiona Campbell and Suba M, for the many hours they all spent looking down the microscope. To all the lab ladies, thank you for making my time in the lab fun and especially for cheering me up on those days when everything was going wrong.

Thanks must also go to the White Lily Ladies who funded my research over the last four years.

To my friends, whom I haven't seen for months whilst I have been writing this, thank you for being there when I needed you. Finally, to my family, who have had to deal with me over the last four years, and particularly over the last six months. . I don't know who is more relieved that I have finished. Many, many thanks for all your encouragement and support. Though, a special mention has to go to my sister, Laura, who spent many hours proof reading all my chapters. Thank you, it is very much appreciated.

I would like to thank everyone who has helped me at any point over the course of the last four years.

Table of Contents

List of Figures

List of Tables

List of Publications

Published Papers

Kirkegaard T, Witton CJ, **McGlynn LM**, Tovey SM, Dunne B, Lyon A & Bartlett JMS (2005) Activation of AKT promotes tamoxifen resistance in breast cancer *J Pathol* 207 (2): 139-146

Kirkegaard T, Edwards J, Tovey SM, **McGlynn LM**, Krishna SN, Mukerjee R, Tam L, Munro AF, Dunne B, Bartlett JMS. Observer variation in immunohistochemical analysis of protein expression, time for a change? *Histopathology* Volume 48, Issue 7, Page 787-794, Jun 2006.

Kirkegaard T, **McGlynn LM,** Campbell FM, Müller S, Tovey SM, Dunne B, Nielsen KV, Cooke TG, Bartlett JMS. Amplified in breast cancer 1 in human epidermal growth factor receptor - positive tumors of tamoxifen-treated breast cancer patients. *Clinical Cancer Reearch* 2007 Mar 1;13(5):1405-11.

Tam L, **Mc Glynn LM**, Traynor P, Mukherjee R, Bartlett JMS and Edwards J. The role of IL-6R/JAK/STAT3 Pathway in hormone refractory prostate cancer. *Br J Cancer*. 2007 Jul 31;97(3):378-83.

Papers in preparation/submitted

McGlynn LM, Witton CJ & Bartlett JMS (2006) Nuclear Ras: A possible therapeutic target for breast cancer. Submitted to Breast Cancer Research & Treatment

McGlynn LM, Kirkegaard T, M S, Campbell FM, Witton CJ & Bartlett JMS (2006) Ras/Raf/MAPK pathway modifies response to tamoxifen but not chemotherapy in breast cancer patients. Submitted to Clinical Cancer Research

McGlynn LM, Traynor P, Kirkegaard T, Campbell FM & Bartlett JMS (2006) The interaction between MAPK and the oestrogen receptor in breast cancer cells. Submitted to Breast Cancer Research & Treatment

Traynor P, Mukherjee R, **McGlynn LM**, Underwood MA, Bartlett JMS and Edwards J (2006) The Role of the Ras family in Hormone Refractory Prostate Cancer. (In preparation)

List of Abbreviations

AF-1	Transactivation Function 1
AF-2	Transactivation Function 2
AI	Aromatase Inhibitors
APS	Ammonium persulphate
ATAC,	Arimidex, Tamoxifen, alone or in combination Trial
BIG-1-98	Breast International Group
BSA	Bovine Serum Albumin
CEB	Cytosol Extraction Buffer
CMF	Cyclophosphamide, Methotrexate and 5-Flourouracil
CNK	Connector Enhancer of KSR
DAB	Diaminobenzidine
DAPI	4'-6-Diamidino-2-phenylindole
DCIS	Ductal Carcinoma *In Situ*
DFS	Disease-Free Survival
DMEM	Dulbecco's Modified Eagle Media
DMSO	Dimethyl Sulphoxide
DPX	Dibutyl Phtalate containing Xylene
DTT	Dithiothreitol
E1	Oestrone
E2	Oestrogen
E3	Oestriol
ECL	Enhanced Chemiluminescence
EGF	Epidermal Growth Factor
EGFR	Epidermal Growth Factor Receptor
ERα	Oestrogen Receptor α
ERβ	Oestrogen Receptor β
ERE	Oestrogen Response Elements
ERK	Extracellular Regulated Kinase
EtOH	Ethanol
FaD	Fluorescein avidin D
FEL	Felodipine
FISH	Fluorescent In Situ Hybridization
FITC	Fluorescein Isothiocyanate
FT	Farnesyl Transferase
FTI	Farnesyl Transferase Inhibitor
GAP	GTPase Activating Protein

GDP	Guanosine 5'-diphosphate (Guanine dinucleotide)
GEF	Guanine Nucleotide Exchange Factors
Grb2	Growth factor Receptor Bound Protein 2
GTP	Guanosine 5'-triphosphate (Guanine Trinucleotide)
HAT	Histone Acetyltransferases
HDAC	Histone-deacetylase
HER2-4.	Human Epidermal Growth Factor Receptor 2-4
HRG	Heregulin
HRP	Horseradish Peroxidase
HSP	Heat Shock Protein
HVR	Hypervariable Region
ICCC	Inter(intra)-class correlation coefficient
IDC	Invasive Ductal Carcinoma
IES	Intergroup Exemestane Study
IF	Immunofluorescence
IHC	Immunohistochemistry
ILC	Invasive Lobular Carcinoma
KSR	Kinase Suppressor of Ras
LBD	Ligand Binding Domain
LCIS	Lobular Carcinoma *In Situ*
LHRH	Luteinising-hormone-releasing hormone
LSAB	Labelled streptavidin-biotin
MAPK	Mitogen activated protein kinase
MEB-A	Membrane-Extraction Buffer-A
MEB-B	Membrane Extraction Buffer-B
NEAT	National breast cancer study of Epirubicin & CMF versus classical CMF Adjuvant Therapy Study Number BR9601
NEB	Nuclear Extraction Buffer
NPI	Nottingham Prognostic Index
OHT	4 Hydroxy-Tamoxifen
OS	Overall Survival
PBS	Phospho-Buffered Saline
pER(ser118)	Phosphorylated ERa at Serine 118
pER(ser167)	Phosphorylated ERa at Serine 167
PI-3K	Phospatidylinositol-3 kinase
PIP2	Phosphatidyl inositol (4,5)- bisphosphate
PIP3	Phosphatidyl inositol (3,4,5)- trisphosphate
PKA	Protein Kinase A
PM	Plasma Membrane

pMAPK	Phosphorylated p44/42 MAPK
PMSF	Phenylmethlysulfonyl fluoride
PNA	Peptide Nucleic Acid
PP2A	Protein Phosphatase 2A
PR	Progesterone Receptor
pRaf(ser259)	Phosphorylated Raf-1 at Serine 259
pRaf(ser338)	Phosphorylated Raf-1 at Serine 338
PVDF	Polyvinylidene Difluoride
R^2	Correlation Coefficient
Rb	Retinoblastoma
RKIP	Raf Kinase Inhibitor Protein
ROT	Recurrence On Tamoxifen
RTK	Receptor Tyrosine Kinase
S.T.W.S	Scots Tap Water Substitute
SDS	Sodium Dodecyl Sulphate
SDS-PAGE	Sodium Dodecyl Sulphate – PolyAcrylamide Gel Electrophoresis
SERM	Selective Oestrogen Receptor Modulator
SH2	Src Homology 2
SOS	Son of Sevenless
STB	Steroid-resistant Tumour Bank
TBS	Tris-Buffered Saline
TEAM	Tamoxifen Exemestane Adjuvant Multinational Trial
TMA	Tissue Micro Array
TR	Texas Red
TTBS	Tris Buffered Saline -Tween

Summary

Tamoxifen and chemotherapy are key treatments for breast cancer patients. Tamoxifen, an oestrogen antagonist, is a non-steroidal that acts as a selective oestrogen receptor modulator (SERM). It competitively inhibits the interaction of oestrogen with the oestrogen receptor, blocking the effects of E2 and inhibiting receptor activity. Chemotherapy uses cytotoxic drugs to kill cancer cells, by preventing them from multiplying, invading and metastasing. Despite the extensive use of both treatments, failure to respond to them is a major clinical problem and this is the cause of significant morbidity and mortality. To overcome this and to improve patients' treatment options, we need to understand the mechanisms regulating the development of resistance.

The Ras/Raf-1/MAPK pathway regulates multiple cellular processes such as proliferation, apoptosis, differentiation, senescence and migration. MAPK activation results in phosphorylation of more than 50 substrates within the cytosol and nucleus. One key substrate of MAPK is the oestrogen receptor (ERα). Activated MAPK directly and indirectly phosphorylates serine 118 and 167, respectively, in the AF-2 domain of the receptor. Stimulation of the Ras pathway results in the ligand-independent activation of the ERα. Consequently, this pathway has been identified as a key player in the development and progression of tumourigenesis. Research suggests that activation of this pathway mediates response to tamoxifen, by activating ERα in a ligand-independent manner, and to chemotherapy, by increasing cell proliferation. This current study investigated the hypothesis that expression and activation of Ras/Raf-1/MAPK influences patient outcome and treatment response, using breast tumours from three different patient cohorts and an immunohistochemical approach. It also examined the relationship

between MAPK and oestrogen receptor, both can localise to the cytoplasm and/or nuclei of cells but it is unclear how and where they interact. Therefore, *in vitro* studies, including immunofluorescence, were performed to investigate the relationship between MAPK and ERα, and their role in driving tamoxifen resistance.

The pilot study, comprised of ER positive and negative patients who received a range of treatments, revealed that increased expression of N-Ras in breast tumours was related to reduced disease-free and overall survival time. It also highlighted the unexpected finding that Ras localised to the nuclei of breast tumour cells. The presence of nuclear Ras was confirmed by *in vitro* studies.

The expression of Ras, Raf-1 and MAPK proteins was investigated further, in tumours from ER positive patients, who were treated with tamoxifen (STB study), and in tumours from ER positive and negative patients who received chemotherapy treatment (NEAT/BR9601 study). These two studies highlighted that the Ras pathway mediated outcome in patients treated with Tamoxifen but not chemotherapy. High expression levels of N-Ras, pRaf(ser338), and MAPK were related to a shortened response time to Tamoxifen. Activated Raf-1 was also associated with a reduced disease-free and overall survival time. The implications of this study was that whilst N-Ras and MAPK were associated with the development of tamoxifen resistance and emphasised the importance of the Ras pathway, it was nuclear pRaf(ser338) that was the principal candidate for identifying patients failing to respond to tamoxifen. Patients with increased tumour expression of pRaf(ser338) were more likely to require additional or alternative therapies such as chemotherapy, aromatase inhibitors or Raf-1 inhibitors. In this STB study elevated levels of activated Raf-1 in tumours appeared to predict for poor response to

tamoxifen, however it also seemed to identify patients who benefited from a combined treatment regime of tamoxifen and chemotherapy. It was therefore speculated that Raf-1 and MAPK partially controlled cells response to chemotherapy. However, analysis of the NEAT study revealed no evidence that either Raf-1 or MAPK were predictive for response to chemotherapy. The exact role of Raf-1 and MAPK in mediating response to chemotherapy is controversial and perhaps further work in a larger cohort of chemotherapy treated patients is required to enhance our knowledge of the mechanism driving resistance.

Having shown a significant link between expression and activation of the Ras pathway and tamoxifen resistance, the interaction between this pathway and ERα was investigated in MCF-7 breast cancer cells. This study confirmed that ligand-mediated phosphorylation was associated with rapid nuclear localisation of ERα, probably due to oestrogen binding and that ERα was phosphorylated at serine 118 in a ligand-independent manner, via MAPK. It suggested that pMAPK has to translocate to the nucleus to induce expression of phosphorylated ER in the nucleus. Preventing nuclear translocation of pMAPK reduced the levels of ligand-independent but not ligand-dependent phosphorylation of ER, confirming that oestrogen phosphorylation of serine 118 is reliant on a kinase other than MAPK. Previous studies have identified CDK7 as the kinase responsible for oestrogen-dependent phosphorylation of serine 118. Additionally, this study suggested that the ligand-independent activation of ERα was dominant over oestrogen-dependent activation. Heregulin mediated signalling determined the subcellular localisation of ER, even in the presence of oestrogen.

This research highlights the impact of the Ras pathway on breast cancer patients' response to treatment. It also reveals some interesting findings regarding the interaction between MAPK and ER, and offers a possible mechanism for the development of Tamoxifen resistance.

1 Introduction

1.1 Breast Cancer: Incidence and prevalence

As the most commonly diagnosed cancer in women, breast cancer accounts for one in three of all female cancers, and is second to lung cancer in causing female-cancer specific deaths. Worldwide, over a million women are diagnosed with breast cancer each year, accounting for a tenth of all new cancers and 23% of all female cancers (1). The lifetime risk of UK women developing breast cancer is 1 in 9. More than 42,000 British women are diagnosed with breast cancer each year (1). In 2002 an estimated 172,000 women were alive in the UK with breast cancer (1). 80% of women survive at least five years after diagnosis. Furthermore, the 20 year survival rate for women has risen from 44% in the early 1990s to 64% in the period 2001-2003. However Britain has one of the highest death rates in Europe; approximately 13,000 women die each year from breast cancer (2).

Several important genetic and environmental risk factors are associated with breast cancer. Approximately 5-10% of breast cancers have a genetic link; two thirds of these cases have mutations in the tumour suppressor genes BRCA1 and BRCA2. Mutations in these genes are associated with familial/hereditary breast and ovarian cancer, early age of onset, and cancer in both breasts (3). The main risk factor for sporadic breast cancer is age: the risk of developing breast cancer by the age of forty is 0.5%; by the age of eighty; it is 10% (4). Other risk factors include family history of breast cancer, prolonged exposure to oestrogen (onset of menstruation before age 12, menopause after age 50, first child born after the age of 30), alcohol abuse and obesity.

1.2 Breast Cancer Pathology

1.2.1 Normal Breast Anatomy

The female breasts are milk-producing glands, composed of lobules/glands, milk ducts, fat and connective tissue. Each breast contains 15-20 lobes, comprising lobules, which end in glands that produce milk in response to hormone signalling, arranged in a circular fashion. Ducts deliver milk to the nipple, thus connecting lobes, lobules and glands. Fatty tissue fills the spaces between the lobules and the ducts (Fig 1.1). Blood and lymph vessels form a network throughout each breast. The mammary gland undergoes three key phases of development and differentiation under the control of hormones and growth factors (5;6): lobule development, between the ages of 10-25; glandular development, under the influence of menstrual hormones between the ages of about 13-45, and involution, or shrinkage of the milk ducts, from about age 35.

During the menstrual cycle, oestrogen stimulates milk duct growth; following ovulation, halfway through the cycle the hormone progesterone continues to stimulate milk gland formation. If pregnancy does not occur, the breasts return to normal size and the cycle begins again. During early (mammogenesis) and late (lactogenesis 1) phases of pregnancy, the final stages of development and differentiation occur. Mammogenesis is characterized by proliferation of the distal elements of the ductal tree, creating multiple alveoli (acini) of variable size and shape. Lactogenesis 1 occurs later and is characterized by differentiation of resting mammary cells into lactocytes, with the potential to secrete the unique fats, carbohydrates, and proteins characteristic of milk. The breast of nulliparous women contains more undifferentiated structures whereas the breast of parous women is comprised of more differentiated lobules (5). During lactation, mammary lobules become enlarged and milk is synthesised and released into the ductal system.

Accumulation of milk in ducts has an inhibitory effect on the production of milk. This results in a series of involutional changes in the mammary gland, which reduces the volume of secretory epithelial cells and inhibits their secretory activity (5).

Hormone regulation is important, not only in the development and differentiation of the breast but also in the development of disorders, such as benign breast disease, and breast cancer.

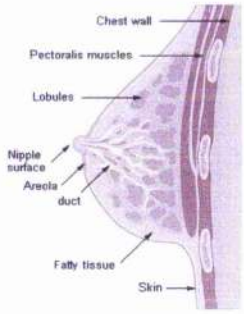

Figure 1.1: Anatomy of female breast
The breast is a milk-producing gland comprised of lobules, lobes, ducts and fatty tissue

1.2.2 Breast Histology

1.2.2.1 Non-neoplastic breast disease

These disorders usually involve alterations of the breast stroma or glands. These changes can be fibrocystic (dilation of ducts to form cysts, apocrine metaplasia, stromal fibrosis) and adenocystic (benign proliferation of glands). Epithelial hyperplasia is an increase in the number of layers of cells lining the ducts (normally two layers). Atypical hyperplasia is an intermediate disorder between hyperplasia and carcinoma in situ, and is associated with an increased risk of developing a carcinoma.

1.2.2.2 Neoplasms of the Breast

- **Benign Neoplasms**

The most common is a fibroadenoma, characterised by proliferation of the breast ducts and stroma. Others include the phyllodes tumour and benign intraduct papilloma. These are associated with a moderate increase in the risk of a carcinoma developing.

- **Carcinoma *In Situ* (Ductal and Lobular Carcinoma *In Situ* DCIS/LCIS)**

DCIS is the most common form of non-invasive breast cancer. Cells within the breast ducts are cancerous; however, the tumour cells proliferate only within the ducts and have not breached the basement membrane and spread throughout the breast tissue and into the lymph nodes. DCIS can be classified into three grades: low, intermediate and high. Higher grade (comedo) DCIS is most likely to develop into invasive cancer (Table 1.1).

Type of *Carcinoma In Situ*	Pathological Characteristics
Solid DCIS	Cancerous cells completely fill the affected breast ducts
Cribriform	Cells are very uniform in size and very regularly placed in relation to one another. Epithelial cells fill and expand the ducts and form defined glandular spaces separated by bridges of cells.
Papillary/Micropapillary	Commonly occurs in association with cribriform DCIS.
Comedo DCIS	Ducts are expanded due to proliferation of large pleomorphic cells. Characterised by mitotic figures and necrosis in the centre of the duct.
LCIS	Cells within breast lobes have undergone morphologic changes but are not cancerous. Lobules are expanded and filled by small, evenly spaced epithelial cells, which do not form ducts.

Table 1.1: Types of Carcinoma In Situ
Carcinoma In Situ can be categorised as Ductal or Lobular.

- **Invasive Ductal Carcinoma (IDC)**

Approximately 70-80% of cancers diagnosed are invasive and ductal, originating in the breast ducts, but invading fatty tissue and metastasising to other parts of the body. Variants include invasive tubular carcinoma (cancerous cells form defined tubular or ductal structure but with no solid nests of cells or single cell invasion), mucinous

carcinoma (malignant cells are suspended in pools of mucin), cribriform, carcinoma, and medullary carcinoma.

- **Invasive Lobular Carcinoma (ILC)**

Approximately 10% of diagnosed cancers are invasive and lobular. ILC has a better prognosis than IDC, but is more likely to be bilateral.

- **Others**

Type of Cancer	Pathological Characterisistics
Inflammatory Breast Cancer	Cancer cells block the lymph ducts in the breast and prevent fluid from being drained from the tissue, resulting in inflammation of the breast.
Paget's Disease	Beginning in the breast ducts, cancer spreads to the nipple and areola.

Table 1.2: Other types of breast cancer
Inflammatory breast cancer and Pagets Disease are two rarer forms of breast cancer, accounting for 1-3% and 1% of all cases respectively.

1.3 Predictive & Prognostic Markers

1.3.1 Breast tumour grade

The grade of a tumour depends on its histological appearance and reflects differentiation associated with neoplasia. Grading breast tumours is based on tubule formation (% of cancer cells composed of tubular structures), nuclear pleomorphism (changes in cell size and uniformity) and mitotic count (rate of cell division), each of which is scored from 1 to 3. Scores are totalled to provide a final score, ranging between 3 and 9, dividing tumours into three grades. Tumours with scores of 3-5 are considered Grade 1, well-differentiated tumours. Grade 2 tumours (score 6-7) are moderately differentiated, whilst tumours scoring 8-9 are Grade 3 (poorly-differentiated). Patients with grade 1 tumours have a better prognosis than those with grade 3 tumours. (7;8).

1.3.2 Breast Tumour Stage

Stage is a measure of tumour size and the extent of disease spread. The TNM staging system - where T represents the size of the primary tumour, N corresponds to nodal involvement, and M confirms whether or not the cancer has metastasised - is commonly applied to breast cancer (Table 1.3). Patients with stage I tumours have a better prognosis than those patients with stage IV tumours (7).

Stage	Tumour Size	Lymph Node Involvement	Metastasis
I	Less than 2cm	No	No
II	2-5cm	No, or in same side of breast (0-3 axillary lymph nodes involved)	No
III	More than 5cm	Yes, on same side of breast (≥ 4 axillary and/or internal mammary lymph node)	No
IV	Any size	Any lymph nodes	Yes

Table 1.3: Breast carcinoma staging system
Staging of a breast tumour depends on the tumour size, lymph node involvement and metastasis, and ranges from stage I to stage IV.

1.3.3 Nottingham Prognostic Index

In 1982, a retrospective analysis was performed to investigate the prognostic capabilities of nine factors in primary, operable breast cancers: age, menopausal state, size, lymph node stage, tumour grade, cellular reaction, sinus histiocytosis, and oestrogen receptor expression (9). Three remained significant, following multivariate analysis. These independent prognostic markers, lymph node stage, histological grade and tumour size were combined to form the Nottingham Prognostic Index (NPI), (8;9) calculated using the following formula:

NPI = (0.2 x tumour size (cm)) + lymph node stage (1-3) + histological grade (1-3)

Rather than determining therapy choice on a single prognostic marker, the NPI score is used to select the appropriate treatment options (Table 1.4).

NPI Score	Annual Mortality	15 years survival	Adjuvant Therapy
< 3.4	3%	80%	No systemic adjuvant treatment
3.4-5.4	7%	42%	Choice dependent on ER/PgR status, menopausal status & axillary disease
> 5.4	30%	13%	Aggressive adjuvant treatment: chemotherapy

Table 1.4: Nottingham Prognostic Index (NPI)
NPI scores, calculated using tumour size, lymph node stage and grade, are used to determine the most appropriate treatment regime for patients.

1.4 Current Treatment Options

1.4.1 Surgery

The objective of surgery is to remove disease and identify extent of disease spread (staging). Surgery to the breast involves either a lumpectomy or partial/segmental mastectomy, removing only the breast lump and a marginal area of normal tissue. A total mastectomy removes the entire breast. However, the more common procedure is a simple mastectomy that removes the entire breast and some of the axillary nodes to assess disease spread beyond the breast.

1.4.2 Radiotherapy

High-energy radiation kills cancer cells. A review of clinical trials involving radiotherapy over the last 40 years showed a significant reduction (~ two-thirds) in the number of patients relapsing following radiotherapy. Radiotherapy reduces breast-cancer related deaths but increases deaths from other causes, in particular vascular-related deaths (10).

1.4.3 Chemotherapy

Adjuvant chemotherapy is standard treatment for women with node-positive breast cancer. In a 10 year overview of approximately 100 clinical trials, for patients treated with adjuvant chemotherapy, recurrence risk was reduced by 22-37%, and risk of death by 14-27% (11). Adjuvant polychemotherapy produced an improvement of about 7-11%

in 10-year survival for women aged under 50 presenting with early breast cancer, and by 2-3% for those aged 50-69 (12). Adjuvant chemotherapy is also beneficial to node-negative breast cancer patients. However, benefits must outweigh the risks of receiving cytotoxic agents. Chemotherapy is recommended for patients with moderately to poorly differentiated invasive tumours larger than 1cm or ER negative tumours (NCI Guidelines). In the UK, patients' NPI scores guide chemotherapy use and the combination of epirubicin and Cyclophosphamide, Methotrexate and 5-Fluorouracil (CMF) is now a common adjuvant practice. In 2002, NICE recommended the use of combined chemotherapy regimes including anthracyclines.

Cyclophosphamide, an alkylating agent that is cell cycle specific, causes DNA strands to break apart, and impairs DNA replication. Methotrexate and 5-fluorouracil are cell cycle phase specific antimetabolites that inhibit the conversion of folic acid to its active form, folinic acid, preventing cell division and killing rapidly dividing cells (13). Anthracyclines, such as epirubicin, are antibiotics that induce apoptosis in tumour cells by disrupting the structure of the DNA. They do this by intercalating into the base pairs in the DNA minor grooves, and by causing free radical damage of the deoxyribose in the DNA (13).

In recent years, taxanes, such as paclitaxel and docetaxel, have been shown to be active cytotoxic antitumour agents(14). Taxanes act by shifting the dynamic equilibrium between tubulin and microtubules in the direction of microtubule assembly. Cells become blocked during the G_2 and M cell cycle phases and cannot form a normal mitotic spindle and divide. Essentially, these microtubules are excessively stable and therefore dysfunctional (15). A recent review demonstrated that treatment with taxanes improved

overall survival, time to progression, and overall response in women with metastatic breast cancer (16).

Despite the use of chemotherapy as adjuvant treatment, failure to respond to chemotherapy is a major problem. Chemotherapy resistance can be categorised into three types: kinetic, biochemical and pharmacologic (13). However, the mechanisms underlying the development of resistance to chemotherapy are not fully understood.

1.4.4 Endocrine Therapy

An important determinant of patient treatment is the tumour hormone receptor status. Between 70-80% of breast cancers are oestrogen receptor (ER) positive and potentially oestrogen dependent. Allred demonstrated that the presence of ER positive cells in breast tumours increases patients' chances of survival following endocrine therapy (17). Front line therapy for locally advanced ER positive breast cancer includes therapies that reduce the levels of oestrogen (Aromatase Inhibitors; Luteinising-hormone-releasing hormone agonists); antagonise the effects of oestrogen on the receptor (SERMS such as Tamoxifen); and down-regulate the receptor (Fulvestrant).

1.5 Oestrogen & Oestrogen Receptor

1.5.1 Oestrogen

Oestrogens are steroid hormones (18). Oestrone (E1), 17β oestradiol (E2) and oestriol (E3) are three naturally occurring oestrogens, of which E2 is the main oestrogen from menarche to menopause. Following menopause, E1 becomes the predominant source of oestrogen. Oestrogens are synthesised in the ovary and testis, but also in peripheral tissues via the aromatisation of androgens. Ovarian synthesis of E2 dramatically declines

at menopause. The majority of breast cancers are diagnosed post-menopause, and non-ovarian sources of E2 are important in breast cancer development and progression.

In addition to its role in female reproduction, oestrogen is required for maintaining bone density and cholesterol levels (18). George Beatson demonstrated over 100 years ago that oophorectomy reduced breast cancer growth (19). Oestrogen antagonists are now vital for the treatment of hormone dependent breast cancer (18).

1.5.2 Oestrogen Receptor

In 1962, Jensen and Jacobson concluded that a receptor protein mediated the effects of E2 (20). In 1986, two groups cloned the oestrogen receptor (ERα) (21;22). There are two known isoforms of the oestrogen receptor, ERα and ERβ (discovered in 1996) (23), encoded by different genes (ERα chromosome 6q and ERβ chromosome 14q) (24;25).

ERα, a member of the steroid hormone nuclear receptor family, is a 65kDA, ligand-activated transcription factor. 15-20% of normal breast cells express ERα, and these cells are generally non-dividing. Oestrogen promotes release of growth factors by ERα positive breast cells, which stimulate proliferation, in a paracrine manner, of neighbouring ERα negative cells. In breast tumours, ERα positive cells undergo proliferation. The causes underlying transformation from non-dividing to proliferating cells are not understood (26). Patients diagnosed with ERα positive tumours have a better prognosis than patients with ERα negative breast cancers. Proliferation rates in ERα negative DCIS cells are greater than in ERα positive DCIS cells (27). Also , ERα tumours are more responsive to hormonal therapy than ERα negative tumours (28-30).

1.5.3 Oestrogen Receptor Structure

ERα comprises six functional domains, annotated as domains A-F. (Figure 1.2) (31-34).

- **A/B Domain (N-terminal):** Poorly conserved, contains the hormone independent activation function (AF-1), which activates target genes by interacting with transcriptional machinery or co-activators. Amino acids 41-150 are required for AF-1 activity; and residues 91-121 for ligand binding domain synergy, which facilitates maximum transcriptional activity.

- **C Domain (DNA binding domain):** Highly conserved DNA binding domain with two zinc finger motifs, each with four conserved cysteines. These zinc finger motifs, in combination with the P-Box (sequence critical for target DNA-DNA recognition and specificity), are responsible for binding to oestrogen response elements (ERE) of target genes, and in combination with a D-box, control dimerisation of the receptor on the EREs.

- **D Domain (Hinge domain):** Allows for ERα "flexibility", contains amino acids required for stable DNA binding. It also stabilises interactions with accessory proteins.

- **E Domain:** Highly conserved, contains ligand binding domain (LBD) and the ligand-dependent transactivation function (AF-2). Comprising 12α helices, forming a ligand binding pocket. Ligand binding changes conformation, and helix 12 caps the pocket, trapping ligands in a hydrophobic environment and forming a surface for co-activators to bind to (35). It contains regions required for anti-oestrogen agonistic activity, dimerisation, nuclear localisation, hsp90 binding and co-activators/co-repressors interactions.

- **F Domain (C-Terminal):** Little is known of this domain. It is thought to contribute to the transactivation function of the ERα and to play a role in distinguishing between agonists and antagonists, perhaps through interactions with cell specific factors.

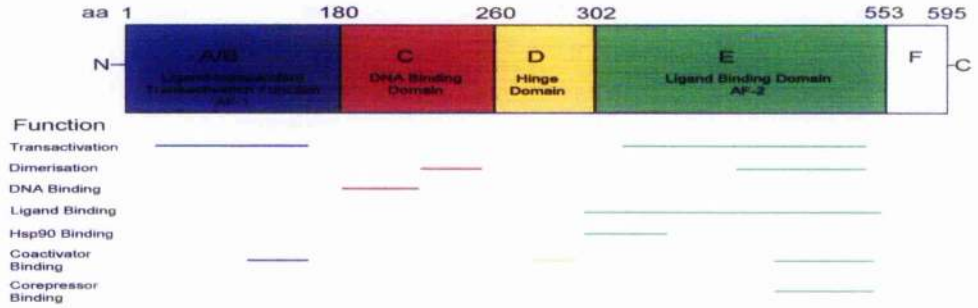

Figure 1.2: Functional Domains of Oestrogen Receptor

The oestrogen receptor comprises six functional domains A-F. The diagram shows the function of each domain.

1.5.4 Oestrogen Receptor Cofactors

ERα interacts with nuclear proteins that modify its effects on transcription. Co-activators interact directly with ERα and enhance transcription, whilst co-repressors suppress ERα-mediated transcription. Inactive ERα, or ERα bound to antagonists, associates with co-repressors. Following ligand binding, ERα undergoes a conformational change that allows it to bind co-activators (35).

- **Co-activators**

There are many co-activators, such as the p160/SRC family, CBP/p300 and the TRAP/DRIP co-activator complex. The p160/SRC family consists of three members: SRC-1 (p160-1, N-CoA1), SRC-2 (TIF-2, GRIP1, NCoA2) and SRC-3 (AIB1, P/CIP, ACTR, RAc3, TRAM1) (35). Co-activators bind to a nuclear-receptor interaction domain, consisting of a LXXLL motif within the AF-2 activation domain (18). The SRC co-activators recruit histone acetyltransferases (HAT) to the promoter region of E2

regulated genes, which facilitates DNA unwinding, allowing transcription to begin. CBP/P300 possess acetyltransferase activity, and its binding requires SRC co-activators (34). The TRAP/DRIP co-activator complex recruits the transcription machinery (36).

- **Co-Repressors**

N-CoR and SMRT are key co-repressors. Both prevent ERα mediated transcription by recruiting proteins that have histone-deacetylase (HDAC) activity to the promoter region of the gene. This prevents transcription by maintaining chromatin in a condensed state and inhibiting access to transcription machinery (37).

1.5.5 Ligand-dependent activation of oestrogen receptor

In the absence of ligand, ERα is maintained in a multiprotein inhibitory complex with Heat Shock Proteins (HSPs). Hsp90 binds regions of the receptor required for homodimerisation, nuclear localisation and DNA binding. It regulates several of the ligand binding functions of ERα and maintains the receptor in its inactive form (32).

The classic "genomic" action of ERα requires ligand binding, which induces phosphorylation, dissociation from Hsps, conformational changes, homodimerisation and nuclear translocation. Nuclear ERα binds directly to ERE sequences in the promoter region of E2 regulated genes (38). This leads to recruitment of co-activators, co-repressors and transcription machinery to the promoter. Depending on cell and promoter context, ERα positively or negatively regulates gene transcription (29;39;40).

ERα also modulates gene expression via AP-1 or Sp-1 sites in an ERE-independent manner. ERα binds indirectly to DNA via transcription factors, such as c-jun or c-fos. Here ERα functions as a co-activator, either stabilising binding of transcription machinery to the DNA, or by recruiting other coactivators (34;41) (Figure 1.3).

Recently, studies have revealed that whilst some ERα binding sites were located directly adjacent to target genes, the majority of binding sites were found significant distances from the transcriptional start sites. It was suggested that ERα interactions with ERE sites were important, but insufficient to enable ERα-chromatin association. Forkhead factor binding sites were present near authentic ERE sites, and Forkhead factor (FoxA1) binding was required for ERα-chromatin interactions. Downregulation of FoxA1 inhibited ERα associating with its binding sites (42).

E2/ERα interaction controls expression of genes involved in cell proliferation, apoptosis, invasion, metastasis and angiogenesis. High-density gene expression profiling of hormone response in ERα positive T-47D breast cancer cells identified 137 ERα-regulated genes, of which only 89 were direct ERα target genes. These 89 genes were also identified as ERα targets in MCF-7 cells and in breast tumours (43)

Activation of ERα requires both AF-1 and AF-2 activation domains. These domains can function independently or synergistically. AF-2 activation requires ligand binding, whereas AF-1 function seems to play a role in both ligand-dependent and ligand-independent mediated transcription, and is regulated via phosphorylation. Binding of E2 stimulates increased phosphorylation of the receptor. However, ERα is also phosphorylated in a ligand-independent manner.

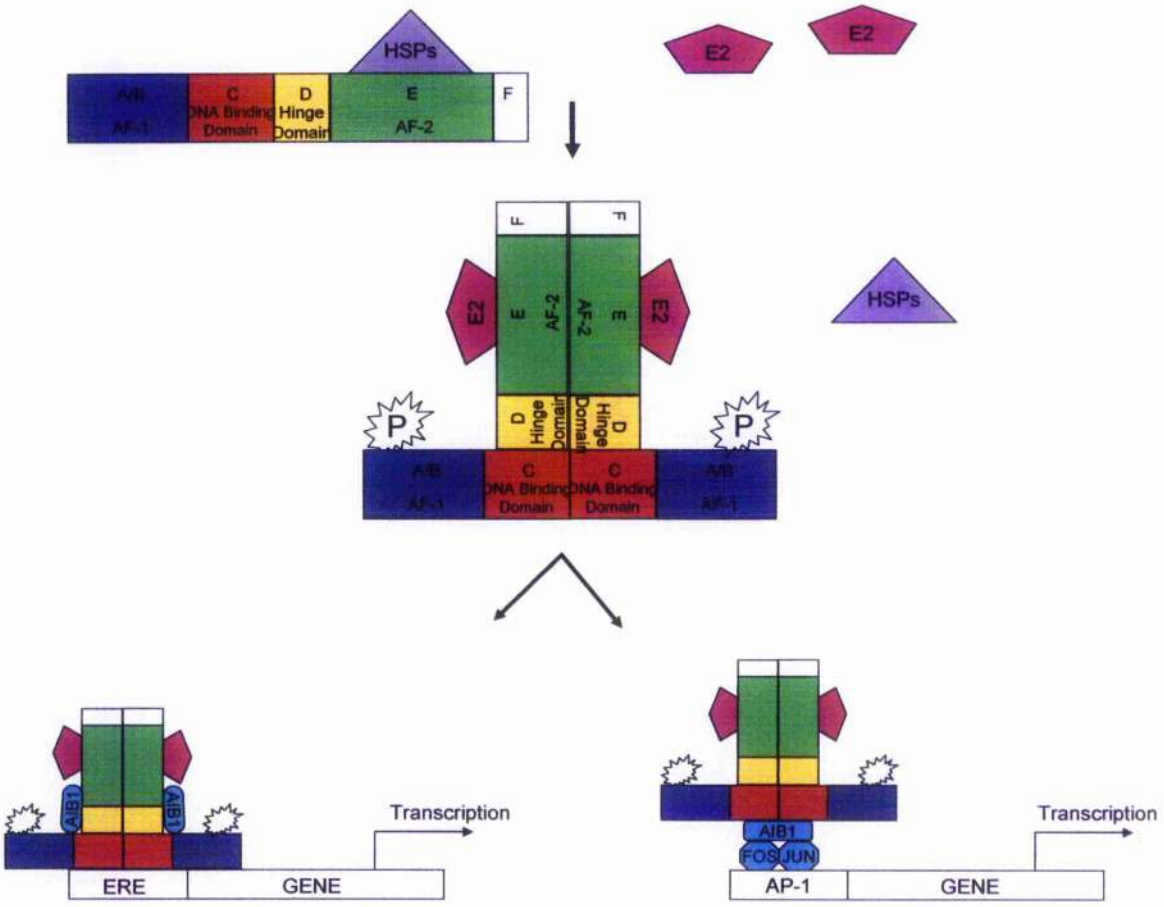

Figure 1.3: Ligand-Dependent Activation of the Oestrogen Receptor
The classic genomic action of the ERα requires ligand binding, which induces ERα to bind directly to the ERE domains in the promoter region of oestrogen regulated genes, leading to the recruitment of coactivators, such as AIB1, and the attachment of transcription machinery to the promoter. Alternatively ERα is able to modulate the expression of genes containing AP-1 or Sp-1 sites in an ERE-independent manner, by binding indirectly to the DNA via other transcription factors, such as c-jun or c-fos. HSPs = Heat shock proteins, E2 = Oestrogen, ERα = Oestrogen Receptor

1.5.6 Oestrogen Receptor Phosphorylation

Phosphorylation of ERα is stimulated in a ligand-dependent manner, via E2 binding, and in a ligand-independent manner, through signal transduction pathways (see below). Key ERα phosphorylation sites include: serine 104/106, 118, 167, 236 and tyrosine 537.

Phosphorylation of AF-1 serine residues 118 and 167 results in transactivation and is mediated by MAPK and AKT pathways. MAPK directly and indirectly

phosphorylates S118 and S167 respectively, in an E2 independent manner. However, Cdk7, and not MAPK, is believed to be the kinase responsible for E2 mediated phosphorylation of S118 (44). The Cdk2 kinase complex phosphorylates serines 104/ 106, (45) increasing receptor trans-activation. Protein Kinase A (PKA) phosphorylates S236 within the DBD, inhibiting ERα dimerisation, in the absence of ligand, or presence of antagonists, and preventing DNA binding (46). Phosphorylation of the AF-2 tyrosine residue 537 is mediated by Src kinases, and regulates ligand binding, dimerisation and trans-activation (47). ERα phosphorylation enhances dimerisation, ligand-binding, nuclear localisation, cofactor recruitment and gene transcription (Figure 1.4).

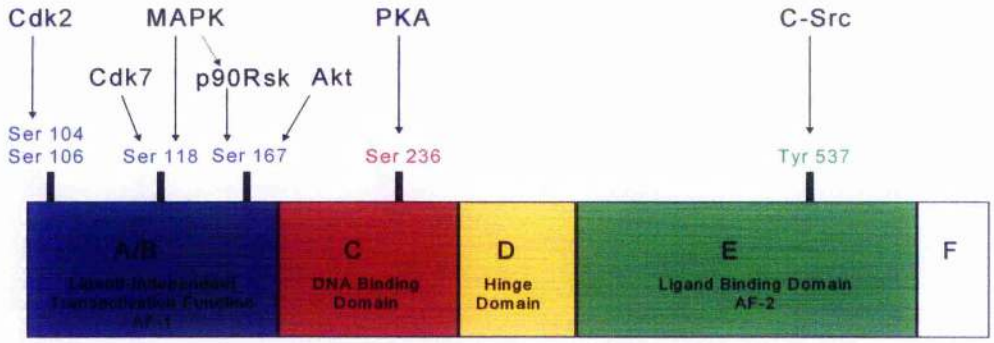

Figure 1.4: Oestrogen Receptor Phosphorylation Sites
The oestrogen receptor is phosphorylated by multiple kinases. The AF-1 domain residues are phosphorylated by the growth factor pathways (MAPK and Akt) and cyclin dependent kinases. PKA phosphorylates serine 226 in the DNA binding domain, whilst Src-kinases are thought to be responsible for phosphorylating Tyrosine 537. Cdk = Cyclin dependent kinase, PKA = Protein Kinase A, Ser = Serine, Tyr = Tyrosine

1.5.7 Ligand-Independent Activation of Oestrogen Receptor

In addition to activation by E2, ERα can be phosphorylated and activated in a ligand-independent manner. Kinases mediate ERα phosphorylation (section 1.5.6) in both the AF-1 and AF-2 domains. Additionally E2 independent phosphorylation of co-activators and co-repressors can increase ERα transcriptional activity.

Multiple signalling pathways activated by growth factors, stress or cytokines are linked to E2-independent activation of the ERα. Activation of the receptor tyrosine kinases (EGFR, HER2-4) results in activation of two key pathways: Ras/Raf/MAPK and Ras/PI3k/AKT, and appears to play a key role in ERα activation (see below).

1.5.8 Non-Genomic Activity of Oestrogen Receptor

The primary function of ERα is to mediate gene transcription (Genomic activity). However, rapid E2 mediated effects (seconds to minutes) and a membrane localised ERα, identified an alternative, non-genomic receptor function. E2 binding to membrane bound ERα activates signal transduction cascades. Membrane-bound ERα effects are rapid and unaffected by transcriptional inhibitors (48). E2 stimulates ERα association with Src and Shc, activating Ras signalling cascades. In vitro studies show increased MAPK and AKT phosphorylation and activation following E2 stimulation, suggesting a positive feed back loop resulting in phosphorylation and activation of nuclear ERα (49-51). Membrane ERα transactivates the epidermal growth factor receptor (EGFR), by activating matrix metalloproteinases, which cleave heparin-bound Epidermal Growth Factor (EGF), which subsequently activates EGFR (52).

1.5.9 Oestrogen Receptor β (ERβ)

There is a relatively high degree of homology between ERα and ERβ in the ligand (60%) and DNA (97%) binding domain. However, there is less similarity in the N-Terminal (18%) domain (38). Expression of ERα and ERβ differ between different tissue types. ERβ appears to have a more limited expression pattern.

ERα and ERβ can form either homo- or heterodimers when co-expressed in cells (53). Although ERα and ERβ interact with the same DNA response elements and have similar binding affinities for E2 (38), ERβ appears to respond differently to E2 agonists and antagonists. A recent study highlighted that E2 induced transcription via ERα bound to AP-1 sites, but that it inhibited transcription via ERβ (54). ER knockout mice revealed that ERα, but not ERβ was required for normal mammary gland development (55;56). The role of ERβ in breast cancer remains controversial. Approximately 70% of breast tumours express ERβ, and most tumours co-express ERα and ERβ (57;58). Expression of both ERs has been associated with higher grade tumours and lymph node positivity (59). A negative correlation was observed between expression of ERβ and the progesterone receptor. ERβ has also been linked to increased cell proliferation and invasiveness (60). However, conflicting studies suggest that expression of ERβ is associated with lymph node negativity, lower grade tumours and improved prognosis (61-63)

1.5.10 Oestrogen and Oestrogen Receptor Targeted Therapies

1.5.10.1 Luteinising-hormone-releasing hormone (LHRH) agonists

LHRH agonists, such as goserelin, are commonly used to treat pre-menopausal breast cancer patients. Goserelin acts by decreasing the secretion of luteinising hormone by the pituitary, resulting in a block in follicular activity, which reduces the production of E2 in the ovaries (64).

1.5.10.2 Tamoxifen

For the last 20 years, Tamoxifen treatment has been the gold standard for ERα positive breast cancer patients. It is currently one of the most effective but least toxic drug

therapies. An oestrogen antagonist, it is a non-steroidal that acts as a selective oestrogen receptor modulator (SERM). It competitively inhibits the interaction of E2 with the ERα, by directly binding to the AF-2 transcriptional activation domain, blocking the effects of E2 and inhibiting receptor activity (Figure 1.5). Tamoxifen binding to the ERα induces a conformational change, so that helix 12 of the LBD is positioned over the co-activator binding sites, preventing their recruitment to the ERα (18;65). Tamoxifen induces co-repressor recruitment, further repressing ERα activation.

Tamoxifen inhibits only AF-2 functions; it does not interfere with AF-1 activation. Consequently Tamoxifen may function as both an ERα antagonist and agonist. Tamoxifen activity depends on the tissue and the availability of co-activators and co-repressors. In breast epithelium, ERα activity is mostly dependent on AF-2 functions, and Tamoxifen acts as an antagonist. However, in the uterus, ERα activity is more reliant on AF-1 activation; therefore Tamoxifen functions as an agonist. Thus Tamoxifen reduces the risk of osteoporosis, but also stimulates endometrial proliferation, which increases the risk of endometrial cancer (~2.5 fold) (66). Other side effects include venous thrombosis, pulmonary embolus and stroke.

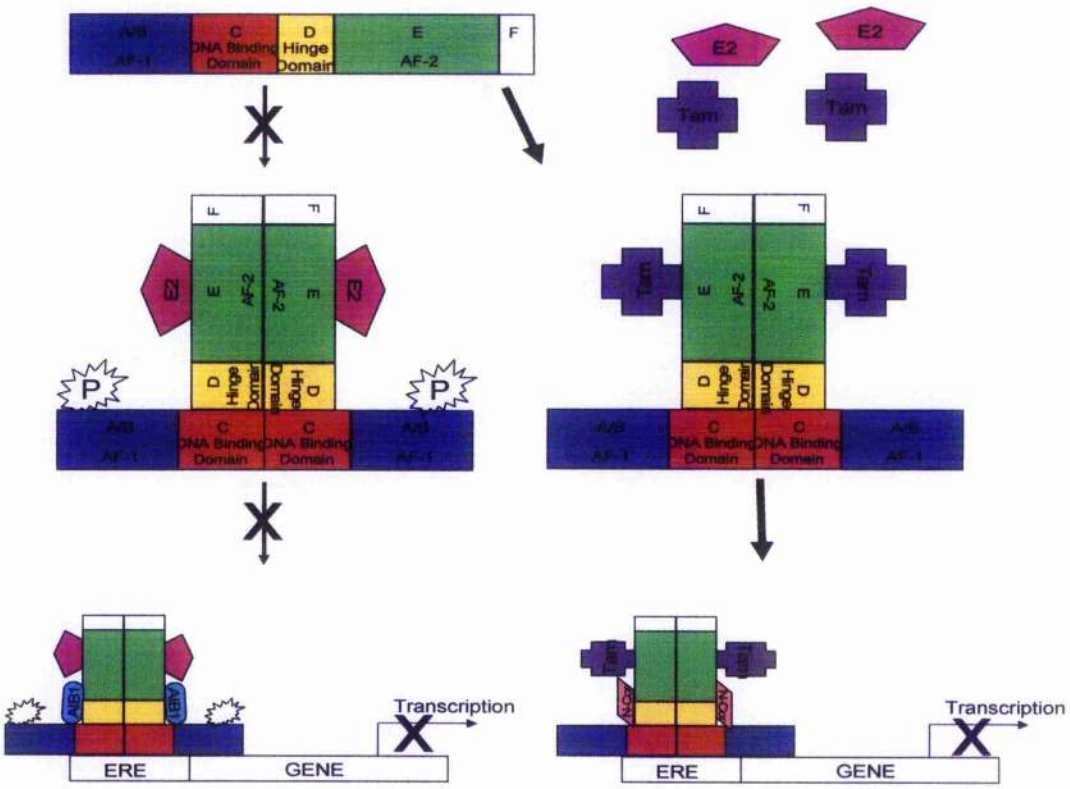

Figure 1.5: Tamoxifen Interaction with Oestrogen Receptor
Tamoxifen binding to the AF-2 domain of the oestrogen receptor prevents E2 from binding. Tamoxifen induces ERα interactions with co-repressors, such as N-CoR, rather than co-activators, such as AIB1.

The standard five-year course of treatment with tamoxifen produces a 51% reduction in recurrence and a 28% reduction in deaths(40). However, approximately 50% of breast cancers, despite being ERα-positive, fail to respond to tamoxifen (67), whilst the majority of women who are initially sensitive to the endocrine therapy develop resistance to the treatment over time (67-69).

1.5.10.3 Fulvestrant

To combat the agonistic effects of Tamoxifen, "pure antioestrogens" that do not demonstrate agonistic behaviour were developed. Fulvestrant (Faslodex), has no

agonistic effects and has a 100 fold greater binding affinity for ERα than Tamoxifen, and is approved for treatment of ERα positive, metastatic, post-menopausal breast cancers. Fulvestrant binds ERα, prevents DNA binding and promotes ERα degradation, markedly reducing cellular receptor levels (70). Tamoxifen resistant cell lines respond to Fulvestrant (71).

1.5.10.4 Aromatase Inhibitors

Post-menopausal women depend on the cytochrome P450 aromatase enzyme for E2 synthesis. Aromatase catalyses the conversion of androgens to oestrogens, in peripheral (e.g. fat, muscle) tissues and locally within tumours. Aromatase inhibitors (AI) inhibit the enzyme, reducing E2 levels by 97% in post menopausal women (72). Type 1 AIs (Exemestane) are steroid analogues of androstenedione, which bind to the aromatase enzyme complex resulting in irreversible inactivation. Type 2 AIs (Anastrazole and Letrozole) are non-steroidal and bind the enzyme complex, reversibly (73).

Recent evidence suggests AIs are superior to other therapies in the treatment of tamoxifen-resistant advanced breast cancers and also in the neoadjuvant setting (74;75). Several clinical trials are underway, investigating the role of the three mentioned AIs as adjuvant treatment in early stage breast cancers. These trials analyse the role of AIs in three different treatment situations; initial adjuvant treatment: (ATAC, TEAM, BIG-1-98), sequenced after 2-3 years of Tamoxifen treatment (IES), or after completing five years Tamoxifen therapy (MA-17). Although the results of these trials cannot be directly compared, they all provide data to suggest that AIs are superior to Tamoxifen in the treatment of breast cancer in terms of disease-free survival (76-78). It is thought that the superiority of AIs over Tamoxifen may be a consequence of aromatase inhibition,

resulting in an increased reduction in tumour proliferation (76). Additionally, treatment with AIs seemed to reduce the adverse side effects observed with Tamoxifen treatment. However, questions remain about the long term safety of AIs (79;80).

As more data regarding the efficiency of AIs from the various trials is released, they might challenge Tamoxifen for the role of first-line therapy. However, to optimize use of such therapies, it would be beneficial to establish predictive markers to identify patients who are likely to develop Tamoxifen resistance and would respond to AI treatment. Results suggest that ERα positive, progesterone receptor (PR) negative breast tumours and HER2 overexpressing tumours are more responsive to AIs than to Tamoxifen (81). A further understanding of the mechanisms driving Tamoxifen resistance is required to enable improved treatment of breast cancer patients.

1.6 Mechanisms of Tamoxifen Resistance

Despite the extensive use of Tamoxifen as first-line therapy for ERα positive breast cancer patients, resistance to tamoxifen treatment, either at primary treatment (*de novo* resistance) or arising during treatment (acquired resistance), causes significant morbidity and mortality.

1.6.1 Down-Regulation of ERα

ERα expression is generally maintained in breast tumours that lose sensitivity to Tamoxifen (40). Several studies highlight that in Tamoxifen-resistant patients, tumour growth and progression is still regulated by the ERα, and that they remain sensitive to other therapies, such as Fulvestrant or AIs (71).

1.6.2 Mutations & Splice Variants of the ERα

ERα mutations that might account for the loss of sensitivity to Tamoxifen have been identified; however, most mutations were silent changes that would not alter ERα amino acid sequence (82). Only 1% of breast tumours present with an ERα mutation within the coding region, and most failed to alter ERα expression at the protein level (83). Alternatively spliced, variant ERα mRNA has been discovered that encodes for a truncated form of the ERα. However, research of clinical samples has failed to reveal a role for these variants in Tamoxifen resistance (82).

1.6.3 Effects of ERβ

ERβ has opposing effects from ERα on tumour growth. A recent study highlighted that when antioestrogens bound to ERβ at an AP-1 site, they functioned as agonists rather than antagonists (54). Likewise, increased ERβ expression is associated with tamoxifen resistance (84;85). However, other studies suggest high ERβ levels inhibit tumour growth if Tamoxifen is present, and ERα positive tumours expressing low ERβ levels are Tamoxifen resistant (86-88).

1.6.4 Hypersensitivity to Oestrogen

Breast tumours can adapt to their environment and become hypersensitive to the oestrogenic effects of Tamoxifen, allowing tumour progression and growth. Tamoxifen-resistant cells show an increase in the basal levels of phosphorylated ERα and tamoxifen promotes, rather than inhibits, growth of these cells (89).

1.6.5 Availability of Co-activators and Co-Repressors

To function as an antagonist, Tamoxifen induces interactions with co-repressors and prevents interactions with co-activators. However, overexpression or mutation of co-

activators could alter response to endocrine therapies. AIB1 is amplified in 5% and overexpressed in 65% of breast tumours (90). These high levels of co-activators may increase the agonistic activity of Tamoxifen (91-93). AIB1 is often co-expressed with HER2 (94), and under these conditions, Tamoxifen acts as an agonist, and ERα binds AIB1, rather than co-repressors (93). It is unclear how co-activators bind to Tamoxifen-bound ERα, since its conformation should prevent them binding. One proposal is that AIB1 binds to the AF-1 domain of ERα, rather than the Tamoxifen bound AF-2 domain. Conversely, if levels of co-repressors are low, this might also facilitate the development of Tamoxifen resistance.

1.6.6 Cross-Talk between ER and Growth Factor Receptor Pathways

The signalling pathways Ras/Raf/MAPK and Ras/PI3K/AKT both phosphorylate and activate the ERα in a ligand-independent manner. Likewise, membrane-associated ERα can activate these two pathways, which ultimately activate the nuclear receptor. Ligand-independent activation of the ERα via signalling pathways, e.g. Ras/Raf/MAPK (29;39;95;96), results in transcription of E2-regulated genes and cell proliferation. Ras activation increases ER sensitivity to low E2 concentrations, via ERα phosphorylation by MAPK and AKT, causing tamoxifen resistance(68;69;97).

1.7 Human Epidermal Growth Factor Receptor (HER) Family

The four members of the Human Epidermal Growth Factor Receptor (HER) family are key factors that interact with and influence ERα activation status.

1. **Epidermal Growth Factor Receptor (EGFR)/HER1**: Localised to chromosome 7p12 encodes a 170kDa transmembrane protein.

2. **HER2**: *Her2* located on chromosome 17q21 encodes a 185kDa transmembrane glycoprotein that has intrinsic kinase activity. Originally identified as a transforming oncogene in rat neuroglioblastomas, the receptor is activated in human breast and ovarian cancer as a result of amplification and overexpression.

3. **HER3**: In 1989 a DNA fragment related to EGFR and HER2 was identified (98) as HER3, a 148kDa transmembrane protein. The gene is located at chromosome 12q13.

4. **HER4**: The *HER4* gene localised to chromosome 2q33 encodes a 180kDa transmembrane protein.

The type I tyrosine kinase receptors (RTKs) control cellular responses to the external environment. Through ligand binding, the receptors activate signal transduction pathways, which determine the fate of the cell. All the receptors have the same basic structure: an extracellular ligand binding domain, containing cysteine rich residues and possible glycosylation sites; a membrane-spanning region; a short intracellular juxta membrane region; a cytoplasmic protein tyrosine kinase domain; and a carboxy tail which contains tyrosine phosphorylation sites (99). There is a high degree of sequence homology in the tyrosine kinase domain of EGFR, HER2 and HER4, highlighting the domains' importance. HER3 has substitutions in four key amino acids in this domain and lacks kinase activity (99). The growth factor receptors remain inactive on the plasma membrane, until ligand binding occurs. Each receptor, with the exception of HER2, binds a narrow spectrum of ligands (Table 1.5). Currently there is no known ligand for HER2.

RECEPTOR	LIGAND
HER1 (EGFR)	Epidermal Growth Factor (EGF), Transforming Growth Factor α (TGFα), β-Cellulin (BTC), Heparin-binding Growth Factor (HB-EGF), Amphiregulin (AR), Epiregulin (EPR)
HER2	Unknown
HER3	Heregulin (HRG), Neuregulins 1 +2 (NRG 1 + 2)
HER4	Heregulin (HRG), Neuregulins 1-4 (NRG 1-4), β-Cellulin (BTC), Heparin-binding Growth Factor (HB-EGF),Epiregulin (EPR)

Table 1.5: Ligands associated with the HER family
All of the HER family members, with the exception of HER2, require ligand binding for activation. The above table lists the ligands for EGFR, HER3 and HER4.

Upon ligand binding, receptors either homo- or hetero-dimerise. The preferred partner for EGFR, HER3 and HER4, is HER2. HER2 increases the binding affinity of these receptors with ligands, resulting in extended activation of signal transduction. Dimerisation activates tyrosine kinase domains, and promotes autophosphorylation of specific tyrosine residues (100). In HER2 overexpressing cells, HER2 is thought to spontaneously homodimerise (99). Receptor activation initiates signal transduction pathways, utilising multiple elements, and integrates signals to the nucleus.

1.7.7 HER family and Breast Cancer

RTKs are expressed on the plasma membrane, and ERα in the nucleus, yet the two show strong evidence of cross-talk, mediated predominantly via the Ras/Raf/MEK/MAPK and PI3-K/AKT pathways (30;69;100;101). Expression of the RTKs is a strong indicator of both prognosis and treatment choice (99;102). Studies within our group indicated increased expression of HER1-3 correlated with reduced survival, while expression of HER4 was associated with improved survival (103-105). It is also accepted that there is a negative correlation between expression of the ERα and EGFR/HER2, and probably HER3.

Approximately 25-30% of all breast cancers overexpress HER2 (19). This is associated with greater proliferation of breast cancer cells and subsequently a poorer prognosis (106). Treatment with Tamoxifen is less effective in patients overexpressing HER family members. The response rate to tamoxifen is reduced from 50% in ERα positive breast cancer with normal HER2 expression to 17% in HER2 overexpressing breast cancer (107), and this effect can be reversed by the use of aromatase inhibitors (81).

1.8 The Ras/Raf/Mek/MAPK Pathway

The mitogen-activated protein (MAP) kinase cascade, is a three-tiered kinase model that conveys signals from the plasma membrane to the nucleus. This model consists of a MAP kinase or Extracellular Regulated Kinase (ERK) being activated by a MAPK/ERK kinase (MEK or MAPKK), which in turn is activated by a MEK kinase (MEKK or MAPKKK). The Ras/Raf/Mek/MAPK pathway is a classic example of this cascade (Figure 1.6).

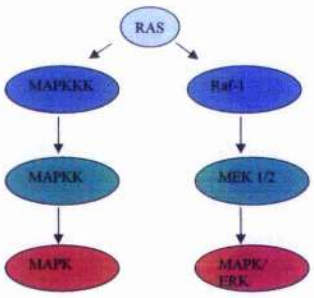

Figure 1.6: Mitogen-activated protein (MAP) kinase cascade
The Ras/Raf/MEK/MAPK is a classic example of the mitogen-activated protein (MAP) kinase cascade. Raf (MAPKK) phosphorylates and activates MEK1/2 (MAPKK), which in turn phosphorylates and activates MAPK (MAPK).

Activation of this pathway follows membrane RTKs binding ligands, dimerising and undergoing autophosphorylation (99;100). RTKs in association with growth factor receptor bound protein 2 (Grb2) and Son of Sevenless (SOS), translocate Ras to the

plasma membrane where it is activated, and promotes Raf-1 phosphorylation and activation (108-115). Raf-1 phosphorylates and activates MEK, which subsequently activates MAPK, which phosphorylates and activates multiple substrates (116;117).

Overexpression and activation of the MAPK cascade is involved in the development and progression of tumours. The pathway regulates proliferation, apoptosis, metastasis and angiogenesis, and links the RTKs, localised to the plasma membrane, with nuclear ERα. MAPK phosphorylates and activates ER in a ligand-independent manner (29;39;95;96). Activation of the Ras pathway is believed to be a key mechanism driving tamoxifen resistance (Figure 1.7).

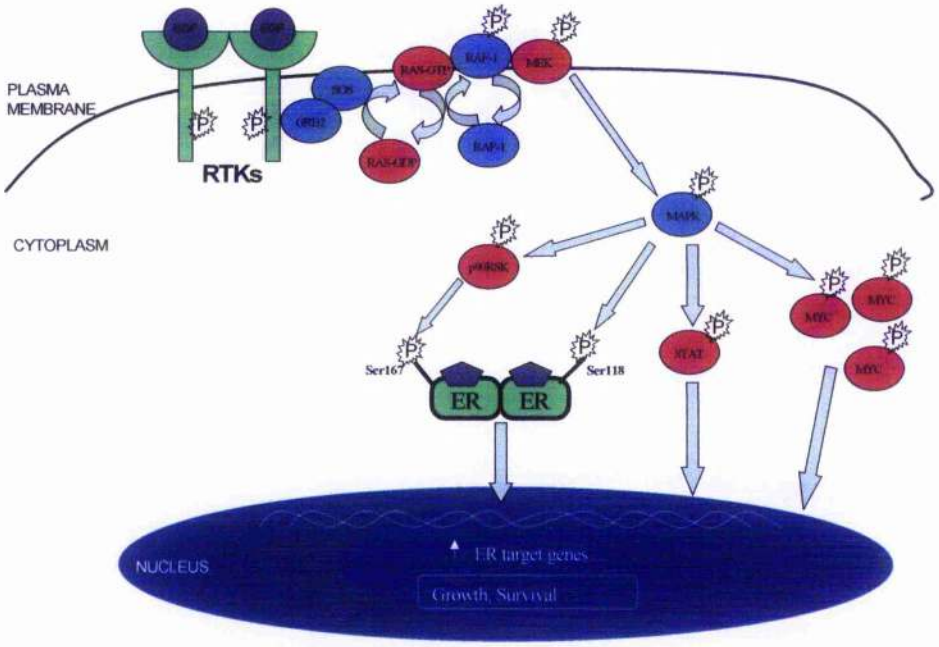

Figure 1.7: Ras/Raf/Mek/MAPK Pathway
Schematic representation of the Ras/Raf-1/MAPK pathway.

1.8.1 Ras

The Ras superfamily of genes, comprising over 65 members, encode GTPases that control multiple cellular processes. These include six subfamilies: Ras, Rho, Rab, Ran

Rad and Arf. The Ras family is further subdivided into four sub-sub-families: Rap (Rap-1A; Rap-1B; Rap-2A; Rap-2B); R-Ras (R-Ras. TC21/R-Ras2, R-Ras3); Ral (RalA, RalB) and Ras (H-Ras, K-RasA, K-RasB and N-Ras) (118).

1.8.1.1 Ras Genes

There are three isoforms of Ras: *Harvey Ras* (*H-Ras*), found on chromosome 11 (11p15.5); *Neuroblastoma Ras* (*N-Ras*), localised to chromosome 1 (1p13); and *Kirsten Ras* (*K-Ras*), found on chromosome 12 (12p12.1) (35,36,37). *H-Ras*, and *K-Ras* genes were identified as viral oncoproteins of Harvey, and Kirsten murine sarcoma viruses, whilst *N-Ras* was discovered in a neuroblastoma cell line (118).

H-, *K-* and *N-Ras* share a similar genetic structure, possessing four exons and a 5' non-coding exon. However, *K-Ras* has two alternative fourth exons (4A and 4B), yielding two protein isoforms (K-RasA and K-RasB). From this point on, K-Ras refers to K-Ras B. There are major differences between the introns of *H-*, *K-*, and *N-Ras* in terms of both size and sequence. The genomic DNA sequences for *K-Ras* spans approximately 35kbp, *N-Ras* only 7 kbp and *H-Ras* only 3 kbp. The Ras genes are regulated by TATA-less but GC rich promoters (111).

1.8.1.2 Ras Protein Structure

The proteins encoded by Ras genes are composed of 188-9 amino acids and are monomeric, membrane localised, guanine nucleotide binding proteins, with a molecular weight of approximately 21kDa. The proteins cycle between an inactive guanine dinucleotide (GDP)-bound state and an active guanine trinucleotide (GTP)-bound state. The proteins contain four domains and appear to have highly conserved regions in their N terminal. Within the N-terminal, catalytic domain, there is 100% homology between the

Ras proteins in the first 86 residues (1st Domain), and approximately 79% homology in the following 78 residues (2nd Domain) (119). However, the homology between the proteins in the final 25 carboxy-terminal residues (residues 165-188/189) is only 10-15%; consequently, this region is termed the hypervariable region (HVR, 3rd domain) (120) (Figure 1.8). The HVR is essential for Ras translocation to, and association with, the plasma membrane (PM) (121). The final four residues of the HVR comprise the carboxy terminal CAAX motif (C=cysteine, A=aliphatic amino acid; leucine, isoleucine or valine, X=serine or methionine, 4th Domain). HVR and the CAAX motif undergo post-translational modifications to enable Ras translocation to the PM. The Effector domain (residues 32-40) is required for Ras binding to its substrates. Five non-contiguous regions are essential for Ras function: residues 5-63, 77-92, 109-123, 139-165 and 186-189 (CAAX motif) (118). There are also two switches present at residues 30-38 (switch I) and 60-76 (switch II). Switch I is involved in the binding of substrates and GTPase activating proteins (GAPs), whilst switch II is implicated in the binding of Guanine nucleotide exchange factors (GEFs). The only structural differences observed between the active and inactive form of Ras are within the two switch domains (122-124)(Figure 1.8).

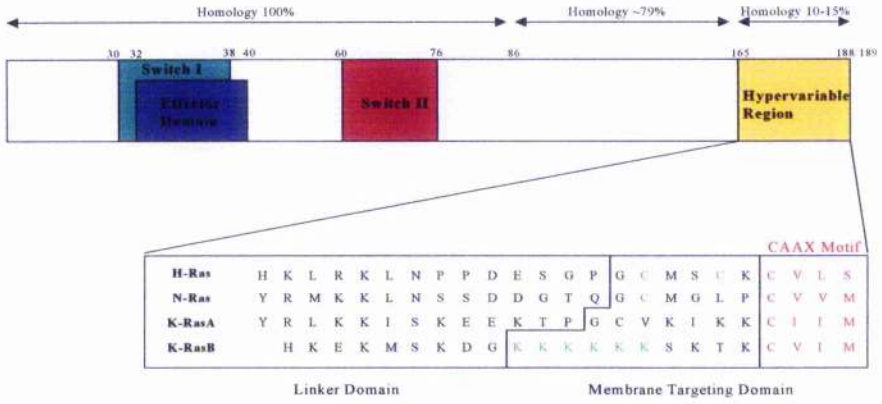

Figure 1.8: Ras Protein Structure

Comparison of the protein sequences highlights a high degree of homology in the N-terminal between the H-, K- and N-Ras proteins. However, there is less homology between the proteins in the hypervariable region. Within the HVR, is the carboxy-terminal, CAAX motif, at residues 186-189 (highlighted in red). There are also residues upstream of the CAAX motif, essential for membrane targeting (highlighted in green). These residues along with the CAAX motif undergo post-translational modifications to enable Ras translocation to the PM.

1.8.1.3 Post-Translational Modifications

Ras proteins are synthesised in the cytosol as inactive precursors. Activation requires post translational modifications and translocation to the plasma membrane (108;111). The first modification involves the addition of a farnesyl (C_{15}) group to the cysteine residue of the CAAX motif, by protein farnesyl transferase (FT). Research suggests that when FT's are inhibited, K-Ras and N-Ras can undergo the alternative modification of geranyl-geranylation (addition of a C_{20} group) (113). Farnesylation directs Ras to the cytosolic surface of the endoplasmic reticulum, where an endopeptidase, Rce1, cleaves the three downstream amino acids (AAX), followed by methylation of the farnesylated-cysteine residue by Isoprenylcysteine carboxyl methyltransferase (Icmt). These modifications

increase the hydrophobicity of the carboxy-terminal region of the protein, thus strengthening the association between proteins and inner surface of the PM (125-127).

Further modifications stabilise the binding of the proteins to the PM. Both H- and N-Ras undergo palmitoylation (addition of palmitic acid) of cysteine residues within the HVR. H-Ras has two palmitoylation sites, cysteine 181 and 184, whereas N-Ras has only one, cysteine 181, (Figure 1.8, cysteine residues highlighted in green) (128). Unlike farnesylation, palmitoylation is reversible (129). Palmitoylation of H- and N-Ras allows them to traffic through the golgi to the lipid rafts of the plasma membrane (127).

K-Ras is farnesylated but not palmitoylated; it has a polybasic stretch of amino acids in the HVR domain (Figure 1.8, highlighted in green) that targets it to the bulky region of the plasma membrane. It is thought that this polybasic domain allows K-Ras to localise to the negatively charged PM via a simple diffusion mechanism, and that there are high-affinity electrostatic interactions between K-Ras and acidic phospholipids and other negatively charged groups on inner surface of the PM. Hence H- and N-Ras are targeted to the PM via the Golgi, whereas K-Ras is relocalised in a golgi-independent manner (117;126-128;130;131). Due to its electrostatic interactions with the PM, K-Ras is localised to its bulky, disordered regions. In contrast, H- and N-Ras are directed to the lipid raft region of the PM. Inactive and active H- and N-Ras cycle between the lipid raft and bulky domain of the plasma membrane. It is thought that the HVR linker domain is crucial for the translocation of Ras from the lipid rafts to the bulky domain (128). Evidence suggests that N-Ras spends a longer period of time in non-raft domains (Figure 1.9)(132;133).

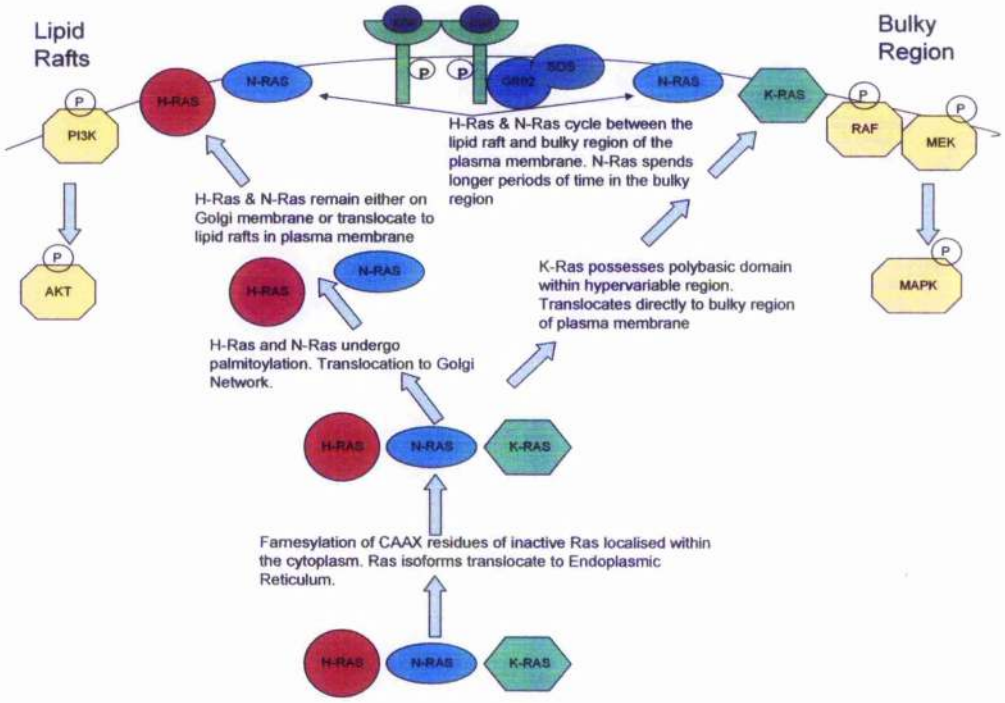

Figure 1.9: Post-translational modifications of Ras
Inactive Ras is located in the cytosol. Activation requires post translational modification and translocation to the plasma membrane (35,38). Post translational modifications include farnesylation and palmitoylation.

1.8.1.4 Ras Activation

Ras acts as a molecular switch and a link between the PM and its downstream signalling cascades. It is activated in response to stimulation of receptor and non-receptor tyrosine kinases, by mitogen and differentiation factors, and by external stimuli, such as UV radiation. Phosphorylation of the tyrosine residues of dimerised HER receptors, permits binding of GRB2, via Src Homology 2 (SH2) domains. GRB2 also contains two SH3 domains, which bind to a proline rich region of SOS. This complex brings SOS into close proximity with Ras, allowing the two proteins to bind (134;135). The docking protein, Shc, can act as an intermediate between the HERs and Grb2. Shc binds to the

phosphorylated receptors at the phosphotyrosine-binding domain (PTB) or at the SH2 domain. Subsequently Shc is phosphorylated and binds Grb2. All four HERs (HER1-4) can bind Grb2 via Shc, but only EGFR, HER2 and HER4, can bind Grb2 directly (136). Shc also mediates Ras binding to non-receptor tyrosine kinases, such as c-Src (137). The binding of SOS to Ras results in a conformational change and catalyses the dissociation of GDP, allowing Ras to bind GTP and become activated. Ras is rapidly deactivated through the hydrolysis of GTP to GDP, via the action of GAPs (108;134;135). Ras has low intrinsic GTPase activity, and requires interactions with GAPs to be inactivated. GAPs bind Ras-GTP and induce a transition state between Ras-GTP and Ras-GDP, reducing the half-life of Ras GTPase activity from minutes to seconds. The most common mutations in the Ras genes, at codons 12, 13, 59 and 61, reduce the intrinsic GTPase activity of Ras and prevent GAP-induced GTP hydrolysis (138).

It was believed that Ras was only activated at the PM; however, recent research has revealed that it can also be activated at the golgi. EGF stimulation results in rapid and transient activation of Ras at the plasma membrane, but a delayed and sustained activation of Ras at the golgi membranes (130;139). The mechanism of Ras activation at the golgi is believed to be different from that at the PM. Growth factors activate Src, which stimulates phospholipase Cγ. This generates diacylglycerol and Ca^{2+}, which activate the Ras guanine nucleotide releasing protein (Ras-GRP) family of GEFs. This causes their translocation to the golgi membrane, where they can mediate Ras activation (140;141)

1.8.1.5 Ras Effectors

There are currently multiple proteins considered to be Ras effectors. Perhaps the most established of these are Raf, PI3K and Ral-GDS. Ras activates Phosphatidylinositol 3-kinase (PI3-K), a lipid kinase. Activated PI3-K then promotes the phosphorylation of phosphatidyl inositol (4,5)- bisphosphate (PIP2) to phosphatidyl inositol (3,4,5)-trisphosphate (PIP3). PIP3 activates AKT/PKB, a serine/threonine kinase, which induces anti-apoptotic responses. Ral-GDS is a guanine nucleotide exchange factor for RalA and RalB. In response to growth signals, Ral-GDS binds to activated Ras and stimulates the exchange of GDP for GTP on Ral (142).

1.8.1.6 Ras Function

Ras proteins regulate multiple cellular processes via activation of signal transduction pathways, such as Raf/MAPK, PI3K/Akt and MEKK1/JNK/SAPK. Ras mutations promote tumour metastasis and angiogenesis, via induction of the angiogenic growth factors and metalloproteinases (143). Ultimately Ras function depends on the cell type, the presence of membrane receptors and duration of Ras activation.

Ras proteins play a key role in the control of the cell cycle. Ras expression is necessary for progression through the G1 phase of the cell cycle. Activated Ras increases Cyclin D1 expression, which shortens the G1 phase of the cell cycle and enhances cell growth. Cyclin D1 is amplified in 15-20% and overexpressed in 30-50% of breast cancers. This increase in expression is thought to be an early event in tumour development (144)

1.8.1.7 Ras Expression & Function: - Differences between the Ras isoforms

H-, K- and N-Ras are not functionally redundant. Ras is expressed in all tissues, though expression of Ras isoforms varies between tissues. H-Ras is highly expressed in skin and skeletal muscles; K-Ras is strongly expressed in colon and thymus; and N-Ras in male germinal tissue and thymus (120). Ras expression was significantly higher in immature cells, as opposed to differentiated cells, suggesting a role for Ras in differentiation (111).

The various Ras isoforms have different functions: K-Ras but not H- or N-Ras is required for development, and K-Ras gene knockout is embryonically lethal (132;145). H-, K-, and N-Ras vary in their ability to induce transformation and stimulate cell motility (133). The different Ras isoforms also vary in their ability to efficiently activate downstream effectors, such as Raf-1 and PI3-K. K-Ras appears to be the most effective activator of Raf-1, whilst H-Ras is the least effective. Conversely, H-Ras is more effective as an activator of the PI3-K/Akt pathway (132;133;135;146). It has been reported that Raf-1 is not involved in the activation of MAPK via H-Ras, but that N-Ras modulates activation of this pathway (138). Differences in function, at least in terms of activating effectors, is partly due to compartmentalisation of H-, K- and N-Ras at the PM.

1.8.1.8 Ras and Breast Cancer

Ras is one of the most commonly mutated genes in cancer (147). H-Ras mutations are found in bladder (10%) and kidney (10%) tumours whilst N-Ras is mutated in melanomas (13%), liver cancer (30%) and acute myelogenous leukaemia (30%). K-Ras mutations are seen in non-small cell lung cancer (33%), colorectal cancer (44%) and pancreatic cancer (90%) (145;148). However, less than 5% of breast tumours present with Ras mutations (118). Regardless, overexpression of Ras occurs in 70% of breast

cancers, and this, in combination with upregulation of Ras activity, means Ras still plays a key role in the development and progression of breast cancer (149).

There are two key explanations for the upregulation of Ras activation. Firstly, RTKs are commonly overexpressed in breast tumours. Increased expression of RTKs is correlated with their increased phosphorylation and activation, which results in activation of Ras. Secondly the adaptor protein, Grb2, is overexpressed in breast tumours compared to normal breast tissue (150). This offers an alternative mechanism by which Ras activation might be enhanced.

Overexpression of Ras both at the mRNA and protein level, has been observed in breast tumours (151-153). However, it is still controversial whether overexpression of Ras is associated with a poor or improved prognosis. *In vitro* and *in vivo* studies revealed that the introduction of constitutively activated Ras into human breast cancer cell lines induces cellular transformation and results in the formation of tumours in nude mice. Furthermore, expression of activated Ras in hormone-dependent MCF-7 cells can induce anchorage-independent growth in the absence of hormone. Activated Ras partially mediates hormone-independent tumour growth in nude mice, suggesting Ras activation is a factor in tamoxifen resistance. Overexpression of the Ras/Raf/MAPK pathway is associated with resistance to chemotherapeutic agents in breast cancer cells (154;155).

1.8.2 Raf

Raf proteins were the first identified Ras effectors. There are three Raf isoforms: A-Raf, B-Raf and Raf-1 (C-Raf). *Raf-1* is localised to chromosome 3 (3p25) (156). A *Raf-1* pseudogene is found on chromosome 4 (157). *A-Raf* and *B-Raf* were identified and localised to the X chromosome (Xp11.4-11.2) and chromosome 7 (7q34) respectively

(158;159). The Raf proteins are a family of serine/threonine kinases, which share a similar structure of three conserved regions (CR1, CR2, CR3). The three isoforms vary in size: A-Raf is the smallest at 68kDa (606 amino acids); *B-Raf* is alternatively spliced and yields proteins ranging from 75 to 100 kDa (765 amino acids); and Raf-1 is 74kDa (648 amino acids). Despite a relatively high degree of homology between the three proteins, there are isoform specific functions and tissue expression patterns.

Raf-1 is ubiquitously expressed, whereas A-Raf and B-Raf have more limited expression. A-Raf is highly expressed in urogenital organs and B-Raf in neuronal tissues (160). These isoforms vary in their basal kinase activity and their ability to interact with and be activated by Ras proteins. Each of the Raf proteins performs different functions. A-Raf is essential for intestinal and neurological development; B-Raf controls vascularisation, neuronal survival and suppresses programmed cell death; while Raf-1 stimulates cellular proliferation and tissue formation (114;161-163). Furthermore, unlike Raf-1 and A-Raf, B-Raf is frequently mutated in human cancers (164). However, of the three isoforms, Raf-1 is the most widely studied.

1.8.2.1 Raf-1 Structure

Raf-1 has two domains – an N-terminal regulatory domain and a C-terminal catalytic domain. The conserved regions, CR1 (residues 55-184) and CR2 (residues 254-269), are localised within the N-terminal, whilst CR3 (residues 349-609) is found in the C-terminal. The CR1 region, containing the Ras binding domain (RBD, residues 55-131) and cysteine rich domain (CRD, residues 139-184), is crucial for Raf-1 translocation to the membrane and activation via Ras binding (112;161;165). The CR2, serine/threonine rich region, when phosphorylated regulates localisation and activation of Raf-1 (112).

CR3 is a catalytic kinase domain, with an activation segment whose function is regulated by phosphorylation (112). The N-Region, located before CR3, possesses a negative charge and phosphorylation sites that are crucial for Raf-1 activation (Figure 1.10).

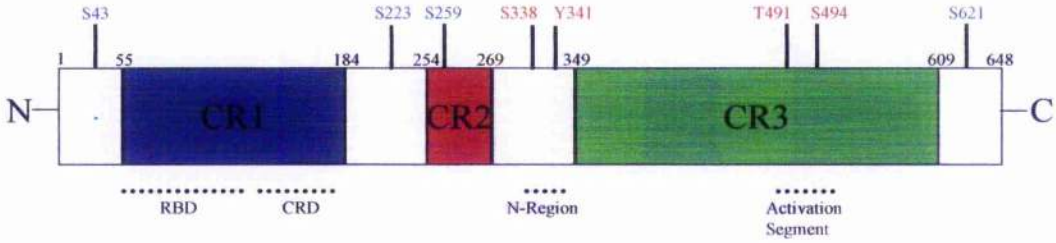

Figure 1.10: Raf-1 Protein Structure
Raf-1 sites highlighted in blue are phosphorylated when Raf-1 is in its inactive form, whereas those sites highlighted in red are phosphorylated when Raf-1 is activated. RBD = Ras Binding Domain, CRD = Cysteine Rich Domain

1.8.2.2 Regulation of Raf-1 by Ras

Raf-1 regulation is dependent on association with activated Ras, interactions with scaffold proteins and key phosphorylation events. However the mechanisms leading to its activation are not completely understood, though binding to Ras is an integral part.

Following RTK activation and transition of Ras-GDP to Ras-GTP, Ras binds Raf-1 and translocates it to the membrane where it can be activated. In order to activate Raf-1, Ras must dimerise (166) allowing Ras to first bind the RBD and then form secondary interactions with the CRD region of Raf-1, via its effector domain (161;167). The CRD negatively controls Raf-1 catalytic activity by interacting with the kinase domain; Ras binding to the CRD overrides inhibition of Raf activity and permits phosphorylation of key sites (114;161). Ras binding also triggers the dephosphorylation of inhibitory sites.

1.8.2.3 Inactive Raf-1: - formation of an auto-inhibitory complex

Inactive Raf-1 is localised to the cytosol, where it forms a multi-protein complex of 300-500 kDa (161). Raf-1 activity is inhibited in the cytoplasm via interactions between the N-terminal regulatory domain and the C-terminal kinase domain. Phosphorylation and association with proteins, such as the heat-shock proteins (Hsp70 and Hsp90) and the dimeric 14-3-3 proteins, also maintain Raf-1 in its inactive form. The Hsps act as chaperones to Raf-1, whilst the 14-3-3 proteins serve to protect Raf-1 from dephosphorylation, and to act as a linker between Raf-1 and other proteins (168). In resting cells, inactive Raf-1 is phosphorylated at three serine sites: S43, S259 and S621 (Figure 1.11) (169). Phosphorylation at S43 prevents the interaction between the effector domain of Ras and Raf-1 RBD (170). Phosphorylation of both S259 and S621 provide docking sites for the 14-3-3 proteins. Binding of 14-3-3 to Raf-1 produces an inactive conformation by bringing the N-terminal domain into contact with the C-terminal (171;172). S259 is a target of both AKT and cAMP activated protein kinase (PKA) (112;173;174). PKA also increases phosphorylation of S43 and S233. This latter site has been identified as a third docking site for 14-3-3 proteins (175).

S259 is a key player in Raf-1 inhibition. Mutations of this residue produce a constitutively active form of Raf-1. Dephosphorylation of S259 is an essential activation step. The binding of Ras to Raf-1 stimulates the dephosphorylation of S259 by destabilising the interaction between 14-3-3 and phospho-S259. Translocation of Raf to the membrane brings it into the vicinity of protein phosphatase 2A (PP2A), which dephosphorylates S259, freeing one arm of the 14-3-3 dimer (176). This enables 14-3-3 to recruit upstream activators and allows the phosphorylation of crucial Raf-1 activation

sites. Only once Raf-1 is dephosphorylated at S259, can it be activated in response to mitogens and other stimuli (Figure 1.11).

1.8.2.4 Activation of Raf-1 mediated by phosphorylation

Raf-1 activation requires phosphorylation of several sites, via direct or indirect signalling from Ras. These include serine-338, tyrosine-341 (upstream of the kinase domain), and threonine-491, serine-494 (within the activation loop) (114;115;161). Of these sites S338 and Y341 are the most studied, and their phosphorylation is required for Raf activation. Mutations of either residue generally render Raf-1 inactive. S338 phosphorylation is induced by growth factors, integrins and Ras, and is a relatively reliable marker of Raf-1 activation. However, debate exists over the kinase(s) responsible for the phosphorylation of S338. It is established that the serine/threonine kinases, PAKs, phosphorylate Raf-1; however, it is thought they do this in a Ras-independent manner (167). It is therefore likely that an unidentified kinase mediates phosphorylation of S338 in a Ras-dependent manner. Phosphorylation of Y341 by Src-family kinases may negate inhibitory effects of the N-terminal on the C-terminal catalytic domain (161).

The final two activating sites, T491 and S494, are located in the activation segment of the CR3 region (167). As with S338, they are both phosphorylated in a mitogen-dependent manner; their mutation prevents Raf activation, although, the kinase that mediates their phosphorylation is unknown. It is speculated that these sites undergo autophosphorylation, in a manner similar to the HERs (177) (Figure 1.11).

1.8.2.5 Regulation of Raf-1 via scaffold proteins

Activation of Raf-1 and the mediation of its effects are also controlled by scaffold proteins. There are scaffold proteins that enhance the effects of Raf-1, such as Sur-8,

KSR (Kinase Suppressor of Ras) and CNK (Connector Enhancer of KSR), whilst those, such as RKIP (Raf Kinase Inhibitor Protein), inhibit Raf-1 signalling. S259 dephosphorylation and the release of one arm of the 14-3-3 dimer enables 14-3-3 to interact with the KSR scaffolding protein. KSR binds MEK and ERK, and links Raf to its downstream substrates (168;178;179). Sur8 complexes with Ras-GTP and Raf-1 and enhances the activation of Raf-1 via EGF and Ras (161). Likewise, CNK binds Raf-1, and with Ras, stimulates Raf-1 activation (177).

RKIP inhibits the Ras/Raf-1/MAPK pathway by binding Raf-1, MEK and MAPK and prevents interaction between Raf-1 and MEK, regardless of Raf-1s activation status (180). Therefore, RKIP prevents activated Raf-1 from stimulating the rest of the kinase cascade. Another important inhibitor of the Raf-1 pathway is Spred, which, through binding Ras, does not prevent Raf translocation to the membrane, but does impede its phosphorylation and activation by an unknown mechanism (167)(Figure 1.11).

1.8.2.6 Negative-feedback regulation of Raf-1

A major point of interest is the termination of Raf-1 activation. The binding affinity that Ras-GTP has for Raf-1 is stronger than that for any other protein with which it interacts, including GAPs. Theoretically this should mean that once Ras-GTP binds Raf-1, this association should be maintained and Ras constitutively activated. However, this is not the case, but the exact mechanism by which Ras dissociates from Raf-1 and Raf-1 activation is inhibited is unknown. Phosphorylation of S43, which prevents interaction between Ras and Raf, is induced by PKA and also growth factors (114). Therefore, growth factors may positively regulate Raf-1 activation via phosphorylation of sites, such as S338, but may also negatively regulate activation by causing Ras to dissociate from

Raf via phosphorylation of S43 (114). However, the kinase that phosphorylates S43 in response to growth factor stimulation is unknown. Downregulation of Raf-1 is also dependent on negative feedback following mitogen stimulation, inhibition of MEK, and MAPK signalling preserved Raf-1 in its active conformation (178;181). Six residues on Raf-1, S29, S43, S289, S296, S301 and S641, become hyperphosphorylated in response to MEK signalling, and this corresponds to Raf-1 inactivation (182). MAPK was identified as the kinase responsible for phosphorylating all sites, bar S43. This study proposed that hyperphosphorylation of Raf-1 induced a conformational change, preventing it from binding to Ras-GTP and responding to growth factor stimulation. Mutations of these residues resulted in increased Ras binding and activation of Raf-1 through phosphorylation of S338. Interestingly, this hyperphosphorylated form of Raf-1 was not a signal for it to be degraded, but rather that it should be recycled into a signalling-competent state ("desensitised"). Raf-1 was maintained in its hyperphosphorylated form for several hours, and it was suggested that all Raf-1 present within the cell, not just the active form, is hyperphosphorylated. PP2A and the prolyl isomerase Pin1 were identified as key proteins responsible for dephosphorylating and inactivating Raf-1, allowing the cycle of activation to begin again (Figure 1.11).

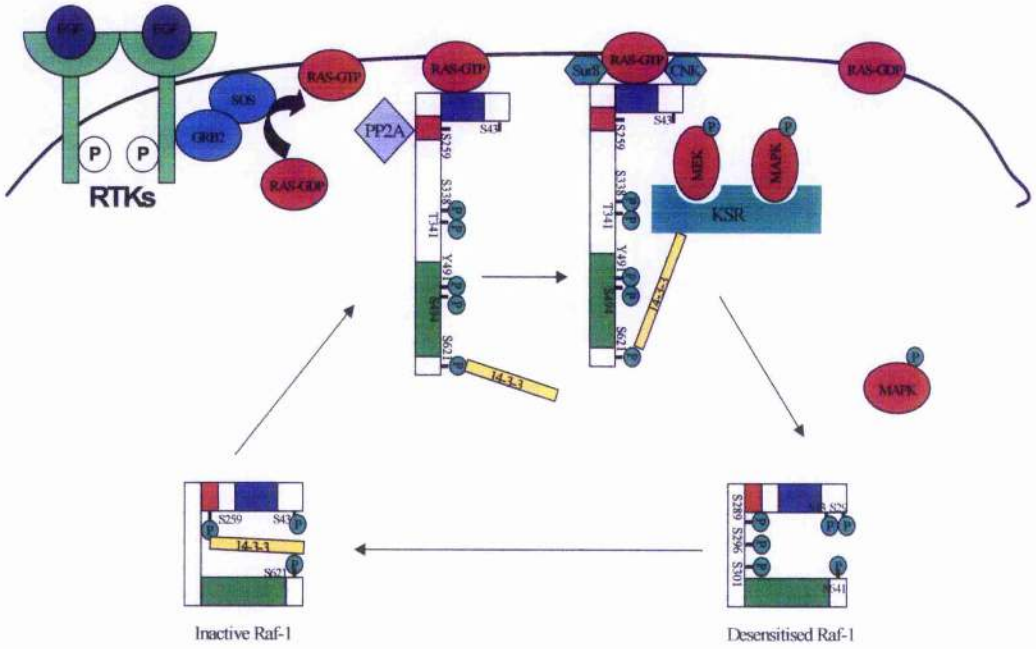

Figure 1.11: Regulation of Raf-1
Raf-1 regulation is dependent on association with activated Ras, interaction with scaffold proteins and key phosphorylation events.

1.8.2.7 Raf-1 Substrates & Function

The most highly characterised substrates of Raf-1 are the dual specific threonine/tyrosine kinases, MEK1 and MEK2. Interestingly, of the three isoforms, Raf-1 is not the most effective activator of MEK1/2: B-Raf binds and phosphorylates MEK1/2 with the most efficiency. B-Raf is the main activator of MEK(177;183); it can phosphorylate MEK1/2 directly, or it can interact with and activate Raf-1, which subsequently phosphorylates MEK1/2. It is now hypothesised that Raf-1 regulates the levels and duration of MEK1/2, activated by B-Raf. MEK1/2 was previously the only identified substrate of Raf-1; however, there is now evidence that Raf-1 can function independently of MEK/MAPK. Raf-1 translocates into the nucleus to bind and phosphorylate the Retinoblastoma (Rb) protein (184), promoting cell cycle progression and proliferation. It is also thought Raf-1 interacts with and phosphorylates Bad, resulting in cell survival (177).

1.8.2.8 Role of Raf-1 in cancer

Due to its key positioning in the MAPK cascade, i.e. downstream of the HERs and upstream of MAPK, and its interactions with other proteins, such as Rb, the activation of Raf-1 is a fundamental step in controlling tumour cell growth, proliferation, apoptosis, metastasis and angiogenesis. Overexpression of HERs, in particular HER2, is associated with a poor outcome in breast cancer patients. This overexpression results in increased activation of Raf-1. HER2, in comparison to EGFR, lengthens the time that Raf-1 is localised to the PM, and prolongs its activation status, enhancing activation of the MAPK cascade (185). This increased activation of Raf-1 via HER2 is perhaps one explanation for the poor prognosis of patients with HER2 overexpressing tumours, and highlights the importance of Raf-1. Down-regulation of Raf-1, using small interfering RNA (siRNA), inhibits tumour growth (186). Raf-1 is not only implicated in the development and progression of breast cancer, but also in the responsiveness of breast tumours to therapies, such as Tamoxifen and chemotherapy.

1.8.3 MEK 1 and MEK2

Mek1 and Mek2 are dual specific threonine/tyrosine kinases. *Mek1* is localised to chromosome 15 (15q21) and *Mek2* to chromosme 7 (7q32). There is approximately 80% homology between the two isoforms. However, there is evidence that the two isoforms have different functions: Mek1 deficient mice die in early gestation while Mek2 deficient mice develop normally (187) . The main activators of Mek1/2 are the Raf kinases (177). However they are also regulated by other kinases, such as MEKK1, Tpl-2 and Mos. Phosphorylation of Mek 1/2 at serine 218 and serine 222, within its activation loop, results in activation. MEK proteins have two consensus kinase motifs, one that regulates

phosphorylation of serine/threonine motifs, and one that controls phosphorylation of tyrosine residues (188). Only MAPK (ERK1 and ERK2) are identified as Mek targets.

1.8.4 MAPK

Several proteins are classified as mitogen activated kinase proteins (MAPKs). These include extracellular regulated kinase 1/2 (ERK1/2, p44/42 MAPK), JNK, p38MAPK and ERK5. However, for the purpose of this thesis, MAPK refers to ERK1/2. *Erk1* is localised to chromosome 16 (16p11.2), whilst *Erk2* is found on chromosome 22 (22p11.2) (189). ERK1 and ERK2 are 44 and 42kDa proline-directed serine/threonine kinases. Both proteins share a high degree of structural and functional similarity.

1.8.4.1 MAPK interaction with MEK

The activation of MAPK is regulated via stimulation of Ras/Raf-1/MEK1/2. MAPK is the only identified effector of activated MEK1/2. However, MEK and MAPK also interact with each other in their inactive forms, via a basic and hydrophobic region within the N-terminal domain of MEK1/2, and several sites within MAPK including a cytosolic retention sequence (CRS) domain, and residues within both the N- and C-terminal domain (190-193). The binding of MEK to MAPK results in the export of inactive MAPK from the nucleus and its retention in the cytoplasm. However, MEK mediated phosphorylation of the Threonine-Glutamine-Tyrosine motif within the activation loop of MAPK (phosphorylation of threonine 202 and tyrosine 204 on ERK1 and threonine 183 and tyrosine 185 on ERK2), results in its activation. This phosphorylation results in approximately 1000-fold increase in the activity of MAPK (194). Furthermore, it causes dissociation from MEK and homo-dimerisation, which facilitates nuclear translocation (195). Phosphorylated MAPK also forms hemi-active dimers with unphosphorylated

MAPK, facilitating the translocation of unphosphorylated MAPK into the nucleus (195). MAPK possess a nuclear export signal (MELDDLPKEKLKEL). However, dimer formation may prevent MAPK nuclear export, as this signal is hidden within the interface of the dimer(195).

MAPK activation results in phosphorylation of more than 50 substrates within the cytosol and nucleus (116;117). MAPK substrates generally contain the consensus sequence, Pro-X-Ser/Thr-Pro. Nuclear substrates include c-Fos and Elk-1. c-Fos, which together with c-Jun, forms AP-1, a transcription factor that regulates early transcriptional events, such as proliferation, differentiation and oncogenic transformation, requires phosphorylation via MAPK to remain in a stabilised state (196). However, MAPK can also promote anti-apoptotic effects through phosphorylation of cytoplasmic substrates, such as p90RSK and BAD (197). Furthermore, cellular response is dependent on the duration of MAPK activation and signalling. Transient activation of MAPK results in an unphosphorylated and unstable form of c-fos, whereas sustained activation leads to p90RSK phosphorylation. This, in combination with MAPK, phosphorylates and stabilises c-fos (198). This generates different biological responses, for example, in PC12 cells, treatment with nerve growth factor stimulates sustained MAPK activation and promotes cell differentiation, whereas treatment with epidermal growth factor results in transient MAPK activity and cell proliferation (199;200).

1.8.4.2 MAPK and the Oestrogen Receptor

ERα is a key substrate of activated MAPK. MAPK directly phosphorylates ERα within the AF-2 domain at S118 (39;201). Residues surrounding S118 comprise the MAPK consensus sequence, Pro-Gln-Leu-Ser-Pro. MAPK also indirectly phosphorylates ERα at

S167 via p90rsk (197). E2 independent phosphorylation of S118 and S167 leads to an increase in the activity of the receptor. Under these circumstances, E2 is not recruited and not required for the activation of the receptor. Phosphorylation of ERα, via MAPK, is rapid and transient in comparison with E2 stimulated phosphorylation (202).

Interestingly, several studies have suggested that the relationship between MAPK and ERα may be even more complex. ERα levels may decrease in response to increasing expression levels of MAPK. Overexpression and increased activation of EGFR/HER2, and subsequently MAPK in ERα positive breast cancer cells, promotes ERα loss and subsequently reduces expression of E2-regulated genes, such as PR (203;204). Furthermore, ERα negative breast tumours tend to present with overexpression of the growth factor receptors and elevated levels of MAPK (203). The relationship between MAPK activation and ERα expression has been examined in MCF-7 breast cancer cells. Several studies have shown that hyperactivation of MAPK results in downregulation of ER levels (205-207). Activation of MAPK in MCF-7 cells corresponds to increased activation of Nuclear Factor-κB, and it is thought that this is partially responsible for the down-regulation of ERα (206). A more recent study suggests that hyper-activation of MAPK in ERα positive cancer cells is a key mechanism in driving the change from an ERα positive to a ERα negative phenotype, and that there is a "hyperactive MAPK signature" set of genes that identify ERα negative tumours (208).

1.8.4.3 MAPK and Breast Cancer

As a result of its role in cell proliferation, differentiation and migration, combined with its relationship with ERα, MAPK has been implicated in the development and progression of breast cancer. *In vitro* studies investigating the effects of MEK inhibitors

revealed that MAPK was associated with cell proliferation and motility in breast cancer cell lines (209;210). Similarly, evidence suggests that MAPK activity is required, not only for the maintained growth of various breast cancer cell lines, but also for their survival (211). The interaction between MAPK and ERα is critical in the progression of tumours. MCF-7 cells, transfected with constitutively active MEK1, displayed increased levels of ER mediated transcription in the presence of low levels of E2. Furthermore, *in vivo* studies highlighted that MEK1 active MCF7 cell tumours were approximately three times larger than the parental MCF-7 cell tumours (212). Breast tumours frequently present with elevated levels of activated MAPK (194). Increased expression of activated MAPK is thought to be associated with breast tumourgenesis and tumour progression. One study showed that approximately 50% of breast cancer patients exhibited an increase in the level of activated MAPK in their primary breast tumours, in comparison with normal breast tissue (213). This study suggested that increased levels of MAPK were associated with tumour metastasis and a poor outcome. This is further supported by another study, indicating that activation of MAPK in tumours is associated with node positive breast cancers, and is linked to a poor outcome (214). However, this relationship is controversial. Studies suggest that activation of MAPK is associated an increased time to patient relapse and improved outcome (215). A recent study indicated that the effect of MAPK activation and expression on patient outcome depended on its subcellular location. Increased expression levels of nuclear MAPK in breast tumours was correlated with a shortened overall survival time, but conversely cytoplasmic expression was associated with an improved outcome, longer disease-free survival time and overall survival time (204).

1.9 The Role of Ras/Raf-1/MAPK in Response to Breast Cancer Treatments

1.9.1 The Ras/Raf-1/MAPK cascade and Tamoxifen resistance

A substantial proportion of the research into the mechanisms driving tamoxifen resistance has focused on the role of the MAPK cascade. One of the outcomes of activation of MAPK is the ligand-independent phosphorylation and activation of the ERα. This ultimately results in the transcription of oestrogen-regulated genes and cell proliferation, which may partially explain the development of Tamoxifen resistance (69;97;107)

Phosphorylation of the AF-1 domain of ERα by kinases, such as MAPK, results in increased interactions with co-activators, rather than co-repressors, and enhances the transcriptional activity of the receptor when bound by Tamoxifen (202). Therefore, this ligand-independent phosphorylation over-rides the antagonistic activity of Tamoxifen and may play an important role in the development of Tamoxifen resistance.

MAPK, in addition to phosphorylating ERα, is able to phosphorylate co-activators, such as SRC-1 and AIB1 (216-218). This enables the co-activator to bind to Tamoxifen-bound ERα and increase ER mediated transcription, and is yet another bypass mechanism of the antagonist effects of Tamoxifen. Furthermore, phosphorylation of the co-repressor, N-CoR, causes it to translocate out of the nucleus, preventing it from inhibiting transcription (202;219) (Figure 1.12).

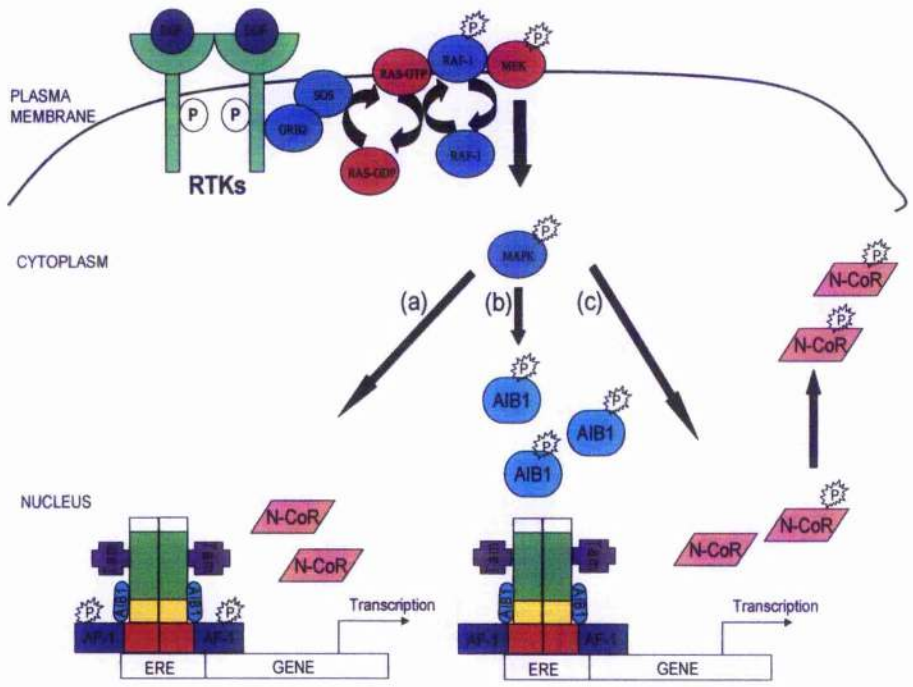

Figure 1.12: Mechanism of Tamoxifen Resistance – Cross talk between growth factor receptors and ER

There is bidirectional cross talk between the growth factor receptors (RTKs) and ERα, and this is thought to be a key mechanism in the development of Tamoxifen resistance. (a) Phosphorylation of the AF-1 domain of the ERα by MAPK, results in increased interactions with co-activators and enhances the transcriptional activity of ERα when Tamoxifen bound. (b)MAPK phosphorylates co-activators, such as AIB1, enabling co-activators to bind to Tamoxifen-bound ERα and increasing ERα mediated transcription. (c) Phosphorylation of the co-repressor, N-CoR, causes it to translocate out of the nucleus, preventing it from binding to ERα and inhibiting transcription. RTKs = Receptor Tyrosine Kinases, Tam = Tamoxifen, ERE = Oestrogen Response Element

In vitro studies have highlighted the importance of growth factor signalling pathways, and in particular MAPK expression and activation, in contributing to the development of tamoxifen resistance. Increased expression of activated Ras induces hormone-independent growth of MCF-7 cells and tumours in nude mice. Constitutive activation of Raf-1 enabled the growth of MCF-7 cells in the absence of oestrogen (220). Analysis of several ERα positive breast cancer cell lines has revealed that increased expression of MAPK is associated with tamoxifen resistance, and that high levels of MAPK support the

growth of these cells during adaptation to long-term oestrogen deprivation (203;221). Tamoxifen-resistant cells also present with elevated levels of phosphorylated EGFR, MAPK and ERα at S118 and S167 (50;222). An immunohistochemistry (IHC) study of clinical breast cancers revealed that approximately 80% of ERα positive patients had an increase in the levels of phosphorylated MAPK in their tamoxifen resistant tumours, in comparison with their tamoxifen sensitive tumour (223). Another study of breast tumours demonstrated that expression of phosphorylated MAPK was associated with a poor response to tamoxifen (224). Increased expression of the activated form of MAPK was observed in the breast tumours of patients who exhibited *de novo* tamoxifen resistance (225). However, contradictory reports suggest MAPK activation is not involved in the development of tamoxifen resistance (212;213), and increased tumour activated MAPK levels are associated with good outcome in tamoxifen treated patients (226).

1.9.2 The Ras/Raf-1/MAPK cascade and Chemotherapy resistance

Failure to respond to chemotherapy is a major clinical problem, and again, the mechanisms underlying the development of resistance to chemotherapeutic agents are not completely understood. The Ras/Raf-1/MAPK pathway is implicated in mediating resistance to chemotherapeutic agents, such as epirubicin and doxorubicin. All research investigating the relationship between the Ras/Raf/MAPK pathway and anthracycline resistance has been performed in cell lines. The role of the MAPK cascade in mediating response to chemotherapy is still controversial. Some studies suggest that increased expression of Raf-1 and MAPK decrease responsiveness to cytotoxic agents and contribute to the development of chemotherapy resistance (227-229). Others suggest that

down-regulation of Raf-1 is linked to paclitaxel resistance, and that MAPK activation promotes cell death in the presence of anthracyclines (230).

1.9.3 Inhibiting the MAPK cascade:- therapeutic implications

The Ras/Raf-1/MAPK pathway is often upregulated in cancer cells, either through mutation or overexpression; hence it represents an appropriate target for anticancer treatments. There are currently drugs that inhibit Ras, Raf-1 and Mek activity, and these, either alone or in combination with other therapies, such as Tamoxifen, offer a possible alternative treatment option for patients.

1.9.3.1 Ras & Therapeutic Implications

As a result of the common occurrence of Ras mutations in human cancers, Ras has become a key therapeutic target. Presently the most effective treatment targeted against Ras are the Farnesyl Transferase Inhibitors (FTIs). FTIs prevent Ras from being farnesylated, thus inhibiting its translocation to the PM and its activation. There are three classes of FTIs: farnesyl pyrophosphate analogues, which compete with the isoprenoid substrates for FT; peptidomimetic inhibitors, which mimic the CAAX motif and compete with Ras for FT; and bisubstrate analogues, which are a combination of the other two (231). Tipifarnib and Ionafarnib are two of the most commonly studied FTIs. Evidence exists that the Ras isoforms have different sensitivities to FTIs. Whilst H-Ras is very sensitive, N-Ras is partially sensitive, and K-Ras is resistant to many FTIs (113;232).

Originally FTIs were designed to combat against Ras mutations; however, they are also effective against wild type Ras. Thus, they are of use in the context of breast cancer. Tipifarnib has been shown to be effective in inhibiting the growth of MCF-7 xenografts (233). It has also been shown that treatment of MCF-7 cells with FTI-277, in

combination with Tamoxifen, is superior to either treatment alone (234). Therefore, since activation of Ras and its signalling pathways is believed to be associated with resistance to treatments, such as Tamoxifen and chemotherapy, it is thought that combined treatment with FTIs might overcome this resistance and improve patient outcome.

1.9.3.2 Raf-1 Inhibitors

The Raf-1 inhibitor, Sorafenib (BAY 43-9006), is a bi-aryl urea that prevents Raf-1 and B-Raf activity (235). It binds to Raf-1 and prevents the activation segment of Raf-1 from binding and phosphorylating downstream substrates (236). BAY 43-9006 exhibits anti-tumour activity in human tumour xenograft models of colon, pancreas, breast and non-small cell lung cancer. In most of these cases, the anti-tumour activity was a consequence of the down-regulation of MAPK activation. BAY 43-9006 is currently in clinical trials.

1.9.3.3 MEK Inhibitors

The specificity of the interaction between MEK1/2 and MAPK means that MEK1/2 represents an ideal target for inhibition of the MAPK cascade. Two of the first MEK inhibitors were PD98059 and U0126. Both these compounds down-regulated MAPK activation and reduced cellular proliferation and activation of MAPK regulated proteins in multiple cancer cell lines (237-239). Unfortunately, neither PD98059 nor U0126 were suitable for clinical testing; hence PD184352, an orally active Mek1/2 inhibitor, was synthesised (240). The binding of inhibitor induces conformational changes in the unphosphorylated form of MEK1/2, rendering it inactive. It is also thought that, whilst in this inactive form, it is insensitive to upstream kinases (241). PD184352 reached phase II trials; however, the results were slightly disappointing. Consequently, a second-generation MEK inhibitor, PD0325901, has been synthesised and shown to have anti-

tumour activity in a range of human tumour grafts (242). It is now currently under testing in phase1/II trials.

It is thought that the use of MEK inhibitors will be most beneficial in combination with cytotoxic agents, such as cisplatin and paclitaxel, to induce apoptosis (242). An *in vitro* study of MCF-7 and MDA-MB-231 cells revealed that treatment with docetaxel was more effective in the presence of U0126 (243). Likewise, if these inhibitors downregulate MAPK activity, they might be of particular use in overcoming the effects of MAPK mediated tamoxifen resistance.

1.10 Statement of Aims

The research presented in this thesis investigated the role of the Ras/Raf-1/MAPK pathway in the development and progression of breast tumourigenesis. Using breast tumours from three different patient cohorts and an immunohistochemical approach, expression of Ras, Raf-1 and MAPK proteins was determined. The various studies tested the hypothesis that increased expression and activation of the components of this pathway in breast tumours, was linked to clinical parameters, such as disease-free and overall survival. Additionally it was speculated that increased expression and activation of the Ras pathway in breast tumours was associated with poor response to tamoxifen and chemotherapy treatment regimes, and this theory was also explored.

As the ligand-independent activation of ERα is believed to be a key step in the development of tamoxifen resistance, the relationship between the Ras/Raf-1/MAPK pathway and ERα was scrutinised. *In vitro* studies were designed in order to compare the effects of E2-dependent versus ligand-independent phosphorylation and activation on the

localisation of ERα. Particular attention was paid to the interaction between MAPK and ERα.

Ultimately the goal of this research was to try and further our understanding of the mechanisms that drive the development of resistance to tamoxifen and chemotherapy in breast cancer patients.

Research Aims

- To determine the levels of Ras and Raf-1 proteins in breast tumours, from a cohort of ER positive and negative patients, and to investigate if protein expression is associated with patient outcome. (Pilot Study)
- To investigate the localisation of Ras proteins in breast tumour cells.
- To determine if increased expression of Ras and Raf-1 is a consequence of gene amplification.
- To determine the levels of Ras, Raf-1, and MAPK proteins in breast tumours, from a cohort of ER positive patients treated with Tamoxifen, and to investigate if increased expression and activation of the Ras pathway is a key mechanism in the development of Tamoxifen resistance.
- To determine the levels of Raf-1 and MAPK proteins in breast tumours, from a cohort of ER positive/negative patients treated with chemotherapy, and to investigate if Raf-1 and MAPK mediate response to chemotherapy.
- To compare the ligand-dependent and ligand-independent phosphorylation and activation of ERα in breast cancer cells.
- To investigate the interaction between MAPK and ERα in breast cancer cells.

2. Materials & Methods

2.1 Patient Cohorts

2.1.1 Pilot Study

This patient cohort was comprised of 206 breast cancer patients treated at Glasgow Royal Infirmary between 1984 and 1993. Patients were selected randomly for inclusion in this study. Consequently these patients represented both ER positive and negative breast cancers, and the treatment regimes varied. Treatment included radiotherapy (37.4% patients), chemotherapy (13.8%), and tamoxifen (74.4%). Clinical and pathological characteristics, including ER status, grade, nodal status, histology, tumour size, NPI and age, are shown in Table 2.1. There were 98 breast cancer specific deaths and 80 breast cancer relapses. Ethical approval was obtained from the Glasgow Royal Infirmary Local Research Ethics Committee.

		Number/Total	%
ER Status	-ve	78/175	44.6
	+ve	97/175	55.4
	Unknown	31	
Histology	Ductal	182/202	90.1
	Lobular	14/202	6.9
	Other	6/202	3.0
	Unknown	4	
Grade	1	30/200	15
	2	75/200	37.5
	3	95/200	47.5
	Unknown	6	
Nodal Status	0	88/176	50.0
	1-3	54/176	30.7
	4+	34/176	19.3
	Unknown	30	
NPI	<3.5	78/170	45.9
	3.5-4.5	54/170	31.8
	4.5	38/170	22.3
	Unknown	36	
Size	T1 (<20mm)	44/198	22.2
	T2 (20-50mm)	130/198	65.7
	T3 (>50mm)	24/198	12.1
	Unknown	8	
Age	<50 years	15/198	7.6
	>50 years	183/198	92.4
	Unknown	8	

Table 2.1: Pilot Study Patient Clinical & Pathological Variables

ER = Oestrogen Receptor. Tumours were considered ER positive if ≥10% nuclei were stained at any intensity. Grade = Bloom and Richardson grade; Nodal Status = Number of positive nodes; Pathological Type: Ductal = invasive ductal carcinoma; Lobular = invasive lobular carcinoma; Others include three medullary, one mucoid, one squamous and one tubular carcinomas.

2.1.2 Steroid Resistant Tumour Bank (STB) Study

This cohort was retrospectively selected from patients presenting with operable breast cancer at the Glasgow Royal Infirmary between the years 1980 and 1999. Initially six hundred and eighty six ER positive or ER unknown patients who had undergone adjuvant treatment with tamoxifen were selected. However, the number of patients was reduced to four hundred and fifty six, as a result of incomplete follow-up (n=52, 8%), or unavailable tissue blocks, or blocks with insufficient tissue, as judged by a pathologist (n=177, 26%). There was no significant difference between the final data set of 456 patients and the original cohort, in terms of patients' age, tumour size, grade or nodal status. Additionally, immunohistochemical staining for ER was performed. Tumours were considered ER positive if ≥10% nuclei were stained at any intensity. 402/ 456 patients had ER positive breast tumours, while 20 had ER negative tumours. For 34 cases there was insufficient material for ER IHC. For all studies only the 402 ER positive cases were analysed.

All 402 patients received adjuvant tamoxifen for a median of 5 years (range 0.03-16 years), and follow-up data was available for a median of 6.45 years (range 0.11-18.42 years). In addition to receiving tamoxifen, 99 patients (24.8%) received chemotherapy (three unknown), whilst 110 patients (27.5%) received radiotherapy (three unknown). Information regarding the clinical and pathological characteristics of these patients, such as age at diagnosis, nodal status, tumour histology, size and grade was also available, and is shown in Table 2.2. There were 74 breast cancer specific deaths and 112 breast cancer relapses, 85 of which occurred during tamoxifen treatment. This allowed for survival analysis in terms of disease free-survival, recurrence whilst on tamoxifen and overall

survival. Ethical approval was obtained from the local research ethics committee. Miss Sian Tovey was responsible for establishing this database and performing the ER IHC.

2.1.3 NEAT Study

The Scottish Cancer Trials Breast Group in conjunction with the CRC Trials Unit established the second group of patients. All the women were part of the Scottish NEAT (National breast cancer study of Epirubicin & CMF versus classical CMF Adjuvant Therapy – Study Number BR9601) clinical trial designed to compare the effects of Cyclophosphamide, Methotrexate and 5-Flourouracil (CMF) alone against that of sequential Epirubicin followed by CMF as adjuvant chemotherapy in women with early breast cancer. The primary objectives were to compare the effects of both treatments on patients, disease-free and overall survival time. The study included women with early breast cancer, with between 4 and 9 positive nodes, though other patients were still eligible if their clinician deemed them suitable for chemotherapy treatment.

Eligible patients were randomly selected for treatment with 4 cycles of epirubicin, followed by 4 cycles of CMF given intravenously every three weeks or treatment with 8 cycles of classical CMF given intravenously every three weeks. In total 318 patients were included in our study. 155 (48.74%) of these patients received the combination treatment of Epirubicin and CMF, while the remaining 163 (51.26%) received only CMF. In addition, 224 (70.44%) received hormone therapy, whilst 255 (80.19%) also received radiotherapy.

For these patients there was a median follow up of 4.95 years (range 0.27-8.52 years). Details regarding the clinical and pathological characteristics of these patients, such as the patient's age, tumour size, grade, ER and nodal status, were also available and

are listed in Table 2.2. In this study there were 84 breast cancer related deaths and 111 breast cancer recurrences (local and distant recurrences).

		STB Patients		McNEAT Patients	
		Number/total	%	Number/Total	%
Histology	Ductal	322/397	81.1		
	Lobular	45/397	11.3		
	Other	30/397	7.6		
	Unknown	5			
Grade	1	99/391	25.32	20/305	6.55
	2	193/391	49.36	100/305	32.79
	3	99/391	25.32	185/305	60.66
	unknown	11		13	
Nodal status	0	193/369	52.3	43/313	13.74
	1-3	107/369	29.0	176/313	56.23
	4+	69/369	18.7	94/313	30.03
	unknown	33		5	
Size	T1 (<20mm)	154/380	40.53	94/308	30.52
	T2 (20-50mm)	204/380	53.68	203/308	65.91
	T3 (>50mm)	22/380	5.79	11/308	3.57
	unknown	22			
NPI	<3.5	128/344	37.21	65/311	20.9
	3.5-4.5	106/344	30.81	148/311	47.59
	4.5+	110/344	31.98	98/311	12.86
	Missing	58		7	
Age	<50 years	73/401	18.2	90/318	28.3
	>50 years	328/401	81.8	228/318	71.7
	Missing	1			
ER Status	+ve	402/402	100.0	174/278	62.59
	-ve			104/278	37.41
	Unknown			40	
Treatment	Epi & CMF	n/a		155/318	48.74
	CMF Alone	n/a		163/318	51.26

Table 2.2: STB & NEAT study patient clinical & pathological characteristics

*Grade = Bloom and Richardson grade, Nodal status = number of positive nodes, NPI = Nottingham Prognostic Index = grade+nodal status+0.02*size in mm. Age = age at diagnosis. ER = Oestrogen Receptor. Tumours were considered ER positive if >10% nuclei were stained at any intensity.*

2.2 Immunohistochemistry

2.2.1 Pilot Study

Immunohistochemistry allows for the detection of a cellular protein or other antigen within cells and tissues using an antibody specific for the desired antigen. The low abundance of many intracellular proteins means that in most cases the signal generated by the "primary" antibody (which binds directly to the target molecule) is "amplified", using an indirect immunohistochemical approach. This involves using a second or "secondary" antibody, labelled with either a visible marker (fluorochrome) or an enzyme, that binds to the primary antibody bound to the antigen. This indirect approach generates an amplified signal. The method for investigating the expression of the Ras and Raf-1 proteins in breast tumour tissue used the LSAB (labelled streptavidin-biotin) visualisation kits. This method relies on the high affinity that avidin has for biotin. Firstly a biotinylated link antibody, which recognises the primary antibody, is applied to the tissue, followed by streptavidin labelled with peroxidase (HRP), which binds to the biotin. This peroxidase then reacts with diaminobenzidine (DAB) to produce an insoluble brown precipitate, which represents the target antigen (Figure 2.1).

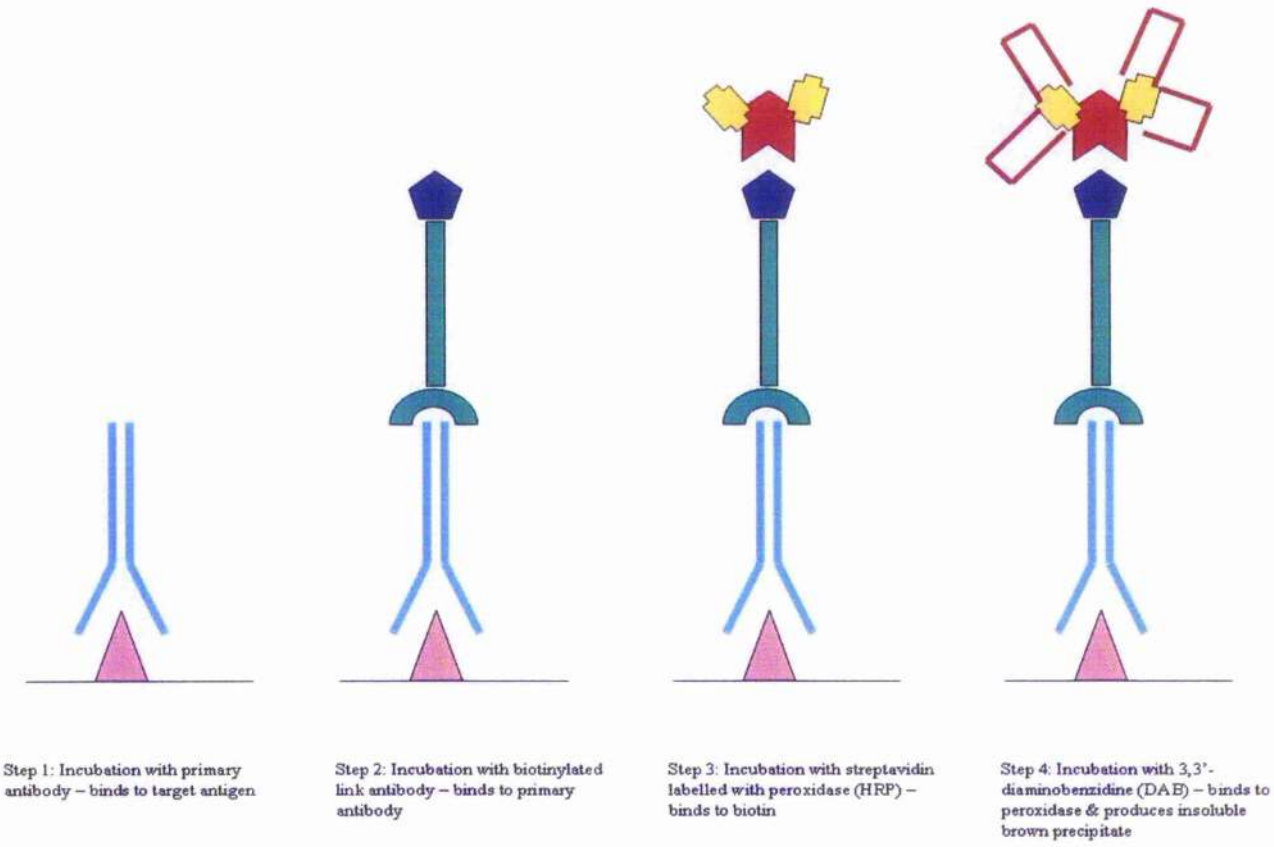

Figure 2.1: Pilot Study Indirect Immunohistochemistry Method

Schematic representation of the indirect immunohistochemistry method used in the pilot study to amplify the signal generated by the primary antibody. This method relies on the high affinity that avidin has for biotin.

- **Tissue Preparation and Dewaxing/ Dehydration**

The tissue specimens were formalin-fixed and embedded in wax and 3-4μm sections were cut and mounted on 3-aminopropylethoxysilane coated slides. Prior to immunohistochemical staining, tissue sections were dewaxed and rehydrated through a series of xylene (2x2minutes) and alcohol (100%(2x2minutes), 90%(1x2minutes), 70%(1x2minutes)) washes.

- **Antigen Retrieval**

As a result of formalin-fixation and wax embedding, the antigen under investigation may lose its immunoreactivity, thus either binding weakly to the appropriate primary antibody or not at all. This is due to the formation of methylene bridges during fixation, which cross link proteins and therefore mask antigenic sites. Thus, it was necessary to include an antigen retrieval step, to break the protein cross-links and expose the antigenic binding site, in order to optimise immunohistochemical staining. Two different heat mediated methods of antigen retrieval were used for the antigens studied. The first involved incubating the tissue sections in 10mM citrate buffer (1:10 dilution of Epitope Retrieval Buffer, DAKO) for twenty minutes at 96°C in a water bath, followed by a twenty minute cool down period. The alternative method heated tissue sections under pressure in 1L of TE buffer (1mM EDTA (Sigma), 5mM Tris (VWR), pH 8.0) for five minutes in a microwave, again followed by a twenty minute cool down period (Table 2.3).

- **Reduction of background staining: - Blocking steps**

Peroxidase reacts with diaminobenzidine, therefore the presence of endogenous peroxidase activity in tissues is a common problem in IHC since it is a cause of background staining. Endogenous peroxidase activity was blocked by incubating the slides in 0.3% hydrogen peroxide (H_2O_2) (VWR) for twenty minutes, followed by a wash in water. A further cause of background staining is the formation of hydrophobic bonds between immunoglobulins and tissue proteins that results in the primary and secondary antibodies binding non-specifically to the tissue section rather than just the target antigen. To reduce this non-specific binding, tissue sections were incubated in 1.5% normal horse serum (Vector Laboratories) in antibody diluent (DAKO). Just as excess peroxidase

produces high levels of background staining, so too does the presence of endogenous biotin since the streptavidin labelled with peroxidase would be able to bind directly to the tissue in addition to the target antigen. Breast tissue generally expresses elevated levels of biotin protein in comparison with other tissues and this in addition to the inclusion of a severe antigen retrieval step often results in false positive staining. Hence a further biotin blocking step (Avidin/Biotin Blocking Kit – Vector Laboratories) was required. This involved pretreating the slides with Avidin D solution for fifteen minutes, to bind any excess biotin on the tissue section. Slides were washed for five minutes in TBS buffer (0.1M Tris/HCl, 1.5M NaCl, pH 7.4) followed by incubation with the biotin solution for fifteen minutes, to block the remaining biotin sites on the avidin. Finally slides were washed in TBS buffer for five minutes before incubation with the desired antibody.

- **Incubation with Primary Antibody**

In this study antibodies for the following proteins were used: H-Ras, N-Ras, Pan-Ras (Pan-Ras Ab and RasAb-1) and Raf-1. For each, a dilution series was performed, investigating various antibody titrations, incubation times and temperatures, to establish the optimal conditions in which to achieve the highest quality of staining, i.e. strongest specific antigen staining with the lowest non-specific background. The required concentration and incubation time for each antibody is recorded in Table 2.3.

- **Quality Assurance**

It was essential to have both a positive and negative control each time IHC was performed. The positive control confirmed that the chosen IHC method was working whilst the negative control checked the specificity of the antibody involved. Tonsil tissue, placenta tissue or breast tissues previously shown to have strong expression of the desired

antigen were incubated with the appropriate antibody and used as positive controls. The same tissues were used for negative controls by treating them with a negative isotype matched control reagent (DAKO).

- **Incubation with Secondary Antibody**

Following incubation with antibody or negative control, the slides were thoroughly washed in TBS buffer for five minutes. Detection of the proteins within breast tissue required binding the primary antibody to a biotinylated secondary antibody, which would then bind to peroxidase-conjugated streptavidin molecules. The visualisation of the antigen occurred via a colour reaction. A substrate chromagen binds to the peroxidase molecules producing a brown coloured product, corresponding to the protein being investigated. In order to do this the DAKO LSAB+ Kit, Peroxidase was utilised. The slides were firstly incubated with Link solution (biotinylated secondary antibody) for thirty minutes at room temperature. Next, the slides were washed in TBS buffer for five minutes and then incubated in the Streptavidin Peroxidase solution for one hour. Slides were then washed in TBS for five minutes.

- **Detection & Visualisation**

The chromagen used for staining the tissue sections was 3,3'-diaminobenzidine (DAB) – (5ml distilled water (dH_2O), 2 drops of buffer solution, 4 drops of DAB stock solution, and 2 drops of Hydrogen Peroxidase solution -Vector Laboratories). Slides were incubated with DAB for five to ten minutes to allow brown staining to develop and were then washed in water for ten minutes.

- **Counterstaining**

Tissue sections were counterstained with haematoxylin and Scott's Tap Water Substitute (S.T.W.S). Slides were immersed in the haematoxylin for approximately thirty seconds, until a red colour was produced in the tissue section; if the tissues appeared to be too red the slides were dipped in acid alcohol to remove some of the colouring. Following this they were then submerged in S.T.W.S for another thirty seconds, to produce a blue colour, in contrast to the brown positive staining of the antigen. The last steps involved dehydrating the tissues through a series of alcohol washes: (70% (1x1min), 90% (1x1min), 100%(2x1min)) and xylene (2x1min), and then mounting the slides onto coverslips using DPX mountant (Dibutyl Phthalate containing Xylene).

Detection of all the proteins, with the exception of Raf-1, was performed as described above. Raf-1 was detected using the Super Sensitive Non-Biotin HRP Detection System (BioGenex, CA, USA). Following antigen retrieval, peroxidase activity was blocked by incubating slides in 3% hydrogen peroxide (H_2O_2) (VWR) for twenty minutes, followed by a wash in water. Tissue sections were then incubated in 1.5% normal horse serum (Vector) in antibody diluent (DAKO), washed in TBS and incubated with the Raf-1 antibody. Afterwards slides were washed in TBS for five minutes and treated with SuperBlock reagent for twenty minutes at room temperature. Sections were then rinsed in TBS for five minutes before being incubated with Poly-HRP reagent for thirty minutes at room temperature. Finally slides were washed three times in TBS for five minutes and then treated with Substrate Solution (one drop (38µl) of DAB Chromagen mixed with

1ml of Substrate Buffer) for ten minutes until brown staining developed. Lastly slides were washed in water for ten minutes. Tissue sections were then counterstained and mounted as described above.

Protein	Antibody	Antigen Retrieval	H_2O_2 Conc^n	Antibody Conc^n	Incubation Time & Temperature
H-Ras	H-Ras Mouse Monoclonal IgG_1 Ab, F235, Santa Cruz	TE Buffer	0.3%	20µg/ml	Overnight at 4°C
N-Ras	N-Ras Mouse Monoclonal IgG1 Ab, F155, Santa Cruz	TE Buffer	0.3%	20µg/ml	Overnight at 4°C
Pan-Ras	Pan-Ras Mouse Monoclonal IgG_{2b} Ab, F132, Santa Cruz	Citrate Buffer	0.3%	20µg/ml	Overnight at 4°C
Pan-Ras	Ras Ab-1 Rabbit Polyclonal IgG_1 Ab, Neomarkers,	Citrate Buffer	0.3%	20µg/ml	30 minutes at room temperature
Raf-1	Raf-1 Mouse Monoclonal IgG1 Ab, E-10, Santa Cruz	TE Buffer	3.0%	5µg/ml	Overnight at 4°C

Table 2.3: Pilot Study Antibody Information

Details of the antibodies used in the pilot study to detect H-Ras, N-Ras, Pan-Ras and Raf-1 proteins. Information regarding the antibody source, antigen retrieval method, concentration and incubation time required are all recorded.
TE Buffer = heating under pressure in 1mM EDTA, 5mM Tris buffer, pH 8.0 for 5 minutes in a microwave, Citrate Buffer = incubation in 10 mM citrate buffer at 96C for 20 minutes. 1.5% Horse Serum blocking reagents was used for all five antibodies

2.2.2 Histoscore Method (Pilot Study)

Two observers, John Bartlett and myself, independently scored all the tissue sections for cytoplasmic and nuclear staining, using a semi-quantitative weighted histoscore method (244). The intensity of staining was categorised as negative (0), weak (1), moderate (2)

and strong (3) and the percentage of tumour cells within each category estimated (Appendix 1 & 2). The histoscore was calculated using the following formula:

Histoscore = 0 x % negative tumour cells + 1 x % weakly stained tumour cells + 2 x % moderately stained tumour cells + 3 x % tumour cells stained strongly

The histoscore ranged from a minimum of zero to a maximum of 300. Agreement between the two observers was monitored. Results were considered discordant if the scores differed by more than 50. These cases were re-evaluated by both observers. Both intra- (variation in individual scoring) and inter- (variation between two observers) class correlation coefficients were calculated (245). Agreement was considered excellent if an ICCC score greater than 0.7 was obtained. Comparison of both LM and JB scores showed that agreement between observers was excellent with ICCC scores between 0.76-0.91. Intra- and inter- class correlation coefficients are shown in Table 2.4.

Protein	Cytoplasmic Scoring	Nuclear Scoring
H-Ras	0.91	0.86
N-Ras	0.82	0.76
Pan-Ras	0.85	0.80
Ras Ab-1	0.82 0.87*	0.88 0.82*
Raf-1	0.73	0.73

Table 2.4: Pilot Study Inter- & Intra*- class correlation coefficients (ICCC)

*Two observers, JB & LM, independently scored breast tissue sections for cytoplasmic and nuclear staining, for H-Ras, N-Ras, Pan-Ras, Ras Ab-1 & Raf-1, using a semi-quantitative weighted histoscore method. Agreement between scores was measured using inter-class correlation coefficients. The intra-class correlation coefficient (variation between individual scorer (myself)) for Ras Ab-1 is shown. The inter-class correlation coefficients for all antibodies are listed in the table. Agreement was considered excellent if an ICCC score was above 0.7. *Intra-class correlation coefficient for Ras Ab-1.*

2.2.3 Tissue MicroArray Construction (STB & NEAT Study)

As a result of the large number of patients in both the STB and NEAT cohorts, it was deemed more appropriate to construct tissue microarrays (TMAs) rather than use whole

tumour tissue sections. Construction of the arrays involved haematoxylin and eosin staining of tissue sections to identify areas of tumour. A pathologist identified tumour areas, and subsequently cores of breast tumour were removed from the designated areas and transferred to recipient paraffin blocks to form the tissue arrays.

For the STB study three 0.6mm^2 cores were removed from each breast tumour to form five different TMAs (TMA A = 100 cores, TMA B = 119 cores, TMA C = 100 cores, TMA D = 60 cores & TMA E =77 cores), each in triplicate. To each of the TMAs, cores of smooth muscle, normal breast, skeletal muscle, lung, skin, testes, prostate, lymph node, placenta and tonsil were added as controls. Each triplicate TMA was constructed from cores from different areas within the same tumour in order to achieve the most accurate representation of the whole tumour section. The use of replicate TMAs also meant that it was more likely that results could be obtained for all cases, since there were three chances of having informative cores.

For the NEAT study three arrays (TMA 1 =117 cores, TMA 2 = 100 cores, TMA 3 = 101 cores) were constructed in quadruplicate from the 318 breast tumours; however, for analysis only three of each arrays were used.

There are several advantages to using arrays as opposed to whole tissue sections. Firstly it is an invaluable way of saving scarce human tissue for research. If whole sections were used only a limited number of studies could be performed, whereas the use of TMAs significantly increases the availability of this resource. Secondly the use of TMAs is far more economical in terms of time and finance. Lastly the use of TMAs enables experimental uniformity since all experiments can be performed on all the

tumour tissue at the same time, which would be highly unlikely in the case of whole tumour tissue sections.

2.2.4 Immunohistochemistry on STB & NEAT TMAs

The same principle as described in section 2.2.1 applies to both the STB and the NEAT study. In the STB study expression and activation of the components of the Ras/Raf/MAPK pathway were investigated: H-Ras, K-Ras, N-Ras, Raf-1, phospho-Raf(ser259), phospho-Raf(ser338), p44/42MAPK and phospho-p44/42MAPK(thr202/tyr204). Whereas in the NEAT study only expression levels of phospho-Raf(ser259), phospho-Raf(ser338), p44/42MAPK and phospho-p44/42MAPK(thr202/tyr204) were examined.

From each of the TMA blocks, 3-4μm thick paraffin wax sections were cut and mounted on 3-aminopropylethoxysilane coated slides. The same basic IHC protocol described in section 2.2.1 was used; however, the signal visualisation steps were different. Slides were dewaxed and rehydrated and antigen retrieval performed. Endogenous peroxidase activity in the tissue was blocked with hydrogen peroxide and non-specific staining reduced by incubating sections in either 1.5% normal horse serum in antibody diluent or Casein (Vector Laboratories) solution. Slides were then incubated with the appropriate antibody. Table 2.5 includes details of the antigen retrieval method, H_2O_2 concentration, blocking solution, antibody concentration and incubation conditions required for each of the proteins investigated.

In the previous protocol the Labelled StreptAvidin Biotin (LSAB) based method was used to visualise the antigens; however, for immunohistochemical staining of the TMAs the Envision system (DAKO) which involves dextran polymer technology was

used. This system enables a large number of enzyme molecules such as horseradish peroxidase to bind to the secondary antibody via a dextran backbone (Figure 2.2). The advantages of this include increased sensitivity and reduced non-specific background staining. The additional biotin-blocking step that was compulsory in the LSAB method was not required when using Envision. The Envision detection method was used for all antigens except K-Ras, which required use of the Super Sensitive Non-Biotin HRP Detection System (as described in section 2.2.1).

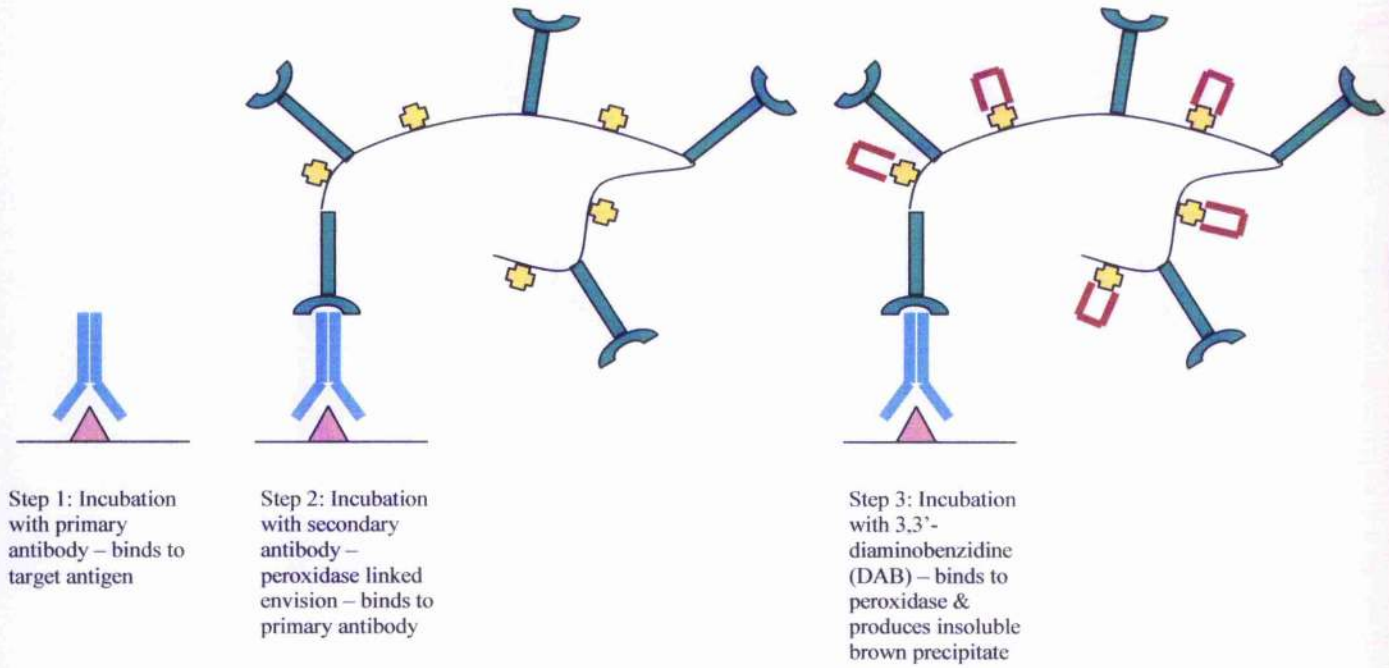

Figure 2.2: Immunohistochemistry Method Using Envision

Schematic representation of the indirect immunohistochemistry method used in the STB and NEAT study to amplify the signal generated by the primary antibody. This method used the Envision system (DAKO), which involves dextran polymer technology. This system enables a large number of enzyme molecules such as horseradish peroxidase to bind to the secondary antibody via a dextran backbone.

Having been incubated with antibody, slides were washed with TBS for five minutes before being treated with Envision solution for thirty minutes at room temperature. Slides were then washed in TBS for five minutes and treated with DAB chromagen (Substrate buffer and DAB+ Chromagen were mixed in a ration of 50:1) (DAKO) for ten minutes to allow brown staining of the antigen to develop. Slides were washed in water for ten minutes and tissue nuclei counterstained with haematoxylin before being dehydrated through a series of alcohol and xylene washes. Slides were then mounted onto coverslips using DPX.

Protein	Antibody	Antigen Retrieval	H_2O_2 Conc[a]	Blocking Solution	Antibody Conc[b]	Incubation Time & Temperature
H-Ras	H-Ras Mouse Monoclonal IgG_1 Ab, F235, Santa Cruz,	TE Buffer	0.3%	1.5% normal horse serum	20µg/ml	Overnight at 4°C
K-Ras	K-Ras Mouse Monoclonal IgG2κ Ab clone 234-4.2 Sigma,	TE Buffer	3.0%	Casein solution	20µg/ml	Overnight at 4°C
N-Ras	N-Ras Mouse Monoclonal IgG1 Ab, F155, Santa Cruz,	TE Buffer	0.3%	1.5% normal horse serum	20µg/ml	Overnight at 4°C
Raf-1	Raf-1 Mouse Monoclonal IgG1 Ab, E-10, Santa Cruz,	TE Buffer	0.3%	1.5% normal horse serum	5µg/ml	Overnight at 4°C
pRaf(ser259)	pRaf(ser259) Rabbit Polyclonal Cell Signaling Technology,	Citrate Buffer	0.3%	Casein solution	4µg/ml	Overnight at 4°C
pRaf(ser338)	pRaf(Ser338) Mouse Monoclonal Upstate	Citrate Buffer	0.3%	Casein solution	4µg/ml	Overnight at 4°C
p44/42 MAPK	p44/42 MAPK Rabbit Polyclonal Cell Signaling Technology,	Citrate Buffer	0.3%	1.5% normal horse serum	0.5µg/ml	Overnight at 4°C
Phospho-p44/42 MAPK	p44/42MAPK (Thr202/Tyr204) Rabbit Polyclonal Cell Signaling Technology,	Citrate Buffer	0.3%	1.5% normal horse serum	0.5µg/ml	Six hours at room temperature

Table 2.5: STB & NEAT Study Antibody Information

Details of the antibodies used in the STB and NEAT study to detect H-Ras, N-Ras, K-Ras, Raf-1 and MAPK proteins. Information regarding the antibody source, antigen retrieval method, blocking reagents and concentration and incubation time required are recorded. All the listed antibodies were used in the STB study, but only pRaf(ser259), pRaf(ser338), MAPK and pMAPK(thr202/tyr204) were used in the NEAT study.

TE = heating under pressure in 1mM EDTA, 5mM Tris buffer, pH 8.0, for 5 minutes in a microwave, Citrate = incubation in 10 mM citrate buffer at 96°C for 20 minutes.

2.2.5 Histoscore Method (STB & McNEAT Study)

The same semi-quantitative histoscore method described in section 2.2.2 was used for scoring cytoplasmic and nuclear staining within tumour cores. Since TMAs were made in triplicate, the final histoscore for each tumour was based on the average score from all available core scores. I scored all tumour cores, whilst 10% of cores were double scored by Dr. Tove Kirkegaard. As before, agreement between the two observers was monitored, and results were considered discordant if the scores differed by more than 50. These cases were re-evaluated by both observers. Agreement was considered excellent if an ICCC score greater than 0.7 was obtained. Comparison of both LM and TK scores showed that agreement between observers was excellent with ICCC scores between 0.75-0.97. Table 2.6 lists the inter-class correlation coefficients for all antibodies for the STB and the NEAT study.

Protein	Cytoplasmic ICCC	Nuclear ICCC
H-Ras	0.91	0.91
N-Ras	0.87	0.75
K-Ras	0.83	0.89
Raf-1	0.89	0.78
pRaf(ser259)	0.92	0.84
PRaf(ser338)	0.86	0.83
MAPK	0.96	0.88
pMAPK	0.88	0.87

Table 2.6: Inter-class correlation coefficients for STB & NEAT studies

Two observers, LM & TK, independently scored breast tumour cores for cytoplasmic and nuclear staining, for H-Ras, N-Ras, K-Ras, Raf-1, pRaf(ser259), pRaf(ser338), MAPK & pMAPK using a semi-quantitative weighted histoscore method. Agreement between scores was measured using inter-class correlation coefficients. The ICCC scores for all antibodies are listed in the table. Agreement was considered excellent if an ICCC score was above 0.7.

2.3 Statistical Analysis for Immunohistochemistry Studies

Statistical analysis was performed using the SPSS statistical package (version 9.0 for Windows). Basic descriptive statistics were performed to calculate the frequencies, mean,

median and inter-quartile ranges for the histoscores for each antibody. These values were then used to establish appropriate cut-off points to define tumours as either low or high expressers of the desired protein.

Correlations between a protein's expression level in the various subcellular compartments and associations between the expression of different proteins were calculated using the Spearman Rank Correlation Test. Pearsons chi-square test was used to correlate protein expression with known prognostic factors, namely tumour size, grade, ER and nodal status.

Kaplan-Meier life-table analysis and Cox's multiple regression (multivariate analysis) were performed to estimate differences in breast cancer related survival, in terms of disease-free survival (DFS), overall survival (OS) and recurrence whilst on tamoxifen (ROT – possible for the STB study only), due to the decreased or increased presence of the protein of interest in patients tumours. Multivariate analysis combined the biological marker of interest with tumour size, grade, ER and nodal status to establish if it was independent of these known predictive markers in influencing patient outcome.

For survival analysis and chi-square tests, patients were split into two groups, those whose tumours expressed high levels of protein and those whose expressed low levels. To establish the relative risk of a patient relapsing or dying as a result of either high or low levels of a particular protein in their breast tumour, hazard ratio analysis was performed.

2.4 Fluorescence In-Situ Hybridisation (FISH)

Fluorescence *In Situ* Hybridization (FISH) is a technique that uses fluorescently labelled DNA probes to visualise gene or chromosome abnormalities. FISH probes are single stranded DNA that can bind to the complimentary DNA strand on the gene/chromosome of interest and subsequently allow the fluorescence detection of the gene/chromosome.

FISH was performed on selected STB TMAs, using probes for H-Ras, N-Ras and Raf-1, produced for this project by DAKO (DAKO, Glostrup, Denmark). Probe mixes consisted of Texas Red-labeled DNA cosmid clones covering the gene (H-Ras, N-Ras or Raf-1) and fluorescein isothiocyanate (FITC)-labeled peptide nucleic acid (PNA) probes for each specific chromosome (chromosomes 11, 1 and 3 respectively). The mix was tested for specificity on metaphase spreads of normal cells.

The FISH experiments were performed using buffers from DAKO's Histology FISH Accessory kit. Initially, the tissue was incubated for one hour at 56°C before being dewaxed and rehydrated through a series of xylene (2 x 5 minutes) and alcohol washes ((100% (2x2minutes), 90% (1x2minutes), 70% (1x2minutes)).

Following this slides were rinsed twice in wash-buffer (diluted 1:20) (DAKO) for three minutes. Tissue sections were then incubated for 10 minutes at 96°C in pre-treatment buffer (diluted 1:20) (DAKO), followed by a 15 minute cool down period. Next the tissue was rinsed twice in wash-buffer (diluted 1:20) for three minutes before treatment with cold ready-to-use Pepsin reagent (DAKO) for 19 minutes at 25°C. The pepsin was removed and the slides rinsed twice in wash buffer. Slides were again rinsed twice in wash buffer for three minutes, dehydrated through a graded series of ethanol washes (70% 1x2minutes, 85% 1x2minutes and 99% 1x2minutes) and subsequently air

dried. The tissue digestion was checked under the microscope. If the digestion was sufficient 10µl of probe was added, and the tissue sections concealed with a coverslip and sealing agent. The probe and tissue was denatured at 82°C for 22 minutes and then the probe allowed to bind to its complementary sequence, by placing slides in a preheated humidified chamber for 14-20 hours at 45°C.

The following morning tissue was rinsed in cold stringent wash buffer (diluted 1:20) and subsequently washed in stringent wash buffer (DAKO) for 10 minutes at 65°C. Slides were rinsed twice in wash buffer for three minutes before being dehydrated through a series of alcohol washes (70% 1x2minutes, 85% 1x2minutes and 99% 1x2minutes). Finally slides were allowed to air dry before being mounted onto coverslips using Vectashield mounting media with 4'-6-Diamidino-2-phenylindole (DAPI) (135µl Vectashield with DAPI: 565µl Vectashield) (Vector Laboratories). DAPI is known to form fluorescent complexes with natural double-stranded DNA, making it a nuclear counterstain in fluorescent techniques. Signals corresponding to both gene and chromosome were visualised using a fluorescent microscope.

I am indebted to Miss Fiona Campbell and Miss Suba M for performing the described FISH experiments.

2.4.1 FISH Scoring

Twenty nuclei from each TMA core were scored, with the number of visible red (H-Ras, N-Ras or Raf-1 gene) and green signals (chromosome) counted. As with the histoscore method one individual scored twenty nuclei in all TMA cores, and a second scorer independently assessed 10% of all cores, in addition to scoring all difficult and borderline cases. Since the TMAs were produced in triplicate, the final FISH score for tumours was

the average of available scores. Gene amplification status was determined as the ratio of red signals to green signals. Genes were considered amplified if the ratio was above 2.0 and deleted if the ratio was below 0.8, according to manufacturers guidelines.

I am grateful to both Miss Suba M and Miss Fiona Campbell for scoring the TMAs.

2.5 *In- vitro* studies

2.5.1 Culturing of breast cancer cell lines

Cell lines used included MCF-7, MDA-MB-231 and MDA-MB-453 (American Tissue Culture Collection ATCC / European Collection of Cell Cultures ECACC). These cell lines represented both ER positive and negative breast cancers, and expressed varying degrees of the tyrosine kinase receptors; EGFR(HER1) and HER2-4. Table 2.7 exhibits the ER and RTK status, growth properties and morphology of the cell lines used.

All the cell lines were grown in Dulbecco's Modified Eagle Media (DMEM) (Invitrogen), supplemented with heat-inactivated foetal calf serum (10%) (Invitrogen), 2mM L-glutamine (Invitrogen) and penicillin/streptomycin (50 units/ml, 50μg/ml) (Invitrogen). Cells were maintained in 5% CO2 at 37°C, with their medium changed regularly; they were grown in T-75 flasks (Gibco).

Before any treatments were performed on cells, they were washed twice in warmed Phospho-Buffered Saline (PBS) (Invitrogen) and then incubated in serum- and phenol red free DMEM (Invitrogen), supplemented with 2mM L-glutamine, penicillin/streptomycin (50 units/ml, 50μg/ml) and 1mM Sodium Pyruvate (Invitrogen) overnight (between 18-20 hours).

Cell Line	Growth Properties	Morphology	ER Status	EGFR Status	HER2 Status	HER3 Status	HER4 Status
MCF-7	Adherent	Epithelial	+		+		
MDA-MB-231	Adherent	Epithelial	-	+			
MDA-MB-453	Adherent	Epithelial	-		+	+	

Table 2.7: ER & RTK status of breast cancer cell lines

Three breast cancer lines were used in the course of this research: - MCF-7, MDA-MB-231 and MDA-MB-453. The oestrogen receptor (ER) and tyrosine kinase receptor status (EGFR, HER2-4) for each cell line is listed.

2.5.2 Trypsinisation of Cells

Cells were routinely passaged to prevent cells becoming too dense and forming clumps. Old medium was removed from the flasks and the cells washed with warmed PBS before Trypsin (Invitrogen) was added to the flask (3mls Trypsin per T-75 flask). Washing the cells with PBS removed serum, which contains trypsin inhibitors, and lowered the concentration of both calcium and magnesium, both of which inhibit trypsinisation. Cells were incubated with trypsin for 3-5 minutes in 5% CO_2, 37°C, in order to detach the cells from the flask. Once cells were no longer adherent, trypsin was inactivated by adding an equal volume of DMEM. Cells were gently pipetted up and down to dislodge any cell clumps that may have formed to produce a single cell suspension to allow for an accurate cell count using a haemocytometer. Having counted the number of cells present within the suspension cells were seeded into new flasks containing 10mls of new DMEM at the required density, this depended on the cell line and experiment being used.

2.5.3 Freezing Cells

Having trypsinised the cells, aliquots of the cells could be stored for future use. The cell suspension was transferred from the flask to a 50ml centrifuge tube and centrifuged at 1200rpm for ten minutes to form a cell pellet. The medium was removed and the pellet

resuspended in 1ml of Freeze Medium (Invitrogen). Since the Freeze Medium contained DMSO, the cells were immediately transferred to -80°C for several hours before being transferred to liquid nitrogen (-180°C) for long-term storage.

If these cell aliquots were required at a later date, they were removed from liquid nitrogen and warmed in a 37°C water bath before being quickly transferred to a flask containing 10mls of pre-warmed DMEM. It was essential not to leave the cells defrosting too long in the freeze medium, as the DMSO would be toxic to them.

2.5.4 Drug Treatments

- **Oestrogen (17-β oestradiol) (Sigma)**

Oestrogen is the ligand for the oestrogen receptor; binding of oestrogen results in receptor phosphorylation and activation. ER positive cells (MCF-7) were treated with 1nM and 10nM oestrogen (E2). These two concentrations were decided upon following an experiment investigating the effects of various concentrations (0.01nM, 0.1nM, 1nM and 10nM) of oestrogen on the nuclear localisation of its receptor. 1nM and 10nM E2 were shown to be the optimal concentrations for the purpose of our studies. A stock solution of 10mM E2 was prepared in Ethanol and stored at 2-8°C, from which 1nM and 10nM solutions were made. Treatment time with E2 ranged from five minutes to three hours.

- **Heregulin α (Sigma)**

Heregulin α (HRG), is the ligand for HER3/4, binding to HER3 results in phosphorylation and dimerisation with HER2 and activation of the growth factor receptor pathways. HER3 positive cell lines (MCF-7, MDA-MB-453) were treated with 1nM and

10nM HRG. Previous studies undertaken in our group had shown 1nM and 10nM HRG to be the most effective concentrations. A stock solution of 1.42μM was made and stored at –20°C. Treatment time with HRG ranged from five minutes to three hours.

- **Epidermal Growth Factor (Sigma)**

Binding of Epidermal Growth Factor (EGF) to its receptor (EGFR) results in phosphorylation and either homo- or hetero-dimerisation, which activates growth factor receptor signalling pathways. The EGFR positive cell line, MDA-MB-231 was treated with 1nM and 10nM EGF. As with HRG, these concentrations were determined in previous studies performed within our group. A stock solution of 10μg/ml was prepared in PBS. Treatment time with EGF ranged from five minutes to thirty minutes.

- **Felodipine (4-(2,3-Dichlorophenyl)-1,4-dihydro-2,6-dimethyl-3,5-pyridinecarboxylic acid ethyl methyl ester) (Sigma)**

Felodipine is a L-type calcium channel blocker. It is a calcium antagonist that has, as one of its properties, the ability to prevent activated MAPK from translocating from the cytoplasm to the nucleus without inhibiting MAPK activation. A 2.6mM stock solution of Felodipine (FEL) was prepared in DMSO and stored at room temperature. Titration experiments using 10μM, 30μM and 100μM FEL, revealed that this drug was most effective in preventing pMAPK nuclear translocation when cells were pre-treated with 30μM FEL for two hours before exposure to growth factors or oestrogen. Treatment time with Felodipine ranged from five minutes to three hours.

- **U0126 (1,4-Diamino-2,3-dicyano-1,4-bis(o-aminophenylmercapto)butadiene) (Sigma)**

A specific inhibitor of MEK1 and MEK2, which prevents phosphorylation and activation of MAPK. A 10mM stock solution of U0126 was prepared by dissolving 5mg in 1.31ml of DMSO. Titration experiments investigating 10μM, 30μM and 100μM U0126, revealed that the optimal inhibition of pMAPK was obtained by using U0126 at a concentration of 10μM. Cells were incubated with this inhibitor for two hours prior to receiving the required treatment for the desired time. Treatment time with U0126 ranged from 5 minutes to thirty minutes.

Details of all the drugs used are listed in Table 2.9

Drug	Molecular Weight (Daltons)	Drug prepared in	Stock Concentration	Final Concentration	Pre-treatment
Oestrogen (E2)	272.38	Ethanol	10mM	1nM & 10nM	NO
Heregulin (HRG)	7000	PBS	1.42μM	1nM & 10nM	NO
Epidermal Growth Factor (EGF)	6200	PBS	1.61mM	1nM & 10nM	NO
Felodipine (FEL)	384.25	DMSO	2.6mM	30μM	YES
U0126	380.49	DMSO	10mM	10μM	YES

Table 2.8: Drug Information

Details of all the drugs used throughout the course of this study; pre-treatment involved exposure to drugs for 2 hours prior to other treatments.

2.6 Immunofluorescence (IF) Studies

Immunofluorescence (IF) is a technique that permits the detection of a specific protein or antigen in cells or tissue sections by fluorescent visualisation. As with IHC there are two types of immunofluorescence staining methods, direct and indirect immunofluorescence.

The first requires using a primary antibody labelled with fluorescent dye, whereas the indirect approach involves the use of a secondary antibody labelled with a fluorescent marker capable of binding to the primary antibody that is bound to the antigen. The protein of interest is then visualised using a fluorescent microscope. This indirect method was used to investigate the expression and localisation of proteins in breast cancer cells following different treatments. In addition to detecting only one protein in treated cells, it was also possible to perform double IF experiments to enable the visualisation of two different proteins within the one cell.

2.6.1 IF of untreated and Heregulin/Epidermal Growth Factor-stimulated MCF-7 & MDA-MB-231 cells with H-Ras, N-Ras, K-Ras

Approximately 1000 MCF-7 or MDA-MB-231 cells were seeded onto 8-well culture slides (VWR) and grown for three days in DMEM. On day 3, DMEM was removed and cells washed twice with warmed PBS before treatment with serum and phenol-red free DMEM, supplemented overnight with 2mM L-glutamine and penicillin/streptomycin (50 units/ml / 50µg/ml) and 1mM sodium pyruvate. On day 4, serum and phenol-red free medium was removed and cells washed with warmed PBS before treatment with either 1nM/10nM HRG or EGF (100µl of drug was added per well) for 0, 5, 15 or 30 minutes.

At each time point there was an untreated control. Cells were treated with serum- and phenol red-free medium only. They were incubated at 37°C, in 5% CO_2. Following drug treatment cells were washed twice with ice-cold PBS, before being fixed to the culture slides by incubation in ice-cold methanol (500µl of methanol per well) for three minutes. Excess methanol was removed by washing the cells three times in dH_20 for five minutes. To reduce non-specific binding of the antibody, cells were incubated in 500µl of

1.5% normal horse serum (Vector) in antibody diluent (DAKO) for twenty minutes. As of this point all steps were performed on an orbital shaker and at room temperature.

Cells were incubated with the appropriate primary antibody for 1 hour (100µl of antibody per well) before being washed three times with TBS for ten minutes. Following this, cells were incubated with either 100µl biotinylated mouse or rabbit secondary antibody (3µg/ml in antibody diluent) (Vector Laboratories) for thirty minutes. Cells were again washed three times with TBS for ten minutes, before being treated with 100µl of Fluorescein Avidin D (diluted 1:100 in TBS) (Vector Laboratories) for thirty minutes. Fluorescein Avidin D has an excitation at 495 nm and an emission at about 515 nm; therefore treated cells fluoresced green. Once the cells were treated with the fluorescent protein, slides were covered in foil and all future steps performed in semi-darkness, to prevent the fluorescence from fading. Finally cells were washed with TBS three times for ten minutes. At this stage culture slides were either mounted onto coverslips, or the procedure continued to enable detection of a second protein.

For double immunofluorescence, following incubation with the first fluorochrome, the cells were incubated in 1.5% horse serum, again for thirty minutes, then with the second primary antibody for one hour, and then with the appropriate secondary for thirty minutes, using the same protocol described above. Since the first protein was detected using Fluorescein Avidin D and would fluoresce green, an alternative fluorochrome was required for the second protein to be visualised. Therefore, Texas Red Avidin D was used. Cells were incubated with 100µl of Texas Red Avidin D for thirty minutes before undergoing three ten minute washes with TBS. Texas Red Avidin D is deep red in colour; it excites at 595 nm and emits at 615 nm. Therefore for

double IF the first protein of interest fluoresces green, whereas the second fluoresces red. Having completed the procedure, culture slides were mounted on to coverslips using Vectashield mounting media with 4'-6-Diamidino-2-phenylindole (DAPI) (635µl mountant media : 65µl mountant media with DAPI)(Vector Laboratories). When bound to double-stranded DNA, DAPI has an absorption maximum at 358 nm and an emission maximum at 461 nm, producing a blue fluorescence, in contrast to the green or red fluorescence of the proteins of interest. There is very little fluorescence overlap between DAPI and green-fluorescent molecules, like fluorescein, or red-fluorescent stains, like Texas Red. DAPI stains nuclei specifically, with little or no cytoplasmic labeling. The protein of interest was then visualised using a fluorescent microscope with either a DAPI (detects both the fluorescien avidin D or Texas Red signal) or green or red filter. Table 2.9 lists the antibodies used in the IF studies, the concentration used, the secondary antibody used and the double IF experiments that were performed.

Originally it was planned to perform IF experiments on MCF-7 and MDA-MB-453 cell lines. However, the MDA-MB-453 cells proved unsuitable for the IF studies, the cells tended to clump together when grown in the culture slide wells, which prevented visualisation of proteins within single cells. Therefore, an alternative ER negative cell line was used, MDA-MB-231 cells.

Antibody	Concentration	Secondary Antibody Used	Single IF	Double IF with
H-Ras	7µg/µl	Mouse	YES (FaD)	N-Ras (TR) K-Ras (TR)
K-Ras	1µg/ml	Mouse	YES (FaD)	H-Ras (FaD) N-Ras (FaD)
N-Ras	7µg/µl	Mouse	YES (FaD)	H-Ras (FaD) K-Ras (TR)

Table 2.9: Ras antibodies used in single and double immunofluorescent studies

This table includes details of the Ras antibodies used in single and double immunofluorescent studies. It highlights the concentration of antibody and the species of the secondary antibody required. The final column reveals what antibodies were used together for double IF experiments. The first protein of interest was visualised with Fluorescein avidin D (FaD), whilst the second was targeted with Texas Red (TR). For example, H-Ras and N-Ras were both visualised together in the same cells – H-Ras was labelled green with FaD and N-Ras was labelled red with TR.

2.6.2 IF of untreated and Heregulin/Estrogen/Felodipine stimulated MCF-7 cells with MAPK, pMAPK, ER, pER(118) & pER(167)

As described in section 2.6.1, MCF-7 cells were grown on culture slides for three days before being treated with serum- and phenol-red free DMEM for approximately 18 hours. MCF-7 cells were then washed twice with warmed PBS before being treated with the required drug. For this experiment the cells were exposed to multiple drug treatments. In total there were 16 treatments over six time points. Cells were incubated with 1nM and 10nM HRG and E2, both individually and in combination, and in the presence and absence of FEL for 5, 15, 30 minutes and 1, 2 and 3 hours. Table 2.10 lists all the drug treatments given to the breast cells.

A problem to be addressed in this study was that three drugs were used, prepared in three different solvents: HRG in PBS, E2 in ethanol, and FEL in DMSO. To ensure experimental uniformity, each of the drug cocktails given to the cells had to have the same concentration of ethanol (0.02M) and DMSO (0.023M) present.

As in the previous study, untreated controls were required for all the time points. However, this time several controls were necessary. First, cells were treated with only serum- and phenol red-free medium, whereas the second required the cells be incubated with serum- and phenol red-free DMEM that contained 0.02M ethanol and 0.023M DMSO. The purpose of this second control was to determine the effects, if any, of ethanol and DMSO on the breast cells, independently of the various drugs. The last control required treating cells with FEL alone, to investigate the effects of this drug on the localisation of MAPK or ER, irrespective of treatment with HRG or E2. Figure 2.3 shows the layout of the culture slides and the drug treatment assigned to each well. All drug combinations were prepared in Eppendorff tubes directly before treatment, to ensure that drugs were thoroughly mixed and that experimental consistency was maintained throughout all the time points. To each well, 100µl of drug or control was added for the required time. Those cells receiving FEL required a two hour pre-treatment with the drug before incubation with HRG, E2, or both plus FEL for the desired time.

5, 15, 30 minutes & 1, 2, 3 hours treatments

10nM E2	10nM E2 10nM HRG
1nM E2	1nM E2 10nM HRG
10nM HRG	10nM E2 1nM HRG
1nM HRG	1nM E2 1nM HRG

30μM FEL 10nM E2	30μM FEL 10nM HRG 10nM E2
30μM FEL 1nM E2	30μM FEL 1nM E2 10nM HRG
30μM FEL 10nM HRG	30μM FEL 10nM E2 1nM HRG
30μM FEL 1nM HRG	30μM FEL 1nM E2 1nM HRG

Control Slides

3hrs UT (with DMSO/EtOH)	2hr UT (with DMSO/EtOH)
1hr UT (with DMSO/EtOH)	30 mins UT (with DMSO/EtOH)
15mins UT (with DMSO/EtOH)	5mins UT (with DMSO/EtOH)
UT w/out DMSO/EtOH	UT w/out DMSO/EtOH

2hrs FEL & 3hrs FEL only	2hrs FEL & 2hrs FEL only
2hrs FEL & 1hr FEL only	2hrs FEL & 30mins FEL only
2hrs FEL & 15mins FEL only	2hrs FEL & 5mins FEL only
2hrs FEL only	2hrs FEL only

Figure 2.3: Slide layout for Immunofluorescent Study

Slide layout of drug treatments and controls for immunofluorescence studies with pMAPK, ER, pER(ser118) and pER(ser167).

Following drug treatment the same protocol as described in section 2.5.1 was employed. Consequently, cells were fixed, incubated in 1.5% horse serum, primary antibody, secondary antibody and lastly Fluorescein Avidin D. As this study was designed to investigate the localisation of MAPK and the ER, the following antibodies were used: pMAPK(thr202/tyr204), ER, pER(ser167) and pER(ser118). Table 2.11 lists the concentration of antibody used and the required secondary antibody.

In addition to investigating the localisation of MAPK and ER proteins in MCF-7 cells it had been hoped to perform similar experiments in a second ER positive cell line,

BT-474 or MDA-MB-361. However, both of these cell lines failed to grow adequately on culture slides.

Drug Treatment	Additional Ethanol or DMSO required
1nM HRG	0.02M EtOH & 0.023 DMSO
10nM HRG	0.02M EtOH & 0.023 DMSO
1nM E2	0.023M DMSO
10nM E2	0.023M DMSO
1nM HRG & 1nM E2	0.023M DMSO
1nM HRG & 10nM E2	0.023M DMSO
10nM HRG & 1nM E2	0.023M DMSO
10nM HRG & 10nM E2	0.023M DMSO
1nM HRG & 30μM Felodipine	0.02M EtOH
10nM HRG & 30μM Felodipine	0.02M EtOH
1nM E2 & 30μM Felodipine	-
10nM E2 & 30μM Felodipine	-
1nM HRG & 1nM E2 & 30μM Felodipine	-
1nM HRG & 10nM E2 & 30μM Felodipine	-
10nM HRG & 1nM E2 & 30μM Felodipine	-
10nM HRG & 10nM E2 & 30μM Felodipine	-
Untreated Control #1 Serum- & phenol-red free DMEM	-
Untreated Control #2 Serum- & phenol-red free DMEM	0.02M EtOH & 0.023M DMSO
Felodipine Control: 30μM Felodipine	0.02M EtOH

Table 2.10: Drug treatments for Immunofluorescent Studies

MCF-7 breast cancer cells were treated with Heregulin (HRG), Oestrogen (E2) and Felodipine for 5, 15 and 30 minutes and 1, 2 and 3 hours. Listed are the nineteen different combinations of treatments. Each drug was dissolved in a different solvent, Heregulin in PBS, Oestrogen in ethanol and Felodipine in DMSO, however all drug treatments had the same final concentration of ethanol (0.02M) and DMSO (0.023M). Therefore this table highlights if treatments required additional ethanol (EtOH) or DMSO.

Antibody	Concentration	Secondary Antibody Used
pMAPK(thr202/tyr204)	0.5µg/ml	Rabbit
ER	0.2mg/ml	Mouse
pER(ser118)	0.3µg/ml	Mouse
pER(ser167)	0.4µg/ml	Rabbit

Table 2.11: MAPK and ER antibodies used in immunofluorescent studies

This table includes details of the MAPK and ER antibodies used in single immunofluorescent studies. It highlights the concentration of antibody and the species of the secondary antibody required.

2.6.3 IF of Heregulin, Oestrogen, Felodipine stimulated MCF-7 cells with pMAPK, and pER(ser118) for 5, 15 and 30 minutes.

This study used the same methods described in sections 2.6.1 and 2.6.2. However, unlike the experiments described in section 2.6.2, the number of time points and drug treatments were reduced. It was established from the first set of experiments in section 2.6.2 that the time points of greatest interest, in terms of changes to protein localisation, were 5, 15 and 30 minutes. Likewise it was deemed more appropriate to investigate only 1nM HRG/1nM E2 and 10nM HRG/10nM E2 drug combinations, as opposed to 1nM/10nM mixtures. Therefore, for this particular study, there were 12 different drug treatments over three time points (5, 15 and 30 minutes), all of which are listed in Table 2.12.

Drug Treatment	Additional Ethanol or DMSO required
1nM HRG	0.02M EtOH & 0.023 DMSO
10nM HRG	0.02M EtOH & 0.023 DMSO
1nM E2	0.023M DMSO
10nM E2	0.023M DMSO
1nM HRG & 1nM E2	0.023M DMSO
10nM HRG & 10nM E2	0.023M DMSO
1nM HRG & 30μM Felodipine	0.02M EtOH
10nM HRG & 30μM Felodipine	0.02M EtOH
1nM E2 & 30μM Felodipine	-
10nM E2 & 30μM Felodipine	-
1nM HRG & 1nM E2 & 30μM Felodipine	-
10nM HRG & 10nM E2 & 30μM Felodipine	-

Table 2.12: Drug treatments for pMAPK and pER(ser118) Immunofluorescent Studies

MCF-7 breast cancer cells were treated with Heregulin (HRG), Oestrogen (E2), and Felodipine for 5, 15 and 30 minutes. Listed are the twelve different combinations of treatments. Each drug was dissolved in a different solvent, Heregulin in PBS, Oestrogen in ethanol, and Felodipine in DMSO; however all drug treatments had the same final concentration of ethanol (0.02M) and DMSO (0.023M). Therefore, this table highlights if treatments required additional ethanol (EtOH) or DMSO.

The controls used remained unchanged, but each treatment was performed in quadruplicate. In addition to this the experiments were performed in triplicate. Therefore, in total there were twelve sets of cells for each treatment condition available for analysis. Figure 2.4 shows the layout of the culture slides and the drug treatment assigned to each well. Following drug treatment the protocol remained unaltered from the one previously described. The final difference between this study and the previous one was that only pMAPK and pER(ser118) protein localisation was monitored. These were both visualised using a fluorescent microscope.

30 MINS (x4 each slide)

10nM E2	10nM HRG 10nM E2
1nM E2	1nM HRG 1nM E2
10nM HRG	30mins UT (with DMSO/EtOH)
1nM HRG	UT w/out DMSO/EtOH

30μM Fel 10nM E2	30μM Fel 10nM HRG 10nM E2
30μM Fel 1nM E2	30μM Fel 1nM HRG 1nM E2
30μM Fel 10nM HRG	2hrs FEL & 30mins FEL only
30μM Fel 1nM HRG	

15 MINS(x4 each slide)

10nM E2	10nM HRG 10nM E2
1nM E2	1nM HRG 1nM E2
10nM HRG	15mins UT (with DMSO/EtOH)
1nM HRG	UT w/out DMSO/EtOH

30μM Fel 10nM E2	30μM Fel 10nM HRG 10nM E2
30μM Fel 1nM E2	30μM Fel 1nM HRG 1nM E2
30μM Fel 10nM HRG	2hrs FEL & 15mins FEL only
30μM Fel 1nM HRG	

5 MINS (x4 each slide)

10nM E2	10nM HRG 10nM E2
1nM E2	1nM HRG 1nM E2
10nM HRG	5mins UT (with DMSO/EtOH)
1nM HRG	UT w/out DMSO/EtOH

30μM Fel 10nM E2	30μM Fel 10nM HRG 10nM E2
30μM Fel 1nM E2	30μM Fel 1nM HRG 1nM E2
30μM Fel 10nM HRG	2hrs FEL & 5mins FEL only
30μM Fel 1nM HRG	2hrs FEL only

Figure 2.4: Slide Layout for Triplicate Immunofluorescent Studies

Slide layout of drug treatments for immunofluorescence studies with pMAPK and pER(ser118).

2.6.4 Immunofluorescent Scoring

In order to semi-quantify the levels of fluorescent protein detected, a scoring method similar to that of the histoscore was devised. Only protein expressed within the nuclei was scored using this method. As with the histoscores, the intensity of nuclear staining was categorised as negative (0), weak/speckled (1), moderate (2) and strong (3) (Appendix 3). Approximately 200 cells, from four random areas (~50 cells per area), were counted in each well as being 0, 1, 2, or 3 positive. From this the percentage of tumour cells within each category was calculated. The IF score was generated using the following formula:

0 x % negative tumour cells + 1 x % weakly stained tumour cells + 2 x % moderately stained tumour cells + 3 x % tumour cells stained strongly

The IF score ranged from a minimum of zero to a maximum of 300.

2.7 Time Course Treatments of MCF-7 breast cancer cell lines

To establish the effects of ligand-dependent and ligand-independent activation of the ER, the ER positive cell line, MCF-7, was treated with E2 and HRG, singly and in combination.

2.7.1 Treatment of MCF-7 cells with Heregulin and Oestrogen for 5, 15 & 30 minutes

MCF-7 cells were grown in T-75 flasks (44 flasks were required) until just below 80% confluence, when the medium was removed and the cells washed twice in warmed PBS. Subsequently, cells were incubated in serum- and phenol red-free DMEM overnight. The next day, medium was removed and the cells rinsed in warmed PBS in preparation for the

appropriate drug treatment. For this study cells were treated with HRG and E2, both singly and in combination (Table 2.13).

Again, as in the IF studies, since E2 was prepared in ethanol, it was essential to ensure that the HRG treatments contained the same final concentration of ethanol (0.02M). Therefore, the 1nM and 10nM HRG solutions were supplemented with 0.02M ethanol. There were three different treatment times, 5, 15 and 30 minutes, and all treatments were performed in duplicate at each time point. There was also an untreated control (cells treated with serum- and phenol red free DMEM with 0.02M ethanol) included at each of these time points. Additionally, there was a completely untreated control, MCF-7 cells, that received nothing but serum- and phenol red-free DMEM (without EtOH).

Drug Treatment	Additional Ethanol or DMSO required
1nM HRG	0.02M EtOH
10nM HRG	0.02M EtOH
1nM E2	-
10nM E2	-
1nM HRG & 1nM E2	-
10nM HRG & 10nM E2	-
Untreated Control #1 Serum- & phenol-red free DMEM	-
Untreated Control #2 Serum- & phenol-red free DMEM	0.02M EtOH

Table 2.13: Drug Treatments for MCF-7 Time Course Experiments

MCF-7 breast cancer cells were treated with Heregulin (HRG) and Oestrogen (E2) for 5, 15 and 30 minutes. Listed are the six different combinations of treatments. Each drug was dissolved in a different solvent: Heregulin in PBS and Oestrogen in ethanol; however all drug treatments had the same final concentration of ethanol (0.02M). Therefore, this table highlights if treatments required additional ethanol (EtOH).

All drugs were prepared in large enough volumes to provide enough for all time points to ensure experimental uniformity. Each flask was treated with 2mls of drug or control, ensuring that all cells were completely covered, and incubated at 37°C in 5%

CO_2 for the required time. All the 30 minute treatments were performed together, followed by the 15 minute treatments, and then finally the 5 minute treatments.

Having been incubated for the desired time, the drug was removed from the flask and cells carefully rinsed twice, with ice-cold PBS. It was important to remove as much of the PBS, using a pipette, as possible, since it would dilute the lysis buffer. From this point onwards all treated flasks were kept on ice. The next step involved lysing the cells to enable collection of the protein. This was done using cell lysis buffer (Cell Signaling Technology) and a non-denaturing method. The buffer used was comprised of the following: 20mM Tris-HCl (pH 7.5), 150mM NaCl, 1mM Na_2EDTA, 1mM EGTA, 1% Triton, 2.5mM sodium pyrophosphate, 1mM beta-glycerophosphate, 1mM sodium orthovanadate (Na_3VO_4), and 1µg/ml leupeptin. Directly before use, this buffer was diluted ten times in dH_20 and 1mM phenylmethlysulfonyl fluoride (PMSF), a serine protease inhibitor, added. This prepared buffer was stored on ice at all times. To each flask 500µl of buffer was added and cells incubated in the buffer on ice for five minutes. Following this cells were scraped from the flask into the buffer, being careful to remove as many of the cells as possible. The cell lysate was transferred to an appropriately labelled 1.5ml eppendorff tube and stored on ice, until all treatments had been performed.

All samples were centrifuged at 14,000 rpm at 4°C to separate the protein from cell debris. The supernatant containing the isolated protein was then carefully transferred to a labelled eppendorff tube and subsequently stored at -70°C.

This experiment was performed twice; therefore, in total there were four protein samples for each treatment condition available for analysis.

2.8 Subcellular Fractionation

Subcellular fractionation was used to study the activation and interaction of proteins, such as MAPK and ER, within the cytoplasm, nuclei and plasma membrane of MCF-7 breast cancer cells.

2.8.1 Fractionation of MCF-7 cells treated with Heregulin for 5, 15 and 30 minutes

A preliminary fractionation experiment was performed on MCF-7 cells. Twenty flasks of MCF-7 cells were grown until nearly 70% confluent, when their medium was replaced with serum and phenol red-free medium overnight. The following morning cells were washed with warmed PBS, and incubated with either 1nM or 10nM HRG for 5, 15 or 30 minutes (2mls per flask). Treatments were performed in duplicate and untreated controls were present at each time point.

After incubation, the drug was removed and cells rinsed twice with ice-cold PBS and trypsinised as described in section 2.5.2. Following trypsinisation, 10mls of DMEM was added, and the cell suspension was centrifuged at 12000 rpm for ten minutes. The supernatant was carefully removed from the pelleted cells, which were washed in 10mls of ice-cold PBS before being centrifuged again at 12000rpm for another ten minutes and the supernatant again discarded. The cell pellet was resuspended in 1ml ice-cold PBS and transferred to an Eppendorf tube. It was stored on ice until all samples were ready to undergo fractionation, using the FractionPREP^{TM} Cell Fractionation System (Biovision), to generate four subcellular protein fractions: - cytosol, membrane, nucleus and cytoskeletal. The following buffers were supplied within the kit: Cytosol Extraction Buffer (CEB), Membrane-Extraction Buffer-A (MEB-A), Membrane Extraction Buffer-B (MEB-B), and Nuclear Extraction Buffer (NEB). Prior to fractionating cells, 2µl of 1M

Dithiothreitol (DTT) and 2µl of Protease Inhibitor Cocktail (both provided in the kit) were added per ml of CEB, MEB-A and NEB. Buffers were stored on ice throughout the experiment, and all centrifugation procedures were performed at 4°C.

The resuspended cell pellets were centrifuged at 700g for 5 minutes and the supernatant discarded. Cell pellets were resuspended in 400µl of CEB-Mix (CEB + DTT + protease inhibitor cocktail), by pipetting the mix up and down several times. Samples were incubated on ice for 30 minutes, with gentle tapping every 5 minutes, before being centrifuged at 700g for 10 minutes. The resultant supernatant was the Cytosolic fraction. This was removed and transferred to a labelled eppendorf tube, and either stored on ice until the end of the experiment or immediately transferred to -80°C for long term storage.

The remaining cell pellets were resuspended in 400µl of MEB-A mix, thoroughly mixed by pipetting and vortexing for 10-15 seconds. To this 22µl of MEB-B was added, samples were vortexed for a further 5 seconds and then incubated on ice for 1 minute. Samples were vortexed again for 5 seconds before being centrifuged at 1000g for 5 minutes. This supernatant contained the membrane fraction, and this was transferred to a pre-chilled, labelled Eppendorf tube. It was either stored on ice or transferred to a -80°C freezer.

The next step generated the nuclear fractions; cell pellets were resuspended in 200µl of NEB-Mix and vortexed for 15 seconds. Samples were stored on ice for 40 minutes, with constant vortexing for 15 seconds every 10 minutes. Finally the samples were centrifuged at top speed for 10 minutes. The resultant supernatant was the nuclear fraction, and this was transferred to a pre-chilled, labelled Eppendorf tube. The residual pellet was the cytoskeletal fraction, and this was very difficult to resuspend. It proved

easiest to add 100µl of SDS-PAGE sample buffer to it. All protein samples were then stored at -80°C for future use.

The protein fractions were shown to be specific for their particular subcellular compartments by western blotting using subcellular markers (Appendix 4).

2.8.2 Fractionation of MCF-7 cells treated for 5 minutes with Heregulin, Oestrogen and Felodipine

From the IF studies (section 2.6.3), it was suggested that the most significant time points for investigating changes in protein localisation, following treatment with either HRG or E2, were 5 and 15 minutes. Therefore, fractionation experiments were performed at these time points.

MCF-7 cells (30 T-75 flasks were required) were grown to just below 70% confluence, when they were washed with PBS and incubated in serum- and phenol-red free DMEM overnight, before undergoing various drug treatments. To ensure conformity with the IF study (section 2.6.3), the same drug treatments and controls were performed on these cells prior to subcellular fractionation commencing. The treatments and controls are shown in Table 2.14.

Drug Treatment	Additional Ethanol or DMSO required
1nM HRG	0.02M EtOH & 0.023 DMSO
10nM HRG	0.02M EtOH & 0.023 DMSO
1nM E2	0.023M DMSO
10nM E2	0.023M DMSO
1nM HRG & 1nM E2	0.023M DMSO
10nM HRG & 10nM E2	0.023M DMSO
1nM HRG & 30μM FEL	0.02M EtOH
10nM HRG & 30μM FEL	0.02M EtOH
1nM E2 & 30μM FEL	-
10nM E2 & 30μM FEL	-
1nM HRG & 1nM E2 & 30μM FEL	-
10nM HRG & 10nM E2 & 30μM FEL	-
Untreated Control #1 Serum- & phenol-red free DMEM	-
Untreated Control #2 Serum- & phenol-red free DMEM	0.02M EtOH & 0.023M DMSO
FEL Control: 30μM FEL	0.02M EtOH

Table 2.14: Five Minute Drug Treatments for MCF-7 Subcellular Fractionation

MCF-7 breast cancer cells were treated with Heregulin (HRG), Oestrogen (E2), and Felodipine (FEL) *for 5 minutes. Listed are the twelve different combinations of treatments and the various controls. Each drug was dissolved in a different solvent, HRG in PBS, E2 in ethanol, and* FEL *in DMSO; however all drug treatments had the same final concentration of ethanol (0.02M) and DMSO (0.023M). Therefore, this table highlights if treatments required additional ethanol (EtOH) or DMSO.*

Again, as described in the IF and time course treatment methods, all drugs and controls, with the exception of untreated control #1, had to be prepared with the same final concentration of DMSO (0.023M) and ethanol (0.02M). Likewise, as in the previous experiments, all treatments were performed in duplicate. Flasks were incubated with 2mls of each drug or control for 5 minutes, and from this point onwards the method was identical to that described in section 2.8.1.

2.8.3 Fractionation of MCF-7 cells treated for 15 minutes with Heregulin, Oestrogen, Felodipine and U0126

The final fractionation study was a slightly modified version of the one described in section 2.8.2. In this particular study cells were again treated with HRG, E2 and Felodipine but also the MEK-1/2 inhibitor, U0126. Table 2.15 displays the various drug combinations and controls used throughout this experiment. Additionally the cells were exposed to the drugs for a longer period of time, 15 as opposed to 5 minutes. With the exception of these changes the protocol used for this experiment was exactly the same as that described in sections 2.8.1 and 2.8.2. This study was performed twice.

Drug Treatment	Additional Ethanol or DMSO required
1nM HRG	0.02M EtOH & 0.023 DMSO
10nM HRG	0.02M EtOH & 0.023 DMSO
1nM E2	0.023M DMSO
10nM E2	0.023M DMSO
1nM HRG & 1nM E2	0.023M DMSO
10nM HRG & 10nM E2	0.023M DMSO
1nM HRG & 30μM FEL	0.02M EtOH
10nM HRG & 30μM FEL	0.02M EtOH
1nM E2 & 30μM FEL	-
10nM E2 & 30μM FEL	-
1nM HRG & 1nM E2 & 30μM FEL	-
10nM HRG & 10nM E2 & 30μM FEL	-
1nM HRG & 10μM U0126	0.02M EtOH
10nM HRG & 10μM U0126	0.02M EtOH
1nM E2 & 10μM U0126	-
10nM E2 & 10μM U0126	-
1nM HRG & 1nM E2 & 10μM U0126	-
10nM HRG & 10nM E2 & 10μM U0126	-
Untreated Control #1 Serum- & phenol-red free DMEM	-
Untreated Control #2 Serum- & phenol-red free DMEM	0.02M EtOH & 0.023M DMSO
FEL Control: 30μM FEL	0.02M EtOH
U0126 Control: – 10μM U0126 alone	0.02M EtOH

Table 2.15: Fifteen minute drug treatments for MCF-7 subcellular fractionation

MCF-7 cells were treated with different combinations of Heregulin (HRG), Oestrogen (E2), Felodipine (FEL), and U0126 for 15 minutes before subcellular fractionation was performed. Three different solvents were used to prepare the drugs. HRG was dissolved in PBS, E2 in Ethanol (EtOH) and FEL and U0126 in DMSO. Therefore, all drug treatments were prepared with 0.02M EtOH and 0.023M DMSO. Also shown are the various controls included in the experiment.

2.9 Western Blotting

Western blotting (immunoblotting) is a technique that enables the detection and quantification of the levels of a specific protein in tissue or cell samples. The basic principle requires preparing protein samples from tissues or cells and then separating the denatured proteins by gel electrophoresis and transferring them to a PVDF membrane. The membrane is then probed with a primary antibody specific to the protein of interest, followed by a secondary antibody that recognises the antibody-antigen complex. Proteins are detected using a chemiluminsecent and chemifluorescent method. This method was used to verify the specificity of all antibodies, and also to measure the levels of proteins in samples from the time course treatment and subcellular fractionation studies.

2.9.1 Determination of Protein Concentration in Prepared Samples

Before performing immunoblotting, it was necessary to determine the concentration of protein present in the samples to be tested. Knowing this enabled experimental consistency, as the same volume of protein was used from all the samples. The method used was Bio-Rad's protein assay, which was based on the Bradford dye-binding procedure (Bradford 1976), and involves a colorimetric assay for measuring total protein concentration.

Samples were prepared for a low-concentration assay in disposable cuvettes (Gibco). First, 200µl of Bio-Rad Protein Assay Reagent (Bio-Rad) was added to the cuvette, followed by 795µl of dH_2O. Subsequently 5µl of protein sample was included to the mix. The solution was thoroughly mixed with a pipette to ensure even distribution of the protein for an accurate concentration reading. In order to have something to compare the concentration of the samples with, protein standards were prepared using Bovine Serum Albumin (BSA) (Sigma). The BSA was supplied at a concentration of 2mg/ml,

but for the purpose of this study it was diluted to 1mg/ml with dH_2O. One reference and seven protein standards were prepared in cuvettes as follows.

Volume of 1mg/ml BSA required (µl)	Volume of dH_2O required (µl)
0 (REFERENCE)	800
1	799
5	795
10	790
15	785
20	780
25	775
50	750

To each of these was added 200µl of Bio-Rad Protein Assay Reagent. A gradual increase in the intensity of the blue colour was observed in parallel to the increasing concentration of the standards. Once prepared the reference and standards were used to calibrate the spectrophotometer (Bio-Rad) Protein 595 assay programme. This assay is based on a colour change of Coomassie brilliant blue G-250 dye in response to the binding of the dye to basic and aromatic acid residues. Protein concentration was determined due to the change in the absorbance of the coomassie dye when bound to protein. When bound it has an absorption spectrum maximum of 595nm, whereas unbound it has an absorbance maximum of 470nm. Therefore, the increase of absorbance at 595nm is proportional to the amount of protein within the sample.

The optical density at 595nm (O.D. 595nm) was measured for the reference and the seven protein standards. The O.D 595 was then read for all the samples and the concentration of protein present generated from the standards concentration. The spectrophotometer calculated the amount of protein (µg/ml) present, but the theory behind it involves plotting a graph of absorbance at 595nm against protein concentration

of standards. This standard curve is then used to determine the concentration of the protein present in the samples from its O.D. 595 value.

However, the concentration (μg/ml) was calculated from a diluted protein sample (1:200). From this the final concentration in mg/ml was determined as follows:

Protein reading (μg/ml) x 0.2 = Final protein concentration (mg/ml)

For western blotting either 25μg or 40μg of protein was used and the volume of sample required was calculated from the final concentration.

2.9.2 Western blotting of Protein Samples

- **Preparation of SDS-PAGE (Sodium Dodecyl Sulphate – PolyAcrylamide Gel Electrophoresis) gels**

All western blots were performed using the Bio-Rad Mini-PROTEAN 3 Electrophoresis System. For all the proteins analysed it was deemed appropriate to use 10% resolving gels, and they were prepared as follows:

Reagents	10% Gel
40% Acrylamide/Bis-Acrylamide (Sigma)	12.49ml
0.5M EDTA	330μl
2M Tris, pH 8.9	8.35ml
10% SDS	500μl
dH_2O	28.33ml
10% APS	300 μl
TEMED	30μl

Gels are formed from the polymerisation of the acrylamide and N-N-methylene-bis-acrylamide (bis). Bis acts as the cross linking agent for the gel, and the TEMED and APS are the catalysts for gel polymerisation. The separation of proteins within the gel is

governed by the size of the pores within the gel, which is determined by the amount of acrylamide-bis present. As the amount of acrylamide present increases, the pore size decreases. Generally a higher percentage of resolving gels are used for smaller proteins, whereas lower percentage gels are more effective for separating larger proteins.

Two gels of different thickness (0.75mm and 1.5mm) were used throughout the various studies; they were produced using either a 0.75mm or a 1.5mm spacer plate respectively. Once the gel mix was prepared with everything but the TEMED and APS added, the gel plates and gel casting apparatus were assembled. Having correctly assembled the plates, the TEMED and APS were added to the resolving gel mix, which was then slowly poured in between the two glass plates, using a plastic pastette, to a level that still allowed for the stacking gel and comb to be added. Finally a layer of isopropanol was applied to the top of the gel to remove any air bubbles and to flatten the top of it. The resolving gel was then left to polymerise for approximately one hour.

Once set, the isopropanol was removed from the top of the resolving gel and the 4.5% stacking gel prepared as follows:

Reagents	**4.5 % Gel**
40% Acrylamide/Bis-Acrylamide	5.63ml
0.5M EDTA	400µl
1M Tris, pH 8.9	6.25ml
10% SDS	500µl
dH_2O	37.22ml
10% APS	30µl
TEMED	10µl

Again, the TEMED and APS were the last two reagents to be added to the gel mix. The stacking gel was then poured onto the resolving gel until it reached the top of the plates;

the gel comb (10 or 15 well comb depending on the number of samples being run) was then inserted and the gel allowed to polymerise for approximately 30 minutes.

At this stage the gel (wrapped in cling film) could be stored at 4°C until required.

- **Protein denaturation**

To enable the primary antibody to recognise and bind to its epitope, it was necessary to denature the proteins, i.e unfold the protein to allow the antibody access. Denaturing the proteins also enabled them to run more efficiently through the gels.

Having previously measured the concentration of protein within each sample, the same amount of protein (either 25µg or 40µg) was removed from each sample and transferred to a new Eppendorf tube. This was stored on ice, and to each sample was added 2X Laemmli's sample reducing buffer which was comprised of:

1.0ml 0.5M Tris-HCl pH 6.8
0.8ml Glycerol
1.6ml 10% sodium dodecyl sulphate (SDS)
0.4ml 2-Mercaptoethanol
0.2ml Bromophenol Blue (0.05% w/v)
4.0ml dH_2O

The samples were thoroughly mixed and then boiled at 100°C for two minutes. The SDS within the sample buffer is a detergent, with a highly negative charge that has a hydrophobic tail that binds to the proteins, causing them to become negatively charged. Additionally, SDS disrupts the tertiary structure of the protein, resulting in their unfolding. The 2-Mercaptoethanol prevented the reformation of disulphide bonds and helped maintain the protein in its denatured state. Boiling the samples also contributed to the denaturing of the proteins by unfolding them completely. Boiled samples were immediately stored back on ice. The molecular weight marker (Biotinylated Protein

Ladder –Cell Signaling Technology) that was used to determine the size of the detected protein was also boiled for two minutes.

- **Gel Electrophoresis**

The principle behind electrophoresis is that an electrical charge moves the proteins down the polyacrylamide gel. This is made possible by the SDS, which transfers a negative charge onto the proteins, thus allowing them to be attracted towards the positive anode. The pores produced by the acrylamide result in smaller protein molecules travelling through the gel at a faster rate than the larger molecules; therefore, they progress further down the gel. Thus, proteins are separated by gel electrophoresis according to their molecular weight.

Gels were placed into the electrode assembly in the mini buffer tank. Combs were removed from gels and the wells rinsed and the tank filled with 1X running buffer (details in table 2.16). Denatured protein samples and ladder (7µl) were then carefully loaded into the wells using a fine tipped pipette. It was important to prevent overspill between the wells. Once all samples were loaded the gel was run at 40mA for approximately one hour.

- **Protein Transfer**

To enable protein detection by a primary antibody, the protein had to be transferred from the polyacrylamide gel to PVDF (polyvinylidene difluoride) membrane. This step proved to be the most problematic, and several different methods were tried, including wet transfer for various times and semi-dry transfer methods. Eventually, optimal transfer was achieved by using the Mini-Trans Blot Cell (Bio-Rad) and transferring the proteins onto the membrane overnight.

Once the proteins had run sufficiently through the gel, protein transfer to the PVDF membrane (Biorad) could begin. For optimal transfer, PVDF membrane, cut slightly bigger than the size of the gel, was pre-treated in 100% methanol for one minute before being soaked in 1X Transfer Buffer (Details of which can be found in table 2.16). Fiber pads and 3M Whatman paper, cut the same size as the membrane, were also soaked in transfer buffer. The gels were then carefully removed from the glass plates; the stacking gel was discarded, and the remaining resolving gel equilibrated, for approximately five minutes in transfer buffer. This step prevented the gel from shrinking during the transfer process.

Next the transfer sandwich, comprised of fiber pads, 3M Whatman paper, gel and PVDF membrane was assembled on the gel holder cassettes, as shown below in Figure 2.5

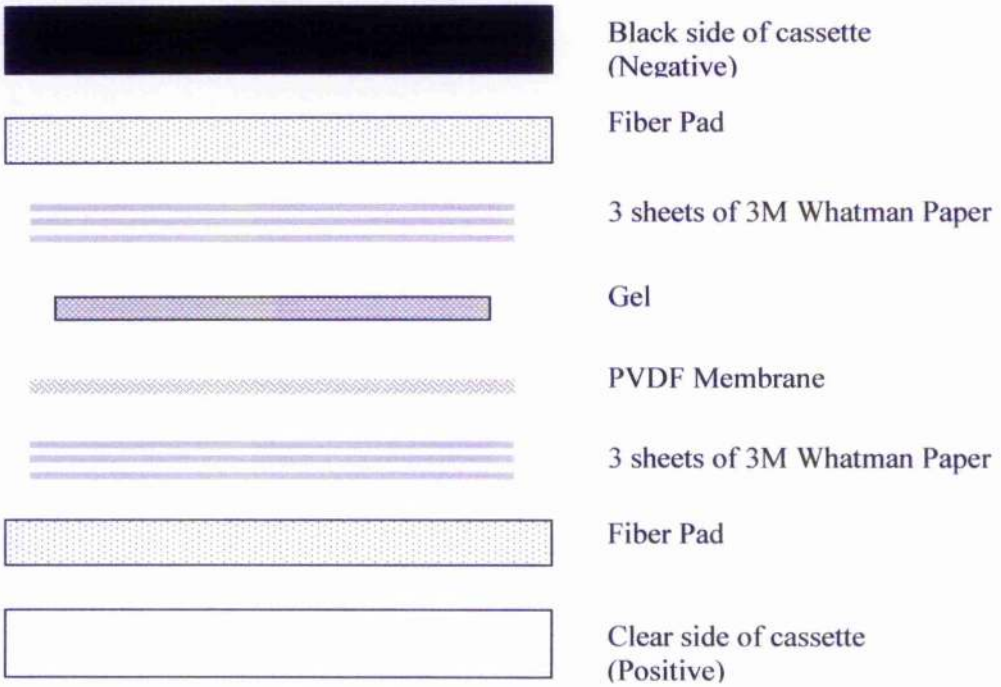

Figure 2.5: Schematic Representation of Western Blot Transfer Sandwich

Schematic representation of the assembly of the transfer sandwich on the cassettes, the sandwich was comprised of fiber pads, 3M Whatman paper, gel and PVDF membrane, all of which had been equilibrated in transfer buffer.

While building the sandwich, it was important to make sure that there were no air bubbles present, as these would prevent efficient transfer; therefore, after each new layer was applied, air bubbles were removed by gently rolling a glass rod over the top surface. The assembled sandwich was then slotted into the electrode assembly and placed in the mini-tank, which was filled with transfer buffer. To reduce the temperature of the buffer during the transfer process, the Bio-Ice cooling unit was used. Additionally a magnetic stirrer was used to maintain even buffer temperature and ion distribution. Proteins were

transferred from the gel (negative/cathode) to the membrane (positive/anode) overnight (approximately 18 hours) at 10 volts.

- **Blocking of Membrane**

Since the proteins transferred from the gel bind to the PVDF membrane, it was equally likely that the antibody used to detect the protein would also bind non-specifically to the membrane. Therefore, to prevent these interactions between antibody and membrane, and to ultimately reduce background staining, it was necessary to mask the membrane.

This was achieved by incubating the membrane in 5% Non-Fat Dry Milk (Marvel) blocking solution, prepared in TBS-Tween (TTBS) (Details of buffers listed in table 2.16) for one hour at room temperature. This step and all future steps were performed on an orbital shaker.

An alternative blocking solution of 5% BSA (Bovine Serum Albumin), prepared in TTBS was also tried, but failed to reduce background staining as efficiently as 5% Non-Fat Dry Milk blocking solution.

At this point it was also possible to stain the gel with Coomassie blue, to determine how efficient the transfer was. Coomassie blue bound to any protein that remained on the gel. The gel was stained for 40 minutes with Coomassie blue and then destained overnight (see table 2.16 for details of both Coomassie blue stain and destain). The following morning any protein that remained on the gel was visible as blue bands.

Buffer	Reagents
10X Running Buffer	200mM Tris, 2M Glycine, 1% SDS (For 1X dilute in dH_2O)
10X Transfer Buffer	248mM Tris, 1.3M Glycine, 20% Methanol (For 1X dilute in dH_2O)
10X TBS	0.1M Tris/HCl, 1.5M NaCl, pH = 7.4 (For 1X dilute in dH_2O)
0.001% TTBS	1000µl of Tween 20 per litre of 1X TBS
Coomassie Blue Stain	1.51mM Coomassie blue R250, 454ml 50% Methanol, 46 ml Glacial Acetic Acid
Destain	25ml Methanol, 37.5ml Glacial Acetic Acid, 437.5ml dH2O

Table 2.16: Buffers used in western blotting

Details of the buffers and solutions used in western blotting

- **Incubation of membrane with primary antibody**

Having sufficiently blocked the membrane, the next step was incubation in primary antibody. All antibodies were prepared in 5% Non-Fat Dry Milk/TTBS solution, to further reduce non-specific binding. Membranes were incubated with primary antibody overnight (approximately 18 hours) at 4°C. For the size of membrane being used 10mls of antibody was adequate to cover the entire membrane. Table 2.17 lists the dilutions/concentrations of all the antibodies used in western blotting.

Antibody	Dilution	Concentration
H-Ras	1:500	0.4μg/ml
K-Ras	1:500	0.2μg/ml
N-Ras	1:500	0.4μg/ml
Pan-Ras	1:100	2μg/ml
Ras Ab-1	1:100	10μg/ml
Raf-1	1:500	0.4μg/ml
pRaf(ser259)	1:500	0.2μg/ml
pRaf(ser338)	1:250	0.4μg/ml
MAPK	1:500	0.2μg/ml
pMAPK(thr202/tyr204)	1:500	0.2μg/ml
ER	1:250	83μg/ml
pER(ser118)	1:250	0.4μg/ml
pERser167)	1:250	0.4μg/ml
Actin	1:1000	0.1μg/ml
Tubulin	1:1000	0.1μg/ml

Table 2.17: Dilutions/Concentrations of antibodies used in western blotting

Details of the dilutions and concentration of all the antibodies used for western blotting. All antibodies were prepared in 5% Non-Fat Dry Milk/TTBS solution and incubated with membranes overnight at 4℃.

- **Incubation of membrane with secondary antibody**

Following incubation with primary antibody, the membrane was washed in TBST three times for 10 minutes, to remove any excess antibody. As in IF, detection of the protein of interest required a secondary antibody bound to either biotin or an enzyme conjugate, such as horseradish peroxidase (HRP) that was species-specific to the primary antibody. The secondary antibodies used were HRP-linked anti-mouse IgG (Cell Signaling Technology) and anti-rabbit IgG (Cell Signaling Technology). The anti-mouse antibody was used at dilution of 1:10000, whereas the anti-rabbit was used at a dilution of 1:5000. In addition to requiring a secondary antibody to recognise the primary antibody bound to its protein, one was also needed for detection of the biotinylated ladder. For this the anti-biotin HRP linked antibody (Cell Signaling Technology) was used at a dilution of 1:1000.

The anti-biotin and anti-mouse/rabbit secondaries were prepared together in 10mls of 5% Non-Fat Dry Milk/TTBS solution and were incubated with the membranes for one hour at room temperature. Table 2.18 lists the required secondary antibody for each primary antibody.

Mouse Secondary	H-, K- & N-Ras Pan Ras & Ras Ab-1 Raf-1 ER & pER(ser118) Actin
Rabbit Secondary	pRaf(Ser259) & pRaf(Ser338) MAPK & pMAPK(thr202/tyr204) pER(167) Tubulin

Table 2.18: Secondary Antibodies for Western Blotting

All the antibodies used for western blotting required either a mouse or a rabbit secondary for detection. Listed are those primary antibodies that required a mouse secondary and those that required a rabbit secondary.

- **Protein visualisation**

The last steps in the western blotting protocol involved detection of the protein of interest using a chemiluminescent method. Luminescence is the emission of light due to the dissipation of energy from a substance in an excited state. Horse-radish peroxidase catalyzes oxidation of luminol, a chemiluminescent substrate, in alkaline conditions. Oxidation results in the luminol being in an excited state which then decays to ground state via a light emitting pathway. For this method ECL plus (Amersham) was used. The principle behind this is that horse-radish peroxidise, conjugated to the secondary antibody, oxidises the ECL Plus chemiluminescent substrate Lumigen PS-3 Acridan, which produces thousands of acridinium ester intermediates per minute. These intermediates then react with the peroxide to produce a sustained, high intensity

chemiluminescence with a maximum emission at 430nm. This light is then detected on autoradiography film.

Following incubation with the secondary antibody, membranes were washed three times in TTBS for ten minutes. While the membranes were washing, the ECL plus reagents were warmed to room temperature. Once the reagents had warmed sufficiently, solution A and solution B were mixed in a ratio of 40:1; 3mls of solution was an adequate amount per membrane. When using the ECL reagents all steps were performed in semi-darkness. Membranes were placed protein side up on a sheet of saran wrap. The ECL solution was pipetted onto the membrane ensuring complete coverage. The membrane was incubated with the reagents for five minutes, and excess solution was then removed and the membrane transferred to a fresh piece of saran wrap, which it was subsequently enveloped in. Finally the membrane was transferred to a film cassette where it was exposed to autoradiography film for various times. Generally the incubation times were 1, 15, 15 and 30 minutes. The film was then developed and both the marker and protein bands visualised.

- **Stripping Membranes**

To prevent re-running of samples, primary antibody was removed from probed membranes using Restore Western Blot Stripping Buffer (Pierce). Membranes were incubated in 20mls of stripping buffer at 37°C for 15 minutes, before being washed in TTBS three times for 10 minutes. Consequently, membranes were blocked in 5% Non-Fat Dry Milk/TTBS and then probed with the next primary and secondary antibody as described above. This was performed a maximum of three times.

3. Pilot Study: Effect of Ras and Raf-1 protein overexpression on breast cancer patients' outcome

3.1 Introduction

Activation of the Ras/Raf-1/MAPK pathway is thought to play a role in the development and progression of breast cancer. However, data on the clinical significance of Ras and Raf-1 expression in breast cancer remains sparse. This pilot study aimed to investigate the expression of Ras and Raf-1 in breast tumours and test the hypothesis that overexpression of these proteins influences disease-free and overall survival in breast cancer. Using an immunohistochemical approach (see Chapter 2.2.1), the expression of pan-Ras, H-Ras, N-Ras and Raf-1 was analysed in breast tumours of patients treated at the Glasgow Royal Infirmary, to determine if expression was linked to reduced survival.

3.2 Expression & Localisation of Ras and Raf in Breast Tumours

Due to the limited availability of breast tumour tissue, the number of patients tested for expression of pan Ras, Ras Ab-1, H-Ras, N-Ras and Raf-1, was 80, 147, 139, 138 and 74 respectively. The pan-Ras and Ras isoform specific antibodies all detected Ras protein in the cytoplasm and nuclei of invasive tumour cells, but not in normal breast epithelial cells. Additionally, almost no membrane staining was detected for any of the Ras antibodies, hence for the rare cases (1%) that displayed membrane staining, this was not scored. Table 3.1 provides details of the descriptive statistics (minimum, maximum, mean, median, lower and upper quartile) for the histoscores of all the antibodies used.

3.2.1 Total Ras Expression in Breast Tumours

Two pan-Ras antibodies were used for this study: the rabbit polyclonal Pan-Ras antibody (Santa Cruz, F132) and the mouse monoclonal Ras Ab-1 antibody (Neomarkers). Both antibodies detected all three Ras isoforms. Ras Ab-1 was produced from a synthetic peptide, corresponding to amino acids 31-43 (EYDPTIEDSYRKQ), from the L2 loop of human Ras protein. Unfortunately the epitope for the Pan-Ras antibody was not mapped.

Both Pan-Ras and Ras Ab-1 detected higher levels of nuclear, rather than cytoplasmic Ras (Figure 3.1a & 3.2a). Ras Ab-1 detected cytoplasmic and nuclear Ras in 92.8% and 99.3% of tumours, while with Pan-Ras the proportions were 86.2% and 98.7%. The frequency and intensity of staining in the cytoplasm and nuclei of tumour cells for both antibodies is shown in Figures 3.1b,c & 3.2b,c.

Results obtained for the expression of nuclear and cytoplasmic pan-Ras were strongly correlated for both antibodies, suggesting the distribution of Ras is linked in both compartments (Spearman Rank Test, $p<0.0005$, pan-Ras $R^2=0.686$, Ras Ab-1 $R^2=0.628$). To evaluate the efficiency of both antibodies in detecting Ras, correlations comparing results for Pan-Ras and Ras Ab-1 antibodies were also performed (Figure 3.3), cytoplasmic Pan-Ras expression correlated with both cytoplasmic and nuclear Ras Ab-1 expression ($R^2 = 0.372$, $p=0.001$ and $R^2=0.296$, $p=0.008$ respectively), whereas nuclear Pan-Ras expression correlated only with nuclear Ras Ab-1 expression ($R^2= 0.248$, $p=0.026$).

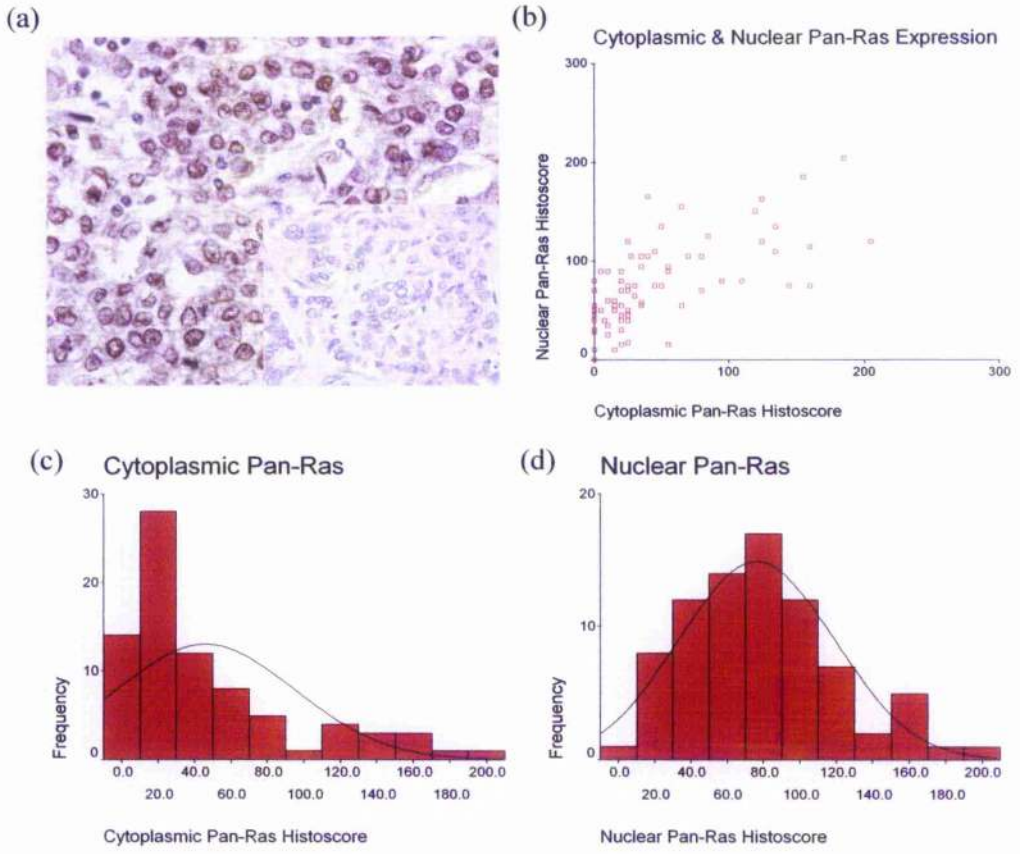

Figure 3.1: Pan-Ras Immunohistochemistry

(a) Breast tumour stained with Pan-Ras antibody. Ras was detected in both the cytoplasm and nuclei of tumour cells. Insert shows the negative control. (b) Scatter graph comparing cytoplasmic and nuclear expression of Ras using Pan-Ras antibody. (c) Histogram showing the intensity of Pan-Ras expression in the cytoplasm of tumour cells. (d) Histogram showing the intensity of Pan-Ras expression in the nuclei of tumour cells.

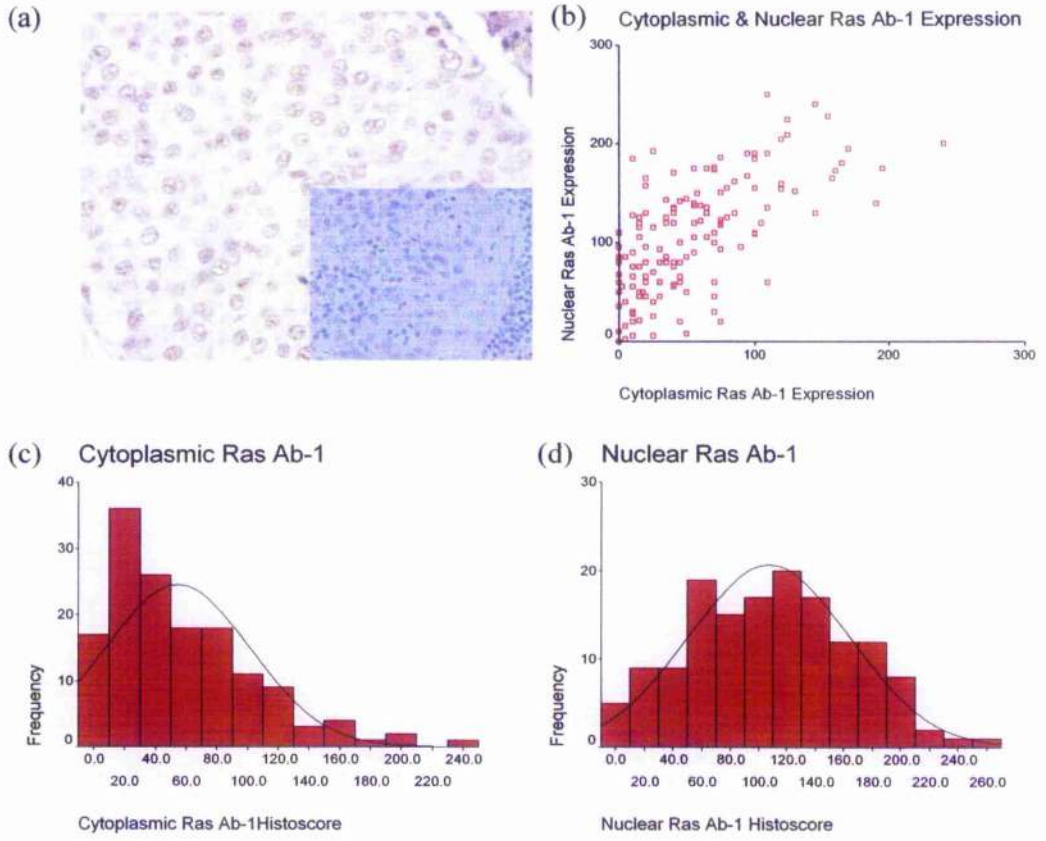

Figure 3.2: Ras Ab-1 Immunohistochemistry

(a) Breast tumour stained with Ras Ab-1 antibody. Ras was detected in both the cytoplasm and nuclei of tumour cells. Insert shown negative control. (b) Scatter graph comparing cytoplasmic and nuclear expression of Ras using Ras Ab-1 antibody. (c) Histogram showing the intensity of total Ras expression in the cytoplasm of tumour cells. (d) Histogram showing the intensity of total Ras expression in the nuclei of tumour cells.

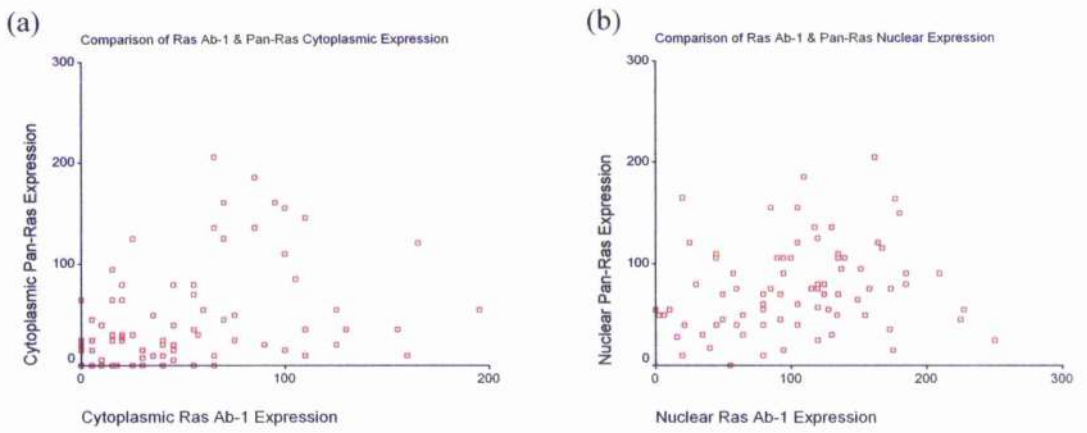

Figure 3.3: Scatter Graphs Comparing Pan-Ras and Ras Ab-1 Expression

Scatter graph comparing the expression of Ras using two different antibodies, Pan-Ras and Ras Ab-1. (a) Scatter graph comparing cytoplasmic Ras expression. (b) Scatter graph comparing nuclear Ras expression.

3.2.2 Specificity of Antibodies

The low correlation coefficients between the expression levels of Ras detected with Pan-Ras and Ras Ab-1 led me to test the specificity of all antibodies used. The specificity of all the antibodies was confirmed by western blotting (Figure 3.4). Western blotting with Pan Ras and Ras Ab-1 suggested that these antibodies were not, in fact, specific for the Ras antigen. Therefore, they were not included in future studies. However, H-Ras, N-Ras and Raf-1 all appeared to be specific for their antigen.

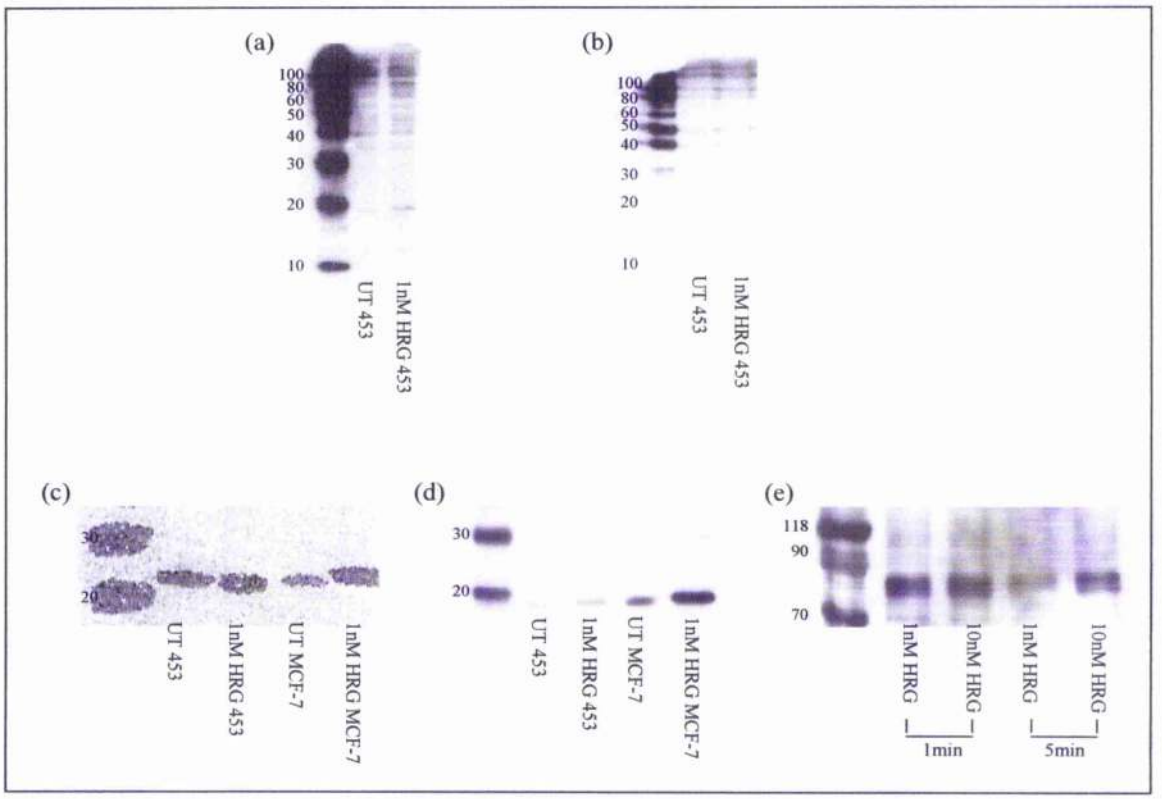

Figure 3.4: Specificity of Antibodies

Western blotting was performed to test the specificity of all the antibodies used. Untreated and 1nM Heregulin (HRG) stimulated MCF-7 and MDA-MB-453 (453) cells were used as controls. The two pan-Ras antibodies (a,b) appeared to be unspecific for the Ras antigen (21kDa). The H-Ras (c) and N-Ras (d) antibodies appeared to be specific for the Ras antigen (21kDa). The Raf-1 antibody (e) seemed to detect only the Raf-1 antigen (74kDa).

3.2.3 H-Ras Expression in Breast Tumours

H-Ras expression was observed in both the cytoplasm and the nuclei of tumour cells in 96.4% and 93.4% of tumours, respectively (Fig 3.5). Generally the cytoplasm of tumour cells exhibited higher expression levels of H-Ras than the nuclei. There was a positive correlation between cytoplasmic and nuclear H-Ras expression: patients whose tumours

strongly expressed cytoplasmic H-Ras tended to express higher levels of nuclear H-Ras ($R^2 = 0.360$, $p<0.0005$).

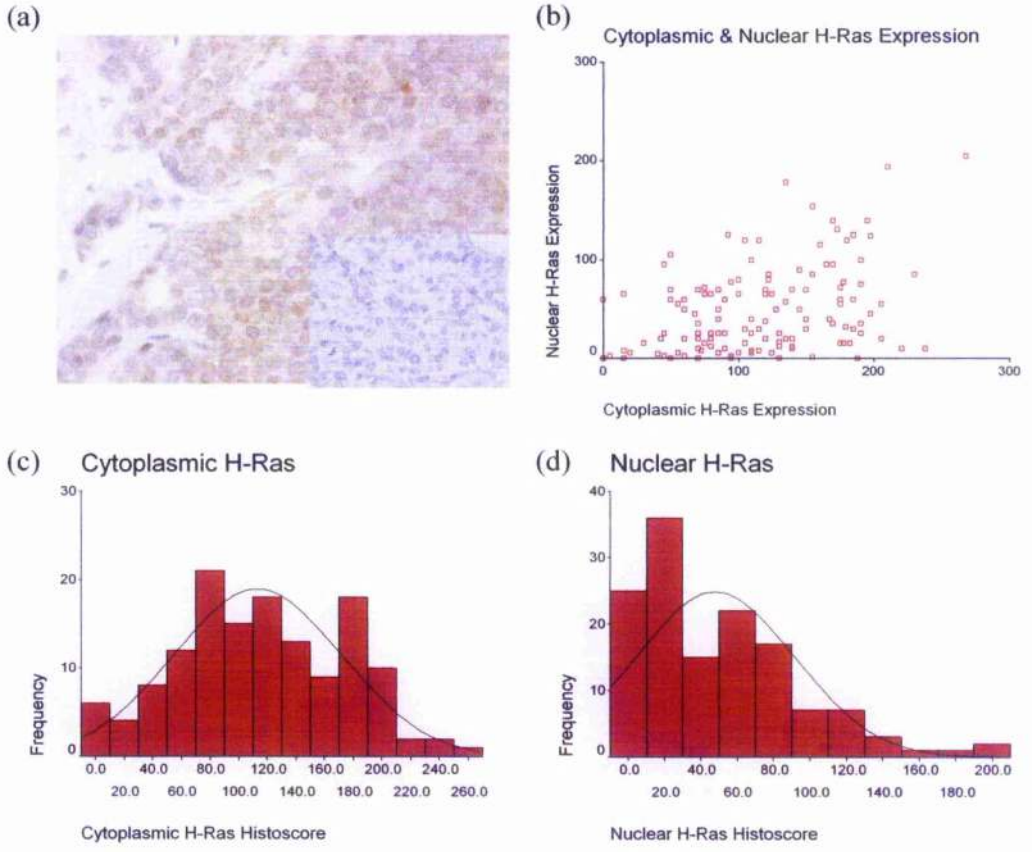

Figure 3.5: H-Ras Immunohistochemistry

(a) Breast tumour stained with H-Ras antibody. H-Ras was detected in both the cytoplasm and nuclei of tumour cells. Insert shows negative control. (b) Scatter graph comparing cytoplasmic and nuclear expression of H-Ras. (c) Histogram showing the intensity of H-Ras expression in the cytoplasm of tumour cells. (d) Histogram showing the intensity of H-Ras expression in the nuclei of tumour cells.

3.2.4 N-Ras Expression in Breast Tumours

N-Ras was detected in the cytoplasm and nuclei of tumour cells in 97.8% and 94.9% of patients respectively (Figure 3.6). Tumours showed elevated levels of cytoplasmic N-Ras expression in comparison to nuclear levels. There was, however, a positive correlation

between the expression of N-Ras in the two subcellular compartments (R^2= 0.452, $p<0.0005$).

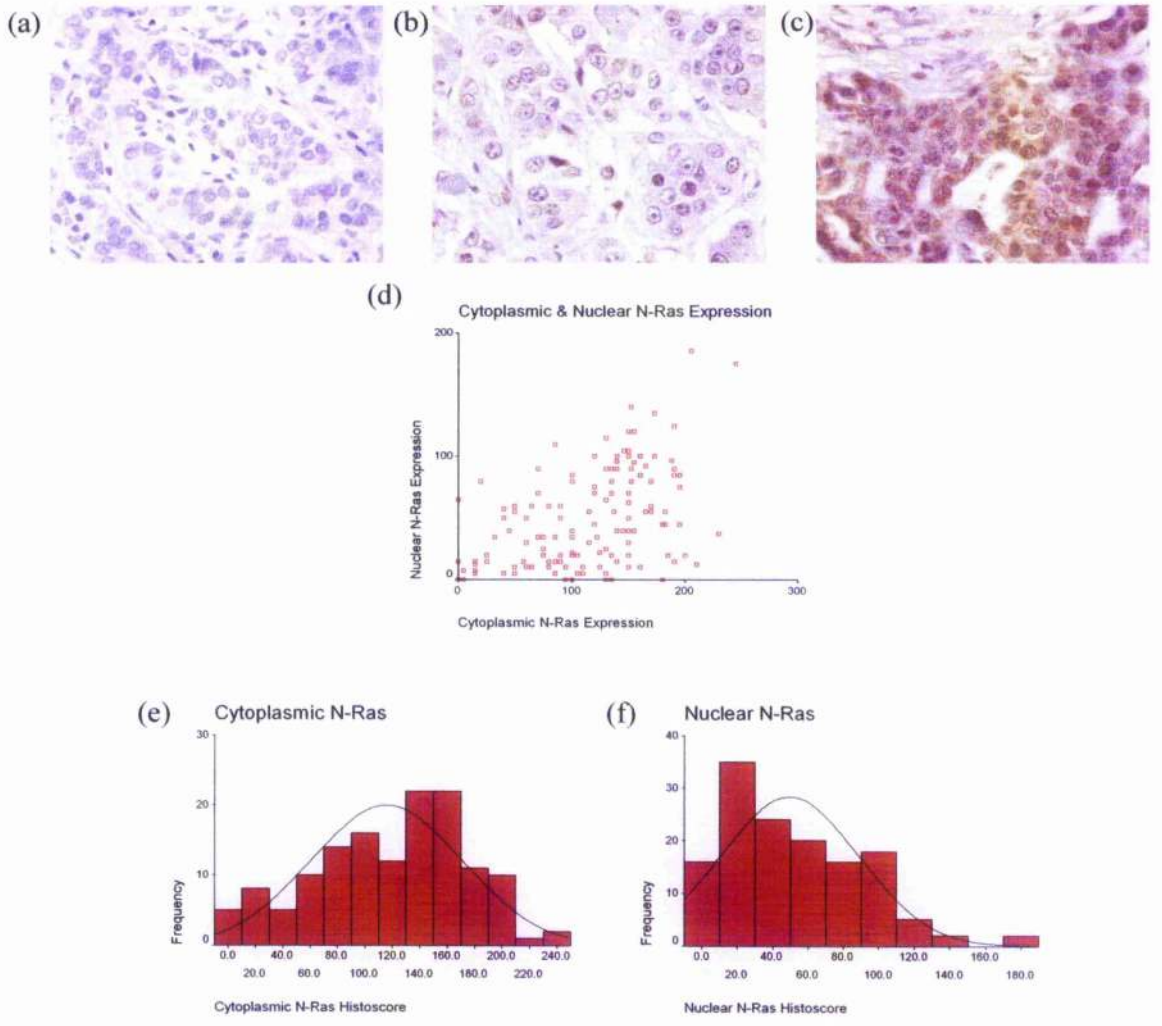

Figure 3.6: N-Ras Immunohistochemistry

(a-c) Breast tumour stained with N-Ras antibody. N-Ras was detected in both the cytoplasm and nuclei of tumour cells. (a) Negative control, (b) Example of tumour with low N-Ras expression (IHC score < UQ), (c) Example of tumour with high N-Ras expression (IHC score > UQ). (d) Scatter graph comparing cytoplasmic and nuclear expression of N-Ras. (e) Histogram showing the intensity of N-Ras expression in the cytoplasm of tumour cells. (f) Histogram showing the intensity of N-Ras expression in the nuclei of tumour cells.

3.2.5 Co-expression of H- and N-Ras in Breast Tumours

Of the 136 breast tumours that were analysed for both H-Ras and N-Ras, three patients did not express H-Ras, whilst only one was negative for N-Ras. No tumour was negative for both isoforms. There did appear to be a relationship between the expression patterns of the two isoforms: tumours that expressed high levels of cytoplasmic H-Ras also expressed increased levels of N-Ras (R^2=0.275, p=0.001) (Figure 3.7). Additionally, tumours with elevated nuclear H-Ras exhibited stronger levels of nuclear N-Ras (R^2=0.264, p=0.002) (Figure 3.7). Tumours were more likely to express the cytoplasmic form of the protein but not the nuclear counterpart. Twelve patients lacked nuclear but not cytoplasmic H- or N-expression. No breast tumour that displayed cytoplasmic Ras was negative for both H- and N-Ras in the nuclei. Furthermore, the median nuclear scores for both H- and N-Ras were significantly lower than their cytoplasmic counterparts (Wilcoxon Signed Ranks Test, p<0.0005 for both)

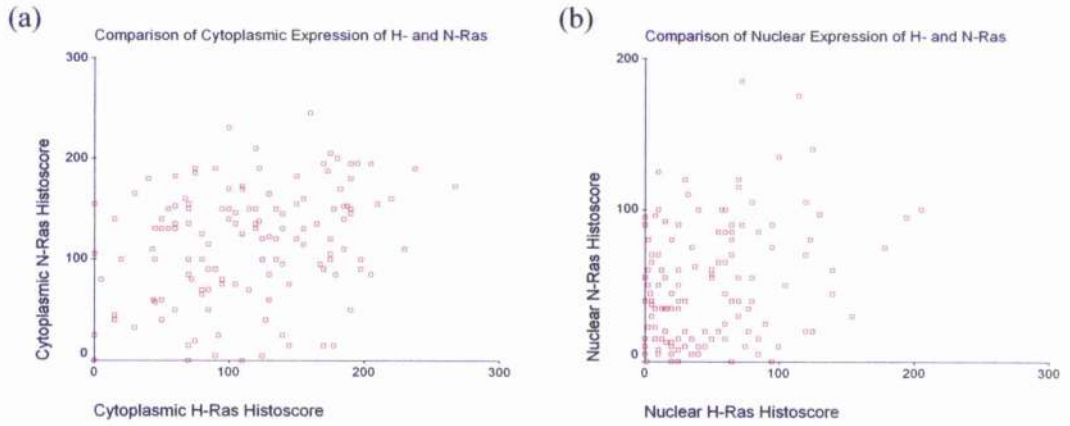

Figure 3.7: Scatter Graphs Comparing H- and N-Ras Expression

(a) Scatter graph comparing H- and N-Ras cytoplasmic expression. (b) Scatter graph comparing H- and N-Ras expression.

3.2.6 Raf-1 Expression in Breast Tumours

Raf-1 protein expression was predominantly localised to the cytoplasm of invasive tumour cells. Weak nuclear staining was evident in some tumours: 94.6% of patients expressed Raf-1 in the cytoplasm of their tumours, whereas only 36.5% exhibited the nuclear form of this protein (Figure 3.8). Additionally, when expressed in the nuclei, the levels were exceedingly low (Median Nuclear Histoscore = 0, IQ Range 0 – 5). Consequently, nuclear Raf-1 was excluded from statistical analysis. Interestingly, there was a negative correlation between H-Ras nuclear expression and Raf-1 cytoplasmic expression (R^2=-0.250, p=0.035). No significant relationship between Raf-1 and N-Ras expression was observed.

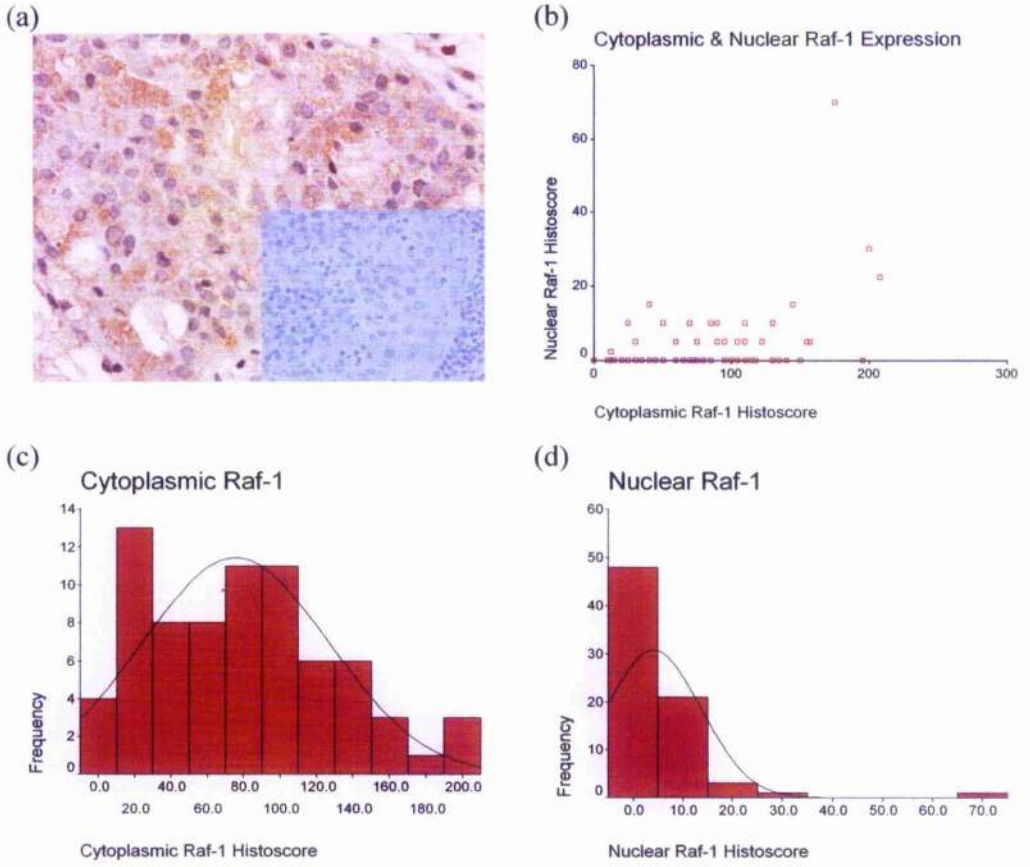

Figure 3.8: Raf-1 Immunohistochemistry

(a) Breast tumour stained with Raf-1 antibody. Raf-1 was detected primarily in the cytoplasm of tumour cells; weak nuclear Raf-1 expression was evident in relatively few tumours. Insert shows negative control. (b) Scatter graph comparing cytoplasmic and nuclear expression of Raf-1. (c) Histogram showing the intensity of Raf-1 expression in the cytoplasm of tumour cells. (d) Histogram showing the intensity of Raf-1 expression in the nuclei of tumour cells.

	Pan-Ras Cyt	Pan-Ras Nuc	Ras Ab-1 Cyt	Ras ab-1 Nuc	H-Ras Cyt	H-Ras Nuc	N-Ras Cyt	N-Ras Nuc	Raf-1 Cyt	Raf-1 Nuc
Minimum	0	0	0	0	0	0	0	0	0	0
Maximum	205	204	240	250	268	205	245	185	208	70
Mean	46	76	55	107	113	48	116	50	76	4
Median	25	73	45	108	110	35	125	40	74	0
LQ	15	45	15	60	70	13	79	15	30	0
UQ	65	105	75	150	165	70	153	80	110	5

Table 3.1: Descriptive Statistics for Histoscores

For each antibody, descriptive statistics were performed on the generated histoscores. The table shows the minimum and maximum histoscore, the mean, median, the lower and upper quartile values for each antibody. LQ=Lower Quartile, UQ=Upper Quartile

3.3 Effects of Ras & Raf Overexpression on Patient Outcome

In this pilot study, patient outcome was measured in terms of disease-free and overall survival, where recurrence and death were the end-points for each respectively. For all proteins under investigation, patients were divided into two groups: those expressing low levels of the protein of interest, and those expressing high levels. The cut-off point for defining low and high expressers for each protein was the upper quartile histoscore value.

3.3.1 Effects of Pan-Ras, H-Ras and Raf-1 expression on Breast Cancer Survival

No significant relationship between total Ras, H-Ras, or Raf-1 expression and patient disease-free or overall survival was observed.

3.3.2 Effects of N-Ras on Breast Cancer Survival

Increased levels of N-Ras in patients' tumours were significantly associated with a reduction in time to relapse and death. Patients with tumours expressing high levels of cytoplasmic N-Ras (IHC score $\geq$ 153) had a reduced disease-free survival time ($p=0.0128$, 5.46 years vs. 7.95 years) and overall survival time ($p=0.0209$, 6.80 years vs. 8.98 years) (Figure 3.9). These patients showed a relative risk of 1.8 (95% CI 1.13 – 2.97, $p=0.0142$) and 1.8 (95% CI 1.1 – 3.1, $p=0.0229$, CR) for relapse and death respectively.

Likewise, patients whose tumours had nuclear staining in the upper quartile (IHC score ≥ 80) showed a significant reduction in time to recurrence (p=0.0345, 5.51 years vs. 8.19 years) and overall survival time (p=0.0071, 6.30 years vs. 9.50 years). The relative risks of relapse or death in cases with high nuclear N-Ras were 1.7 (95% CI 1.0 – 2.8, p=0.0366) and 2.0 (95% CI 1.2 – 3.4, p=0.0083) respectively.

However, multivariate Cox-Regression revealed no evidence that N-Ras expression was independent of tumour size, grade, ER or nodal status in influencing survival. Only ER and nodal status (p<0.00005 and p=0.0005 respectively) proved to be independent markers of patient survival in this dataset.

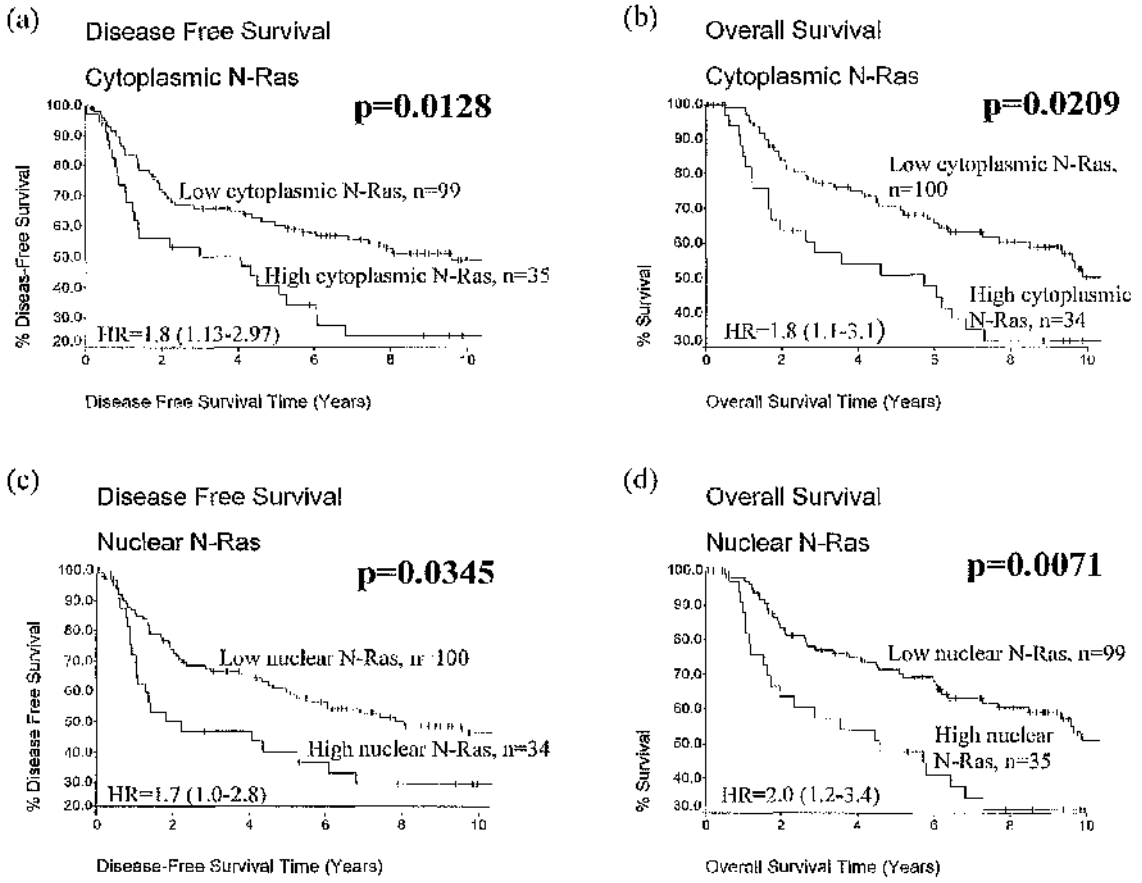

Figure 3.9: N-Ras Disease Free & Overall Survival Curves

Kaplan Meier survival curves showing disease-free and overall survival in patients whose tumours express cytoplasmic or nuclear N-Ras. (a,b) Survival curves showing a significant reduction in disease-free and overall survival time in patients whose tumours express high levels of cytoplasmic N-Ras (p=0.0128 and p=0.0209 respectively). (c,d) Survival curves showing a significant reduction in overall survival time in patients whose tumours express high levels of nuclear N-Ras (p=0.0345 and p=0.0071 respectively).
HR = Hazard Ratio (95% CI)

3.4 Relationship between Ras and Raf-1 expression and known prognostic markers

The expression of Ras and Raf-1 proteins was analysed to establish if there was a link between increasing levels of these proteins and known prognostic markers, namely tumour size, grade, nodal and ER status.

It was observed that patients whose tumours over-expressed cytoplasmic N-Ras were more likely to present with a tumour of a higher grade (grade=3) (χ^2 p=0.016). There was no significant relationship between N-Ras expression and tumour size, nodal or ER status.

Increasing levels of cytoplasmic H-Ras were also associated with tumours of a higher grade (grade=3) (χ^2 p=0.003). Additionally, patients' tumours expressing higher levels of cytoplasmic H-Ras were more likely to be ER negative (χ^2 p=0.019). Expression levels of H-Ras did not significantly impact on either tumour size or nodal status.

Similarly, no correlation was observed between pan-Ras or Raf-1 expression and tumour size, grade, nodal status, or ER status.

3.5 Discussion

There were two main discoveries in this pilot study: the first was the novel observation that Ras localised to the nuclei of tumour cells, and the second was that N-Ras expression influences patient outcome.

Until recently, it was thought that Ras and Raf-1 localised only to the cytoplasm and plasma membrane. However, it is now accepted that the Ras/Raf-1 pathway is also activated at the endoplasmic reticulum and the golgi (246). It is also acknowledged that Raf-1 is expressed in the nucleus, since several studies demonstrate that activated Raf -1

translocates to the nucleus, in order to bind and phosphorylate the retinablastoma (Rb) protein (184). Our data suggests that a nuclear function for Ras may also exist. The recent findings that the Ras/Raf-1/MAPK pathway is activated at sites other than the plasma membrane might suggest that the nucleus is another subcellular location for activation of this pathway.

In this pilot study, both Ras and Raf-1 were shown to localise to the nucleus. Other reports have shown that GRB2 is also overexpressed in breast tumour cells, and that it predominantly localises to the nuclei (150). These factors suggest a role for the Ras/Raf-1 pathway in the nucleus. Perhaps activation within the nucleus enables Raf-1 to interact with and inactivate Rb, which enables cell cycle progression and cell proliferation.

Wurzer et al identified an oncogenic form of Ras, H-Ras^{Val12,} that showed both cytoplasmic and nuclear localisation (247). However, since less than 5% of breast tumours show mutation of Ras, it seems unlikely that levels of nuclear Ras detected in our subset of breast tumours is due to expression of mutated Ras. Another explanation is that the detected nuclear Ras is due to alternative splicing of the Ras, pre-mRNA, which generates a modified Ras protein. Guil et al demonstrated that H-Ras pre-RNA can undergo alternative splicing of its last encoding exon, and that the product of this, p19 Ras, localises to both the cytoplasm and nucleus (248). The unexpected finding that Ras was localised to the nuclei of tumour cells directed a proportion of the later studies. Having identified nuclear Ras in breast tumour tissue, the subcellular localisation of Ras was further investigated *in* vitro. The findings from these studies are discussed in the proceeding chapter.

Expression of cytoplasmic and nuclear N-Ras was associated with early relapse and reduced overall survival time (Figure 3.9), confirming previous results linking Ras with poor prognosis (249;250) in breast cancer. High N-Ras expression was associated with increased tumour grade, but not tumour size, stage or ER status, all of which independently affect patient outcome. These results suggest that high N-Ras expression may identify a group of patients who require alternative therapies, e.g., farnesyl transferase inhibitors, in order to improve their long-term prognosis. Increased cytoplasmic H-Ras expression positively correlated with high tumour grade and ER negativity. Surprisingly, however, our results imply that H-Ras expression does not significantly impact on patient disease free or overall survival.

There are several possible explanations as to why N-Ras but not H-Ras expression influences patient outcome. It is well documented that the various Ras isoforms have different functions. H- and N-Ras vary in their ability to induce transformation and stimulate cell motility (251). There is also increasing evidence that membrane localisation of Ras is dependent on post-translational modifications, which differ between the isoforms, and thus modify the compartmentalisation and function of these proteins. H- and N-Ras undergo farnesylation and palmitoylation that targets them to the plasma membrane lipid rafts, via the Golgi and endoplasmic reticulum (117;246). Differences in plasma membrane localisation influence the ability of Ras to activate its downstream effectors, since concentrations of Raf-1 and PI3-K vary within plasma membrane microdomains. Raf-1 is believed to be activated at the bulky region of the plasma membrane, whereas PI3-K is present in the lipid rafts (252). Activated H- and N-Ras cycle between the lipid raft and bulky domain of the plasma membrane, and there is

evidence that N-Ras spends a longer period of time in the non-raft domain. Accordingly, N-Ras appears to be the more effective activator of Raf-1, whilst H-Ras is more effective as an activator of the PI3-K/Akt pathway (132;251). Therefore, it is plausible that Akt, as opposed to H-Ras, is a better predictor of patient survival. Likewise, activated Raf-1 or MAPK may be more appropriate predictive markers than N-Ras. It has been reported that Raf-1 is not involved in the activation of MAPK via H-Ras, but that N-Ras modulates activation of this pathway (138). The association between increased N-Ras expression and reduced patient survival could reflect greater activation of MAPK via Raf-1, resulting in enhanced tumour proliferation and subsequently poorer survival. Work from our group suggests that Raf-1 activation of MAPK may be associated with the development of hormone resistance in prostate cancer (253).

Evidence also exists that the Ras isoforms have different sensitivities to farnesyl transferase inhibitors: whilst H-Ras is very sensitive, N-Ras is only partially sensitive (113). This further supports the hypothesis that H- and N-Ras have different functional properties mediated via their different locations on the plasma membrane. The effect of differential plasma membrane localisation of H- and N-Ras on protein function and patient survival requires further investigation.

This is one of the first studies to show evidence of Ras expression in the nuclei of tumour cells and to suggest that N-Ras expression significantly influences patient survival. It highlights that Ras, in particular N-Ras, may represent an important therapeutic target in breast cancer.

The findings from this pilot study directed the course of the majority of the later studies. As previously mentioned, the novel nuclear localisation of Ras was investigated

and is discussed in the following chapter. In addition, having highlighted the possible importance of Ras, particularly N-Ras, in mediating breast cancer progression and ultimately patients' outcome, the role of these proteins in a larger cohort of patients and in the context of different treatment regimes was investigated. It was deemed appropriate to determine the importance of the Ras pathway, rather than Ras itself; therefore, the investigation was extended further downstream to Raf-1 and MAPK. The role of the Ras/Raf-1/MAPK pathway was therefore analysed in patient cohorts treated with tamoxifen or chemotherapy. The findings from these studies are discussed in later chapters.

4. Localisation of Ras Proteins

4.1 Introduction

Analysis of the expression of Ras in breast tumours from the pilot study (chapter 3) revealed an unexpected finding. H-Ras and N-Ras were both localised to the cytoplasm but were also expressed in the nuclei of tumour cells. As discussed in chapters 1 and 3, inactive Ras is localised to the cytoplasm but translocates to the plasma membrane to be activated. The literature previously suggested that Ras could only be activated and stimulate kinase cascades at the plasma membrane, but more recently it has been reported that Ras can function at the ER and Golgi. However, few studies have shown a nuclear form of this protein. The findings from the pilot study, that Ras localised to the nuclei and that expression of nuclear N-Ras was associated with a poor outcome, led to further investigation of Ras localisation, in particular N-Ras, in breast cancer cell lines, using immunofluorescent and subcellular fractionation techniques.

4.2 Immunofluorescent detection of H-, K-, and N-Ras in breast cancer cells

Immunofluorescent (IF) techniques (described in chapter 2) were used to examine the localisation of the three Ras isoforms, H-, K-, and N-Ras, in MCF-7 and MDA-MB-231 breast cancer cells. MCF-7 and MDA-MB-231 cells were either untreated or stimulated with Heregulin (HRG, MCF-7) or Epidermal Growth Factor (EGF, MDA-MB-231) for 5, 15 and 30 minutes. Subsequently the subcellular location of each of the individual Ras isoforms was monitored (Single IF). However, it was also necessary to investigate the co-localisation patterns of the Ras isoforms. Co-localisation studies were performed in pairs: H- and K-Ras; H- and N-Ras; and K- and N-Ras (Double IF).

4.2.1 Localisation of H-, K-, and N-Ras in MCF-7 & MDA-MB-231 cells

4.2.1.1 H-Ras

In untreated MCF-7 cells, H-Ras was localised to the cytoplasm. It remained in the cytoplasm following a 5-minute treatment with 1nM HRG; however extended stimulation for 15 and 30 minutes induced low levels of H-Ras to translocate into the nucleus. The presence of nuclear Ras was most apparent following the 30-minute treatment (Figure 4.1). A similar pattern was observed when cells were stimulated with 10nM HRG. However, using 10nM HRG triggered more rapid translocation of H-Ras into the nucleus. Nuclear H-Ras was detectable following the 5-minute treatment, with higher levels noticeable after the 15 and 30-minute stimulations. Expression of cytoplasmic H-Ras was maintained throughout the course of the timed treatments (Figure 4.1).

A different expression pattern for H-Ras was observed in MDA-MB-231 cells. As with MCF-7 cells, no detectable nuclear H-Ras was evident in untreated MDA-MB-231 cells. However, stimulation with 1nM and 10nM EGF failed to promote nuclear translocation of H-Ras. Even after 30 minute treatments, H-Ras was undetectable in the nuclei of MDA-MB-231 cells. Furthermore, cytoplasmic H-Ras expression appeared to be considerably weaker than, and not as uniformly expressed as, that observed in the MCF-7 cells. Instead H-Ras was compartmentalised in a region next to the nuclei. It was speculated that this location was in fact the golgi complex and, perhaps, the endoplasmic reticulum (Figure 4.2).

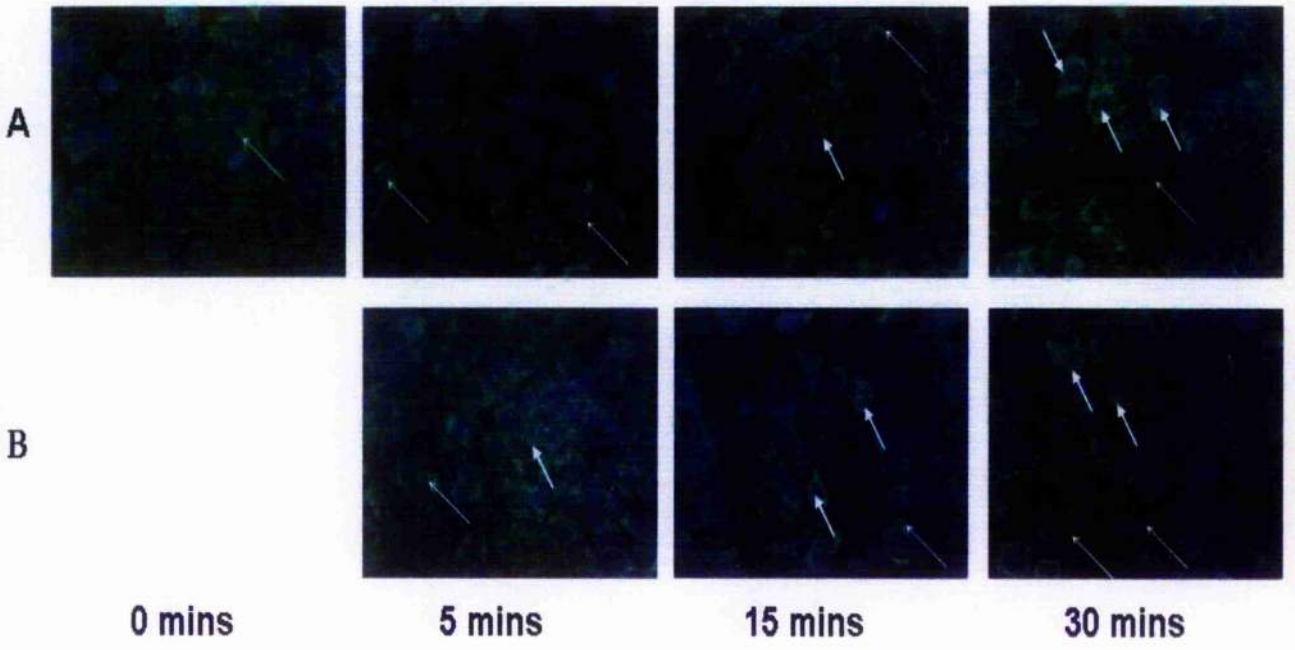

Figure 4.1: H-Ras Immunofluorescence on MCF-7 cells

Immunofluorescence of MCF-7 cells stimulated with 1nM Heregulin (A) and 10nM Heregulin (B) for 0, 5, 15 and 30 minutes and treated with H-Ras antibody and Fluorescein avidin D. H-Ras was localised to the cytoplasm and nuclei of MCF-7 cells. Block Arrows highlight cells expressing nuclear Ras. Thin arrows highlight cells expressing cytoplasmic Ras.

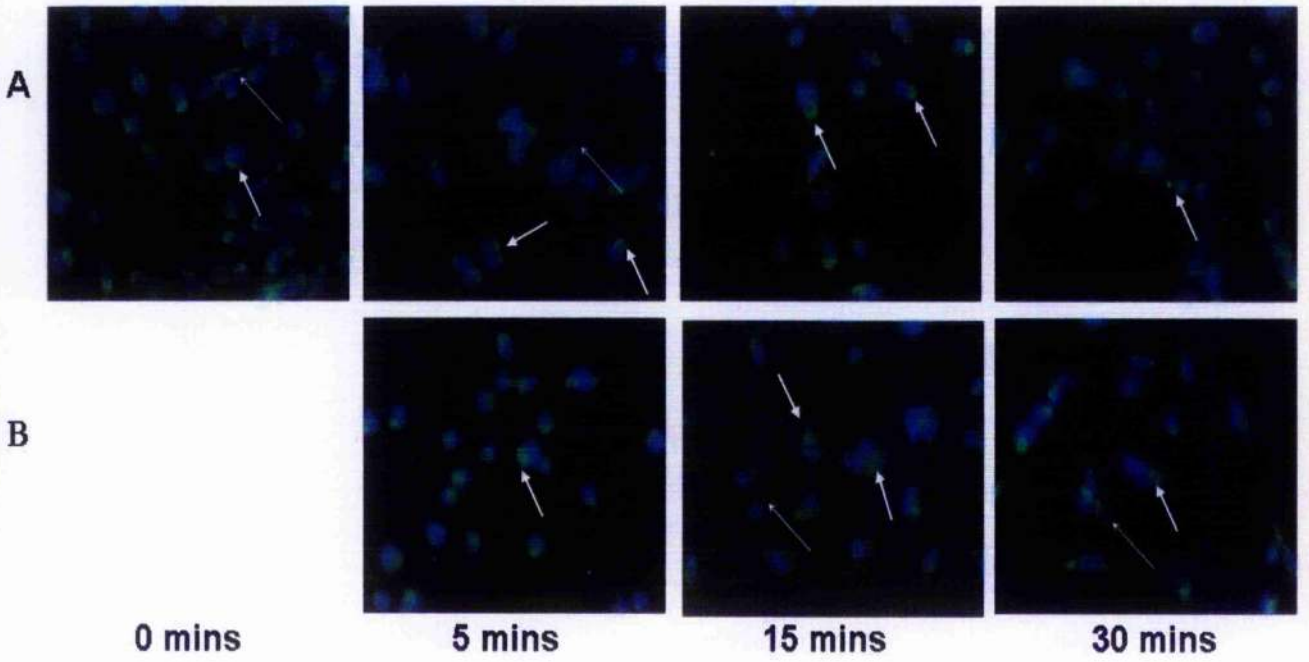

Figure 4.2: H-Ras Immunofluorescence on MDA-MB-231 cells

Immunofluorescence of MDA-MB-231 cells stimulated with 1nM EGF (A) and 10nM EGF (B) for 0, 5, 15 and 30 minutes and treated with H-Ras antibody and Fluorescein avidin D. H-Ras was compartmentalised to a region next to the nuclei, hypothesised to be the golgi and the endoplasmic reticulum. Low levels of H-Ras were also detected in the cytoplasm. Block Arrows highlight cells expressing Ras at the golgi/endoplasmic reticulum. Thin arrows highlight cells expressing cytoplasmic Ras.

4.2.1.2 K-Ras

K-Ras was detectable only in the cytoplasm of untreated MCF-7 cells. Upon stimulation with HRG, K-Ras was predominantly localised to the cytoplasm but was also present within some nuclei. After only 5 minutes of 1nM HRG treatment, low levels of nuclear K-Ras were evident. But as with H-Ras, the highest levels of nuclear K-Ras were observed after the 30 minute treatment. However, the levels of nuclear K-Ras were slightly lower when treated with 10nM HRG (Figure 4.3).

The K-Ras isoform failed to localise to MDA-MB-231 nuclei, despite stimulation with EGF. However, in contrast to the H-Ras pattern of expression, K-Ras was detected at relatively strong levels throughout the cytoplasm of the cells at all time points. Consequently, K-Ras did not appear to localise to the same confined subcellular body (golgi and endoplasmic reticulum) as H-Ras. K-Ras was observed at this location in only a few cells (Figure 4.4).

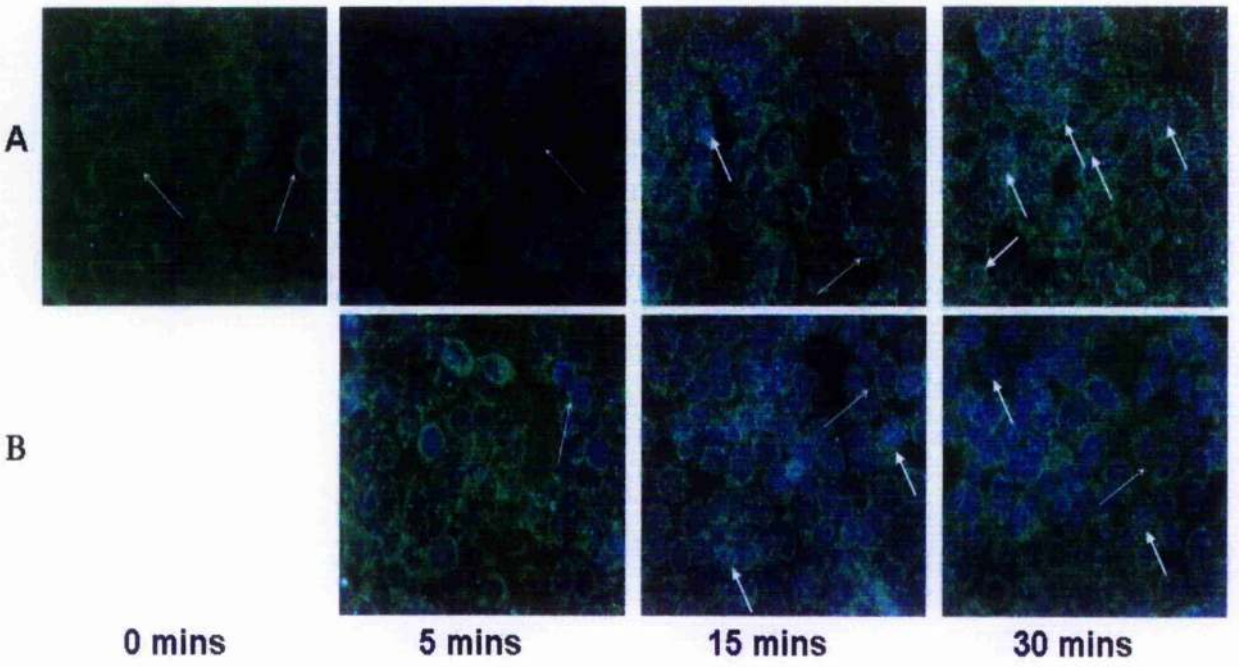

Figure 4.3: K-Ras Immunofluorescence on MCF-7 cells

Immunofluorescence of MCF-7 cells stimulated with 1nM Heregulin (A) and 10nM Heregulin (B) for 0, 5, 15 and 30 minutes and treated with K-Ras antibody and Fluorescein avidin D. K-Ras was localised to the cytoplasm and nuclei of MCF-7 cells. Block Arrows highlight cells expressing nuclear Ras. Thin arrows highlight cells expressing cytoplasmic Ras.

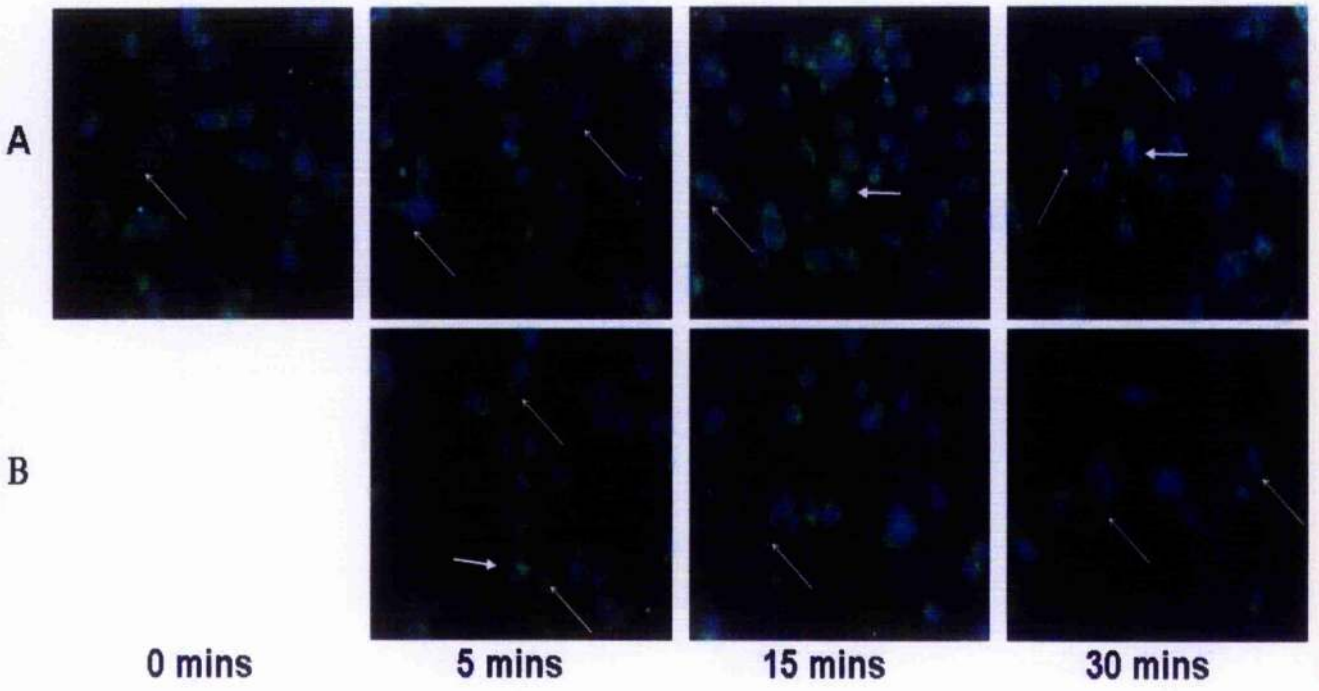

Figure 4.4: K-Ras Immunofluorescence on MDA-MB-231 cells

Immunofluorescence of MDA-MB-231 cells stimulated with 1nM EGF (A) and 10nM EGF (B) for 0, 5, 15 and 30 minutes and treated with K-Ras antibody and Fluorescein avidin D. K-Ras was predominantly localised to the cytoplasm of cells, but weaker levels were detected at a region next to the nuclei, hypothesised to be the golgi and the endoplasmic reticulum. Block Arrows highlight cells expressing Ras at the golgi/endoplasmic reticulum. Thin arrows highlight cells expressing cytoplasmic Ras.

4.2.1.3 N-Ras

Only cytoplasmic N-Ras was evident in untreated MCF-7 cells. The level of N-Ras present within the cytoplasm seemed to remain fairly constant throughout the timed treatments. Stimulation with HRG induced N-Ras to translocate into the nuclei of the cells. The 15 minute treatment with both 1nM and 10nM HRG produced the strongest levels of nuclear N-Ras (Figure 4.5).

The expression and localisation of N-Ras in the MDA-MB-231 cells paralleled that observed with H-Ras. Yet again, there was no evidence of N-Ras being localised to the nuclei of cells, and expression in the cytoplasm was sparse. However, strong levels were detected at the proposed site of the golgi complex and the endoplasmic reticulum (Figure 4.6).

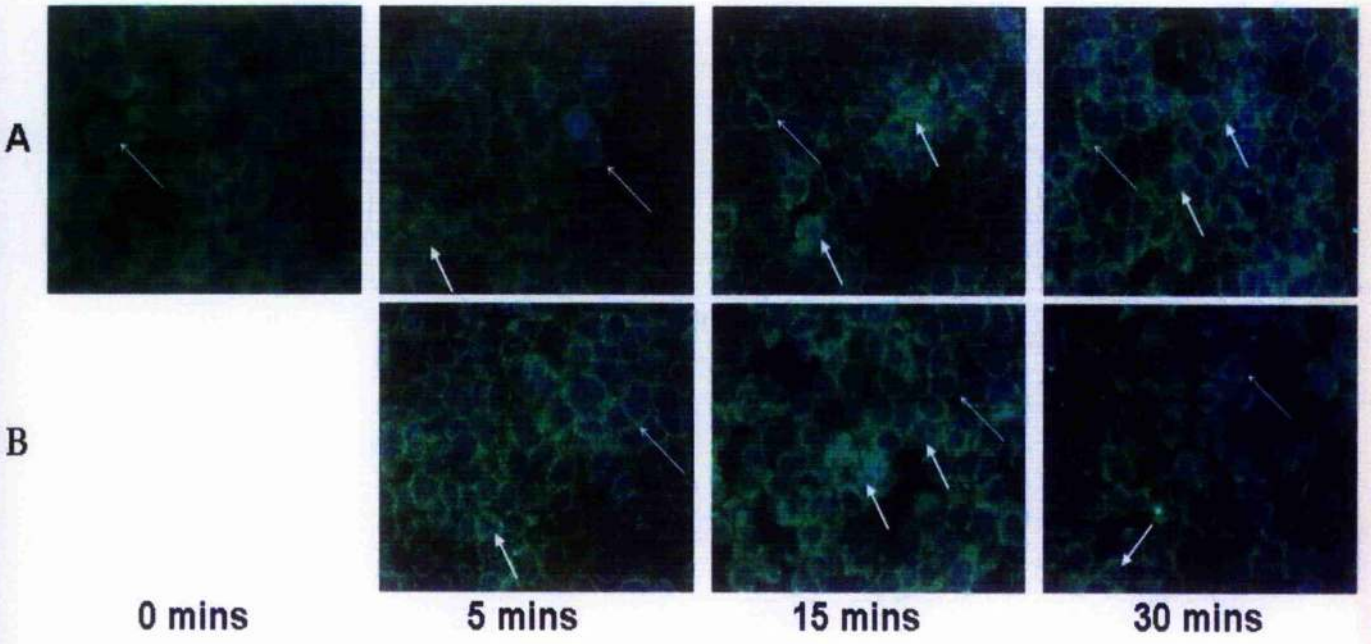

Figure 4.5: N-Ras Immunofluorescence on MCF-7 cells

Immunofluorescence of MCF-7 cells stimulated with 1nM Heregulin (A) and 10nM Heregulin (B) for 0, 5, 15 and 30 minutes and treated with N-Ras antibody and Fluorescein avidin D. N-Ras was localised to the cytoplasm and nuclei of MCF-7 cells. Block Arrows highlight cells expressing nuclear Ras. Thin arrows highlight cells expressing cytoplasmic Ras.

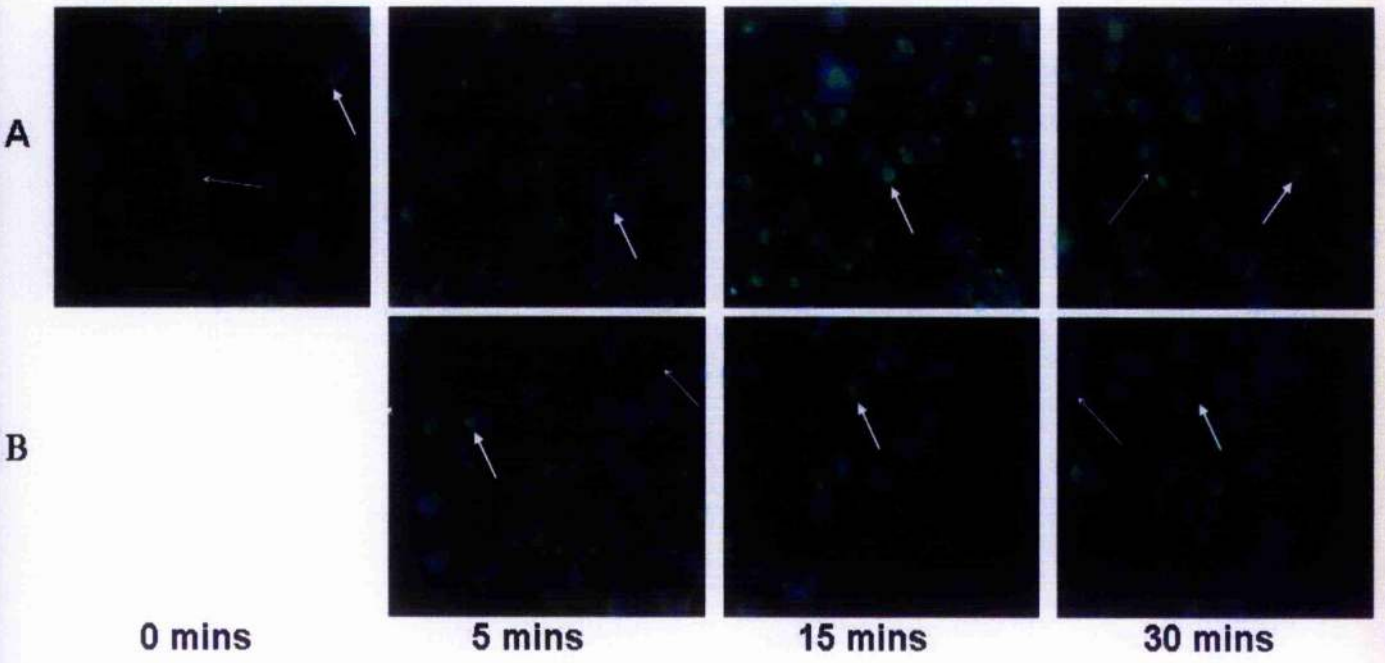

Figure 4.6: N-Ras Immunofluorescence on MDA-MB-231 cells

Immunofluorescence of MDA-MB-231 cells stimulated with 1nM EGF (A) and 10nM EGF (B) for 0, 5, 15 and 30 minutes and treated with N-Ras antibody and Fluorescein avidin D. N-Ras was compartmentalised to a region next to the nuclei, hypothesised to be the golgi and the endoplasmic reticulum. Low levels of N-Ras were also detected in the cytoplasm. Block Arrows highlight cells expressing Ras at the golgi/endoplasmic reticulum. Thin arrows highlight cells expressing cytoplasmic Ras.

4.2.2 Co-localisation of H-, K-, and N-Ras in MCF-7 and MDA-MB-231 cells

4.2.2.1 Co-localisation of H- and K-Ras

For the double IF studies, H-Ras was detected using green fluorescence (Fluorescein avidin D), whilst K-Ras was detected with a red fluorochrome (Texas Red). Consequently, when the two proteins co-localised, a yellow fluorescence was evident. In the MCF-7 cells, H-Ras and K-Ras co-localised to the cytoplasm, evident from the yellow fluorescence throughout the cytoplasm. However, within the untreated cells, there were regions of the cytoplasm where K-Ras was more apparent than H-Ras, depicted by the red fluorescence. Surprisingly, only very low levels of both H-Ras and K-Ras were detected in the nuclei of cells (Figure 4.7).

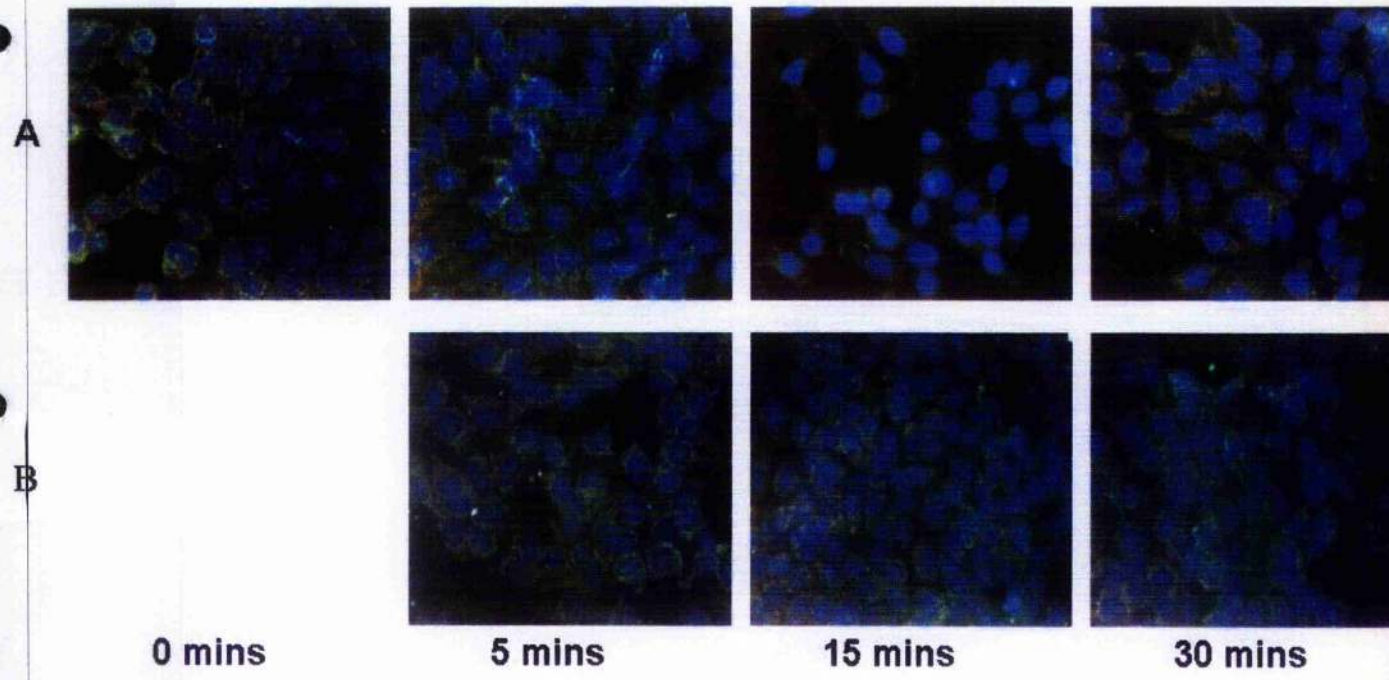

Figure 4.7: Co-localisation of H-Ras & K-Ras in MCF-7 cells

Immunofluorescence of MCF-7 cells stimulated with 1nM Heregulin (A) and 10nM Heregulin (B) for 0, 5, 15 and 30 minutes and treated with H-Ras antibody and Fluorescein avidin D (green) followed by K-Ras antibody and Texas Red (red). When H-Ras and K-Ras were co-expressed in cells, a yellow fluorescence was emitted. H-Ras and K-Ras co-localised to the cytoplasm and, to a lesser extent, to the nuclei of MCF-7 cells.

4.2.1.2 Co-localisation of H- and N-Ras

As described above, H-Ras was detected in cells using the green Fluorescein avidin D, whilst N-Ras was detected with Texas Red. Again, when the two proteins were co-expressed, a yellow fluorescence was emitted. Both H- and N-Ras were co-expressed in the cytoplasm of the MCF-7 cells throughout all timed treatments. Once more very low levels of nuclear Ras, either H- or N-Ras, were detected (Figure 4.8).

In the MDA-MB-231 cells, H- and N-Ras were again shown to co-localise. As observed in the single IF studies, both H- and N-Ras expression was very weak in the cytoplasm, but both were co-localised and strongly expressed in the subcellular compartment thought to be the golgi and endoplasmic reticulum (Figure 4.9).

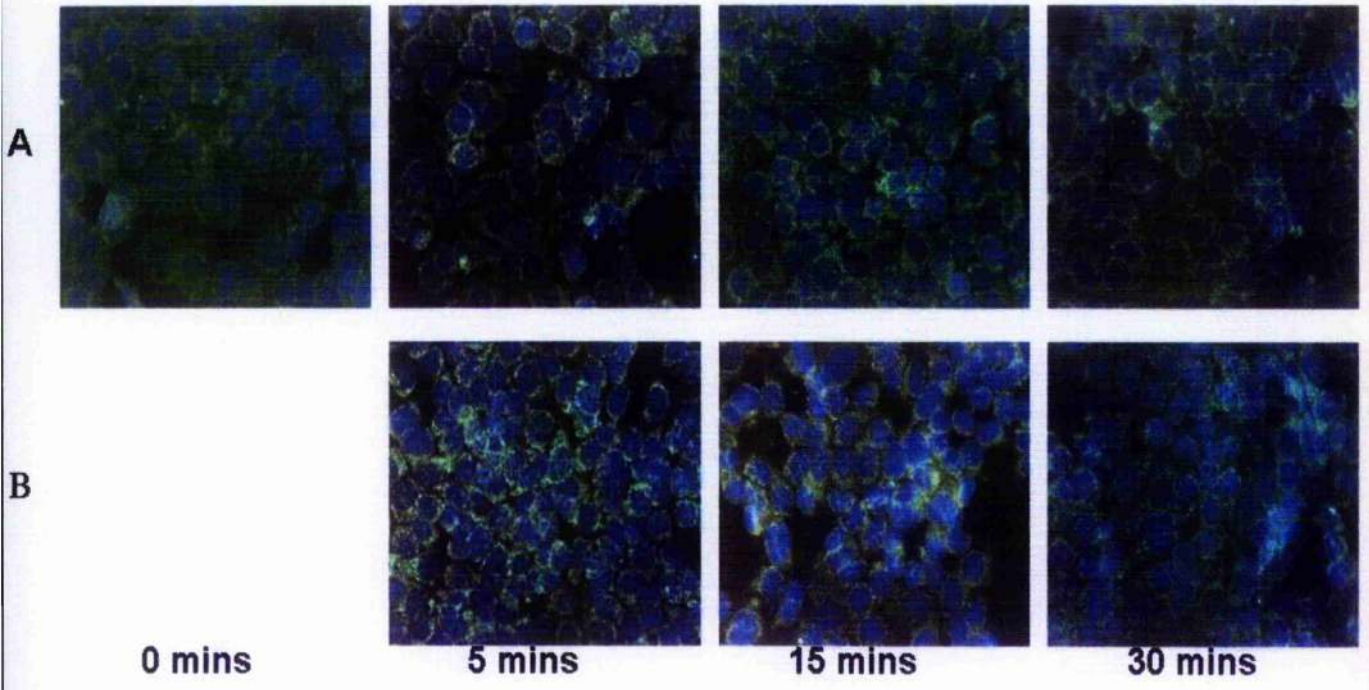

Figure 4.8: Co-localisation of H-Ras & N-Ras in MCF-7 cells

Immunofluorescence of MCF-7 cells stimulated with 1nM Heregulin (A) and 10nM Heregulin (B) for 0, 5, 15 and 30 minutes and treated with H-Ras antibody and Fluorescein avidin D (green) followed by N-Ras antibody and Texas Red (red). When H-Ras and N-Ras were co-expressed in cells, a yellow fluorescence was emitted. H-Ras and N-Ras co-localised to the cytoplasm and, to a lesser extent, to the nuclei of MCF-7 cells.

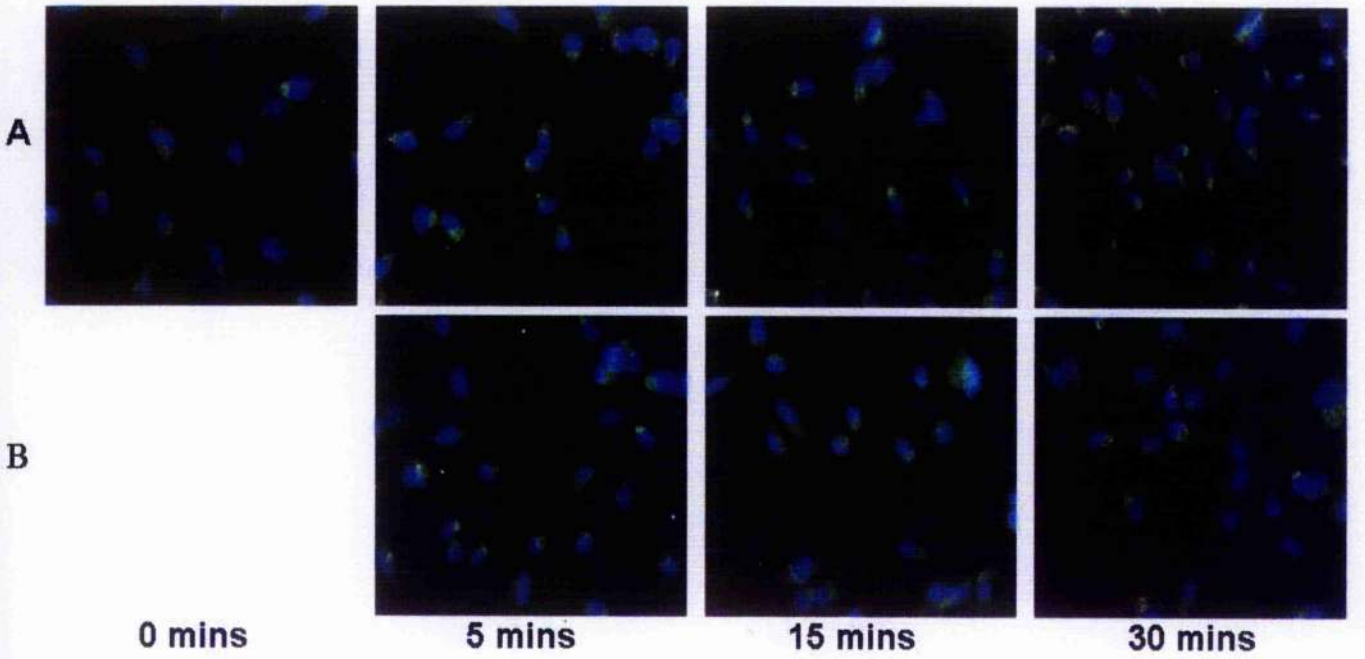

Figure 4.9: Co-localisation of H-Ras & N-Ras in MDA-MB-231 cells

Immunofluorescence of MDA-MB-231 cells stimulated with 1nM EGF (A) and 10nM EGF (B) for 0, 5, 15 and 30 minutes and treated with H-Ras antibody and Fluorescein avidin D (green) followed by N-Ras antibody and Texas Red (red). When H-Ras and N-Ras were co-expressed in cells, a yellow fluorescence was emitted. H-Ras and N-Ras co-localised to the cytoplasm and to the supposed Golgi and endoplasmic reticulum region.

4.2.1.3 Co-localisation of K- and N-Ras

In order to investigate the co-localisation of K- and N-Ras, N-Ras was bound to Fluoroscein Avidin D, whilst K-Ras was bound to Texas Red. In the MCF-7 cells, the cytoplasm fluoresced yellow, indicating that both K-Ras and N-Ras were co-expressed in the cytoplasm. As in the single IF experiments, the levels of cytoplasmic Ras appeared to remain constant throughout the timed treatments (Figure 4.10).

As perhaps expected, following the results from the single IF performed on the MDA-MB-231 cells, K-Ras and N-Ras exhibited slightly different expression patterns. Only K-Ras was prominently localised to the cytoplasm of the cells. However, both were co-expressed at the Golgi and endoplasmic reticulum. As before, neither Ras isoform was expressed in the nuclei, even when stimulated with EGF (Figure 4.11).

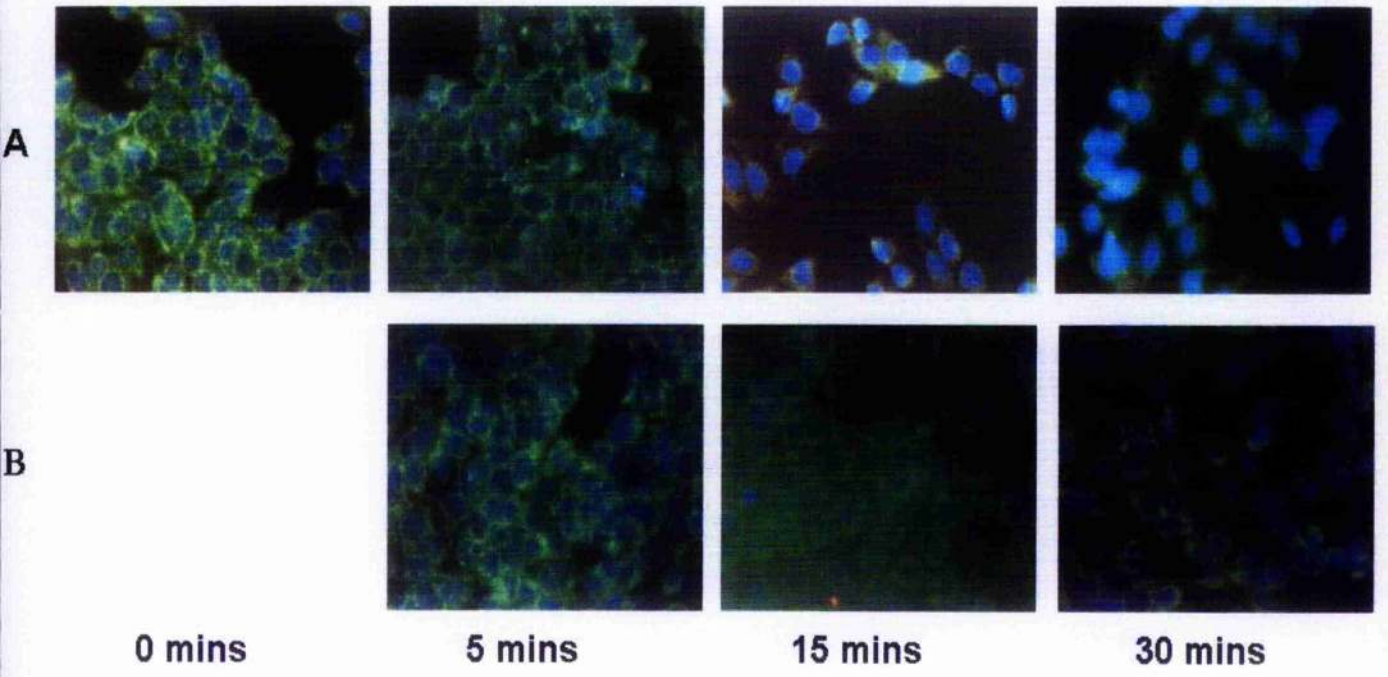

Figure 4.10: Co-localisation of K-Ras & N-Ras in MCF-7 cells

Immunofluorescence of MCF-7 cells stimulated with 1nM Heregulin (A) and 10nM Heregulin (B) for 0, 5, 15 and 30 minutes and treated with N-Ras antibody and Fluorescein avidin D (green) followed by K-Ras antibody and Texas Red (red). When N-Ras and K-Ras were co-expressed in cells, a yellow fluorescence was emitted. N-Ras and K-Ras co-localised to the cytoplasm and, to a lesser extent, to the nuclei of MCF-7 cells.

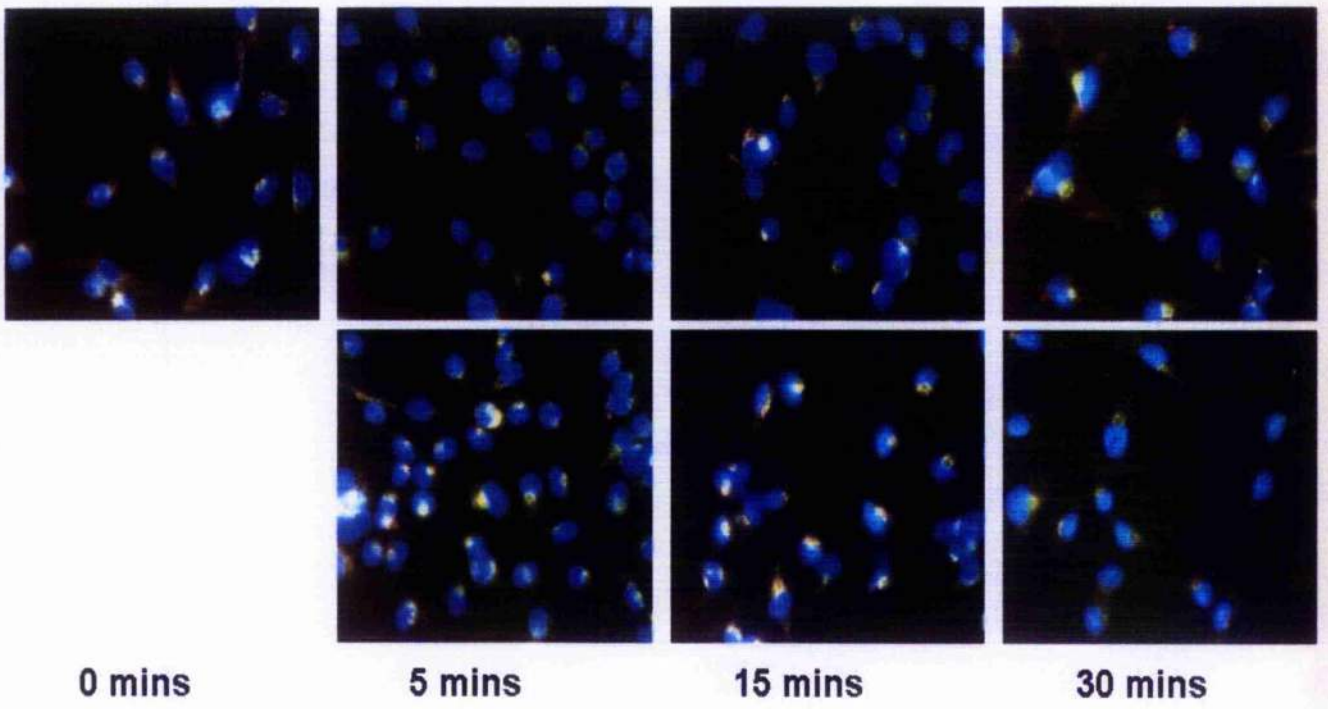

Figure 4.11: Co-localisation of K-Ras & N-Ras in MDA-MB-231 cells

Immunofluorescence of MDA-MB-231 cells stimulated with 1nM EGF (A) and 10nM EGF (B) for 0, 5, 15 and 30 minutes and treated with N-Ras antibody and Fluorescein avidin D (green) followed by K-Ras antibody and Texas Red (red). When K-Ras and N-Ras were co-expressed in cells, a yellow fluorescence was emitted. K-Ras and N-Ras co-localised to the cytoplasm and to the supposed Golgi and endoplasmic reticulum region. However, K-Ras expression seemed to be more predominant in the cytoplasm than N-Ras.

4.3 Investigation of N-Ras localisation in MCF-7 cells using subcellular fractionation

To further verify the existence of a nuclear form of Ras, subcellular fractionation was performed on MCF-7 cells. The preliminary fractionation experiment investigated the localisation of N-Ras in membranous, cytoplasmic, nuclear and cytoskeletal fractions of MCF-7 cells that were either untreated, or had been stimulated with HRG. This experiment again highlighted that N-Ras was expressed in the nuclei of breast cancer cells. N-Ras was detected in the membrane, cytoplasmic and nuclear fractions but not in the cytoskeletal fractions of both untreated and stimulated cells (Figure 4.12).

The localisation of N-Ras was further probed in MCF-7 cells that had been treated with HRG, E2 and MAPK inhibitors, Felodipine and U0126. These subcellular fractionation experiments provided further evidence of the presence of a nuclear form of N-Ras. Figures 4.13 and 4.14 highlight the localisation of N-Ras to the membrane, cytoplasm and nuclei of MCF-7 cells.

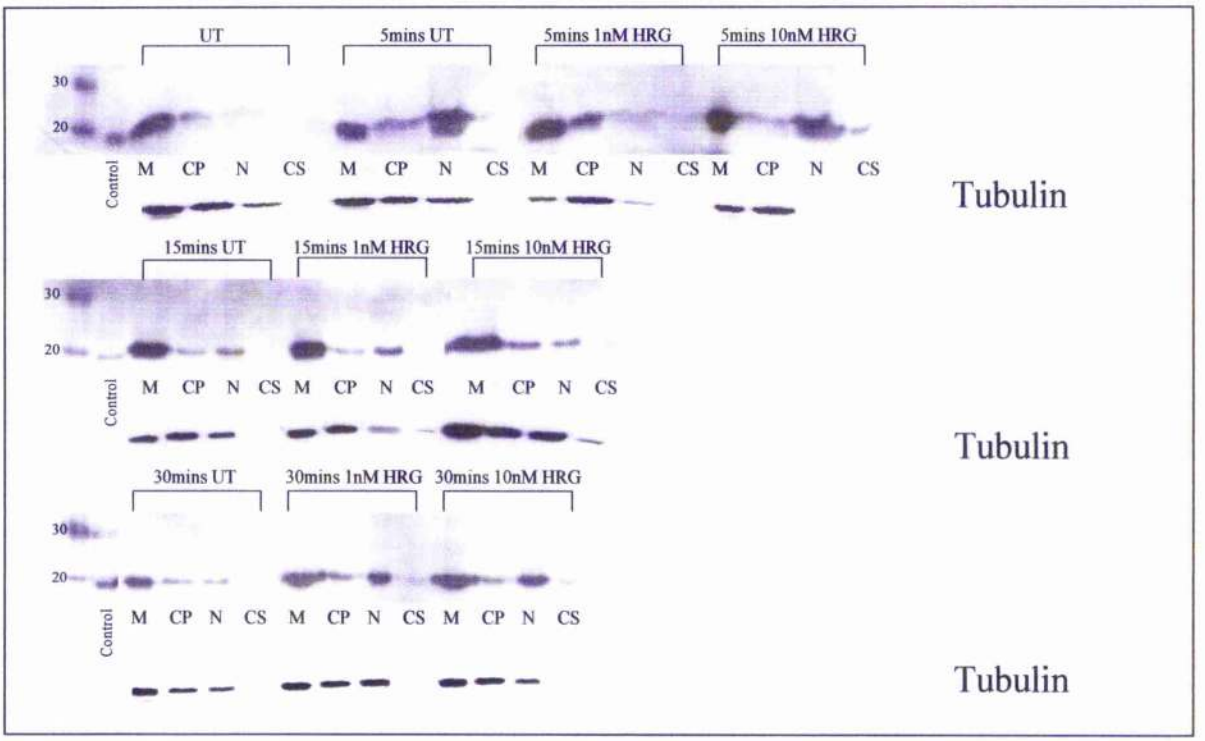

Figure 4.12: Subcellular Fractionation of MCF-7 Cells

Western blot of MCF-7 protein fractions probed for N-Ras (21kDa). MCF-7 cells were either untreated or stimulated with 1nM and 10nM Heregulin (HRG) for 5, 15 and 30 minutes before subcellular fractionation was performed. N-Ras was detected in the membrane, cytoplasmic and nuclear fraction. Tubulin was used as a loading control.
C= Control (untreated MDA-MB-453 cells), M = Membrane fraction, CP = Cytoplasmic fraction, N = Nuclear fraction, CS = Cytoskeletal fraction

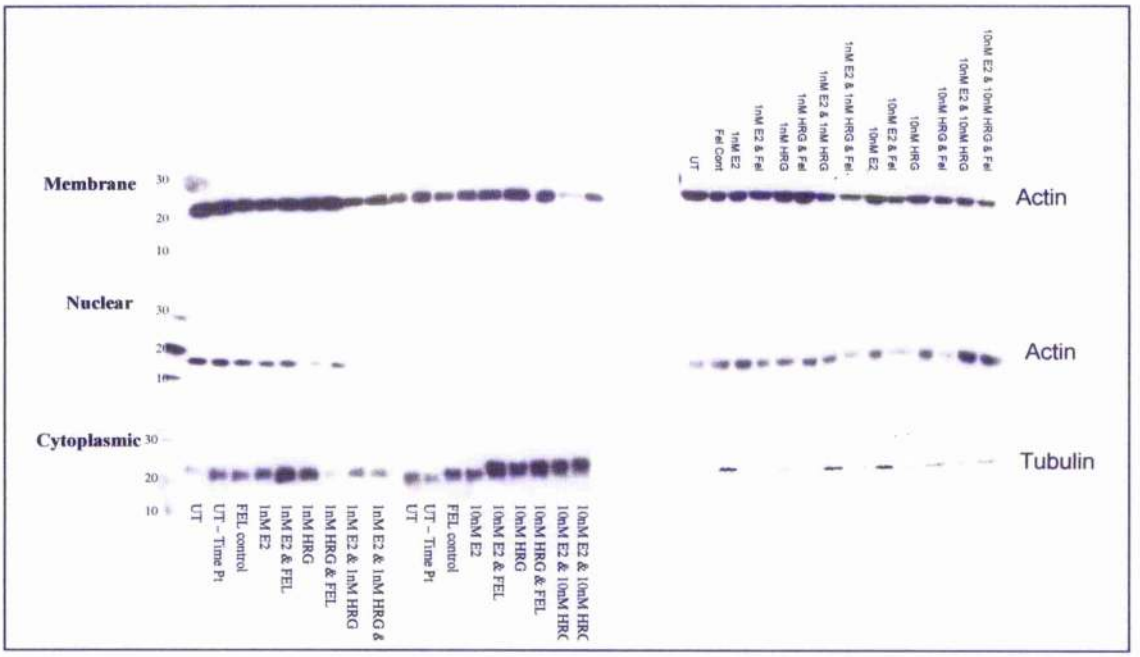

Figure 4.13: Detection of N-Ras in protein fractions following 5 minute treatment with HRG, E2 and FEL

MCF-7 cells were treated with 1/10nM Heregulin (HRG) and Oestrogen (E2), singly and in combination, and in the presence or absence of Felodipine (FEL), for 5 minutes. Subcellular fractionation was then performed, generating membranous, cytoplasmic and nuclear fractions. Western blotting was performed on 25μg of membrane, nuclear and cytoplasmic protein fractions and samples probed for N-Ras (21kDa) expression. Tubulin and Actin were used as loading controls.
UT= Untreated control without DMSO & EtOH, UT time pt = 5 minute untreated control with DMSO & ETOH, FEL control= 30μM Felodipine only

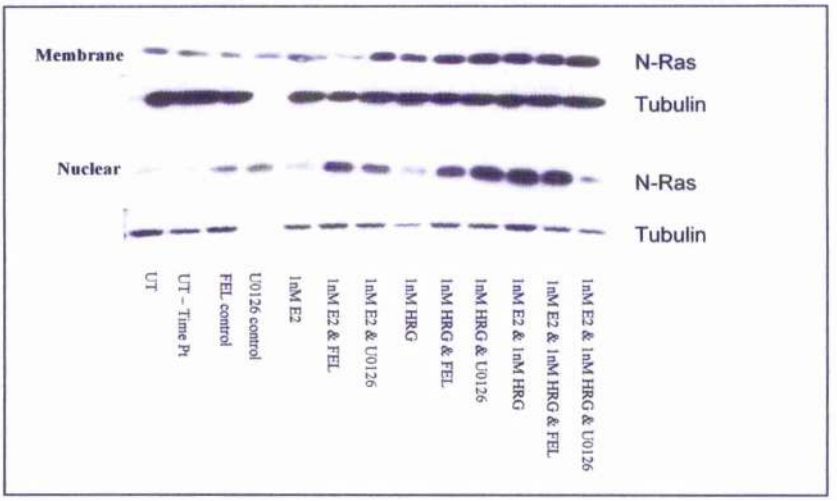

Figure 4.14: Detection of N-Ras in protein fractions following 15 minute treatment with HRG, E2, FEL and U0126

MCF-7 cells were treated with 1nM Heregulin (HRG) and Oestrogen (E2), singly and in combination, and in the presence or absence of Felodipine (FEL) and U0126, for 15 minutes. Subcellular fractionation was then performed, generating membranous, and nuclear fractions. Western blotting was performed on 25μg of membrane and nuclear protein fractions and samples probed for N-Ras (21kDa) expression. Tubulin was used as a loading control.

UT= Untreated control without DMSO & EtOH, UT time pt = 5 minute untreated control with DMSO &, ETOH, FEL control= 30μM Felodipine only, U0126 control = 10mM U0126 only

4.4 Discussion

This *in vitro* study confirmed the pilot study observation (Chapter 3) that Ras localises to the nuclei of breast tumour cells. Using both immunofluorescence and subcellular fractionation techniques, H-, K- and N-Ras were all localised to the nuclei of MCF-7 breast cancer cells. As discussed in the previous chapter, only a few reports support the findings of a nuclear form of Ras. One study identified an oncogenic form of Ras, H-Ras^{Val12}, that presented in the nuclei of cells (247). However, there is no indication that MCF-7 cells carry this mutation. In fact, Ras mutations are a very rare occurrence in breast cancer cells. Additionally, it has been shown that H-Ras mRNA can undergo

alternative splicing of its last encoding exon, to produce a 19kDa product that localises to both the cytoplasm and nuclei of cells (248). However, this may justify the presence of H-Ras in the nucleus, but does not offer any explanation for the localisation of either K-Ras or N-Ras to the nucleus. There is no evidence that N-Ras mRNA undergoes alternative splicing to produce a nuclear isoform, and while it is well established that K-Ras has two alternative fourth exons that yield K-RasA and K-RasB, there has been no indication that there is a nuclear K-Ras isoform. Consequently, there must be other, as of yet undiscovered, explanations for the presence of the Ras isoforms in the nuclei of cells.

As previously mentioned, until recently it was thought that Ras could only be activated at the plasma membrane. However, it is now well established that Ras can be activated at the Golgi and the endoplasmic reticulum, and that this activation is sufficient to stimulate phosphorylation and activation of MAPK (130;139;141). It is, therefore, feasible to hypothesise that the nucleus is an additional subcellular location for the activation of Ras, or that activation of Ras, at either the plasma membrane or the Golgi, induces it to translocate into the nucleus. Analysis of the MCF-7 IF studies highlight that Ras is not detectable in the nucleus of untreated cells, but that treatment with HRG induced the expression of Ras in the nucleus, generally after 15 minutes. Since the antibodies used throughout this study detect total Ras, i.e, inactive and active forms, this perhaps suggests that Ras is activated outside the nucleus and then translocates in. The delay in expression of nuclear Ras is particularly interesting since several studies have demonstrated that there are distinct differences between the kinetics of Ras activation at the plasma membrane, versus the golgi and endoplasmic reticulum. Evidence suggests that activation of Ras at the plasma membrane is rapid (< 5 minutes) and transient, whilst

activation at the Golgi is delayed (10-20 minutes) and sustained (130;139). Furthermore, it has been proposed that inactivation of Ras at the plasma membrane and its activation at the Golgi are regulated by the Src/Phospholipase Cγ/RasGRPI pathway. Growth factors activate Src, which mediates phosphorylation of Phospholipase Cγ (PLCγ), which increases the levels of intracellular calcium ions. This subsequently results in the activation of the GEF, RasGRP1, which is translocated to the Golgi, where it assists in the activation of Ras. Simultaneously increased levels of calcium ions cause the GAP, CAPRI, to move to the plasma membrane, where it facilitates in the inactivation of Ras (141;254). Perhaps, activation of the RTKs initially stimulates activation of Ras at the plasma membrane, and then induces its inactivation, but simultaneously it promotes its activation at the golgi and its translocation into the nuclei. It is of interest that in the pilot study, a negligible percentage of breast tumours presented with membranous Ras, whereas approximately 94% exhibited the nuclear form of Ras. Analysis of MCF-7 cells may have confirmed the findings from the pilot study, but the MDA-MB-231 IF experiments generated slightly different results.

Despite Ras being detected in the nuclei of MCF-7 cells, in both IF and subcellular fractionation experiments, it was not evident in the nuclei of MDA-MB-231 cells. Even following stimulation of the cells with EGF, Ras failed to localise to the nuclei of MDA-MB-231 cells. There were, in fact, several crucial differences in the expression and localisation of Ras between the two cell lines. All three Ras isoforms were shown to co-localise in the MCF-7 cells, whereas in the MDA-MB-231 cells, the patterns of expression were very similar for H- and N-Ras, whilst K-Ras showed a more distinct expression profile. H-Ras and N-Ras expression was very limited in the

cytoplasm of MDA-MB-231, in contrast to the strong and uniform MCF-7 cytoplasmic expression. However, both appeared to be compartmentalised to a region next to the nuclei. It was speculated that this region was in fact the Golgi and the endoplasmic reticulum. Evidence from other studies investigating the expression of proteins at the Golgi using IF methods support this hypothesis (255-258).

K-Ras, on the other hand, was predominantly expressed in the cytoplasm of cells, with weaker levels detected at the proposed site of the Golgi and ER. The differences between the localisation of H-/N-Ras and K-Ras confirm previous findings that H- and N-Ras are targeted to the plasma membrane, via the Golgi and endoplasmic reticulum, but that K-Ras is relocalised from the cytoplasm to the membrane in a Golgi-independent manner (117;126-128;130;131).

This IF study raised the question: why was the localisation of the Ras isoforms different in the two breast cancer cell lines? In an attempt to answer this, the differences between the two cell lines must be addressed. There were two major distinctions between the MCF-7 and MDA-MB-231 cells. The first is that MCF-7 cells are ER positive whilst the MDA-MB-231 cells are ER negative. The second difference relates to the expression of the RTKs: MCF-7 cells express HER2 and HER3 whereas MDA-MB-231 cells are EGFR positive. Perhaps, the localisation of Ras to the nuclei is dependent on the presence of either the ER or the RTKs. It is worth noting that the EGFR has a stronger association with Src, than HER2/HER3. Possibly the presence of EGFR in the MDA-MB-231 cells stimulates the Ras pathway at the Golgi via its interaction with Src.

This study, combined with the pilot study, provides evidence of nuclear Ras in both clinical tumour samples and in a breast cancer cell line, using three different

tecniques, immunohistochemistry, immunofluorescence and subcellular fractionation. Nonetheless, the proposal that Ras localises to the nucleus will undoubtedly be met with scepticism. However, it should be noted that, until recently, the theories that activated Raf localised to the nucleus, and that a membranous form of ERα existed were both rejected. Now, it is accepted that Raf translocates into the nucleus to bind and activate the retinoblastoma protein, and that ERα is expressed at the membrane to mediate the rapid effects of E2 (48;184).

This study confirms that Ras localises to the nucleus; however, the mechanism by which it does this and its function requires further investigation. This is particularly important, as the results from the pilot study suggest that expression of nuclear N-Ras is associated with shortened disease-free and overall survival time. As mentioned above, the nucleus is possibly another subcellular compartment where Ras can activate signal transduction cascades, such as the MAPK pathway. This theory is supported by the finding that Grb2, which facilitates the activation of Ras, is overexpressed in breast cancer cells and is predominantly localised to the nuclei of cells (150). An alternative explanation is that Ras remains bound to Raf when it translocates into the nucleus, to maintain Raf in its active conformation. Further research must be performed to enable us to understand the mechanisms by which Ras translocates into the nucleus and to reveal its function. Due to the interesting results obtained from both studies, investigation of the role of Ras and also its downstream targets in regulating breast cancer progression and patient outcome continued. Consequently, this directed the focus of my research towards two key studies examining the role of the Ras pathway in mediating breast cancer

patients' response to endocrine and chemotherapeutic treatments. The results of these will be discussed in the following chapters.

5 Expression and localisation of Ras, Raf and MAPK proteins in breast tumour tissue microarrays.

5.1 Introduction

The previous two chapters highlighted the unexpected localisation of Ras proteins to the nuclei of tumour cells, and the pilot study suggested that increased expression levels of N-Ras in breast tumours significantly influenced patient survival. It was therefore appropriate to further investigate the expression and localisation of all three Ras isoforms in a larger cohort of breast tumours. The expression levels of proteins downstream of Ras, namely Raf-1 and MAPK, were also monitored. H-, K- and N-Ras and Raf-1 expression was investigated in the Steroid-Resistant Tumour Bank (STB) cohort, whilst the inactivated and activated form of Raf-1, pRaf(ser259) and pRaf(ser338) respectively, and MAPK and pMAPK, were analysed in both the STB and NEAT/BR9601 cohort of patients. As in the pilot study, expression of all proteins was monitored using an immunohistochemical approach (chapter 2.2). Additionally, genetic modifications of H-Ras, N-Ras and Raf-1 were examined in a subset of patients from the STB cohort, using FISH. This chapter aims to present the data generated from the IHC and FISH studies, in terms of the distribution and localisation of the Ras, Raf-1 and MAPK proteins. The relationship between gene and protein expression for H-Ras, N-Ras and Raf-1 is also investigated. The effects of these proteins on patient outcome and response to treatment are discussed in the next two chapters.

5.2 Specificity of antibodies

The specificity of all the antibodies was confirmed by western blotting (Figure 5.1). The specificity of H-Ras, N-Ras and Raf-1 was confirmed previously (Chapter 3, Figure 3.5).

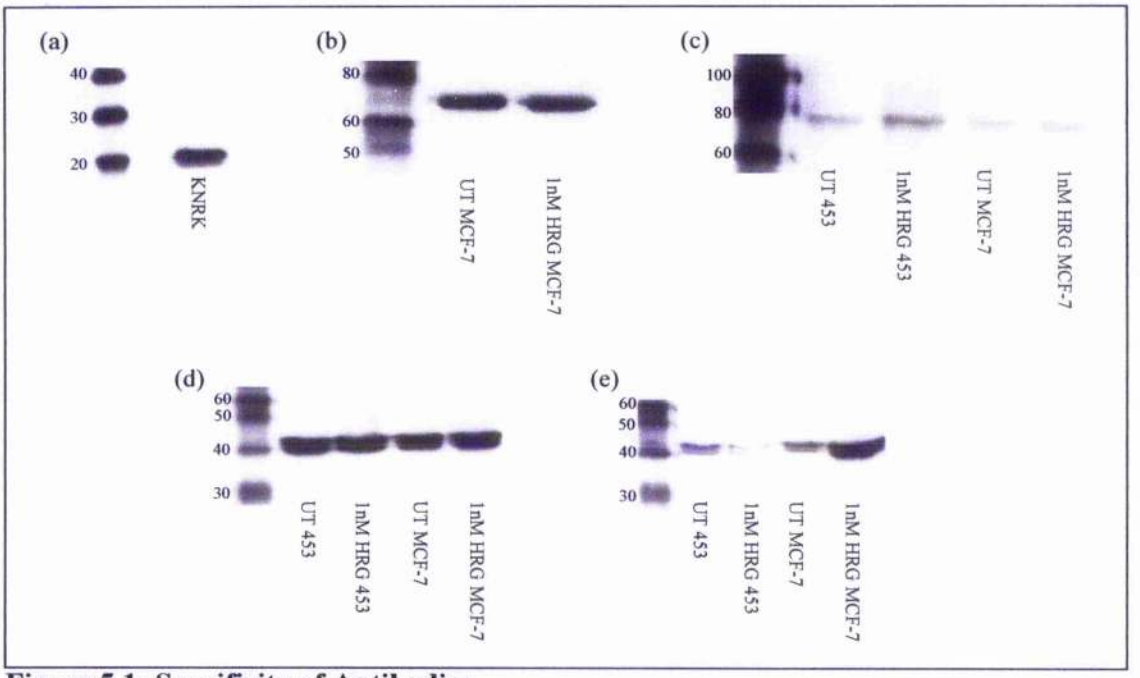

Figure 5.1: Specificity of Antibodies

Western blotting was performed to test the specificity of all the antibodies used. Untreated and 1nM Heregulin (HRG) stimulated MCF-7 and MDA-MB-453 (453) cells were used as controls for all antibodies except K-Ras. KNRK (a normal rat kidney [NRK] cell line transformed by Kirsten murine sarcoma virus) control cells were used for testing the specificity of the K-Ras antibody. All antibodies appeared to be specific for their antigen: (a) K-Ras (21kDa); (b) pRaf(ser259) (74kDa); (c) pRaf(ser338) (74 kDa); (d) p44/42 MAPK (44/42kDa); (e) Phospho-p44/42MAPK (44/42kDa).

5.3 Ras expression in Steroid-Resistant Tumour Bank (STB) Tissue MicroArrays (TMAs)

As previously shown, H- and N-Ras proteins were localised to both the cytoplasm and nuclei of tumour cells. K-Ras, like the other two Ras isoforms, was also expressed in both subcellular compartments. Very few tumours were shown to express any of the Ras isoforms at the plasma membrane. Table 5.1 provides details of the descriptive statistics (minimum, maximum, mean, median, lower and upper quartile) for the histoscores for the Ras isoforms. Negative controls for all Ras antibodies are shown in Appendix 5.

	H-Ras Cyto	H-Ras Nuc	K-Ras Cyto	K-Ras Nuc	N-Ras Cyto	N-Ras Nuc
Minimum	0	0	0	0	28	5
Maximum	232	150	162	130	250	200
Mean	122	47	56	34	146	98
Median	125	40	53	23	147	10
LQ	90	20	27	8	113	80
UQ	157	70	85	50	180	117

Table 5.1: Descriptive Statistics for Ras Histoscores

For each antibody, descriptive statistics were performed on the generated histoscores. The table shows the minimum and maximum histoscore, the mean, median, lower and upper quartile values for each antibody. LQ=Lower Quartile, UQ=Upper Quartile

5.3.1 H-Ras Expression

Localisation and expression of H-Ras in breast tumours was investigated in 391/402 (97.3%) STB patients (Figure 5.2). Only four tumours failed to express any H-Ras protein, whereas 363/391 (92.8%) tumours displayed both cytoplasmic and nuclear forms of this protein. The remaining patients either expressed only cytoplasmic (22 patients) or nuclear (2 patients) H-Ras in their tumours. As in the pilot study, H-Ras appeared to be expressed at higher levels in the cytoplasm as opposed to the nuclei of tumour cells. However, unlike the pilot study, no correlation was observed between the expression levels of cytoplasmic and nuclear H-Ras.

Patients were split into two groups, those that were defined as expressing low levels of H-Ras and those defined as expressing higher levels of the protein. For all proteins analysed, it was deemed most appropriate to use the histoscore upper quartile value as the cut off point for characterising the patients. The upper quartile value was chosen, since the range of histoscore values for each of the proteins for both nuclear and

cytoplasmic expression was not normally distributed. For cytoplasmic and nuclear H-Ras, the histoscore cut-off values were 157 and 70 respectively. 106 and 104 patients expressed high levels of H-Ras in the cytoplasm and nuclei of their tumours respectively. However, only 7.7% tumours (30 cases) overexpressed both cytoplasmic and nuclear H-Ras.

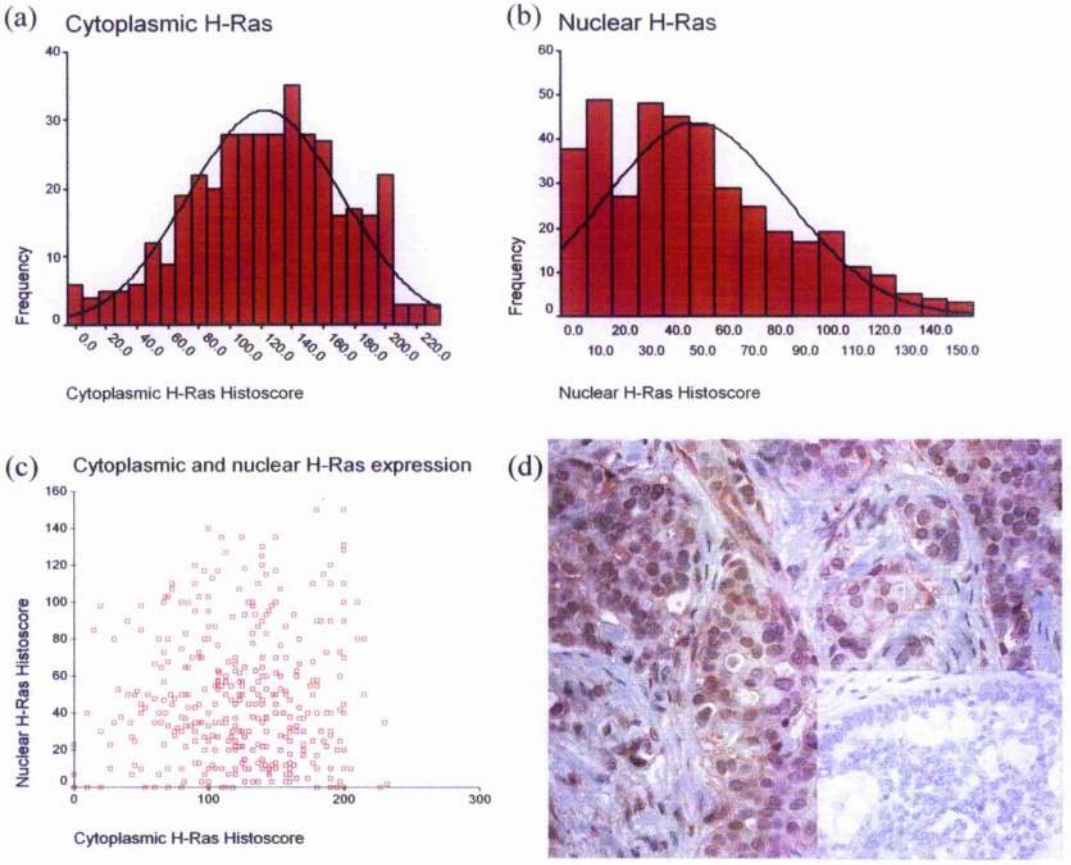

Figure 5.2: H-Ras Immunohistochemistry

(a) Histogram showing the intensity of H-Ras expression in the cytoplasm of tumour cells. (b) Histogram showing the intensity of H-Ras expression in the nuclei of tumour cells. (c) Scatter graph comparing distribution of cytoplasmic and nuclear H-Ras expression. (d) Breast tumour stained with H-Ras antibody. H-Ras was detected in both the cytoplasm and nuclei of tumour cells. Insert shows negative control.

5.3.2 K-Ras Expression

As with H- and N-Ras, K-Ras was expressed in both the cytoplasm and nuclei of breast tumour cells but not at the plasma membrane. A total of 388 (96.5%) tumours were analysed for K-Ras expression, of which only four were negative for this protein. 342/388 (88.1%) tumours presented with both cytoplasmic and nuclear K-Ras

expression; 13/388 (3.4%) tumours expressed only nuclear K-Ras, whereas 29/388 (7.5%) of patients' tumours were positive only for cytoplasmic K-Ras (Figure 5.3). Despite the high frequency of patients expressing both cytoplasmic and nuclear K-Ras, there was no significant relationship between the expression levels of K-Ras in the two locations.

As described for H-Ras, patients were separated into two groups using the K-Ras cytoplasmic (IHC score $\geq$ 85) and nuclear (IHC score $\geq$ 50) histoscore upper quartile values. Accordingly, 99 and 101 patients expressed high levels of K-Ras in the cytoplasm and nuclei of their tumours. Furthermore, 29 patients (7.5%) presented with tumours that expressed high levels of K-Ras in both subcellular locations.

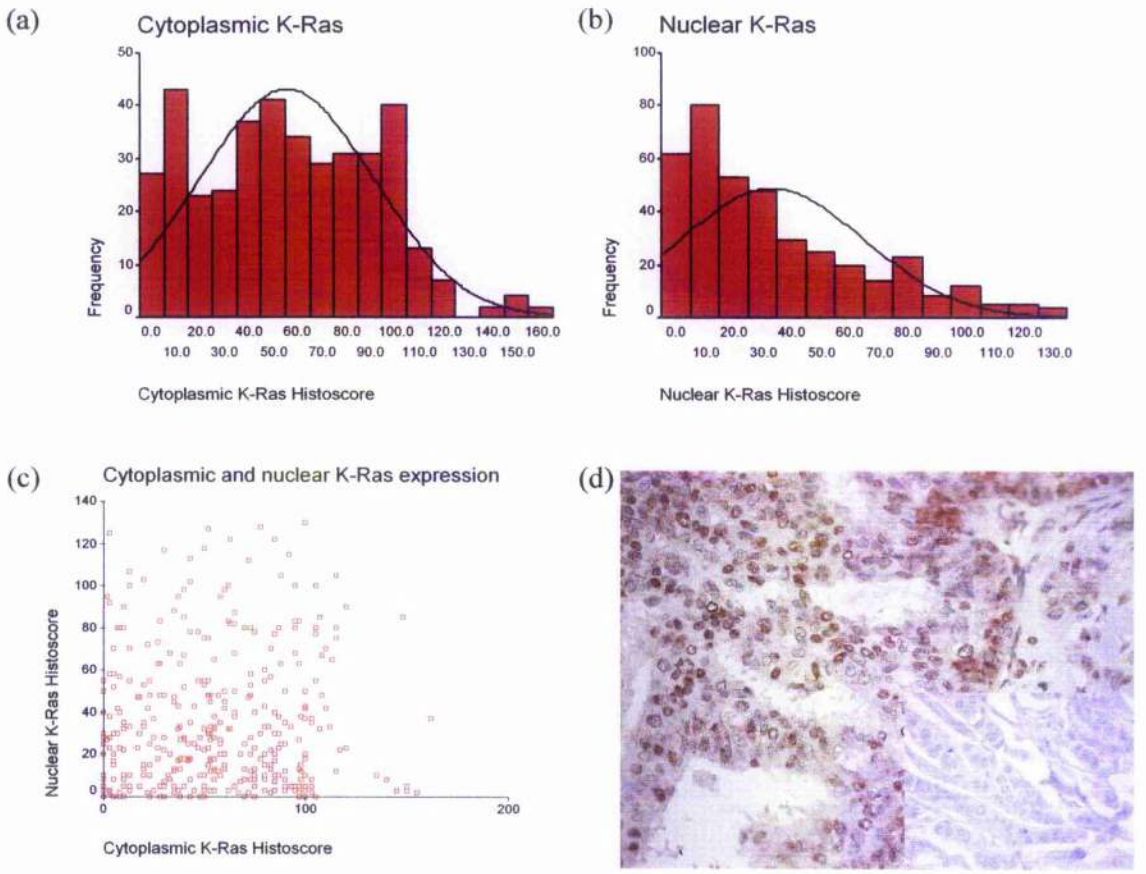

Figure 5.3: K-Ras Immunohistochemistry

(a) Histogram showing the intensity of K-Ras expression in the cytoplasm of tumour cells. (b) Histogram showing the intensity of K-Ras expression in the nuclei of tumour cells. (c) Scatter graph comparing distribution of cytoplasmic and nuclear K-Ras expression. (d) Breast tumour stained with K-Ras antibody. K-Ras was detected in both the cytoplasm and nuclei of tumour cells. Insert shows negative control.

5.3.3 N-Ras Expression

Expression levels of N-Ras were determined in 387/402 (96.3%) tumours. Unlike H- and K-Ras, all 387 patients' tumours exhibited both cytoplasmic and nuclear N-Ras protein

expression (Figure 5.4). However, cytoplasmic levels of N-Ras tended to be higher than those observed in the nuclei of tumour cells.

Cytoplasmic histoscores ≥ 180 and nuclear histoscores ≥ 118 were used to split the patients into those expressing either low or high levels of N-Ras in their tumours. Consequently 100 patients were defined as expressing high levels of cytoplasmic N-Ras in their tumours, whilst 96 presented with high tumour levels of nuclear N-Ras. Only 26 patients (6.7%) had high levels of both cytoplasmic and nuclear N-Ras in their tumours.

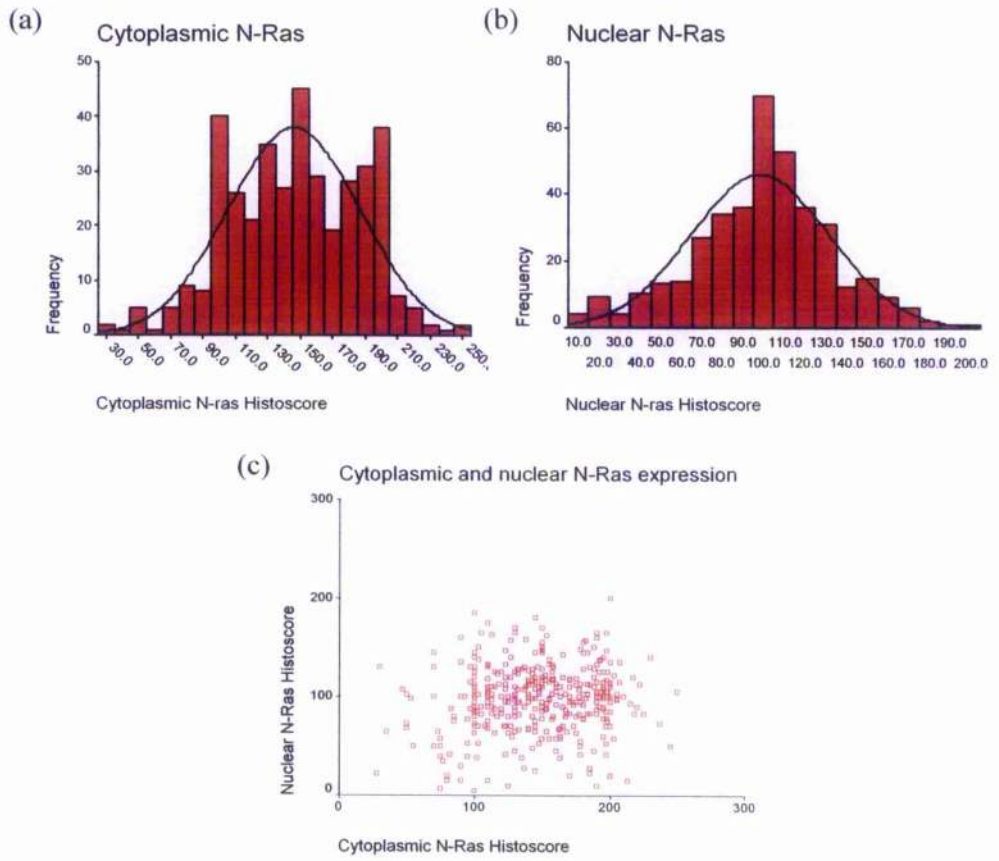

Figure 5.4: N-Ras Immunohistochemistry

(a) Histogram showing the intensity of N-Ras expression in the cytoplasm of tumour cells. (b) Histogram showing the intensity of N-Ras expression in the nuclei of tumour cells. (c) Scatter graph comparing distribution of cytoplasmic and nuclear N-Ras expression. (d-f) Breast tumour stained with N-Ras antibody. N-Ras was detected in both the cytoplasm and nuclei of tumour cells. (d) Negative control, (e) Example of tumour with low N-Ras expression (IHC score < UQ), (f) Example of tumour with high N-Ras expression (IHC score > UQ).

5.3.4 Combined Expression of H-, K-, and N-Ras in breast tumours

A total of 373 patients' tumours was investigated for expression of all three Ras isoforms. Of all the tumours analysed, 315 were positive for H-, K- and N-Ras expression in both the cytoplasm and nuclei of tumour cells, whereas 328 and 356 tumours expressed all three isoforms in the nuclei and cytoplasm of tumour cells respectively. Table 5.2 presents the frequency and percentage of patients whose tumours expressed increased levels of none, one, two or all three of the Ras isoforms in the cytoplasm or nuclei.

	Cytoplasmic		Nuclear	
No. of Ras isoforms highly expressed (0, 1, 2 or 3)	No. of patients (Total no of patients =373)	% Patients	No. of patients (Total no of patients =373)	% Patients
0	181	48.5	177	47.5
1	108	29.0	118	31.6
2	63	16.9	63	16.9
3	21	5.6	15	4.0

Table 5.2: Frequency of patients overexpressing 0, 1, 2 or 3 Ras isoforms in cytoplasm or nuclei of tumour cells.

A total of 373 patients' tumours were analysed for expression of all three Ras isoforms. Listed in the table is the frequency and percentage of patients who expressed high levels of none, one, two or three of the isoforms (H-, K- and N-Ras) in the cytoplasm and nuclei of tumour cells.

Further analysis suggested that there was a relationship between the expression of H-, K- and N- Ras in the cytoplasm and in the nuclei. Tumours that expressed high levels of one Ras isoform in the cytoplasm were more likely to display increased levels of the other two isoforms. The same trend was observed for the nuclear localisation of the three Ras isoforms (Table 5.3). However, these results should be treated with some caution, albeit that the p- values are less than 0.05, which is generally the value considered to be

statistically significant. The correlation coefficients (R^2) are low (<0.4) for some of the correlations. For a correlation to be considered statistically significant, the correlation coefficient values should ideally be higher. Therefore, examination of the scatter plots (Figure 5.5) for the various correlations suggest that, despite various correlations appearing to be statistically significant, the strongest relationship is between H- and N-Ras protein expression, in both the cytoplasm and the nuclei of tumour cells.

	H-Ras Cyto	H-Ras Nuc	K-Ras Cyto	K-Ras Nuc	N-Ras Cyto	N-Ras Nuc
H-Ras Cyto		R^2 =0.058 p=0.251	***R^2=0.279*** ***p<0.0005***	*R^2=-0.106* *P=0.039*	***R^2=0.437*** ***p<0.0005***	*R^2=-0.104* *P=0.044*
H-Ras Nuc			R^2=-0.023 p=0.661	***R^2=0.230*** ***p<0.0005***	R^2 =0.058 p=0.251	***R^2=0.410*** ***p<0.0005***
K-Ras Cyto				R^2=0.042 p=0.413	***R^2=0.441*** ***p<0.0005***	R^2=0.066 p=0.199
K-Ras Nuc					R^2=0.056 p=0.277	***R^2=0.225*** ***P<0.0005***
N-Ras Cyto						*R^2=0.100* *p=0.049*

Table 5.3: Correlations between H-, K- and N-Ras expression in breast tumours

Spearman-Rank correlations were performed to analyse the relationship between expression of the three Ras isoforms in the cytoplasm and in the nuclei of tumour cells. Those correlations deemed to be statistically significant, taking into account the p-value and correlation coefficient, are highlighted in bold. R^2 = correlation coefficient, p-values < 0.003 were deemed statistically significant, using Bonferroni's correction.

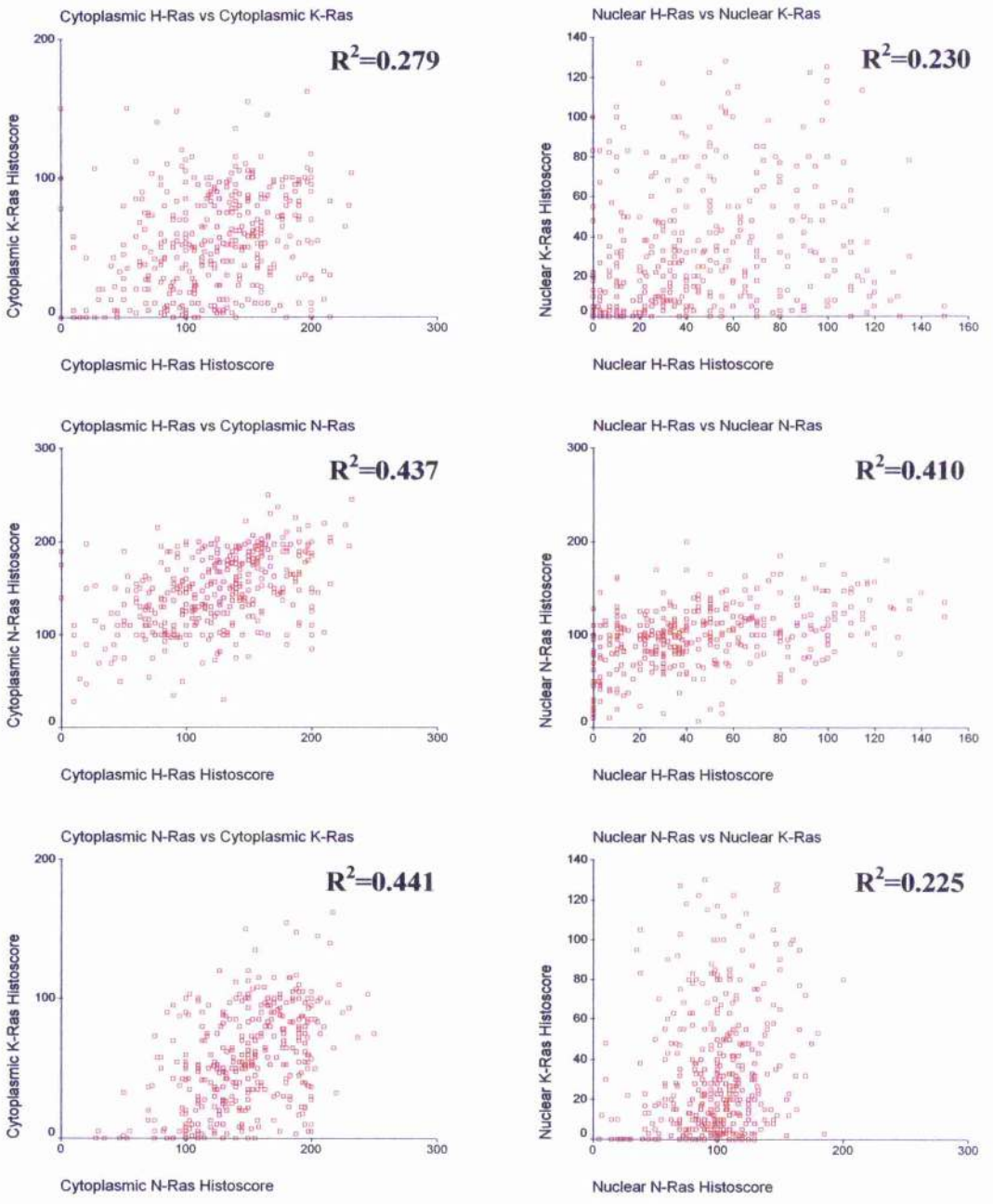

Figure 5.5: Scatter Graphs comparing H-, K-, N-Ras expression in breast tumours

The above scatter graphs show the relationship between H-, K- and N-Ras. Spearman Rank correlations produced p values <0.0005 for all correlations. However, the scatter plots suggested that correlation coefficients (R^2) > 0.4 identify the statistically significant correlations. Hence the strongest observed correlation was between H- and N-Ras expression in the cytoplasm and the nuclei of tumour cells.

5.4 Raf expression in Steroid Resistant Tumour Bank (STB) and NEAT Studies

In addition to investigating the expression and localisation of total Raf-1 in breast tumours, the inactive (pRaf(ser259)) and active (pRaf(ser338)) form of the protein was also examined. Negative controls are in Appendix 5. Table 5.4 displays the minimum, maximum, mean, median, lower quartile and upper quartile histoscore values for all three forms.

	Raf-1 Cyto	Raf-1 Nuc	pRaf(ser259) Cyto	pRaf(ser259) Nuc	pRaf(ser338) Cyto	pRaf(ser338) Nuc
Minimum	0	0	0	0	30	5
Maximum	280	200	285	93	290	225
Mean	120	107	81	5	152	136
Median	123	108	71	0	157	137
LQ	83	91	30	0	120	113
UQ	153	123	120	3	185	160

Table 5.4: Descriptive Statistics for Raf Histoscores

For each antibody, descriptive statistics were performed on the generated histoscores. The table shows the minimum and maximum histoscore, the mean, median, lower and upper quartile values for each antibody. LQ=Lower Quartile, UQ=Upper Quartile

5.4.1 Raf-1 Expression (STB Only)

A total of 356 (88.6%) patients' tumours were analysed for Raf-1 expression. Raf-1 was detected in both the cytoplasm and nuclei of tumour cells (Figure 5.6). In the pilot study, Raf-1 was primarily expressed in the cytoplasm of tumour cells. However, in the STB study, there was a positive correlation between the levels of cytoplasmic and nuclear Raf-1. Those tumours that expressed increased levels of cytoplasmic Raf-1 expressed higher levels of nuclear Raf-1 ($R2=0.375$, $p<0.0005$). One patient was negative for both cytoplasmic and nuclear Raf-1, whereas three patients expressed only nuclear Raf-1.

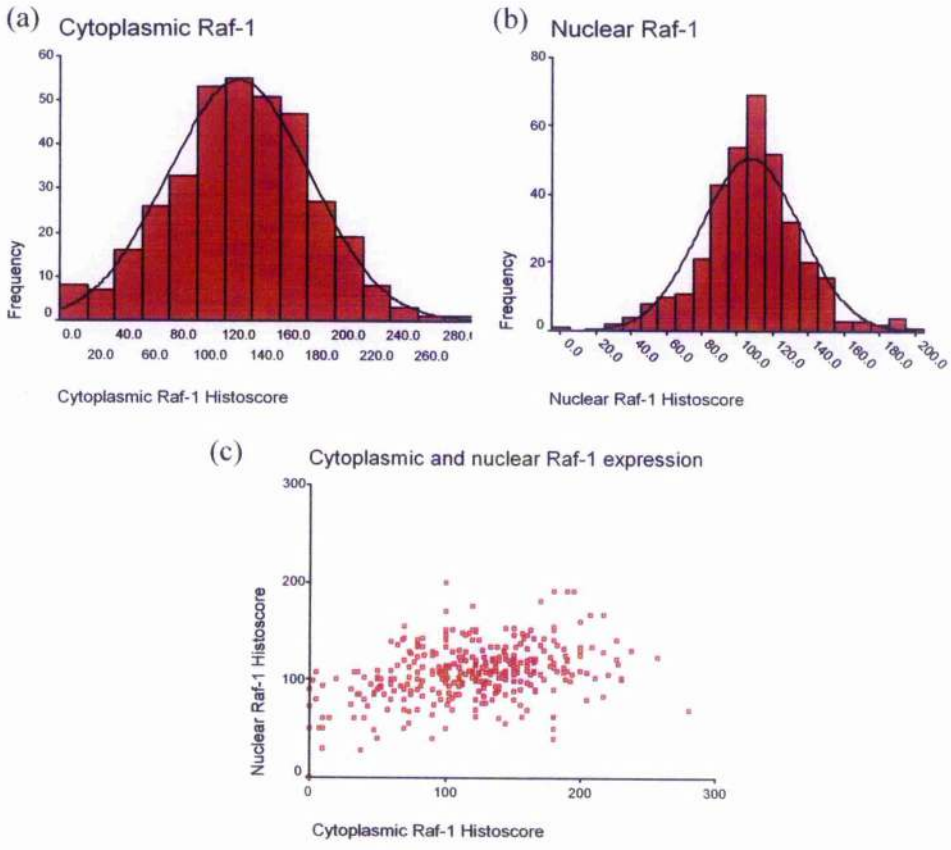

Figure 5.6: Raf-1 Immunohistochemistry

(a) Histogram showing the intensity of Raf-1 expression in the cytoplasm of tumour cells. (b) Histogram showing the intensity of Raf-1 expression in the nuclei of tumour cells. (c) Scatter graph comparing distribution of cytoplasmic and nuclear Raf-1 expression. (d-f) Breast tumour stained with Raf-1 antibody. Raf-1 was detected in both the cytoplasm and nuclei of tumour cells. (d) Negative control, (e) Example of tumour with low Raf-1 expression (IHC score < UQ), (f) Example of tumour with high Raf-1 expression (IHC score > UQ).

The cut-off histoscores for high levels of cytoplasmic and nuclear Raf-1 expression were 153 and 123 respectively. Of the 356 patients, 90 and 89 individuals were classified as expressing high levels of Raf-1 in the cytoplasm and nuclei of their tumours respectively. Furthermore, 109 patients (30.7%) expressed high levels of Raf-1 in one subcellular compartment, either in the cytoplasm or the nuclei, whereas 35 patients (9.9%) exhibited increased expression of both cytoplasmic and nuclear Raf-1 in their tumours.

5.4.2 pRaf(ser259) Expression (STB & NEAT)

A total of 683 (316 NEAT & 367 STB patients) patient tumours were analysed for expression of inactive Raf-1, pRaf(ser259). Generally pRaf(ser259) was only expressed in the cytoplasm of tumour cells; very low levels of inactive Raf-1 were detected in the nuclei. A total of 352 tumours were negative for pRaf(ser259) expression in the nuclei (51.5%), whilst only 72 tumours (10.4%) failed to express cytoplasmic pRaf(ser259). The frequency and intensity of pRaf(ser259) staining is shown in Figure 5.7.

High levels of cytoplasmic pRaf(ser259) (IHC score $\geq$ 120) were detected in 173 patients. Due to the large proportion of tumours that were negative for nuclear pRaf(Ser259), any tumour with a nuclear histoscore $\geq$ 3 was considered to express high levels of nuclear pRaf(ser259). There were 232 such tumours. Of all the patients, 51.2 % (350 patients) failed to express high levels of either nuclear or cytoplasmic pRaf(ser259) in their tumours, 38.2% (261 patients) expressed high levels of either cytoplasmic or nuclear inactive Raf-1, whilst 10.5% (72 patients) expressed high levels of both.

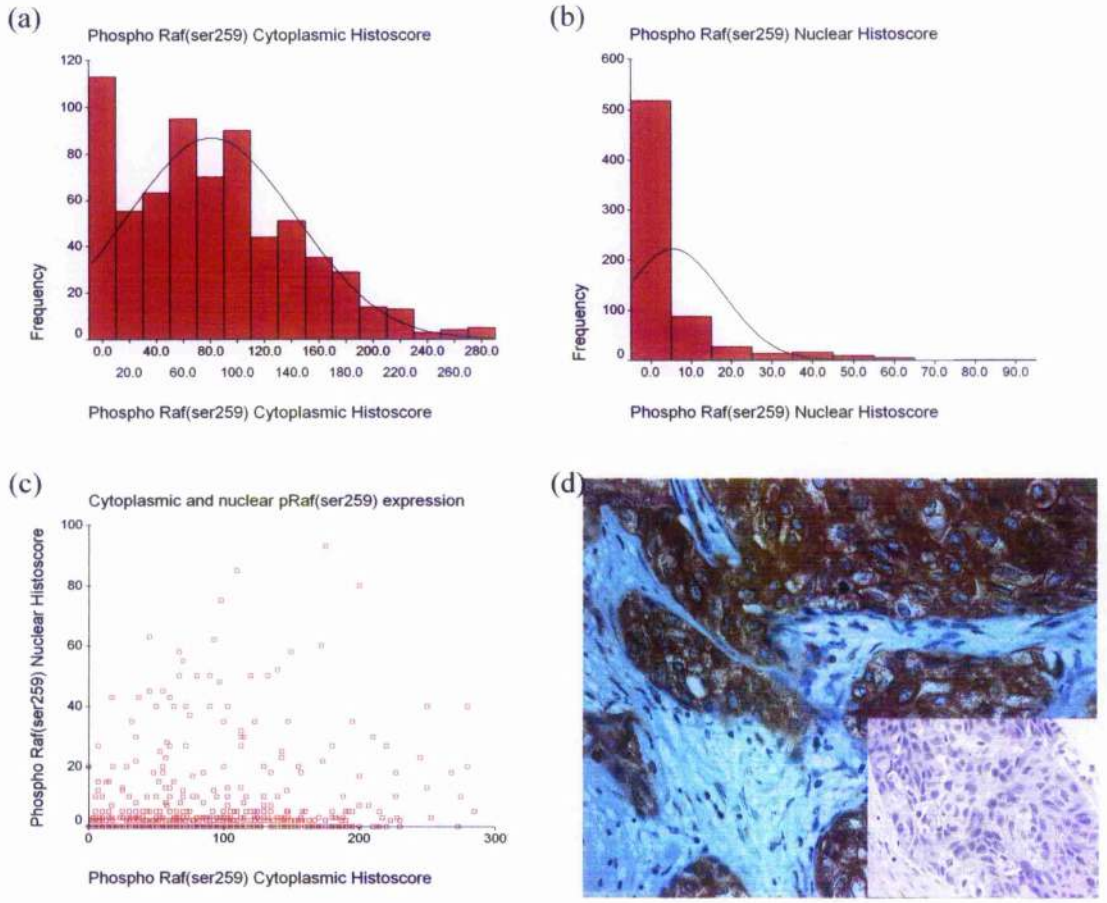

Figure 5.7: pRaf(ser259) Immunohistochemistry

(a) Histogram showing the intensity of pRaf(ser259) expression in the cytoplasm of tumour cells. (b) Histogram showing the intensity of pRaf(ser259) expression in the nuclei of tumour cells. (c) Scatter graph comparing distribution of cytoplasmic and nuclear pRaf(ser259) expression. (d) Breast tumour stained with pRaf(ser259) antibody. pRaf(ser259) was detected primarily in the cytoplasm of tumour cells. Insert shows negative control.

5.4.3 pRaf(ser338) Expression (STB & NEAT)

A total of 671 patients' tumours (313 NEAT patients & 358 STB patients) were analysed for the activated form of Raf-1, pRaf(ser338). The protein was detected in both the

cytoplasmic and nuclear compartments of tumour cells. The frequency and intensity of pRaf(Ser338) staining is shown in Figure 5.8.

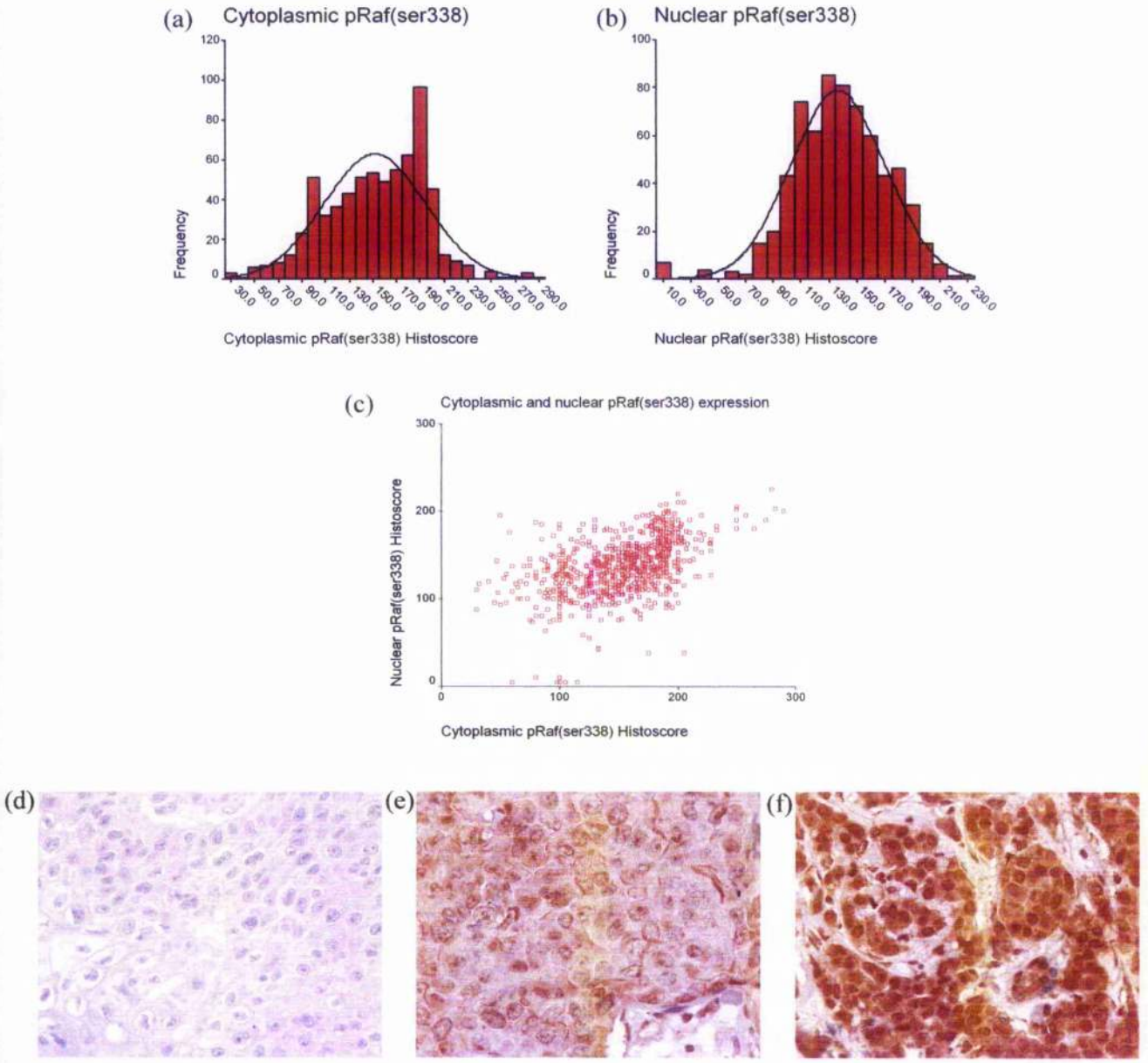

Figure 5.8: pRaf(ser338) Immunohistochemistry

(a) Histogram showing the intensity of pRaf(ser338) expression in the cytoplasm of tumour cells. (b) Histogram showing the intensity of pRaf(ser338) expression in the nuclei of tumour cells. (c) Scatter graph comparing distribution of cytoplasmic and nuclear pRaf(ser338) expression. (d-f) Breast tumour stained with pRaf(ser338) antibody. pRaf(ser338) was detected in both the cytoplasm and nuclei of tumour cells. (d) Negative control, (e) Example of tumour with low pRaf(ser338) expression (IHC score < UQ), (f) Example of tumour with high pRaf(ser338) expression (IHC score > UQ).

No tumour was negative for cytoplasmic or nuclear pRaf(ser338) expression. Tumours that exhibited elevated levels of cytoplasmic pRaf(ser338) also tended to present with strong nuclear expression (R^2=0.488, p<0.0005). A total of 179 and 172 patients presented with tumours that expressed high levels of cytoplasmic (IHC score ≥ 185) or nuclear (IHC score ≥ 160) pRaf(ser338) respectively. Of these patients, 145 (21.6%) overexpressed only one form of pRaf(ser338) (cytoplasmic or nuclear) whereas 103 (15.4%) overexpressed both.

5.4.4 Relationship between Raf-1 and phosphorylated Raf expression (STB Study Only)

Increased expression of Raf-1, in both the cytoplasm and nuclei, was associated with elevated levels of both the inactive and active phosphorylated forms of Raf, pRaf(ser259) and pRaf(ser338) respectively (Table 5.5).

	Raf-1 Cyt	**Raf-1 Nuc**
pRaf(ser259) Cyt	$R^2 = 0.440$ p<0.0005	$R^2 = 0.245$ p<0.0005
pRaf(ser338) Cyt	$R^2 = 0.461$ p<0.0005	$R^2 = 0.276$ p<0.0005
pRaf(ser338) Nuc	$R^2 = 0.181$ p =0.001	$R^2 = 0.401$ p<0.0005

Table 5.5: Correlations between Raf-1 and pRaf expression

Spearman-Rank correlations were performed to analyse the relationship between expression of Raf-1 and pRaf(ser259)/pRaf(ser338) in the cytoplasm and in the nuclei of tumour cells. R^2 = correlation coefficient, p values < 0.008 deemed statistically significant, using Bonferroni's correction.

5.5 p44/42 MAPK & phospho-p44/42 MAPK expression in Steroid Resistant Tumour Bank (STB) and NEAT Studies

The expression and localisation of p44/42 MAPK and phospho-p44/42 MAPK (pMAPK) was investigated in both the STB and NEAT patient cohorts. Table 5.6 presents the minimum, maximum, mean, median, lower quartile and upper quartile histoscore values for both proteins.

	p44/42 MAPK Cyto	p44/42 MAPK Nuc	Phospho-p44/42 MAPK Cyto	Phospho-p44/42 MAPK Nuc
Minimum	0	0	0	0
Maximum	285	210	235	193
Mean	110	76	64	68
Median	110	75	60	68
LQ	68	50	25	40
UQ	147	100	95	95

Table 5.6: Descriptive Statistics for MAPK Histoscores

For each antibody, descriptive statistics were performed on the generated histoscores. The table shows the minimum and maximum histoscore, the mean, median, lower and upper quartile values for each antibody. LQ=Lower Quartile, UQ=Upper Quartile

5.5.1 p44/42 MAPK Expression

MAPK expression was investigated in tumours from 692 patients (377 STB & 315 NEAT patients). MAPK protein was detected in the cytoplasm and nuclei of invasive tumour cells. Generally the levels of cytoplasmic MAPK were greater than those observed in the nuclei (Figure 5.9). A strong positive correlation was evident between cytoplasmic and nuclear localisation of MAPK (R^2=0.492, $p<0.0005$). Two patients were shown to be negative for MAPK expression in their tumour, 4 patients expressed only cytoplasmic MAPK, whilst 5 patients were positive for nuclear MAPK alone.

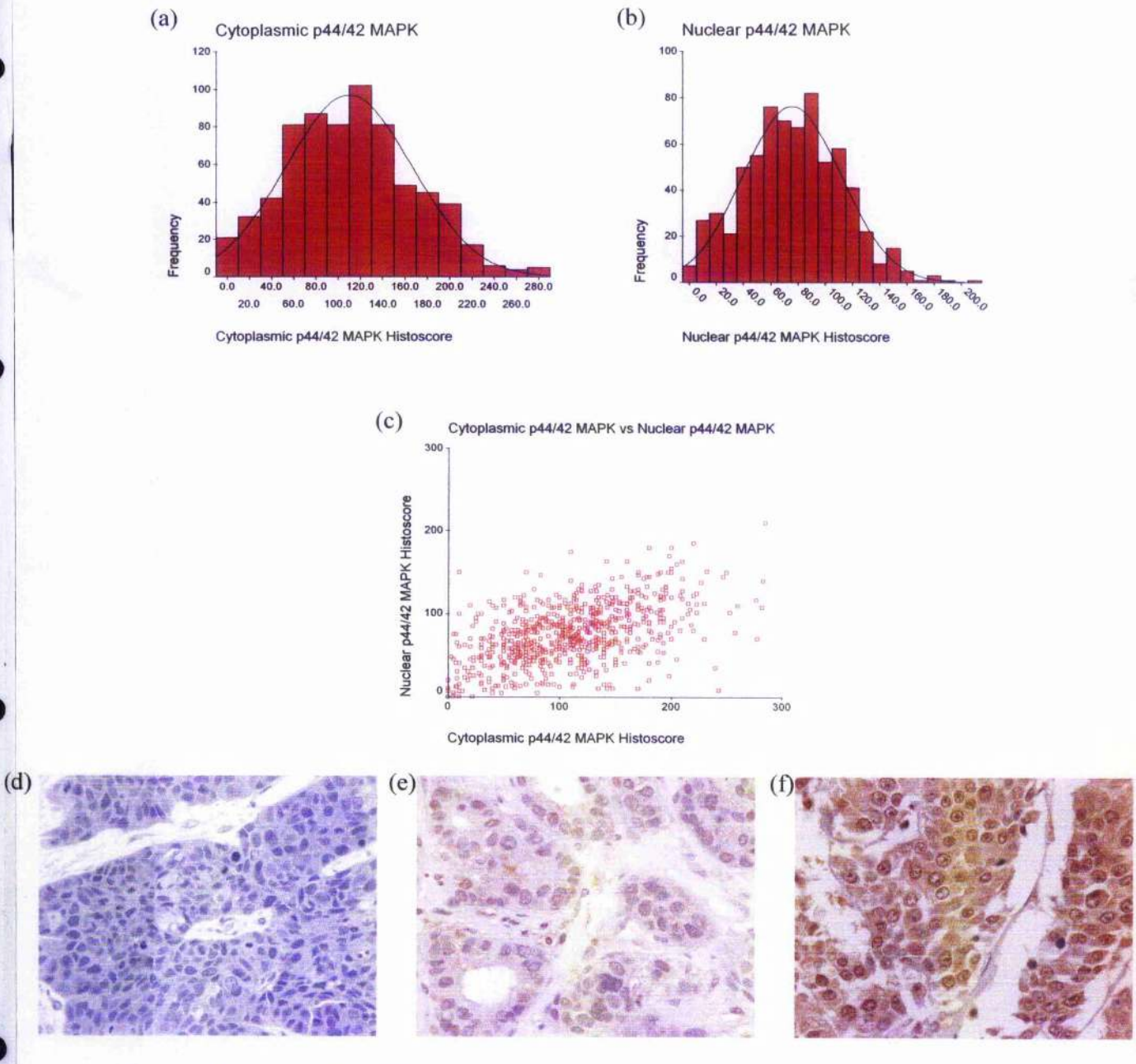

Figure 5.9: p44/42 MAPK Immunohistochemistry

(a) Histogram showing the intensity of p44/42 MAPK expression in the cytoplasm of tumour cells. (b) Histogram showing the intensity of p44/42 MAPK expression in the nuclei of tumour cells. (c) Scatter graph comparing distribution of cytoplasmic and nuclear MAPK expression. (d-f) Breast tumour stained with MAPK antibody. MAPK was detected in both the cytoplasm and nuclei of tumour cells. (d) Negative control, (e) Example of tumour with low p44/42MAPK expression (IHC score < UQ), (f) Example of tumour with high p44/42MAPK expression (IHC score > UQ).

High levels of MAPK were defined using histoscore values of 147 for cytoplasmic and 100 for nuclear. A total of 176 and 186 patients expressed high levels of MAPK in the cytoplasm and nuclei of their tumours. Additionally, 170 (24.6%) patients presented with high tumour levels of either cytoplasmic or nuclear MAPK, whilst 96 (13.9%) patients expressed high levels of both in their tumours.

5.5.2 Phospho-p44/42 MAPK Expression

Expression levels of phospho-p44/42 MAPK (pMAPK) were determined in 681 patients (368 STB & 313 NEAT patients). As with MAPK, the phosphorylated form of this protein was localised to both the cytoplasm and nuclei of tumour cells. Three patients' tumours were negative for cytoplasmic and nuclear pMAPK, and two were negative only for nuclear pMAPK. However, 43 patients (6.3%) presented with only nuclear pMAPK in their tumours. Nonetheless, cytoplasmic and nuclear pMAPK expression was positively correlated (R^2=0.509, $p<0.0005$). Figure 5.10 displays the frequency and intensity of pMAPK staining in the cytoplasm and nuclei of tumour cells.

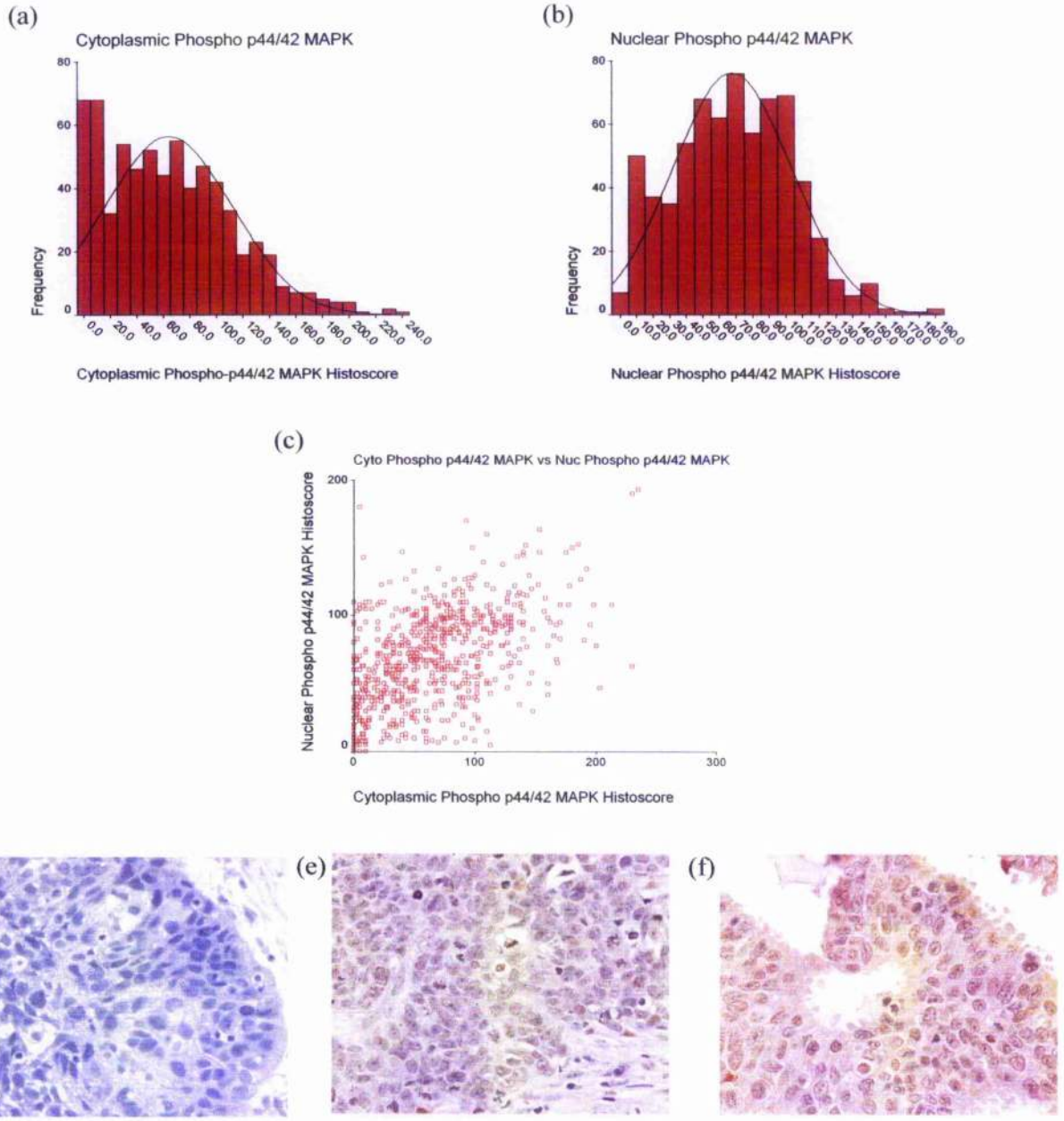

Figure 5.10: Phospho-p44/42 MAPK Immunohistochemistry

(a) Histogram showing the intensity of phospho-p44/42 MAPK expression in the cytoplasm of tumour cells. (b) Histogram showing the intensity of phospho-p44/42 MAPK expression in the nuclei of tumour cells. (c) Scatter graph comparing distribution of cytoplasmic and nuclear phospho-MAPK expression. (d-f) Breast tumour stained with phospho-MAPK antibody. Phospho-MAPK was detected in both the cytoplasm and nuclei of tumour cells. (d) Negative control, (e) Example of tumour with low phospho-p44/42MAPK expression (IHC score < UQ), (f) Example of tumour with high phospho-p44/42MAPK expression (IHC score > UQ).

Again, patients were split into two groups: 176 tumours expressed high levels of cytoplasmic pMAPK (IHC score ≥ 95) and 184 overexpressed nuclear pMAPK (IHC score ≥ 93). A total of 88 tumours overexpressed both cytoplasmic and nuclear pMAPK, whereas 183 overexpressed pMAPK in only one cellular compartment.

5.5.3 Relationship between MAPK and pMAPK expression

There was a positive correlation between expression of total cytoplasmic MAPK and expression of its phosphorylated counterpart in the cytoplasm and the nuclei of breast tumour cells ($p<0.0005$ for both). A weak association was evident between nuclear MAPK and nuclear pMAPK (Table 5.7). Scatter graphs of the four correlations suggest that these correlations are believable, though the relationships between cytoplasmic MAPK and pMAPK and nuclear MAPK and pMAPK are the strongest (Figure 5.11).

	MAPK Cyt	MAPK Nuc
pMAPK Cyt	$R^2 = 0.399$ $p<0.0005$	$R^2 = 0.167$ $p<0.0005$
pMAPK Nuc	$R^2 = 0.290$ $p<0.0005$	$R^2 = 0.308$ $p = 0.001$

Table 5.7: Correlations between MAPK and pMAPK expression

Spearman-Rank correlations were performed to analyse the relationship between expression of MAPK and pMAPK in the cytoplasm and in the nuclei of tumour cells. R^2 = correlation coefficient, p values < 0.01 deemed statistically significant, using Bonferroni's correction.

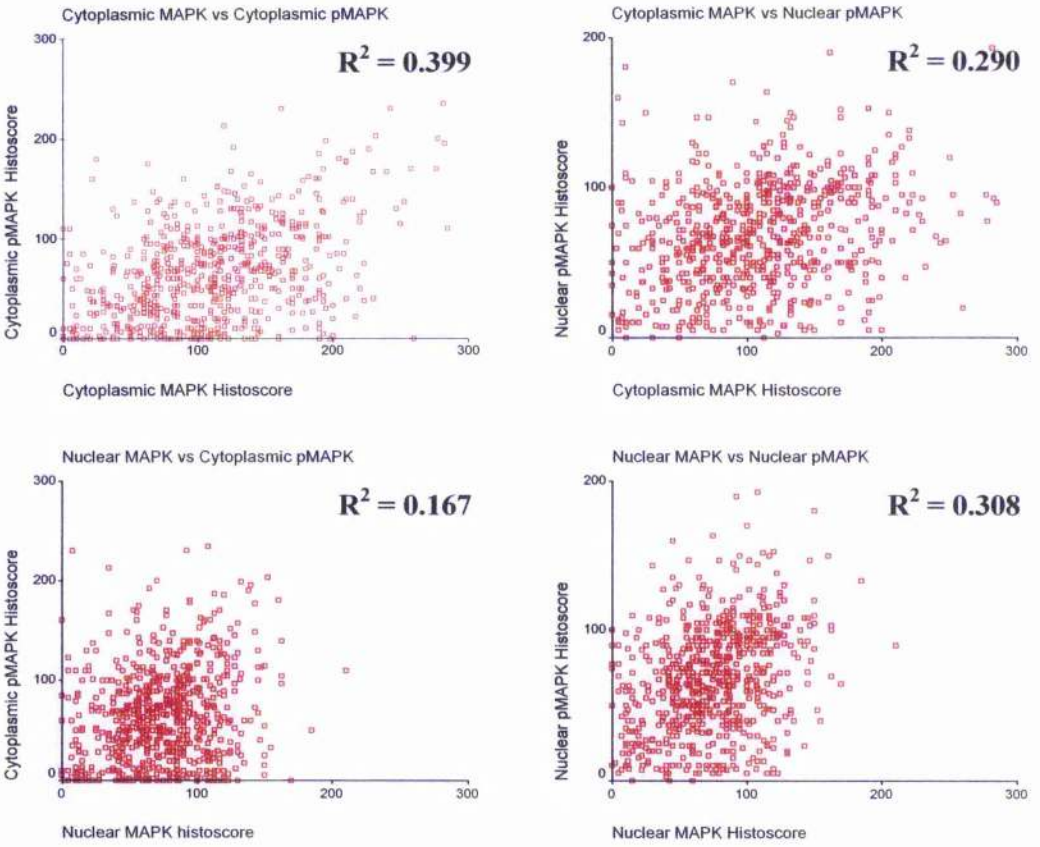

Figure 5.11: Scatter graphs comparing expression of MAPK and pMAPK in breast tumours

The above scatter graphs highlight the relationship between total MAPK and its phosphorylated form, pMAPK, in the cytoplasm and in the nuclei of tumour cells.

5.6 Increased expression levels of H-Ras, N-Ras and Raf-1 in breast tumours is not a result of gene amplification

119 patients from the STB cohort were analysed for modifications of H-Ras, N-Ras and Raf-1, at the genetic level using FISH. Genes were considered amplified if the ratio was above 2.0 and deleted if the ratio was below 0.8, as recommended by the manufacturer.

5.6.1 H-Ras FISH

FISH was successfully performed on tumours from 90 patients. No H-Ras amplifications were detected in any of the tumours. However, 3 patients exhibited deletions of this gene: these patients had an average H-Ras copy number of 1.56 and an overall ratio of 0.74. All other patients presented with normal ratios of H-Ras copy number to chromosome 11 (range 0.8 – 1.9, mean = 1.1). Figure 5.12 displays the frequencies of H-Ras copy number and chromosome 11 and the overall ratios.

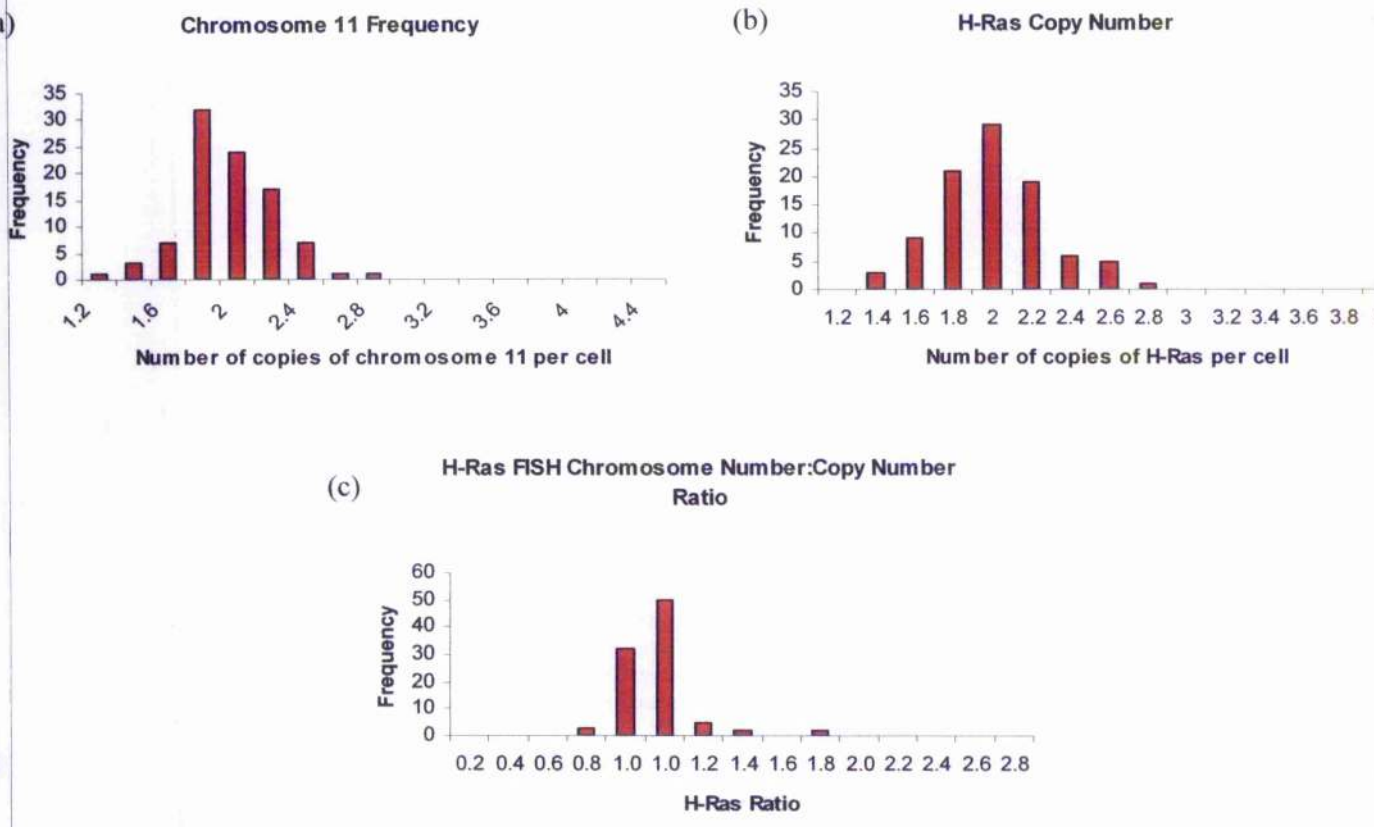

Figure 5.12: H-Ras FISH
(a) Histogram displaying the frequency of the number of copies of chromosome 11 per tumour cell. (b) Histogram displaying the frequency of the number of copies of H-Ras gene per tumour cell. (c) Histogram showing the overall ratio of chromosome number to H-Ras copy number in tumour cells. Genes were considered amplified if the ratio was above 2.0 and deleted if the ratio was below 0.8.

5.6.2 N-Ras

Breast carcinomas from 83 patients were successfully analysed for genetic modifications of N-Ras: no amplifications of the gene were observed. However, 3 tumours exhibited a deletion of this gene. The average gene/chromosome ratio for these patients was 0.6 (Range 0.48 – 0.78). All other patients presented with normal ratios of N-Ras copy

number to chromosome 1 (range 0.92 – 1.79, mean = 1.23). Figure 5.13 displays the frequencies of N-Ras copy number and chromosome 1 and the overall ratios in tumour cells.

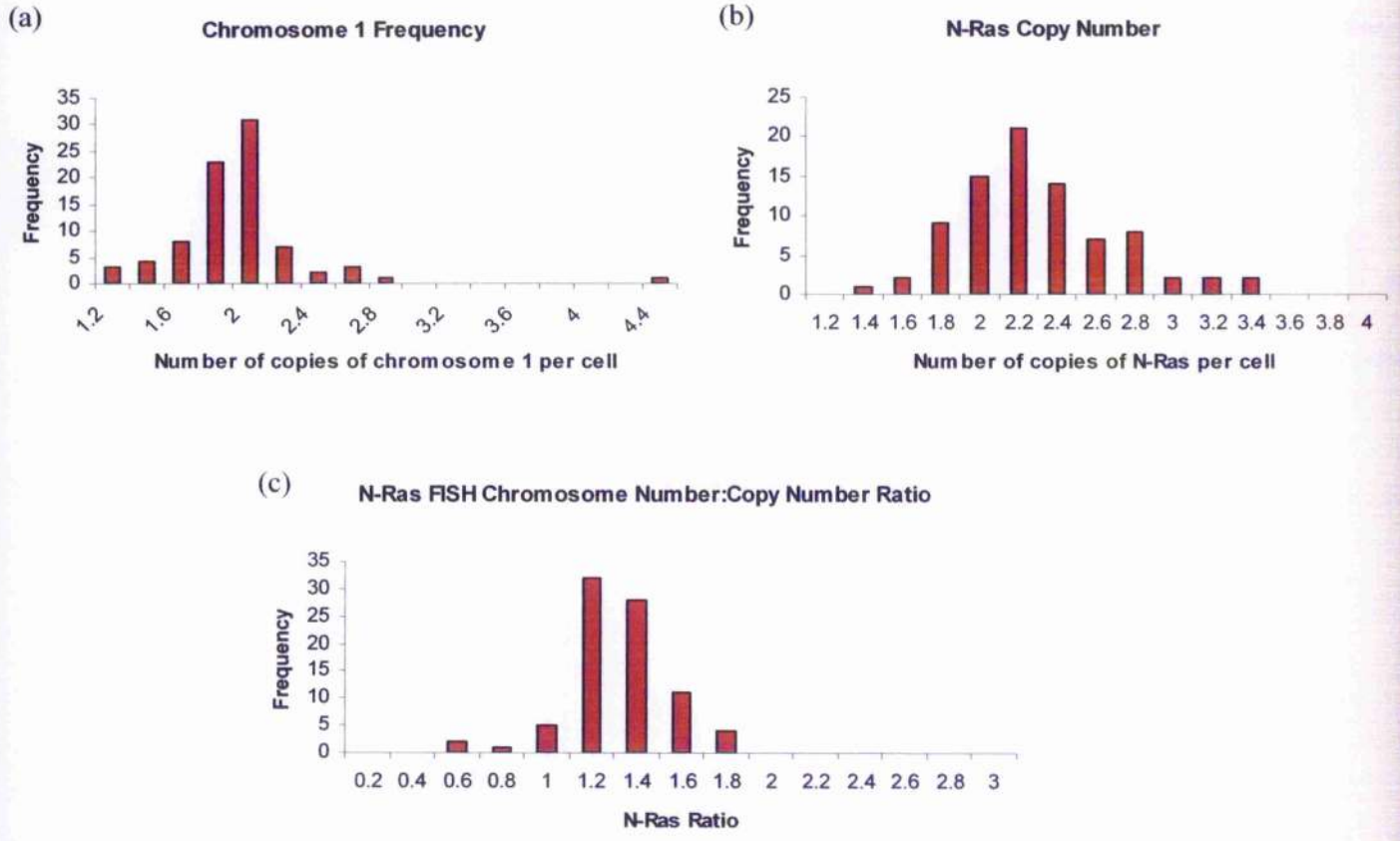

Figure 5.13: N-Ras FISH

(a) Histogram displaying the frequency of the number of copies of chromosome 1 per tumour cell. (b) Histogram displaying the frequency of the number of copies of N-Ras gene per tumour cell. (c) Histogram showing the overall ratio of chromosome number to N-Ras copy number in tumour cells. Genes were considered amplified if the ratio was above 2.0 and deleted if the ratio was below 0.8.

5.6.3 Raf-1

Of the 119 tumours, 90 were successfully analysed for Raf-1 and no amplifications were detected. Only one tumour was shown to have a deletion of this gene (overall ratio = 0.58). All other tumours exhibited a normal ratio of chromosome 3 to Raf-1 copy number (Range 0.81 – 1.63, mean = 1.1). Figure 5.14 displays the frequencies of Raf-1 copy number and chromosome 3 and the overall ratios in tumour cells.

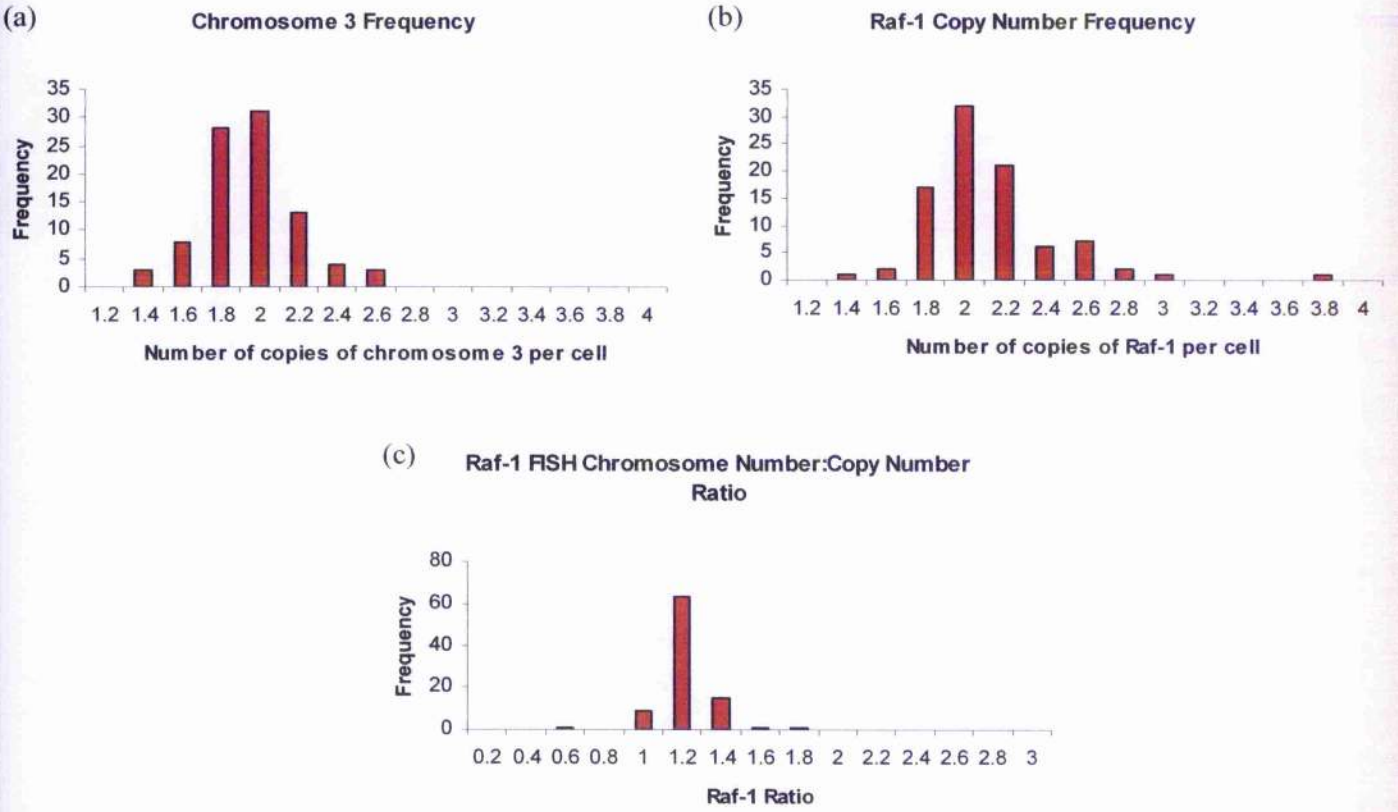

Figure 5.14: Raf-1 FISH

(a) Histogram displaying the frequency of the number of copies of chromosome 3 per tumour cell. (b) Histogram displaying the frequency of the number of copies of Raf-1 gene per tumour cell. (c) Histogram showing the overall ratio of chromosome number to Raf-1 copy number in tumour cells. Genes were considered amplified if the ratio was above 2.0 and deleted if the ratio was below 0.8.

5.7 Discussion

It is well established that the function and activity of a protein is often dependent on its subcellular location. A classic example of this is the ER. As discussed in chapter 1, the ER is known to localise to the cytoplasm, nuclei and membrane of cells. In the nucleus the ER mediates transcription of E2 regulated genes, whilst membranous ER exerts more rapid non-genomic effects.

In the two previous chapters a nuclear form of Ras was identified and validated. As discussed in these chapters, this was an unexpected finding, and as yet, there is no known function for this nuclear protein. However, in the pilot study (chapter 3), increased expression of nuclear N-Ras was associated with shortened disease-free and overall survival time. In keeping with these findings, H-, K- and N-Ras were all detected in the nuclei as well as the cytoplasm of breast tumours treated with Tamoxifen (STB group). As in the pilot study, expression levels of nuclear Ras, for all three Ras isoforms, were generally lower than those observed in the cytoplasm of tumour cells. No positive correlations were observed between the expression levels of H-, K- or N-Ras in the cytoplasm and nuclei of tumour cells. However, there was evidence of a relationship between H-Ras and N-Ras expression. In both the cytoplasm and nuclei of tumour cells, increased expression of H-Ras in either the cytoplasm or nuclei was positively correlated with increased expression of N-Ras. This is particularly significant, since in chapter 4, H- and N-Ras were shown to co-localise to a greater extent with each other, in comparison to K-Ras. Furthermore, as discussed in detail in chapters 1 and 3, both H-Ras and N-Ras undergo the same post-translational modifications and translocation to the plasma membrane, which differ from those that regulate K-Ras (117;139). One can perhaps

speculate that the mechanism by which H- and N- Ras are translocated to the nuclei is also slightly different from the one that induces translocation of K-Ras.

In the pilot study, increased expression of cytoplasmic and nuclear N-Ras was associated with an increased risk of relapse and death, suggesting that nuclear Ras serves an important, albeit unknown function. However, only cytoplasmic N-Ras expression was found to correlate with tumour grade and hence differentiation. Possibly this implies that there are diverse functions associated with the different subcellular forms of Ras. This theory is discussed in more detail in the next chapter.

Considering the hypothesis that the subcellular location of a protein is influenced by its activation, this study highlighted that the localisation of Raf-1, a protein expressed in the cytoplasm and nuclei, as well as at the plasma membrane, is dependent on its activation status. Inactive Raf-1, pRaf(ser259) was shown to be predominantly expressed in the cytoplasm of tumour cells, whereas the activated form, pRaf(ser338), was expressed in both the cytoplasm and the nuclei of cells. In recent years it has been established that a nuclear form of Raf-1 exists, which binds to and phosphorylates the Retinoblastoma protein (184). This IHC study confirms that Raf-1 is expressed in the nuclei of breast tumour cells, but also suggests that Raf-1 is activated at the plasma membrane and then translocates into the nucleus. The absence of pRaf(Ser259) from the nucleus infers that Raf-1 cannot be activated within the nucleus. Therefore, there must be some unknown mechanism or signal that promotes nuclear translocation of Raf-1. It should be noted that all three antibodies specific for Raf-1 (total, inactive or active Raf-1) detected negligible levels of the membranous form of the protein in breast tumours. The same was also true for the antibodies that recognised the three Ras isoforms. This is

perhaps surprising since the plasma membrane is the site for activation of both Ras and Raf-1. The lack of membranous Ras and Raf-1 possibly suggests that there is a rapid turnover of the activated proteins. Evidence indicates that activation of Ras, and hence Raf-1, at the plasma membrane is rapid and transient (130;139). It also emphasises that IHC represents only a "snapshot" of the inactivation/activation cycle of proteins.

The localisation of MAPK, like Raf-1, is to a certain extent indicative of its phosphorylation/activation status. Inactive, unphosphorylated MAPK is generally localised to the cytoplasm, partly through its interaction with MEK. Yet, because of its small size (<50 kDa), MAPK is able to diffuse into the nucleus, but it is rapidly relocalised back to the cytoplasm (195). In this study, a positive correlation was observed between cytoplasmic and nuclear MAPK expression (R^2=0.492, $p<0.0005$). Phosphorylation of cytoplasmic MAPK results in its dimerisation and its nuclear translocation. Consequently, the nuclear form of MAPK is thought to be representative of phosphorylated MAPK. A strong positive correlation was observed between the cytoplasmic and nuclear phosphorylated forms of MAPK. Additionally there was a correlation between total MAPK expression and expression of phosphorylated MAPK in both the cytoplasm and nuclei of tumour cells. As expected, the strongest correlations were observed between cytoplasmic MAPK and pMAPK (R^2=0.399, $p<0.0005$) and nuclear MAPK and pMAPK (R^2=0.308, $p<0.0005$).

Since one mechanism by which protein expression is upregulated is gene amplification, it was deemed appropriate to investigate H-Ras, N-Ras and Raf-1 at the genetic level. However, this study failed to show any link between gene amplification and increased protein expression. For all three genes, no amplifications were detected.

Accordingly, it was decided to investigate the hypothesis that increased expression of Ras, Raf-1 and MAPK proteins in breast tumours is associated with a poor outcome and failure to respond to tamoxifen and chemotherapy. The results of these studies are discussed in the following two chapters.

6. The role of the Ras/Raf-1/MAPK pathway in the development of Tamoxifen resistance: Steroid Resistant Tumour Bank (STB) Study

6.1 Introduction

Tamoxifen, an oestrogen antagonist, is currently the most successful and least toxic drug treatment for the 70-80% of patients diagnosed with ER positive breast cancer (see Section 1.5.10.2). Despite the extensive use of tamoxifen as adjuvant treatment, failure to respond to treatment is a major clinical problem. Resistance to tamoxifen, either primary (*de novo* resistance) or arising during treatment (acquired resistance) causes significant morbidity and mortality. Alternative therapies, such as aromatase inhibitors, inhibit or evade tamoxifen resistance pathways. In order to optimise use of such therapies they should, ideally, be targeted to those patient sub-groups who are most likely to acquire tamoxifen resistance.

The mechanisms controlling the development of tamoxifen resistance are not fully understood. Previous studies show patients whose tumours overexpress HER1-3 are less likely to respond to tamoxifen treatment (103-105;107). The ligand-independent phosphorylation and activation of the ER via signal transduction pathways, such as Ras/Raf-1/MEK/MAPK, is also a key factor (see Sections 1.6.6 and 1.9.1). Tamoxifen-resistant cells show an increase in the basal levels of phosphorylated ERα and tamoxifen promotes, rather than inhibits, growth of these cells (89). It has been speculated that activation of the Ras pathway modifies cells response to oestrogen, increasing ERα activity and sensitivity to low concentrations of oestrogen, via the ability of MAPK to

directly phosphorylate the ERα. This may partially explain the development of Tamoxifen resistance (29;69;107) .

Therefore, this study investigated whether expression and activation of the key components of the Ras pathway influenced clinical outcome in patients treated with tamoxifen. This study tested the hypothesis that activation of the Ras/Raf-1/MAPK pathway drives resistance to tamoxifen in clinical breast cancers. Patients from the STB cohort were analysed for Ras, Raf-1 and MAPK expression and activation (discussed in Chapter 4), and survival analysis was performed, in terms of disease-free survival (DFS), overall survival (OS), and recurrence whilst on tamoxifen (ROT).

6.2 Patient Cohort & Treatment

This study cohort was comprised of 402 ERα positive breast cancer patients. All patients received tamoxifen treatment for a median of five years (range 0.03-16 years). A total of 303 patients (75.4%) received only tamoxifen, whilst the remaining 99 patients (24.6%) were treated with chemotherapy in addition to tamoxifen. Consequently, survival analysis was performed on all 402 STB patients, as a whole, but also on the sub-group of patients, that received tamoxifen alone (303 patients). Due to the small number of patients receiving both tamoxifen and chemotherapy (99 patients), it was deemed inappropriate to perform analyses on this sub-group.

6.3 Predictive value of Ras/Raf-1/MAPK pathway activation.

6.3.1 Disease Free Survival (DFS) & Recurrence on Tamoxifen (ROT) in 402 STB patients

For the purpose of this study, the end point for disease-free survival was defined as breast cancer recurrence. In total 112/402 patients (27.9%) relapsed. Of these patients, 85

relapsed whilst receiving tamoxifen treatment. Therefore, in this study, it was deemed appropriate to analyse both disease-free survival (DFS) – including all patients who relapsed regardless of treatment status – and recurrence on tamoxifen (ROT) – including only those patients who relapsed whilst receiving tamoxifen treatment. Table 6.1 categorises patients in terms of recurrence status. As discussed in chapters 2 and 5, patients were split into two groups: those that were defined as expressing low levels of protein in their tumours and those that expressed higher levels. For all proteins analysed, it was deemed most appropriate to use the histoscore upper quartile value as the cut off point for characterising the patients.

Recurrence Type	No. of Patients
NONE	289
Overall Recurrence	112
Recurrence on Tamoxifen (ROT)	85
Recurrence < 3 years on Tamoxifen	53
Recurrence > 3 years on Tamoxifen	32
Recurrence after tamoxifen withdrawal	27

Table 6.1: Recurrence Type

Table highlighting the number of patients with the different types of recurrences. Overall Recurrence – all patients who relapsed. Recurrence on tamoxifen (ROT) = only patients who relapsed whilst receiving tamoxifen treatment. Recurrence < 3 years on Tamoxifen = patients who relapsed in the first three years of tamoxifen treatment. Recurrence > 3 years on Tamoxifen – patients who relapsed after three years on tamoxifen. Recurrence after tamoxifen withdrawal = patients who relapsed after treatment with tamoxifen ceased.

6.3.2 Raf-1 activation is associated with decreased disease-free survival time.

Activation of Raf-1 was associated with an increased risk of recurrence. Increased expression of activated Raf-1, pRaf(ser338), in the cytoplasm of tumour cells (IHC score ≥ 185), was associated with a reduced time to recurrence in patients treated with

tamoxifen (p=0.0022, 10.18 years vs. 13.10 years, Figure 6.1a). Similarly patients whose tumours expressed increased levels of nuclear pRaf(ser338) (IHC score ≥ 165) had a shorter DFS (p=0.0064, 10.55 years vs. 12.51 years, Figure 6.1b). The relative risks for relapse associated with elevated expression of cytoplasmic or nuclear pRaf(ser338) in patients tumours were 1.84 (95% CI 1.24 - 2.75, p= 0.0026) and 1.78 (95% CI 1.17 – 2.71, p=0.0071) respectively. Multivariate Cox-Regression revealed no evidence that pRaf(ser338) expression was independent of tumour size, grade or nodal status.

Increased expression of all three Ras isoforms, Raf-1, inactive Raf-1 (pRaf(ser259)), MAPK and pMAPK, failed to show any significant association with DFS time of patients treated with tamoxifen.

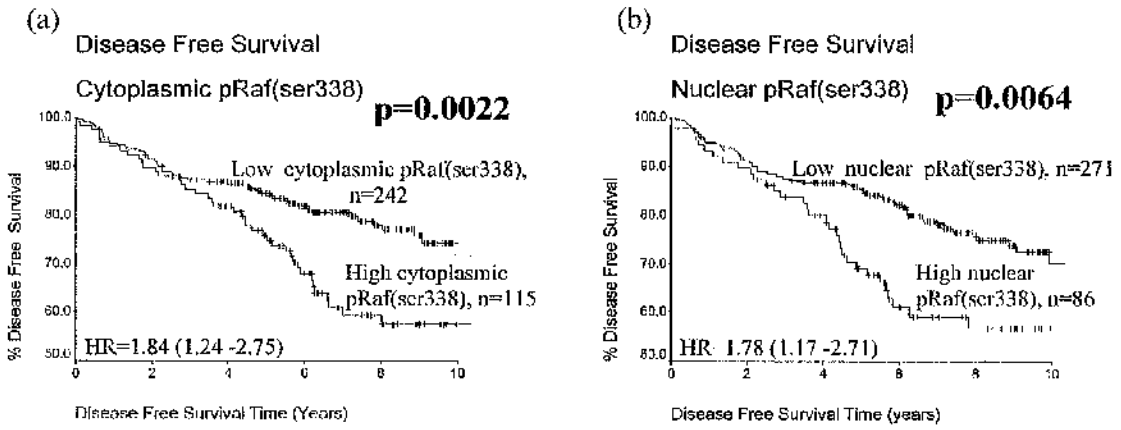

Figure 6.1: pRaf(ser338) Disease Free Survival Curves

Kaplan Meier survival curves showing disease-free survival (DFS) in patients whose tumours express cytoplasmic and nuclear pRaf(ser338). (a) Survival curve showing a significant reduction in DFS in patients whose tumours express high levels of cytoplasmic pRaf(ser338) (p=0.0022). (b) Survival curves showing a significant reduction in DFS in patients whose tumours express high levels of nuclear pRaf(ser338) (p=0.0064). High levels were defined as scores ≥ upper quartile value. p values represent log rank testing of the differences in survival. HR=Hazard Ratio (95% CI)

6.3.3 The N-Ras/Raf-1/MAPK pathway and Tamoxifen resistance

Expression of N-Ras, pRaf(ser338) and MAPK were each associated with an increased risk of relapse during tamoxifen treatment. Patients whose tumours expressed high levels of cytoplasmic N-Ras (IHC Score ≥ 180), but not H- or K-Ras, were more likely to relapse whilst receiving tamoxifen than patients with low tumour cytoplasmic N-Ras (p=0.0318, 9.97 years vs. 12.27 years; relative risk 1.64, 95% CI 1.04 – 2.58, p=0.0337, Figure 6.2a).

Likewise, patients expressing elevated levels of nuclear pRaf(Ser338) had a significantly shortened disease-free survival time during tamoxifen treatment (p=0.0052, 10.97 years vs. 12.63 years; relative risk 1.98, 95% CI 1.23 - 3.19, p=0.0048, Figure 6.2b). Expression of cytoplasmic pRaf(ser338) and pRaf(ser259) was not related to relapse whilst on tamoxifen. Neither N-Ras nor pRaf(ser338) were independent markers of tamoxifen resistance in a multivariate analysis.

Patients whose tumours expressed high levels of cytoplasmic MAPK were also candidates for developing resistance to tamoxifen; patients whose tumours displayed high levels of MAPK were more likely to relapse whilst on tamoxifen (p=0.0012, 7.60 years vs. 12.81 years; relative risk 2.08, 95% CI 1.32 – 3.27, Figure 6.2c). Furthermore, multivariate Cox-regression analysis revealed that MAPK expression was independent of tumour size, grade and nodal status in predicting recurrence whilst on tamoxifen (p=0.0368) (Table 6.2). However, neither cytoplasmic nor nuclear pMAPK tumour expression was associated with patients' relapse whilst on tamoxifen.

Both N-Ras and MAPK were responsible for events controlling early relapse on Tamoxifen, i.e., relapse within the first three years of treatment. Increased expression of pRaf(ser338) influenced later events in the progression of the disease (Figure 6.2).

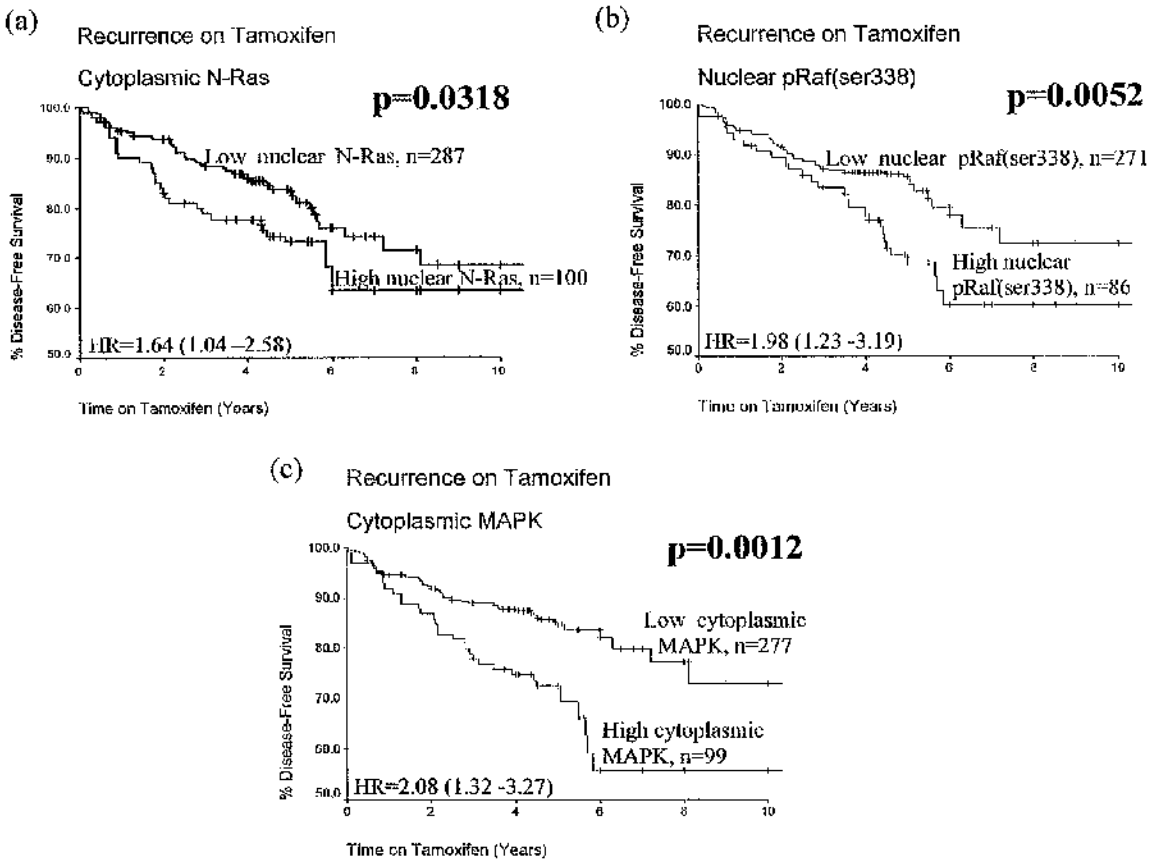

Figure 6.2: Recurrence on Tamoxifen Survival Curves

Kaplan Meier survival curves showing the differences in survival, in terms of recurrence on tamoxifen. (a)The survival curve shows a significant increase in the number of patients who express high levels of cytoplasmic N-Ras relapsing during tamoxifen treatment in comparison to those whose tumours express low levels (p=0.0318). (b)The survival curve shows a significant increase in the number of patients who express high levels of nuclear pRaf(ser338) relapsing during tamoxifen treatment in comparison to those whose tumours express low levels (p=0.0052). (c)The survival curve shows a significant increase in the number of patients who express high levels of cytoplasmic MAPK relapsing during tamoxifen treatment in comparison to those whose tumours express low levels (p=0.0012). High levels were defined as scores ≥ upper quartile value. p values represent log rank testing of the differences in survival. HR=Hazard Ratio (95% CI)

Factor	Hazard Ratio	p-value
Nodal Status	2.18 (1.54 3.07)	p<0.00005
Tumour Grade	1.6 (1.09 – 2.33)	p=0.0138
Tumour Size	1.94 (1.19 – 3.15)	p=0.0074
Cytoplasmic MAPK	1.79 (1.04 – 3.07)	p=0.0368

Table 6.2: Recurrence on Tamoxifen Cox-Regression

Cox-Regression multivariate analysis revealed that cytoplasmic MAPK expression was independent of known prognostic markers, nodal status, tumour size and grade in influencing response to tamoxifen treatment. p-value < 0.05 were deemed statistically significant. Hazard ratio = relative risk associated with development of tamoxifen resistance (95% CI).

6.3.4 Increased expression of pRaf(338) in breast tumours may identify patients more likely to relapse after three years of tamoxifen treatment

Survival analysis was also performed on the sub-group of patients who remained disease-free after three years on Tamoxifen. In these patients, only increased tumour levels of cytoplasmic and nuclear pRaf(ser338) were shown to have a significant impact on time to relapse and death after the first three years of tamoxifen treatment. High cytoplasmic levels of pRaf(ser338) were associated with an increased risk of recurrence (p=0.0006, 8.94 years vs. 11.83 years) and death (p=0.0084, 11.76 years vs. 13.75 years) following the initial three years of tamoxifen treatment. The relative risks associated with relapse and death were 2.66 (95% CI 1.49 – 4.75, p=0.001) and 2.94 (95% CI 1.27 –6.8, p=0.0119) respectively. Likewise, patients with strong nuclear pRaf(338) expression in their tumours had a significantly shortened disease free (p=0.0029, 9.43 years vs. 11.20 years) and overall survival time (p=0.0001, 11.03 years vs. 13.80 years). These patients showed a relative risk of 2.40 (95% CI 1.33 – 4.36, p=0.0038) and 4.78 (95% CI 2.06 – 11.06, p= 0.0003) for relapse and death respectively (Figure 6.3).

Multivariate Cox-regression analysis revealed that both cytoplasmic and nuclear pRaf(Ser338) expression were independent of tumour size, grade and nodal status in predicting for relapse and death after three years of tamoxifen treatment (Table 6.3)

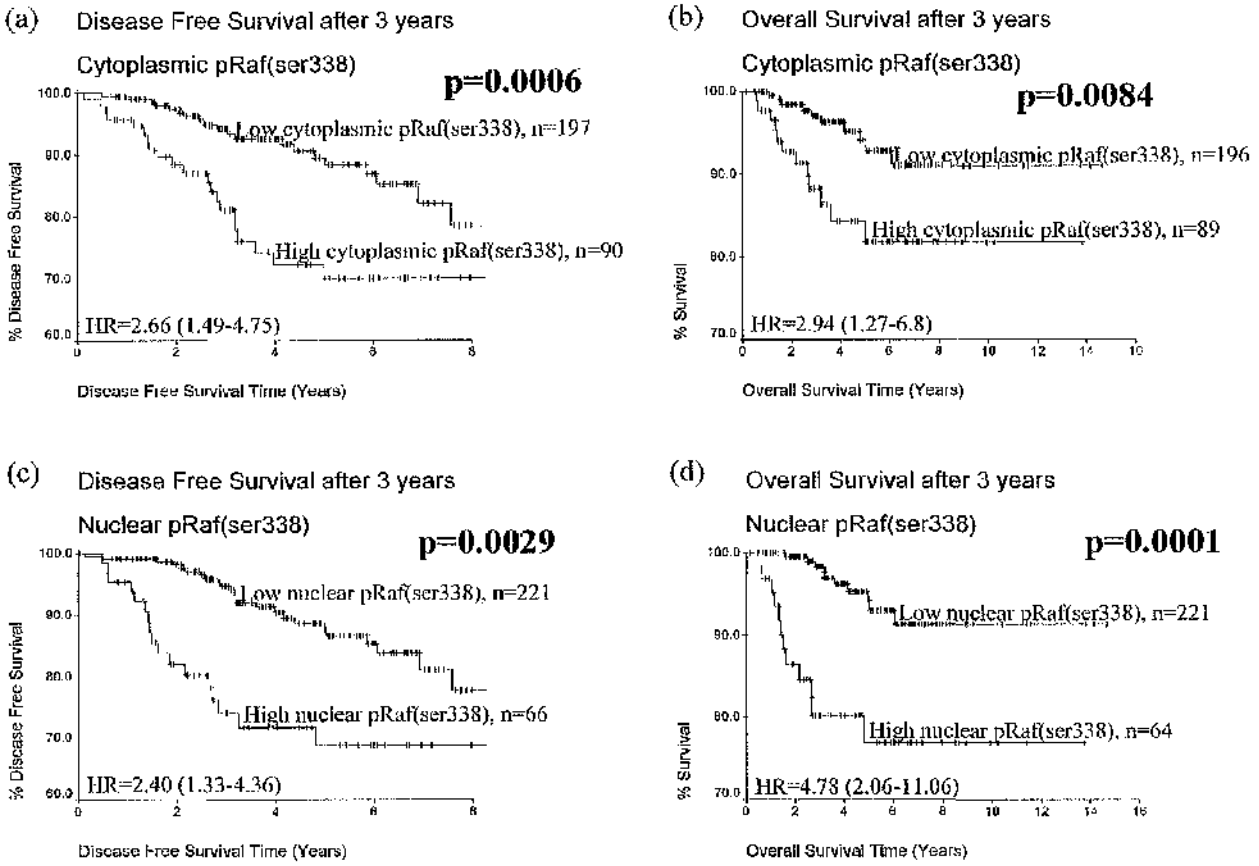

Figure 6.3: pRaf(ser338) Survival Curves after 3 years tamoxifen treatment

Kaplan Meier survival curves showing the effects of low and high tumour levels of pRaf(ser338) on disease-free and overall survival time in patients who remained disease-free after three years on tamoxifen. (a,b) Survival curves showing a significant reduction in disease-free and overall survival time, following three years of tamoxifen treatment, in patients whose tumours express high levels of cytoplasmic pRaf(ser338) (p=0.0006 and p=0.0084 respectively). (c,d) Survival curves showing a significant reduction in disease-free and overall survival time, following three years treatment with tamoxifen, in patients whose tumours express high levels of nuclear pRaf(ser338) (p=0.0029 and p=0.0001 respectively). High levels were defined as ≥ upper quartile value. p values represent log rank testing of the differences in survival. HR=Hazard Ratio (95% CI)

	Factor	Hazard Ratio	p-Value
Disease-Free Survival after 3 years tamoxifen treatment	**Nodal Status**	1.72 (1.09-2.74)	0.0204
	Tumour Grade	1.12 (0.69-1.80)	-
	Tumour Size	1.72 (0.94-3.15)	0.0705
	Cyto pRaf(ser338)	2.55 (1.26-5.14)	0.0056
Overall Survival after 3 years tamoxifen treatment	**Nodal Status**	2.22 (1.18-4.18)	0.0041
	Tumour Grade	1.64 (0.79-3.38)	-
	Tumour Size	1.55 (0.69-3.50)	-
	Cyto pRaf(ser338)	3.16 (1.14-8.74)	0.0059
Disease-Free Survival after 3 years tamoxifen treatment	**Nodal Status**	1.74 (1.11-2.73)	0.126
	Tumour Grade	1.23 (0.77-1.98)	-
	Tumour Size	1.74 (0.93-3.26)	0.624
	Nuc pRaf(ser338)	2.49 (1.22-5.09)	0.0131
Overall Survival after 3 years tamoxifen treatment	**Nodal Status**	2.14 (1.16-3.95)	0.0102
	Tumour Grade	1.77 (0.85-3.69)	0.0903
	Tumour Size	1.37 (0.57-3.29)	-
	Nuc pRaf(ser33)	4.70 (1.75-12.66)	0.0015

Table 6.3: Patient outcome Cox-regression after three years tamoxifen treatment

Cox-Regression multivariate analysis revealed that cytoplasmic and nuclear pRaf(ser338) expression was independent of known prognostic markers, nodal status, tumour size and grade, in influencing disease free and overall survival following three years of tamoxifen treatment. p-value < 0.05 were deemed statistically significant. Hazard ratio = relative risk associated with development of tamoxifen resistance (95% CI).

6.4 Does increased expression of Ras/Raf-1/MAPK pathway affect overall survival time in 402 STB patients?

6.4.1 Overall Survival Time (OS)

The end point for overall survival was a breast cancer related death. In total there were 74 breast cancer related deaths in this group of 402 patients.

6.4.2 Activation of Raf-1 reduces overall survival time of patients treated with tamoxifen.

Activation of Raf-1 was linked to a poor outcome in patients treated with tamoxifen. Patients whose tumours expressed increased levels of cytoplasmic or nuclear pRaf(ser338) exhibited a shortened OS time (p=0.0229, 13.76 years vs. 14.87 years) and (p=0.0006, 11.82 years vs. 15.49 years) respectively (Figure 6.4). Elevated levels of cytoplasmic or nuclear pRaf(ser338) increased the risk of death in patients treated with tamoxifen by 1.74 (95% CI 1.07 – 2.81, p=0.0247) and 2.29 (95% CI 1.41 – 3.74, p=0.0009) times respectively. However, multivariate Cox-Regression revealed no evidence that pRaf(ser338) expression was an independent factor in influencing survival.

Overall survival (OS) time for patients treated with tamoxifen was not affected by expression of Raf-1, pRaf(ser259), MAPK or pMAPK. Increasing levels of H-, K- and N-Ras in patients' tumours also failed to influence OS.

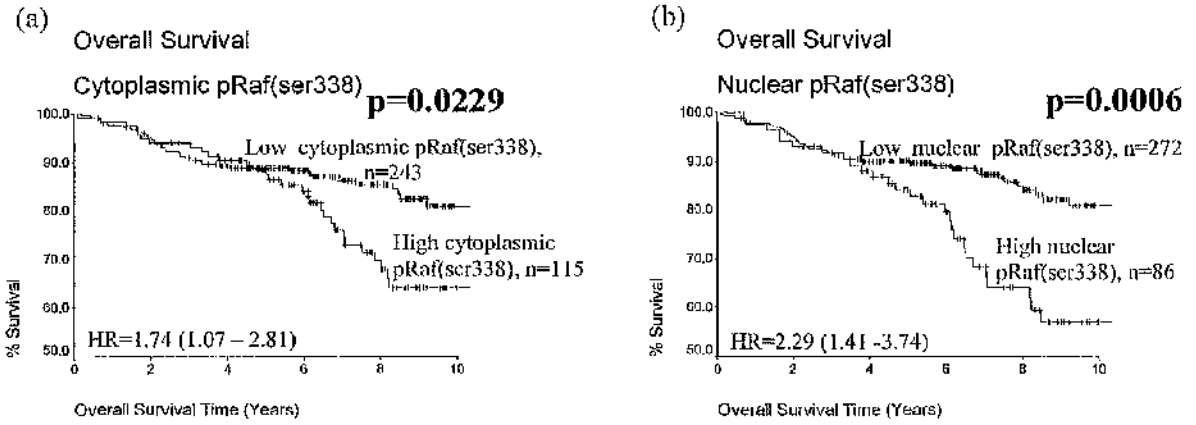

Figure 6.4: pRaf(ser338) Overall Survival Curves

Kaplan Meier survival curves showing overall survival in patients whose tumours express cytoplasmic and nuclear pRaf(ser338). (a) Survival curve showing a significant reduction in overall survival time in patients whose tumours express high levels of cytoplasmic pRaf(ser338) (p=0.0229). (b) Survival curve showing a significant reduction in overall survival time in patients whose tumours express high levels of nuclear pRaf(ser338) (p=0.0006). High levels were defined as scores ≥ upper quartile value, p values represent log rank testing of the differences in survival. HR=Hazard Ratio (95% CI)

6.5 Effect of increased expression of Ras/Raf-1/MAPK on disease-free survival of patients treated with only tamoxifen.

6.5.1 Disease Free Survival (DFS) and Recurrence on Tamoxifen (ROT)

As in section 6.3.1, the end point for disease-free survival for patients was defined as a breast cancer relapse. In this sub group, the 303 tamoxifen only treated patients were analysed. In total there were 82 patients (27.1%) who relapsed. Of these, 61 relapsed whilst receiving tamoxifen treatment. As before, both DFS – including all patients who relapsed regardless of treatment status – and ROT – including only those patients who relapsed whilst receiving tamoxifen treatment were analysed.

6.5.2 Activation of Raf-1 and MAPK is associated with a reduced disease free survival time in patients treated only with tamoxifen.

Increased expression of activated Raf-1 was linked to a reduction in DFS time. Patients whose tumours expressed increased levels of cytoplasmic (p=0.0023, 10.15 years vs. 13.27 years) and nuclear pRaf(ser338) (p=0.0020, 10.28 years vs. 12.83 years) were more likely to relapse quicker (Figure 6.5). Those patients with elevated tumour expression of either cytoplasmic or nuclear pRaf(ser338) were 2.02 (95% CI 1.27-3.21, p=0.0028) and 2.08 (95% CI 1.29-3.33, p=0.0025) times more likely to relapse than those patients with low tumour levels.

Phosphorylation of MAPK was also associated with an increased risk of recurrence in patients. Increased expression of pMAPK in the cytoplasm of tumour cells was associated with a reduced time to recurrence in patients treated with only tamoxifen (p=0.0104, 8.52 years vs. 12.94 years, Figure 6.6a). Similarly, those patients whose tumours expressed increased levels of nuclear pMAPK had a shorter DFS (p=0.0425, 11.38 years vs. 12.52 years, Figure 6.6b). The relative risks for relapse associated with higher expression levels of cytoplasmic or nuclear pMAPK in patients were 2.04 (95% CI 1.17-3.55, p=0.0121) and 1.61 (95% CI 1.01-2.55, p=0.0444) respectively.

Multivariate Cox-Regression analysis revealed that only nuclear pRaf(ser338) expression was independent of tumour size, grade or nodal status in influencing relapse (p=0.0307) (Table 6.4).

DFS time for patients treated only with tamoxifen was not affected by overexpression of the three Ras isoforms, Raf-1, pRaf(ser259) or MAPK.

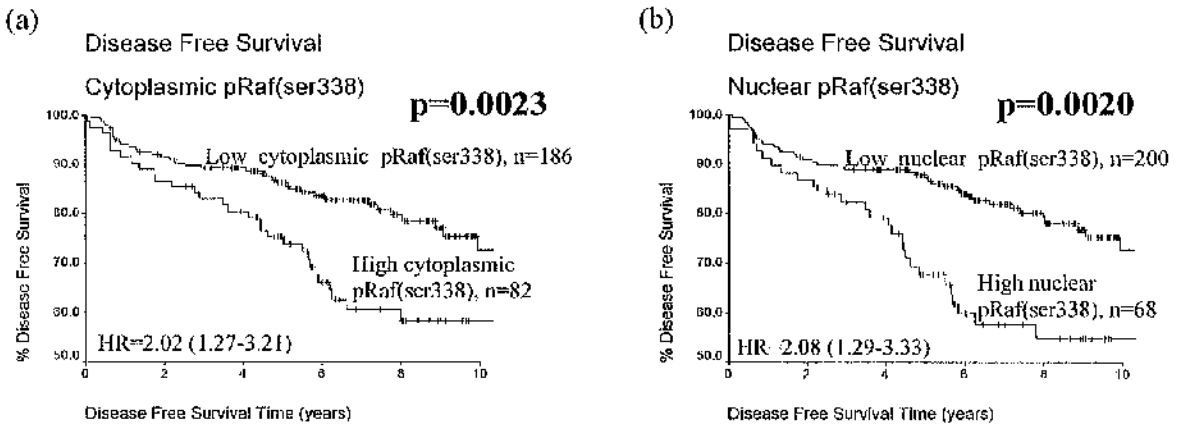

Figure 6.5: Tamoxifen only treated patients disease free survival curves

Kaplan Meier survival curves showing disease-free survival in patients treated only with Tamoxifen whose tumours express cytoplasmic and nuclear pRaf(ser338). (a) Survival curve showing a significant reduction in disease-free survival time in patients whose tumours express high levels of cytoplasmic pRaf(ser338) (p=0.0023). (b) Survival curves showing a significant reduction in disease survival time in patients whose tumours express high levels of nuclear pRaf(ser338) (p=0.0020). High levels were defined as scores ≥ upper quartile value. p values represent log rank testing of the differences in survival. HR=Hazard Ratio (95% CI).

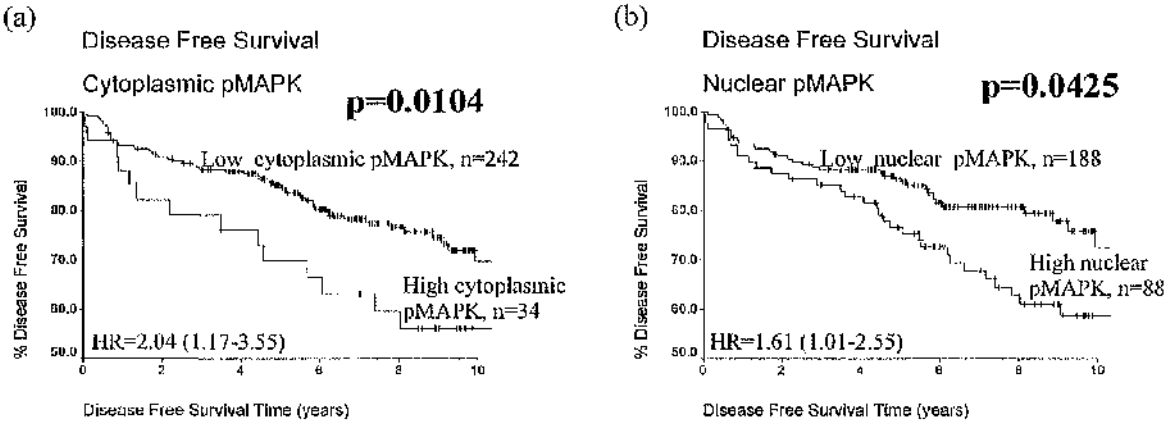

Figure 6.6: Tamoxifen only treated patients disease free survival curves

Kaplan Meier survival curves showing disease-free survival in patients treated only with tamoxifen whose tumours express cytoplasmic and nuclear pMAPK. (a) Survival curve showing a significant reduction in disease-free survival time in patients whose tumours express high levels of cytoplasmic pMAPK (p=0.0104). (b) Survival curves showing a significant reduction in disease survival time in patients whose tumours express high levels of nuclear pMAPK (p=0.0425). High levels were defined as scores ≥ upper quartile value. p values represent log rank testing of the differences in survival. HR=Hazard Ratio (95% CI)

Factor	Hazard Ratio	p-value
Nodal Status	2.01 (1.41 – 2.87)	p=0.0002
Tumour Grade	1.47 (0.99 – 2.20)	p=0.0552
Tumour Size	2.23 (1.31 – 3.81)	p=0.0027
Nuclear pRaf(ser338)	1.94 (1.09 – 3.45)	p=0.0307

Table 6.4: Disease-free survival Cox-regression of patients treated only with tamoxifen

Cox-Regression multivariate analysis revealed that nuclear pRaf(Ser338) expression was independent of known prognostic markers; nodal status, tumour size and grade, in influencing disease-free survival time in patients treated only with tamoxifen. p-values < 0.05 were deemed statistically significant. Hazard ratio = relative risk associated with development of tamoxifen resistance (95% CI).

6.5.3 Increased expression of nuclear pRaf(ser338) and cytoplasmic MAPK is involved in the development of tamoxifen resistance in patients treated only with tamoxifen.

Increased expression of nuclear, but not cytoplasmic pRaf(ser338), in patients' tumours was associated with the development of tamoxifen resistance. These patients had a significantly shorter response time to tamoxifen (p=0.0006, 10.70 years vs. 13.23 years, Figure 6.7a). The relative risk associated with recurrence whilst on tamoxifen was 2.51 (95% CI 1.45-4.34, p=0.0010).

Increased expression of cytoplasmic MAPK was also associated with ROT. Patients whose tumours displayed high levels of MAPK were more likely to relapse whilst on tamoxifen (p=0.0021, 7.68 years vs. 13.20 years, Figure 6.7b). The relative risk for these patients was 2.28 (95% CI 1.33-3.91, p=0.0028)

Furthermore, Cox-regression analysis revealed that nuclear pRaf(ser338) expression was independent of tumour size, grade and nodal status in influencing recurrence whilst on tamoxifen (p=0.0368) (Table 6.5).

Expression of the Ras isoforms, pRaf(ser259) and pMAPK, was not associated with ROT in those patients treated only with tamoxifen.

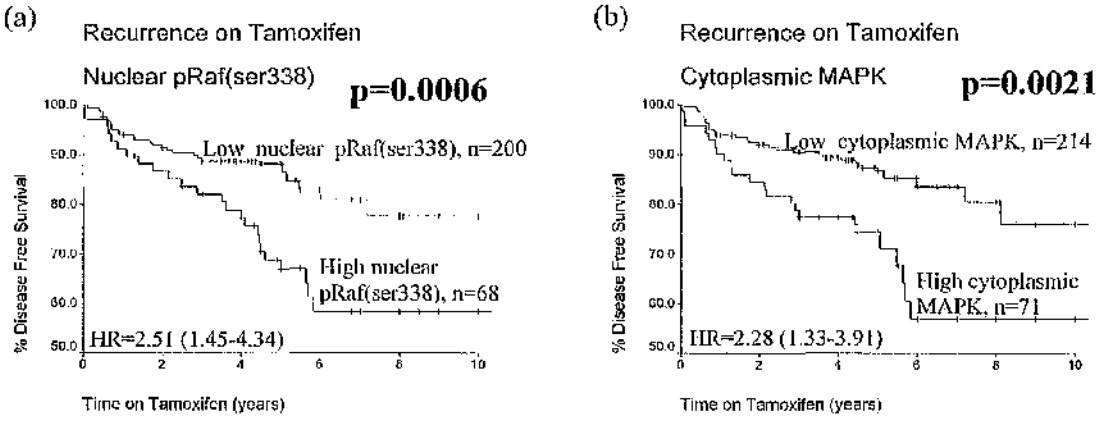

Figure 6.7: Recurrence on Tamoxifen survival curves for patients treated only with Tamoxifen

Kaplan Meier survival curves showing the differences in survival in terms of recurrence whilst on tamoxifen for patients whose tumours express either low or high levels of pRaf(Ser338) or MAPK. (a) The survival curve shows a significant increase in the number of patients who express high levels of nuclear pRaf(ser338) relapsing during tamoxifen treatment in comparison to those patients whose tumours express low levels (p=0.0006). (b) The survival curve shows a significant increase in the number of patients who express high levels of cytoplasmic MAPK relapsing during tamoxifen treatment in comparison to those patients whose tumours express low levels (p=0.0021). High levels were defined as scores ≥ upper quartile value. p values represent log rank testing of the differences in survival. HR=Hazard Ratio (95% CI)

Factor	p-value	Hazard Ratio
Nodal Status	p=0.0011	2.02 (1.33 – 3.05)
Tumour Grade	p=0.0094	1.93 (1.16 – 3.23)
Tumour Size	p=0.0194	2.10 (1.12 – 3.93)
Nuclear pRaf(ser338)	p=0.0439	2.01 (1.03 – 3.92)

Table 6.5: Recurrence on Tamoxifen Cox-regression for patients treated only with tamoxifen

Cox-Regression multivariate analysis revealed that nuclear pRaf(Ser338) expression was independent of known prognostic markers, nodal status, tumour size and grade, in influencing recurrence whilst receiving tamoxifen in patients treated only with tamoxifen. p-values < 0.05 were deemed statistically significant. Hazard ratio = relative risk associated with development of tamoxifen resistance (95% CI).

6.6 Effect of increased expression of Ras/Raf-1/MAPK pathway on overall survival of patients treated only with tamoxifen

6.6.1 Overall Survival (OS)

The end point for overall survival was a breast cancer related death. In total there were 55 breast cancer related deaths in this group of 303 patients.

6.6.2 Expression and activation of Raf-1 and MAPK is linked to a reduction in overall survival time of patients treated only with tamoxifen.

Activation of Raf-1 was linked to a poor outcome in patients treated only with tamoxifen. Patients whose tumours expressed high levels of cytoplasmic or nuclear pRaf(ser338) exhibited a shortened OS time (p=0.0154, 13.60 years vs. 15.06 years) and (p=0.0008, 11.80 years vs. 15.72 years) respectively (Figure 6.8). Increased expression of cytoplasmic or nuclear pRaf(ser338) raised the risk of death in patients treated with tamoxifen by 1.96 (95% CI 1.13-3.42, p=0.0175) and 2.52 (95% CI 1.44-4.41, p=0.0012) times respectively.

Increased expression of MAPK and pMAPK were also associated with a significant reduction in OS time. Patients whose tumours expressed higher levels of cytoplasmic and nuclear MAPK were more likely to die sooner than those with low levels (p=0.0331, 13.15 years vs. 15.55 years) and (p=0.0395, 13.11 years vs. 15.60 years) respectively (Figure 6.9a,b). The relative risk for these patients was 1.84 (95% CI 1.04-3.26, p=0.0359) and 1.78 (95% CI 1.02-3.12, p=0.0423) for cytoplasmic and nuclear MAPK respectively.

Likewise, patients with elevated tumour levels of nuclear pMAPK exhibited a shortened OS time (p=0.0336, 13.50 years vs. 16.10 years, Figure 6.9c). Increased

expression of nuclear pMAPK increased the risk of death in patients treated with tamoxifen by 1.83 (95% CI 1.04-3.24, p=0.0363) times.

Multivariate analysis failed to demonstrate that pRaf(ser338), MAPK or pMAPK were independent factors in influencing overall survival in patients treated only with tamoxifen.

Again, expression of H-, K-, N-Ras and inactive Raf-1 failed to influence outcome in patients treated only with tamoxifen.

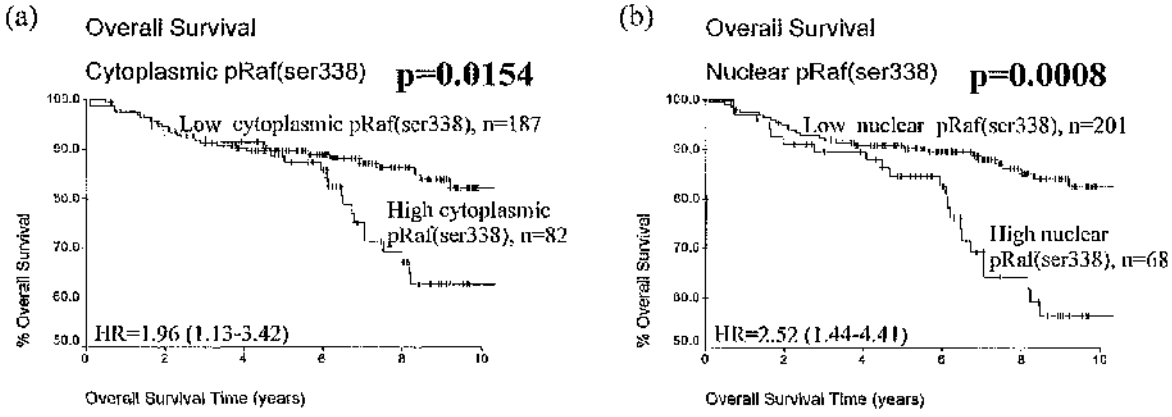

Figure 6.8: Tamoxifen only treated patients pRaf(ser338) overall survival curves

Kaplan Meier survival curves showing overall survival in patients whose tumours express cytoplasmic and nuclear pRaf(ser338). (a) Survival curve showing a significant reduction in overall survival time in patients whose tumours express high levels of cytoplasmic pRaf(ser338) (p=0.0154). (b) Survival curve showing a significant reduction in overall survival time in patients whose tumours express high levels of nuclear pRaf(ser338) (p=0.0008). High levels were defined as scores ≥ upper quartile value. p values represent log rank testing of the differences in survival. HR=Hazard Ratio (95% CI).

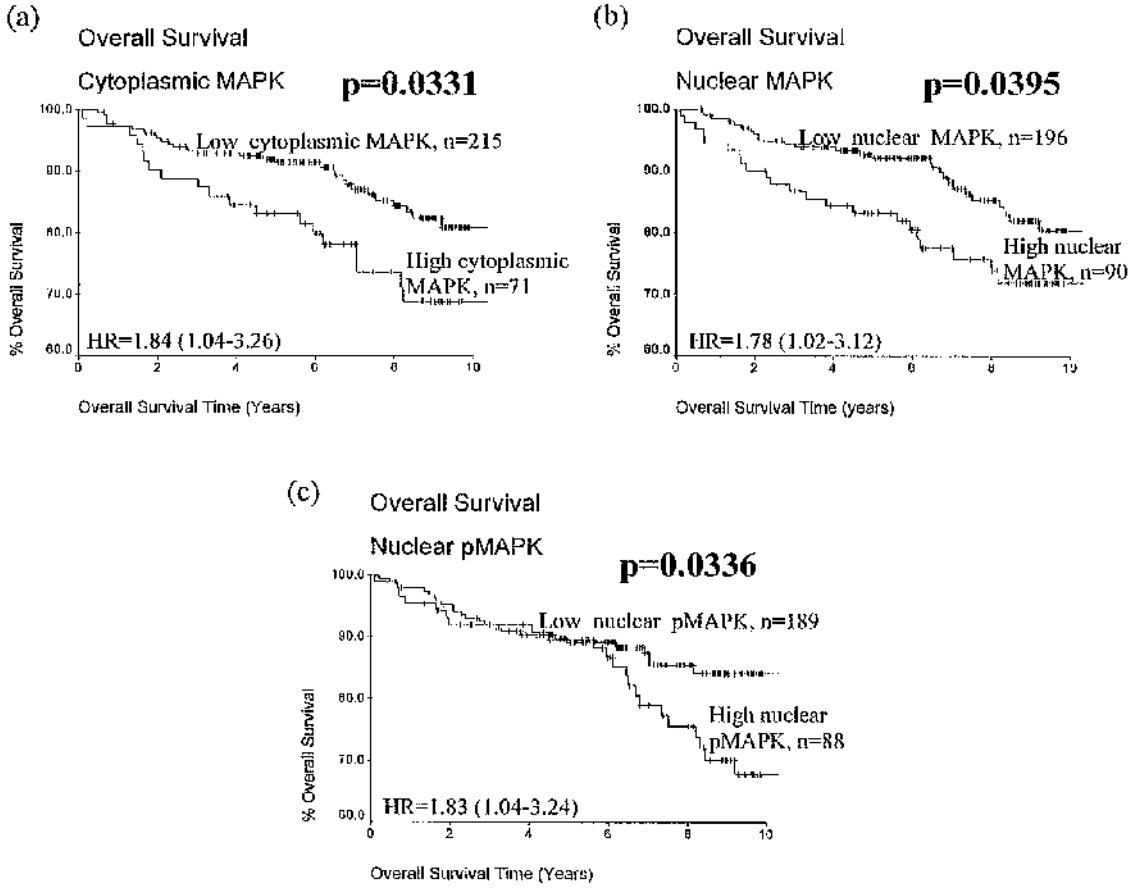

Figure 6.9: Tamoxifen only treated patients MAPK & pMAPK overall survival curves

Kaplan Meier survival curves showing overall survival in patients whose tumours express cytoplasmic and nuclear MAPK and nuclear pMAPK (a) Survival curve showing a significant reduction in overall survival time in patients whose tumours express high levels of cytoplasmic MAPK (p=0.0331). (b) Survival curve showing a significant reduction in overall survival time in patients whose tumours express high levels of nuclear MAPK (p=0.0395). (c) Survival curve showing a significant reduction in overall survival time in patients whose tumours express high levels of nuclear pMAPK (p=0.0336). High levels were defined as scores ≥ upper quartile value. p values represent log rank testing of the differences in survival. HR=Hazard Ratio (95% CI)

6.7 The Ras/Raf-1/MAPK pathway modifies patient outcome and response to treatment

The Ras/Raf-1/MAPK pathway appeared to play a crucial role in the progression of breast cancer and response to treatment, though the effects mediated by Raf-1 and MAPK

seemed to be partially dependent on the patient's treatment regime. Figure 6.10 summarises the impact of Ras, Raf-1 and MAPK on DFS, OS and ROT, in the entire STB cohort, and in the tamoxifen only treated patients.

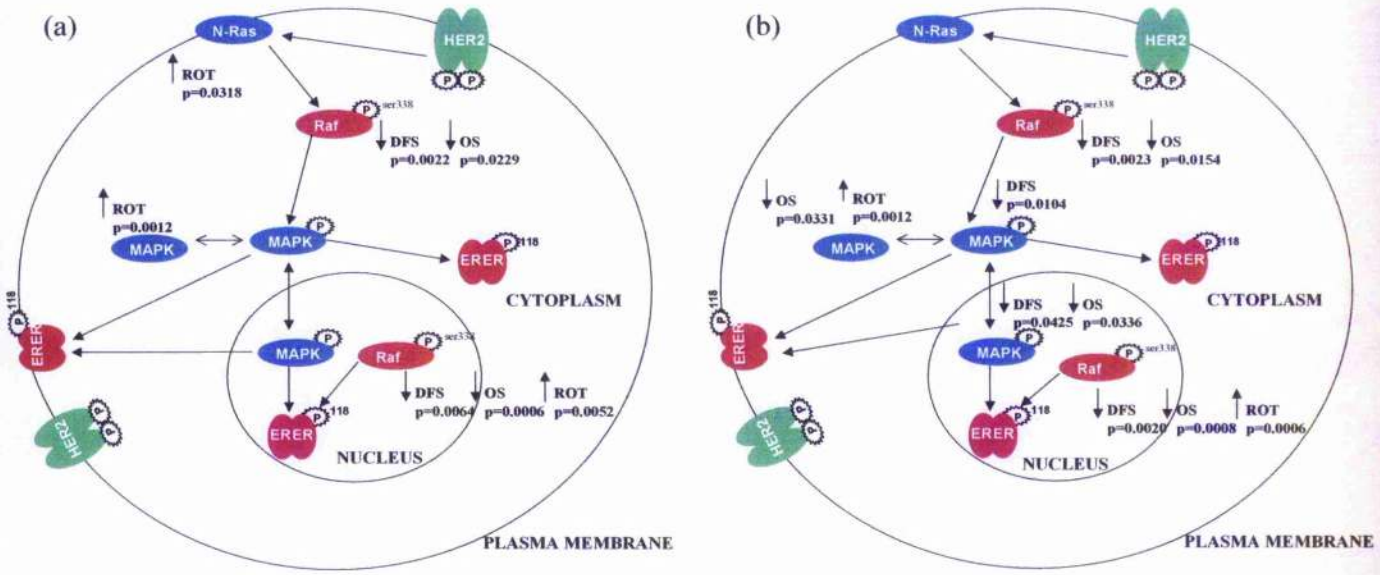

All 402 STB Patients (303 tamoxifen only & 99 tamoxifen/chemotherapy treated patients)

303 tamoxifen only treated patients

Figure 6.10: Association between Ras/Raf-1/MAPK pathway and patient outcome

Schematic representation of the interaction between the Ras pathway and the oestrogen receptor and highlights the factors associated with DFS, OS and ROT in (a) the entire STB cohort and (b) in the tamoxifen only treated patients. DFS= Disease Free Survival, OS = Overall Survival, ROT = Recurrence on Tamoxifen. p values represent log rank testing of the differences in survival, values < 0.05 were deemed statistically significant.

6.8 Association between Ras/Raf-1/MAPK expression and known prognostic markers

Pearsons chi-square analysis was performed to establish if there was any link between expression/activation of Ras, Raf-1, MAPK and tumour grade, size or nodal status.

6.8.1 H-Ras

Cytoplasmic H-Ras was positively correlated with tumour grade (p=0.015). Patients with high levels of cytoplasmic H-Ras in their tumour were more likely to present with a grade 3 tumour. No correlations were observed between H-Ras expression and tumour size or nodal status.

6.8.2 K-Ras

Expression of nuclear K-Ras was associated with nodal status (p=0.019). Patients who presented with increased levels of nuclear K-Ras in their tumour tended to be node-positive. However, no correlation was evident between K-Ras expression and tumour grade or size.

6.8.3 N-Ras

A negative correlation between expression of nuclear N-Ras and tumour grade was evident (p=0.0001). Tumours that overexpressed nuclear N-Ras had a tendency to be of a lower grade (grade 1or 2). There was no evidence of an association between N-Ras expression and tumour size or nodal status.

6.8.4 Raf-1

There were no correlations observed between Raf-1 expression and tumour size, grade or nodal status.

6.8.5 pRaf(ser259)

No associations were evident between pRaf(ser259) expression and tumour grade, size or nodal status.

6.8.6 pRaf(ser338)

Nuclear pRaf(ser338) expression was positively correlated with node positivity ($p=0.009$), but not tumour size or grade, whilst overexpression of cytoplasmic pRaf(ser338) was associated with increased tumour grade ($p=0.012$), but not size or nodal status.

6.8.7 MAPK

Cytoplasmic MAPK expression was positively associated with tumour grade ($p=0.025$), size ($p=0.002$) and nodal status ($p<0.0005$). No correlations were observed between nuclear MAPK and known prognostic markers.

6.8.8 pMAPK

No associations were evident between pMAPK expression and tumour grade, size or nodal status.

6.9 Is the Ras/Raf-1/MAPK pathway activated in breast tumours?

Having shown that increased expression of the individual components of the Ras/Raf-1/MAPK pathway were associated with patient outcome, it was logical to assess whether the pathway was activated in tumours. Spearman Rank tests suggested a trend that increased levels of Ras expression, in particular N-Ras, was associated with increased activation of Raf-1, which subsequently was linked to increased phosphorylation of MAPK. However, the correlations should be observed with caution, since all the correlation coefficients for the various interactions were very low (Tables 6.6 & 6.7, Figures 6.11, 6.12 & 6.13). In particular, the scatter graphs examining the relationship between the Ras isoforms and inactive Raf-1, pRaf(ser259), highlight that the p-values should be viewed with some scepticism (Figure 6.12).

		pRaf(ser338)		pRaf(ser259)
		Cytoplasmic	Nuclear	Cytoplasmic
H-Ras	Cyto	$R^2 = 0.130$ p=0.015	$R^2 = -0.052$ p=0.329	$R^2 = 0.138$ p=0.009
	Nuc	$R^2 = -0.163$ p=0.002	$R^2 = 0.066$ p=0.213	$R^2 = -0.161$ p=0.002
K-Ras	Cyto	$R^2 = 0.226$ p<0.0005	$R^2 = 0.067$ p=0.212	$R^2 = 0.139$ p=0.008
	Nuc	$R^2 = 0.061$ p=0.250	$R^2 = 0.143$ p = 0.007	$R^2 = 0.249$ p<0.0005
N-Ras	Cyto	$R^2 = 0.274$ p<0.0005	$R^2 = 0.028$ p=0.603	$R^2 = 0.170$ p=0.001
	Nuc	$R^2 = -0.217$ p<0.0005	$R^2 = -0.002$ p=0.971	$R^2 = -0.117$ p=0.027

Table 6.6: Correlations between Ras and Raf-1

Spearman Rank Tests were performed to analyse the relationship between overexpression of the three Ras isoforms and phosphorylation of Raf-1, at serine 259 and serine 338, in the cytoplasm and nuclei. Only cytoplasmic pRaf(ser259) was analysed, because only very low levels of nuclear pRaf(ser259) were detected. R^2 = correlation coefficient. p values < 0.003 were deemed statistically significant, using Bonferroni's correction. ns = non-significant.

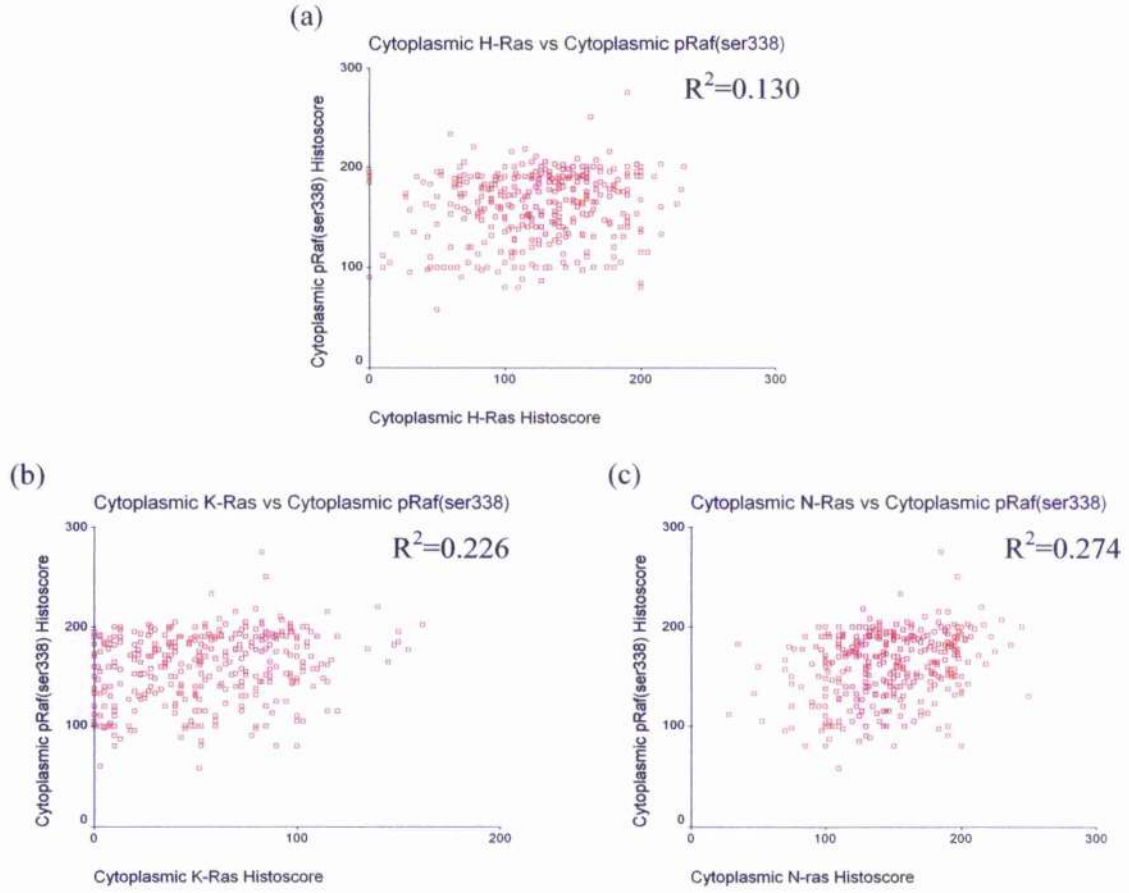

Figure 6.11: Scatter graphs of the interaction between Ras and pRaf(ser338)

The above scatter graphs highlight the relationship between expression of the three Ras isoforms in the cytoplasm and expression of cytoplasmic pRaf(ser338). The scatter plots and the correlation coefficients (R^2) suggest that the strongest correlation was between the expression of cytoplasmic N-Ras and cytoplasmic pRaf(se338).

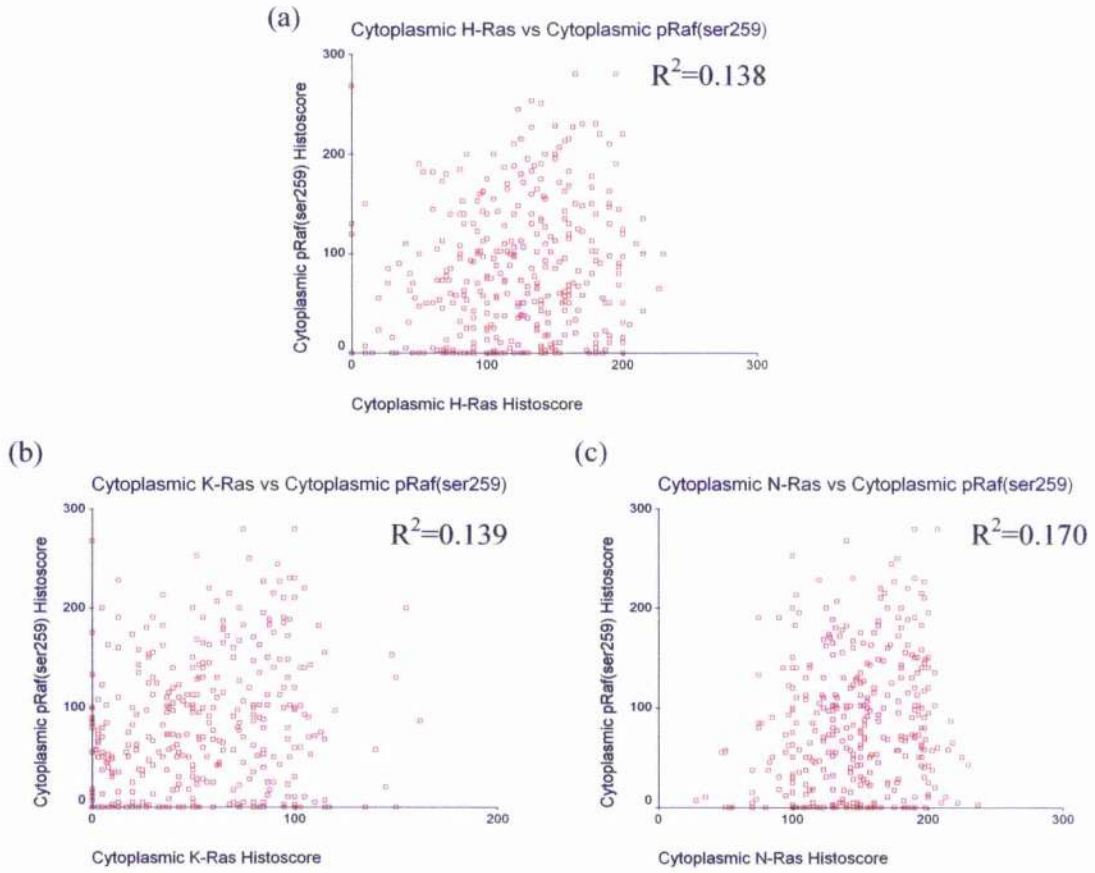

Figure 6.12: Scatter graphs of the interaction between Ras and pRaf(ser259)

The above scatter graphs highlight the relationship between expression of the three Ras isoforms in the cytoplasm and expression of cytoplasmic pRaf(ser259). The scatter plots and the correlation coefficients (R^2) suggest that the correlations should be interpreted with caution.

	pMAPK Cyt	pMAPK Nuc
pRaf(ser259) Cyt	$R^2 = 0.495$ $p < 0.0005$	$R^2 = 0.377$ $p < 0.0005$
pRaf(ser338) Cyt	$R^2 = 0.333$ $p<0.0005$	$R^2 = 0.213$ $P<0.0005$
pRaf(ser338) Nuc	$R^2 = 0.262$ $P<0.0005$	$R^2 = 0.300$ $P<0.0005$

Table 6.7: Correlations between pRaf and pMAPK expression

Spearman Rank Tests were performed to analyse the relationship between expression of pRaf(ser259) and pMAPK, pRaf(ser338) and pMAPK. R^2 = correlation coefficient, p values <0.008 deemed statistically significant, using Bonferroni's correction.

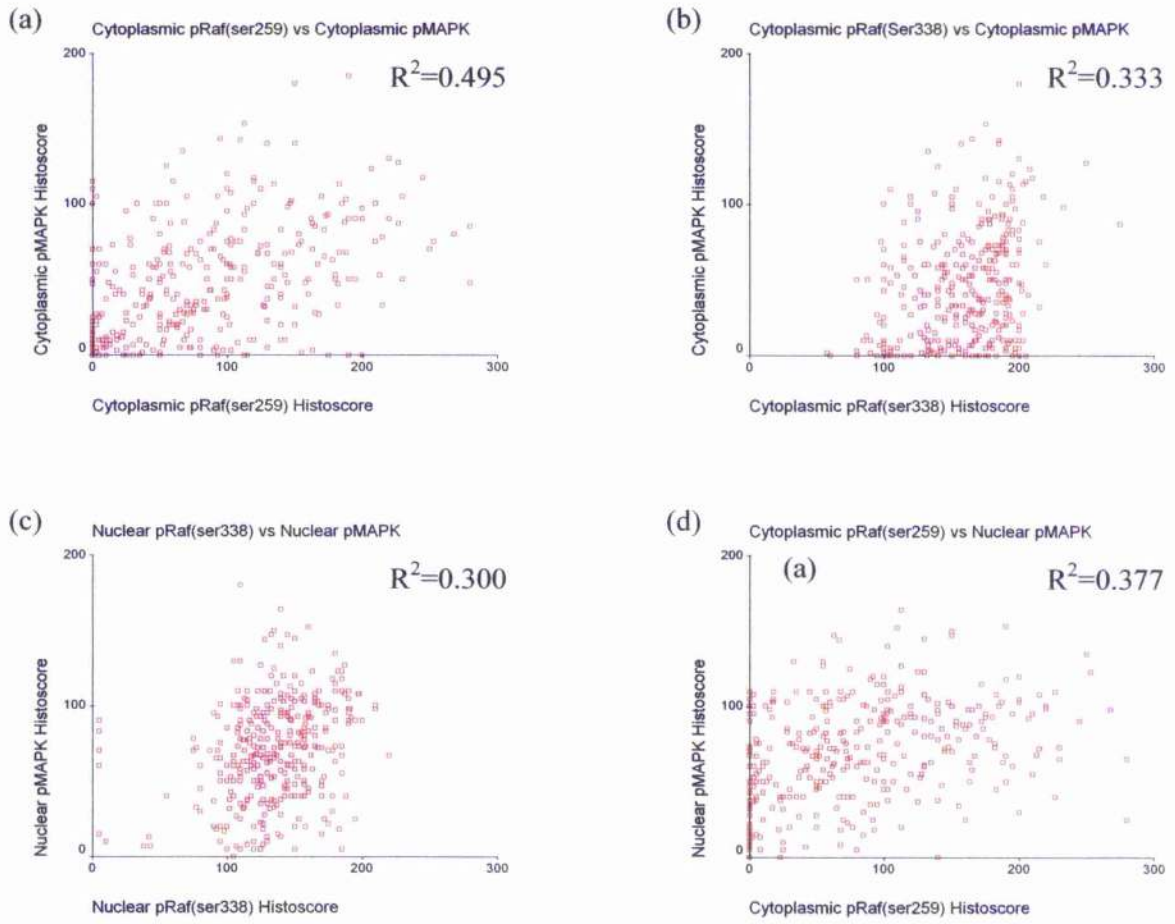

Figure 6.13: Scatter graphs of the interaction between pRaf and pMAPK

The above scatter graphs highlight the relationship between expression of pRaf-1 and pMAPK. The scatter plots and the correlation coefficients (R^2) suggest that despite p-values <0.008 the correlations should be observed with caution.

6.10 Relationship between the Ras/Raf-1/MAPK pathway and the activation and localisation of the oestrogen receptor.

Having shown that increased activation of Raf-1 and expression of MAPK was associated with increased risk of tamoxifen resistance, and knowing that MAPK can activate ERα in a ligand independent manner, it was deemed appropriate to investigate the relationship between activation of the Ras pathway and expression and phosphorylation of ERα. Spearman Rank Tests were performed to analyse the relationship between expression of pRaf(ser338)/MAPK/pMAPK and ER/pER(ser118)/pER(ser167) in the various subcellular compartments. Immunohistochemistry for ER, pER(ser118) and pER(ser167) had previously been performed by Miss Sian Tovey.

6.10.1 Relationship between MAPK and ER expression

Analysis revealed that there was a very weak inverse relationship between expression of nuclear MAPK and ER expression (Table 5.8). There appeared to be a trend towards tumours with increased levels of nuclear MAPK expressing lower levels of cytoplasmic and nuclear ER ($p<0.0005$ and $p=0.031$ respectively). Again, the correlation coefficients were very low, and these results should be observed with caution.

	MAPK Cyto	MAPK Nuc
ER Cyt	ns	$R^2 = -0.180$ $p<0.0005$
ER Nuc	ns	$R^2 = -0.111$ $p=0.031$

Table 6.8: Relationship between MAPK and ER expression

Spearman Rank Tests were performed to analyse the relationship between expression of MAPK and ER in the cytoplasm and nuclei of tumour cells. R^2 = correlation coefficient. p values < 0.01 were deemed statistically significant, using Bonferroni's correction.

6.10.2 Relationship between Ras/Raf-1/MAPK pathway and pER localisation.

At first glance, Spearman Rank Tests suggested that there were several statistically significant interactions between Raf-1, MAPK and ERα. However, closer examination of the p-values, correlation coefficients and scatter plots highlighted that only the interaction between nuclear pMAPK and nuclear pER(ser167) could be deemed believable (R^2=0.298, p<0.0005) (Table 6.9, Figure 6.14). Figure 6.14 also shows two examples of scatter graphs of correlations that appear statistically significant, but have relatively low correlation coefficients and, therefore, should be regarded with scepticism.

	pER(ser118)			pER(ser167)		
	Cyto	**Nuc**	**Memb**	**Cyto**	**Nuc**	**Memb**
pRaf(Ser338) Cyto	**R^2=0.201 p<0.0005**	R^2= 0.068 P=0.204	R^2=0.136 **p=0.01**	R^2=0.109 p=0.045	**R^2=0.205 p<0.0005**	R^2=0.159 p=0.003
pRaf(ser338) Nuc	R^2= 0.023 p=0.663	R^2=0.170 P=0.001	R^2= 0.078 p=0.140	R^2= -0.053 p=0.334	R^2=0.173 p=0.001	R^2=0.139 p=0.011
MAPK Cyto	R^2= 0.083 p=0.111	R^2= 0.066 P=0.205	R^2=0.140 p=0.007	R^2= 0.027 p=0.608	R^2= 0.020 p=0.711	R^2=0.176 p=0.001
MAPK Nuc	R^2 -0.086 p=0.102	R^2= -0.101 P=0.053	R^2=0.108 p=0.036	**R^2=-0.248 p<0.0005**	R^2=-0.172 P=0.001	R^2= -0.010 p=0.850
pMAPK Cyto	R^2=0.164 p=0.002	R^2= 0.102 P=0.054	**R^2=0.228 p<0.0005**	**R^2=0.206 p<0.0005**	R^2=0.115 p=0.033	**R^2=0.234 <0.0005**
pMAPK Nuc	R^2= 0.085 p=0.107	R^2=0.106 P=0.045	R^2=0.172 p=0.001	R^2=0.165 p=0.002	**R^2=0.298 p<0.0005**	R^2=0.124 p=0.021

Table 6.9: Relationship between Raf-1/MAPK expression & pER expression

Spearman Rank Tests were performed to analyse the relationship between expression of pRaf(ser338)/MAPK/pMAPK and pERser(118)/pER(ser167) in the three subcellular compartments, namely cytoplasm, nuclei and plasma membrane. R^2 = correlation coefficient. p values < 0.001 were deemed statistically significant, using Bonferroni's correction.

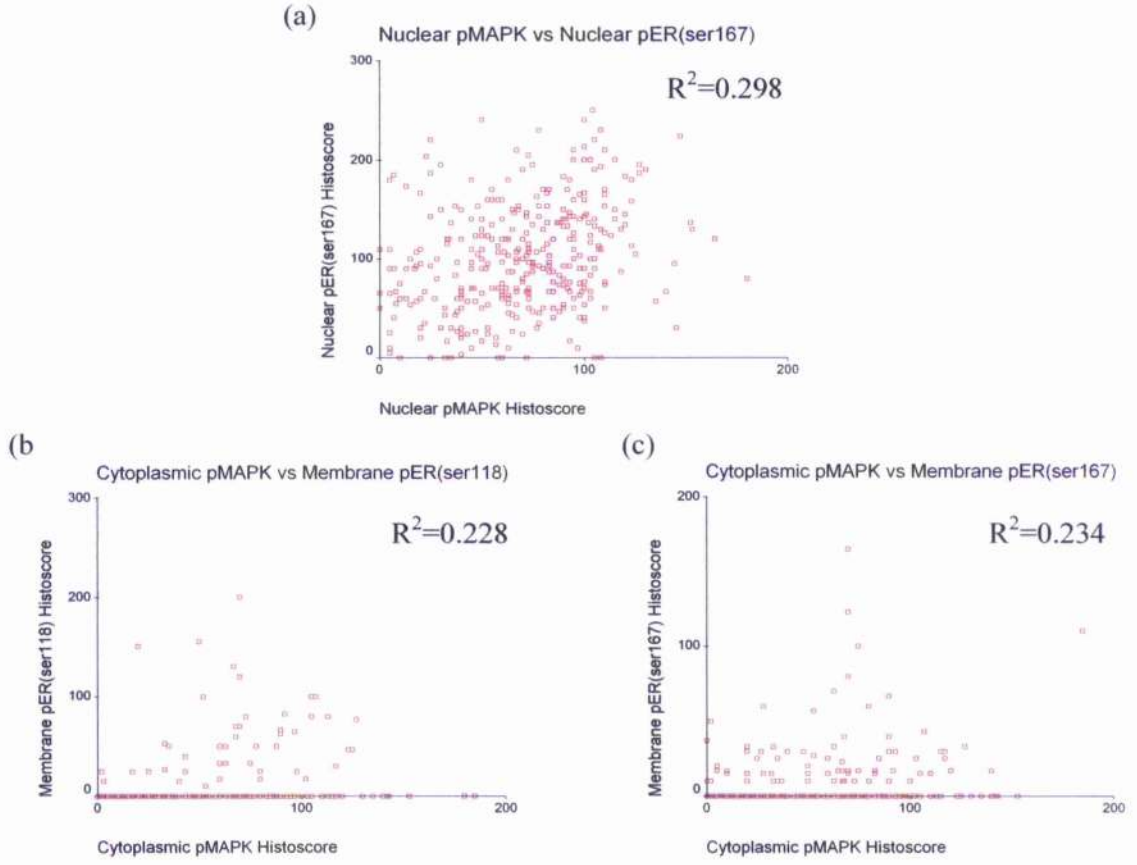

Figure 6.14: Scatter graphs of the interactions between MAPK and ER

Spearman Rank Tests suggested there were several statistically significant correlations between Raf-1, MAPK and ERα. However, examination of the correlation coefficients revealed that the only believable interaction was between nuclear pMAPK and nuclear pER(ser167) (a). Graphs b,c show that despite p-values <0.0005, the correlations between cytoplasmic pMAPK and membrane pER must be viewed with some scepticism.

6.11 Discussion

It has long been hypothesised that the interaction between growth factor receptor pathways and ERα mediates tamoxifen resistance. This study presents clinical evidence that expression and activation of the components of the Ras/Raf-1/MAPK pathway in clinical breast tumours is associated with a poor outcome, in particular the failure to respond to tamoxifen treatment (tamoxifen resistance).

While the Ras/Raf-1/MAPK pathway serves multiple purposes, two key functions are modulation of cell proliferation and modification of ERα. Tamoxifen functions by down-regulating ERα activity, inhibiting activation of oestrogen regulated genes and reducing cell proliferation. That Ras, Raf-1 and MAPK proteins appear to be predictive markers for response to treatment for patients treated with tamoxifen implies that the modification of ERα by the Ras pathway is crucial in the development, progression, and treatment responsiveness of tamoxifen treated breast tumours.

Initial analysis of the entire STB cohort (303 tamoxifen only and 99 tamoxifen and chemotherapy treated patients) revealed that the development of tamoxifen resistance was partially dependent on the expression and activation of the Ras cascade. Patients whose tumours overexpressed cytoplasmic N-Ras ($p=0.0318$) and nuclear pRaf(ser338) ($p=0.0052$) exhibited a shortened time to relapse whilst receiving tamoxifen. Furthermore, pRaf(ser338) was the only factor related to reduced disease-free and overall survival time. That of the three isoforms, only N-Ras appears to be involved in the mechanism that drives tamoxifen resistance confirms previous findings that the various Ras isoforms differ in their functions and ability to activate their downstream effectors, such as Raf-1 and PI3K. K- and N-Ras are believed to be the more effective activators of Raf-1, whereas H-Ras is more efficient in activating the PI3K/Akt pathway

(132;133;218). This, too, was suggested in our study, of the three isoforms, N-Ras expression appeared to be the most significantly correlated with activation of Raf-1. Consequently, the various Ras isoforms may regulate different pathways that mediate response to alternative treatments. Overexpression and activation of the N-Ras/Raf-1/MAPK pathway is perhaps fundamental in the acquisition of tamoxifen resistance. This theory is further supported by the findings from this study that MAPK is a potential predictive marker of response to tamoxifen treatment, since patients expressing high levels of MAPK in their tumours were more likely to relapse whilst receiving tamoxifen ($p=0.0012$). Additionally, MAPK, unlike Ras or Raf-1, was shown to be independent of known prognostic markers, namely tumour size, grade and nodal status, in predicting response to treatment.

MAPK controls multiple cellular processes through phosphorylating and activating substrates within the cytoplasm and the nuclei of cells. However, of particular interest is its ability to modify the activation status of ERα and ERα regulated genes. The relationship between MAPK and ERα has been well documented; it is known that MAPK directly phosphorylates ERα at serine 118, and indirectly at serine 167, via p90rsk (39;197;201). This ligand-independent phosphorylation of ERα results in its increased interactions with co-activators rather than co-repressors, which subsequently increases ERα-mediated transcriptional activity. It is thought that this contributes to tamoxifen resistance by promoting tumour growth in the presence of low levels of oestrogen. In addition, MAPK phosphorylates ERα co-activator proteins, such as SRC-1 and AIB1, enabling them to interact with ERα, which further enhances transcriptional activity and may promote the agonistic rather than antagonistic nature of Tamoxifen (216;217).

Alternatively, tumour ERα levels may decrease in response to increasing expression levels of MAPK. Several studies have shown that overexpression and increased activation of the EGFR/HER2 pathways in ERα positive breast cancer cells can promote ERα loss and subsequently reduce expression of oestrogen-regulated genes, such as the progesterone receptor (204;208;225). Furthermore, ERα negative breast tumours tend to present with overexpression of the growth factor receptors and elevated levels of MAPK (259). Elevated MAPK activity was prominent in the tumours of patients exhibiting *de novo* tamoxifen resistance (225). Activation of MAPK in MCF-7 cells corresponds to increased activation of Nuclear Factor-κB, and it is thought that this is partially responsible for the down-regulation of ERα (206). A more recent study suggests that hyper-activation of MAPK in ERα positive cancer cells is a key mechanism in driving the change from an ERα positive to a ERα negative phenotype, and that there is a "hyperactive MAPK signature" set of genes that identify ERα negative tumours (208). Data from our study also suggests the trend that tumours expressing high levels of nuclear MAPK exhibit lower levels of ERα. Previous research demonstrated that patients whose tumours exhibited lower levels of ER had a poorer prognosis (223). Our findings support this, in that patients with increased levels of MAPK presented with more aggressive tumours. These patients were more likely to be node positive and have tumours that were both larger in size and higher in grade, all of which are known to be poor prognostic markers. However, ERα levels can be restored in MCF-7 breast cancer cells (205) using MEK inhibitors, therefore, the same approach might be appropriate in patients whose tumours overexpress MAPK.

To further probe the role of the Ras pathway in driving tamoxifen resistance, it was deemed appropriate to analyse the effects of Ras, Raf-1 and MAPK expression on the outcome of those patients treated only with tamoxifen, thus avoiding the potential compounding effects of combined endocrine and chemotherapy treatments. Whilst clearly exploratory, due to the reduced sample size, these sub-analyses confirmed initial findings that activation of the Ras pathway is a crucial mechanism in the progression of breast cancer and development of tamoxifen resistance. In this sub-group, both elevated levels of pRaf(ser338) and pMAPK were associated with reduced disease free and overall survival time, strengthening the argument that activation of the Ras pathway is linked to a poor outcome.

The original analysis of the entire STB cohort failed to show a relationship between pMAPK expression and patient outcome. Previous studies have been inconclusive in confirming whether expression levels of pMAPK influence patient survival and resistance to treatment. Two clinical studies suggested that patients with low levels of pMAPK were more responsive to tamoxifen (223;225). Whereas *in vitro* analysis showed that tamoxifen significantly inhibited the growth of MCF-7 cells transfected with constitutively activated MEK, and that activation of MAPK was not contributing to tamoxifen resistance (212). Another study investigating pMAPK, in untreated patients and in a mixture of differently treated patients, showed that, in only the untreated patients, did pMAPK correlate with overall survival (224). The differences observed in terms of the role of pMAPK in influencing outcome may be because we are comparing *in vivo* and *in vitro* studies. It might also be that the phosphorylated form of MAPK does not necessarily represent the activated form of the protein. It has been shown

that both the dimerisation and nuclear localisation of MAPK are dependent on its phosphorylation, but not its activation status (195). It may also reflect the difficulty in finding reliable phosphorylated antibodies.

As in the original analyses, overexpression of nuclear pRaf(ser338) and cytoplasmic MAPK were once again linked with relapse whilst receiving tamoxifen treatment. Conversely, though, in this tamoxifen only treated group, it was pRaf(ser338) expression and not MAPK expression that proved to be independent of tumour size, grade and nodal status in predicting for tamoxifen resistance. Additionally pRaf(ser338) was also shown to be an independent predictive marker of reduced disease free survival. These findings, together with those from the analysis of the entire STB cohort, suggest that pRaf(ser338), as opposed to MAPK, is a better predictor of patient outcome in tamoxifen treated patients.

There are several implications from these findings. The first is that, whilst N-Ras and MAPK are associated with the development of tamoxifen resistance and emphasise the importance of the Ras pathway, it is nuclear pRaf(ser338) that is the principal candidate for identifying patients failing to respond to tamoxifen. The second is that elevated levels of activated Raf-1 in tumours may predict for poor response to Tamoxifen; however it also appears to identify patients who benefit from a combined treatment regime of tamoxifen and chemotherapy. Finally, that MAPK was not an independent predictive marker in the tamoxifen only treated patients, but was in the cohort of tamoxifen and chemotherapy treated patients, perhaps suggests that MAPK partially controls cells response to chemotherapy.

Raf-1 is a serine-threonine kinase that plays a role in cell proliferation, differentiation and apoptosis, and is prominent in controlling tumour angiogenesis and metastasis (260). This study illustrated that upregulated activity of Raf-1 in tumours was related to poorly differentiated tumours (high grade) and tumour spread (node positivity). A recent study demonstrated that targeting of Raf-1 inhibited tumour growth, and that this represented an important therapeutic strategy (186). Additionally, the Ras pathway has been shown to interact with and activate ERα. The finding that the Ras/Raf-1/MAPK pathway, in particular Raf-1, are predictive markers for survival and response to tamoxifen may suggest that the interaction between this pathway and ERα is fundamental in influencing patient outcome in response to tamoxifen.

As discussed above, the ligand-independent phosphorylation of ERα at serine 118 is believed to be a major contributor to the development of tamoxifen resistance. However, increased expression of neither nuclear pMAPK nor pER(ser118) (unpublished data from our group) demonstrated a significant association with relapse on tamoxifen treatment. This implies that, whilst MAPK driven phosphorylation of ERα is important, it is not the only contributing factor in the development of tamoxifen resistance. It also suggests that the mechanism by which nuclear pRaf(ser338) influences tamoxifen resistance is independent of MAPK.

It is perhaps surprising, considering the vast quantities of research that is undertaken to investigate the Ras/Raf-1/MAPK pathway, that Raf-1 is not the only effective activator of Mek1/2 and subsequently MAPK. B-Raf is considered to be a main activator of MEK (261-263). Activation of Raf-1 is thought to result in the transient phosophorylation of MAPK (261). Consequently, there are thought to be other cellular

targets for Raf-1, and research has revealed other functions of Raf-1, such as its ability to regulate Rho signalling independently of MAPK (264). One other key Raf-1 substrate is the Retinoblastoma (RB) tumour suppressor protein.

Research has highlighted that nuclear Raf-1 binds and phosphorylates Rb protein independently of the MAPK cascade (184). Phosphorylation of Rb results in its inactivation, and the subsequent dissociation from and activation of E2F. This ultimately results in the cell cycle progressing from G1 to S phase. Therefore, translocation of Raf-1 into the nucleus can facilitate cell proliferation. Studies have shown that prevention of the interaction between Raf-1 and Rb prevents tumour growth and angiogenesis (265). This corresponds with our findings that increased Raf-1 is associated with poor patient outcome. Furthermore, it is postulated that Rb is a key target of oestrogen, and that inactivation of Rb is connected to the development of resistance to antioestrogen therapies, such as tamoxifen (266). Additionally, the antioestrogens, ICI 164,384 and OHT (4-Hydroxy Tamoxifen), were shown to be able to prevent oestrogen-induced hyperphosphorylation of Rb, in T57D cells. Tamoxifen, however, was unable to do this (267). Interestingly, Rb has been shown to be a co-activator of the androgen receptor in prostate cancer cells (268;269). These results imply that activation and translocation of Raf-1 to the nucleus inactivates Rb, which results in increased cellular proliferation, even in the presence of antioestrogens.

Elevated levels of activated Raf-1 in tumours predicted for poor response to Tamoxifen; however it also seemed to identify those patients who would benefit from a combined treatment regime of tamoxifen and chemotherapy. Chemotherapy targets highly proliferating cells. In tumours, cell growth is driven by the classical proliferative

factors, such as c-fos, but also by the Ras/Raf-1/MAPK-ERα interactions, which will enhance cells sensitivity to oestrogen, and ultimately increase proliferation. Furthermore, the interaction between nuclear Raf-1 and Rb will stimulate cell proliferation and growth. One might, therefore, predict that tumours which overexpress Ras/Raf-1/MAPK might be more responsive to chemotherapy. Accordingly, it seemed that those patients who overexpressed pRaf(ser338) had an improved outcome when treated with chemotherapy, in addition to tamoxifen. Comparison of the survival curves from the tamoxifen only treated group with the tamoxifen only and tamoxifen plus chemotherapy cohort suggested that chemotherapy delayed tamoxifen relapse in those patients expressing high levels of pRaf(ser338) but not MAPK. In the tamoxifen only treated group, increased expression of pRaf(ser338) and MAPK seemed to mediate early events in the development of tamoxifen resistance. This pattern fits with previous research that suggests that changes in the MAPK cascade are important in the early stages of development and maintenance of tamoxifen resistance (270). However, supplementary chemotherapy treatment seemed to temporarily negate the effects of elevated pRaf(ser338). Activation of Raf-1 seemed to be associated with a lack of response after 3 years of tamoxifen treatment. Increased tumour levels of pRaf(ser338) are indicative of poor response to Tamoxifen, but perhaps also of an enhanced response to chemotherapy. This supports previous findings that increased expression of Raf-1 in cell lines makes them more responsive to chemotherapeutic agents (271). Perhaps this signifies that pRaf(ser338) is a potential marker to identify patients for whom tamoxifen alone is insufficient adjuvant systemic therapy. Those patients who overexpress pRaf(Ser338) in their tumours may require treatments such as chemotherapy or aromatase inhibitors, in addition to tamoxifen.

Studies are currently underway investigating the benefits of switching from tamoxifen to aromatase inhibitors (AIs) after 2-3 years of tamoxifen treatment (IES study)(272). Analysis of patients who remained disease-free after 3 years tamoxifen treatment revealed that overexpression of pRaf(ser338) was significantly associated with shortened time to relapse and death. These results, again, raise the possibility that activated Raf-1 is a suitable marker for identifying patients who require other treatments besides tamoxifen. However, further research, perhaps in the TEAM or ATAC trial, is required to test the ability of activated Raf-1 to function as an effective predictive marker for response to tamoxifen treatment.

Unlike the expression of activated Raf-1, MAPK expression was an independent marker of tamoxifen resistance in the entire STB cohort perhaps suggesting that MAPK regulates response to chemotherapy. To investigate this hypothesis and to establish the role of both Raf-1 and MAPK in mediating response to chemotherapy, a similar study to this one was performed on a cohort of breast cancer patients from the NEAT/BR9601 trial who had received adjuvant chemotherapy. The results are discussed in the following chapter.

In recent years, the localisation of ERα has been the focus of much research. Previously the presence of membrane ERα had been ignored; however, it is now acknowledged that ERα is localised to the cytoplasm, nuclei and membrane of cells, and that the functions of nuclear and membranous ERα differ. Nuclear ERα exerts genomic effects through regulating transcription of oestrogen-regulated genes, whereas membranous ERα mediates non-genomic effects via activating signal transduction cascades, such as the Ras/Raf-1/MAPK pathway (48-51). It is, therefore, becoming

increasingly obvious that the subcellular localisation of proteins, as well as the extent of their expression, is an important factor when attempting to establish new prognostic and predictive markers. This was particularly apparent from the analyses of Ras and Raf-1 proteins. Overexpression of the activated form of Raf-1, pRaf(ser338), was linked to reduced disease-free and overall survival in patients. pRaf(ser338) altered patient outcome, regardless of whether it was expressed in the cytoplasm or nuclei of tumour cells. However, only nuclear pRaf(ser338) was associated with recurrence on Tamoxifen, suggesting that the cytoplasmic and nuclear forms of these proteins have different functions. This argument is further strengthened by the fact that patients who overexpressed cytoplasmic pRaf(ser338) in their tumours were more likely to present with higher grade tumours (grade=3), whereas those patients who overexpressed nuclear pRaf(ser338) in their tumours were predisposed to be node positive. These results suggest that cytoplasmic pRaf(Ser338) is involved in regulating cellular differentiation, whereas nuclear pRaf(ser338) perhaps regulates cell motility and tumour metastasis.

The varying function of proteins, depending on their localisation, was evident from the findings regarding the role of Ras in breast cancer. In both this study and the pilot study (chapter 3), H-, K- and N-Ras were localised to both the cytoplasm and nuclei of tumour cells. In the pilot study, overexpression of both cytoplasmic and nuclear N-Ras was associated with a reduced time to relapse and death. However, in this study, only cytoplasmic N-Ras was linked to an increased risk of tamoxifen resistance. Nonetheless, this study highlights, that like Raf(ser338), the cytoplasmic and nuclear Ras isoforms seem to have different functions. Cytoplasmic N-Ras may be linked to an increased risk of relapse on tamoxifen, but its nuclear counterpart was inversely correlated with tumour

grade. Those patients who overexpressed nuclear N-Ras were more likely to present with a lower grade tumour. Likewise, differences were observed between cytoplasmic and nuclear H-Ras. Increased expression of cytoplasmic, but not nuclear H-Ras, was associated with higher grade tumours, suggesting a role for cytoplasmic H-Ras in regulating differentiation. Similar differences were observed with K-Ras. The nuclear, but not cytoplasmic form of this protein, was associated with node positivity. Therefore, this study highlighted, not only the importance of subcellular specific functions of proteins, but also confirmed previous findings that the various Ras isoforms have different abilities to control cellular processes, such as differentiation and cell motility. Additionally, it again underlines the importance of the newly identified nuclear Ras, especially K- and N-Ras, and highlights the necessity of establishing the function of this nuclear protein.

This is the first study to investigate the function of the Ras/Raf-1/MAPK pathway in tumours of breast cancer patients treated with tamoxifen. It has demonstrated that this proliferative pathway is activated in breast tumours, and that this activation significantly contributes to the development of tamoxifen resistance in patients. These results suggest that activated Raf-1 is a potential predictive factor for identifying patients who are least likely to respond to tamoxifen and would require either additional or alternative therapies, such as chemotherapy, AIs or even Raf-1 inhibitors. Furthermore, this study laid the foundations for the research investigating the role of the Ras pathway in chemotherapy response, and the interactions between MAPK and ERα in breast cancer cell lines, all of which are discussed in the proceeding chapters.

7. The role of the Ras/Raf-1/MAPK pathway in the development of resistance to chemotherapy

7.1 Introduction

The results from the STB study (chapter 6) suggested that activation of the Ras/Raf-1/MAPK pathway was associated with the development of tamoxifen resistance. Activated Raf-1 was identified as a possible predictive marker for tamoxifen resistance. However, this study also inferred that increased expression of pRaf(ser338) in tumours identified a group of patients who would benefit from the combined treatment of both tamoxifen and chemotherapy. Furthermore, it raised questions regarding the role of MAPK in predicting patients' response to chemotherapy.

Adjuvant chemotherapy is generally accepted as the treatment for women with node-positive breast cancer. This involves the use of cytotoxic drugs to kill cancer cells by direct toxic actions (as opposed to tamoxifen, which modulates a biological target). Following the NEAT (National breast cancer study of Epirubicin & CMF versus classical CMF Adjuvant Therapy) clinical trial, the combination of epirubicin and CMF is now a common practice in the UK.

Despite the extensive use of chemotherapy as adjuvant treatment, failure to respond to treatment is a major clinical problem. For the majority of chemotherapeutic agents to function efficiently, the tumour cells must be proliferating and in a growth phase. Patients who present with tumours that have only a small percentage of cells in growth phase, are more likely to develop resistance to chemotherapeutic agents (13). The exact mechanisms underlying the development of resistance to chemotherapy are not fully understood. However, several studies have suggested that the Ras/Raf-1/MAPK

pathway may be involved in the development of resistance to epirubicin and doxorubicin.

This study investigated whether expression and activation of Raf-1 and MAPK influenced clinical outcome following treatment with chemotherapy. It tested the hypothesis that activation of the Ras/Raf-1/MAPK pathway drives resistance to chemotherapy in clinical breast cancers. Patients from the NEAT/BR9601 cohort were analysed for Raf-1 and MAPK expression and activation (discussed in Chapter 4), and survival analysis was performed, in terms of disease-free survival (DFS), and overall survival (OS).

7.2 Patient cohort & treatment

Patients from the BR9601 (NEAT) trial were randomly allocated to receive treatment of 4 cycles of epirubicin, followed by 4 cycles of CMF given intravenously every three weeks, or treatment with 8 cycles of classical CMF given intravenously every three weeks (Table 7.1). Three hundred and eighty four patients were randomised in the original trial, and we retrieved tissue samples from 318 of these cases (84%). 155 patients (48.74%) received the combined treatment of Epirubicin and CMF, while the remaining 163 patients (51.26%) received only CMF. Survival analysis was performed on all 318 NEAT patients, but also on the two sub-groups of patients: those that received CMF alone and those that received it in combination with epirubicin.

The results from chapter 6 suggested that pRaf(Ser338) and MAPK expression might predict for response to chemotherapy in tamoxifen treated patients. To investigate this further, it was deemed appropriate to combine the two patient cohorts for survival analysis. In total there were 264 ERα positive patients (165 NEAT patients and 99 STB patients) who received both tamoxifen and chemotherapy. Additionally 25 ERα negative

and 34 ERα unknown patients received both tamoxifen and chemotherapy, but these patients were excluded from further sub-analyses. Ninety-four patients from the NEAT study were treated with chemotherapy but not tamoxifen (79 ERα –ve, 9 ERα+ve, 6 ERα Unknown). Consequently, survival analysis was performed on the two sub-groups of patients: those that received tamoxifen in combination with chemotherapy (264 patients) and those that received only chemotherapy (94 patients). Table 7.2 provides details of the various treatments.

Treatment	Dose
CMF	Cyclophosphamide: 750mg/m^2 iv Methotrexate: 50mg/m^2 iv 5-fluorouracil: 600mg/m^2 iv
Epirubicin	Epirubicin: 100mg/m^2 iv

Table 7.1: BR9601/NEAT Chemotherapy Treatment

Treatment	STB Patients	NEAT Patients	Combined Patients
Tamoxifen	303	na	303
Tamoxifen & Chemotherapy	99	165	264
Chemotherapy	na	ERα +ve: 9 ERα –ve: 79 ERαunknown: 6	94

Table 7.2: Treatment regimes from STB and NEAT studies

The STB and NEAT cohort of patients were combined for survival analysis. Patients were treated with one of three regimes: tamoxifen alone, tamoxifen and chemotherapy combined, or chemotherapy alone.

7.3 Ras/Raf-1/MAPK pathway is activated in breast tumours

As in the STB study, Spearman Rank Tests revealed that the Raf-1/MAPK pathway was activated in the tumours of the NEAT patients. Patients who expressed higher levels of activated Raf-1 in either the cytoplasm or nuclei of tumour cells, also presented with increased levels of cytoplasmic and nuclear pMAPK (Table 7.3).

	pMAPK Cyt	pMAPK Nuc
pRaf(ser259) Cyt	R^2=0.505 p<0.0005	R^2=0.413 p<0.0005
pRaf(ser338) Cyt	R^2=0.588 p<0.0005	R^2= 0.234 p<0.0005
pRaf(ser338) Nuc	R^2= 0.403 p<0.0005	R^2 =0.296 p<0.0005

Table 7.3: NEAT pRaf and pMAPK correlations

Spearman Rank Tests were performed to analyse the relationship between expression of pRaf(ser259) and pMAPK, pRaf(ser338) and pMAPK. R^2 = correlation coefficient. Using Bonferroni corrections, p values <0. 008 deemed statistically significant.

7.4 Relationship between Ras/Raf-1/MAPK pathway and disease-free survival in patients treated with chemotherapy.

7.4.1 Disease Free Survival (DFS)

The end point for measuring disease-free survival, regardless of treatment received, was local, regional or distant recurrence. In total 111 patients (34.9%) relapsed, 87 patients suffered from an initial distant recurrence (metastasis), whilst regional and local recurrences occurred in 10 and 14 patients respectively. A further 20 patients whose first relapse was either local or regional also suffered from a secondary distant recurrence (Table 7.4). Survival analyses were performed on all patients who relapsed, regardless of their type of recurrence, and on only those patients who suffered a distant recurrence. Additionally, analyses were performed on the two treatment groups (Epi/CMF & CMF alone) in combination and individually. As described in chapter 5, for survival analysis, patients were split into two groups: those that were defined as expressing low levels of protein and those that expressed higher levels. For all proteins analysed, it was deemed most appropriate to use the histoscore upper quartile value as the cut off point for characterising the patients into their groups.

Recurrence	Recurrence Type	Total No.	Epi/CMF	CMF only
	NONE	207	113	94
1st	Distant	87	37	50
	Regional	10	3	7
	Local	14	2	12
2nd	Distant	20	5	15

Table 7.4: NEAT Recurrence Type

The end point for disease-free survival was a local, regional or distant recurrence. Information was available regarding patients' primary and secondary recurrences. The table presents the frequency of each type of recurrence and highlights the number of patients from each treatment group who relapsed.

7.4.2 Overexpression of Raf-1 and MAPK does not impact on patients' disease-free survival.

Survival analyses performed on all patients (Epi/CMF & CMF alone) revealed no significant association between tumour expression of pRaf(ser259), pRaf(ser338), MAPK, or pMAPK and risk of breast cancer recurrence whilst receiving chemotherapy. There was also no evidence of pRaf(Ser259), pRaf(ser338), MAPK or pMAPK being linked to tumour metastasis (distant recurrences only).

7.4.3 Overexpression of neither Raf-1 nor MAPK preferentially affects disease-free survival time in patients treated with either Epirubicin/CMF or CMF alone.

Patients were split into their two treatment groups (Epi/CMF vs CMF alone) and disease-free survival analysis performed. However, in both treatment groups, increased expression of Raf-1 (inactive or active) and MAPK failed to alter disease-free survival time.

7.5 Relationship between Ras/Raf-1/MAPK pathway and overall survival in patients treated with chemotherapy.

7.5.1 Overall Survival (OS)

The end point for overall survival was a breast cancer related death. Within this study there were 84 breast cancer related deaths; 50 of these were patients receiving only CMF

treatment, while the remaining 34 patients received both Epirubicin and CMF. Again, analyses were performed on the patient group, as a whole, and individually on the two treatment groups.

7.5.2 Overexpression of Raf-1 and MAPK does not impact on patients' disease-free survival.

Overall survival (OS) time for all NEAT patients (treated with Epi/CMF or CMF alone) was not affected by overexpression of pRaf(ser259), pRaf(ser338), MAPK or pMAPK.

7.5.3 Overexpression of neither Raf-1 nor MAPK affects overall survival time in patients treated with either Epirubicin/CMF or CMF alone.

Again, patients were split into their two treatment groups (Epi/CMF vs CMF alone) and overall survival analysis performed. However, in both treatment groups overexpression of inactive or active Raf-1, MAPK and pMAPK was not associated with reduced overall survival time.

7.6 Role of Raf-1 and MAPK in predicting outcome in patients treated with tamoxifen and chemotherapy

A total of 264 patients from both the NEAT and STB cohorts were treated with both tamoxifen and chemotherapy. Within this sub-group of patients there were 79 breast cancer relapses and 51 breast cancer related deaths. Survival analysis was performed relative to disease-free survival (DFS) and overall survival (OS), to investigate the effects of receiving both tamoxifen and chemotherapy on patient outcome. Relapse whilst on tamoxifen (ROT) was not analysed, as data regarding tamoxifen relapse was not available for the NEAT patients.

7.6.1 Raf-1 and MAPK are not predictive factors for outcome in patients treated with both tamoxifen and chemotherapy

Survival analyses performed on patients receiving both treatments revealed no significant association between tumour expression of pRaf(ser259), pRaf(ser338), MAPK, or pMAPK and shortened DFS or OS time.

7.7 Role of Raf-1 and MAPK in predicting outcome in patients treated only with chemotherapy

Ninety-four patients from the NEAT cohort received only chemotherapy, of which 38 patients experienced a breast cancer recurrence whilst 35 patients suffered a breast cancer related death. Survival analysis was performed for disease-free and overall survival.

7.7.1 Raf-1 and MAPK are not predictive for response to chemotherapy treatment

Expression of inactive or active Raf-1, MAPK, and pMAPK was not associated with outcome in patients treated only with chemotherapy.

7.8 Association between Raf-1/MAPK expression and known prognostic markers

Pearsons chi-square analysis was performed to establish if there was any link between expression/activation of Raf-1 and MAPK and tumour grade, size, ERα or nodal status.

No associations were evident between pRaf(ser259) and pRaf(ser338) expression and tumour grade, size, ERα or nodal status. However, nuclear MAPK and cytoplasmic pMAPK expression were negatively correlated with tumour grade ($p=0.011$ and $p=0.017$ respectively). Tumours that expressed high levels of either nuclear MAPK or cytoplasmic pMAPK were more likely to be of a lower grade (grade =1 or 2). There were no significant correlations between MAPK and pMAPK expression and tumour size, ERα or nodal status.

7.9 Discussion

As the incidences of breast cancer in women continue to increase, so too does the need to establish new treatments while also improve existing therapies. One way to do this is to further our understanding of the mechanisms that cause current therapies to fail. Chemotherapy is known to improve patient survival, yet resistance to chemotherapeutic agents is an ever-increasing problem. The factors driving resistance are unconfirmed. This study tested the hypothesis that Raf-1 and MAPK, factors that regulate cell proliferation, ultimately predict outcome in terms of disease-free and overall survival in patients treated with chemotherapy.

The Ras/Raf-1/MAPK pathway is a key regulator of cell proliferation and the effectiveness of chemotherapy is believed to be dependent on cellular proliferation. It is perhaps surprising that this study revealed no evidence that expression or activation of the components of this pathway influenced response to chemotherapeutic agents.

Neither Raf-1 (active or inactive) nor MAPK expression levels were shown to influence the disease-free or overall survival time of patients treated with either CMF or CMF and Epirubicin. These results suggest that the Ras/Raf-1/MAPK pathway is not primarily involved in the acquisition of chemotherapy resistance.

The function of Raf-1 and MAPK in mediating response to chemotherapeutic agents is controversial. Previously all research investigating the relationship between the Ras/Raf-1/MAPK pathway and anthracycline resistance had been performed in cell lines. These studies suggested that both Raf-1 and MAPK played a role in the development of resistance to epirubicin and doxorubicin. Two studies (154;227) showed that increased expression and activation of Raf-1 was associated with resistance to doxorubicin induced apoptosis in MCF-7 breast cancer cells. Conversely, another study suggested that down-

regulation of Raf-1 was associated with paclitaxel resistance in breast cancer cells (271). Likewise, the extent to which p42/44 MAPK influences resistance to anthracycline treatment is also complex. Anthracyclines can induce and inhibit activation of MAPK under certain conditions. As a result, MAPK activation has sometimes been associated with protecting cells from drug-induced apoptosis, while in other incidences it promotes cell death (230;273). A more recent study (274) highlighted that treatment with anthracyclines leads to activation of MAPK in breast epithelial and carcinoma cells, and that this activation may in turn inhibit the anti-tumour activity of the anthracyclines. The increase in MAPK activity was also shown to correlate with an increase in phosphorylation of p90RSK and BAD. Phosphorylation of BAD at Serine 112 is anti-apoptotic, since it prevents it from binding to Bcl-x_L. It would seem from this study that activation of the MAPK pathway inhibits the anti-tumour effects of anthracyclines. Preliminary studies by this same group suggested that inhibition of MAPK enhanced doxorubicin or epirubicin induced apoptosis.

However, our study failed to reveal any significant relationship between either expression/activation of Raf-1 and MAPK and chemotherapy resistance. A previous study investigating the response of prostate cancer cells to either doxorubicin or paclitaxel failed to show a link between the Ras cascade and drug resistance (275). Nonetheless, a study of chemotherapy resistance in MCF-7 breast cancer cells suggested that PI3K/Akt pathway, as opposed to the Raf-1/MAPK pathway, may play a more significant role in mediating chemo-resistance (229). A similar finding was observed in the study of small cell lung cancer cells, which showed that inhibition of the PI3K/Akt, but not the Ras/Raf-1/MAPK pathway, overcame resistance to chemotherapy (276). For

chemotherapy to be effective, cell death has to outweigh cell proliferation. It may be necessary to analyse both the proliferative Ras/Raf-1/MAPK pathway and the anti-apoptotic PI3K/Akt pathway in the NEAT study. Perhaps in clinical breast tumours the anti-apoptotic proteins downstream of Raf-1 and MAPK, such as p90RSK, Bcl-2 or Bad, may be more appropriate targets for predicting chemotherapy resistance. This was suggested in a study of MCF-7 cancer cells, which demonstrated that activation of Raf-1 in Bcl-2 overexpressing cells resulted in greater resistance to doxorubicin, in comparison with cells lacking Bcl-2 overexpression (227).

In addition to highlighting pRaf(ser338), and to a lesser extent, MAPK as predictive markers for tamoxifen resistance, results from the previous STB study (chapter 6) suggested the possibility that overexpression of pRaf(ser338) identified patients who benefited from the combined treatment of tamoxifen and chemotherapy, and that MAPK perhaps controlled response to chemotherapy. Unfortunately, these hypotheses were not proven, as this study failed to demonstrate any predictive capabilities of Raf-1 or MAPK for chemotherapy response in patients treated with chemotherapy alone or in combination with tamoxifen.

Tamoxifen down-regulates ERα activity, inhibiting activation of oestrogen regulated genes and reducing cell proliferation. Chemotherapy targets proliferating cells either directly, in the case of antimetabolites, such as methotrexate, or indirectly via production of DNA damage. Our findings that Raf-1 and MAPK expression is predictive for Tamoxifen but not chemotherapy response can be interpreted in two ways. The Ras/Raf-1/MAPK pathway is responsible for phosphorylating multiple substrates, such as the pro-proliferative c-fos and the anti-apoptotic p90RSK. One other key substrate is the

ER. Therefore, the unexpected finding that Ras/Raf-1/MAPK are predictive markers for survival and response to Tamoxifen but not chemotherapy may indicate that it is the interaction between this pathway and the ER that fundamentally influences patient outcome. If this is true, then perhaps Raf-1 and MAPK are only predictive for response in ER positive patients; therefore, possibly the NEAT study was underpowered in terms of ER positive patients, preventing full investigation of the effects of the Ras pathway on chemotherapy response. A larger cohort of ER positive chemotherapy treated patients is required to analyse the potential of Raf-1 and MAPK as predictive markers. However, if their predictive power is dependent on its interaction with ER, they may not be the most appropriate markers for response to chemotherapy: it may be more advisable to investigate anti-apoptotic factors downstream of MAPK, such as BAD.

Chemotherapy targets highly proliferating cells. In tumours, cell growth is driven by classical proliferative factors, such as c-fos, but also by the MAPK-ERα interactions that will enhance cells sensitivity to oestrogen, ultimately increasing proliferation. Perhaps the reason we failed to demonstrate Raf-1 or MAPK as predictive for chemotherapy response is that, in the ER positive NEAT, patients the chemotherapy cancels out the effects of the MAPK-ERα driven proliferation. These results suggest that the combined treatment of tamoxifen and chemotherapy is beneficial in patients who overexpress Raf-1 and MAPK, to such an extent that they have a prognosis similar to those patients who expressed lower levels of the proteins. This argument was strengthened by our observation that, in the 303 tamoxifen only treated patients, Raf-1 and MAPK continued to predict for response on tamoxifen (Chapter 6). However, neither Raf-1 nor MAPK expression was predictive for outcome or response to chemotherapy in

all the NEAT chemotherapy treated patients or in the 264 patients from both STB and NEAT cohorts who received both tamoxifen and chemotherapy. Possibly this signifies that pRaf(ser338), and to a lesser extent, MAPK is a potential marker to identify patients for whom tamoxifen alone is insufficient adjuvant systemic therapy. Those patients who overexpress pRaf(Ser338) and MAPK in their tumours may require treatments, such as chemotherapy or aromatase inhibitors, in addition to tamoxifen. As discussed in the previous chapter, further research, in larger studies, such as the TEAM or ATAC study, is needed to confirm our findings.

When undertaking this study, the role of the Ras/Raf/MAPK pathway in mediating response to chemotherapy was unconfirmed. Work from the STB study (Chapter 6) had alluded to the possibility that overexpression of pRaf(ser338) in tumours identified patients who benefited from the combined treatment of tamoxifen and chemotherapy, and that MAPK was involved in controlling response to chemotherapy. However, the NEAT study failed to demonstrate any significant association between expression of either of these proteins and chemotherapy treated patients' outcome. Consequently, the roles of Raf and MAPK in driving chemotherapy response remain controversial, and further work, perhaps in larger patient cohorts, is required to try and enhance our understanding of the phenomenon that is chemotherapy resistance.

8. Relationship between MAPK and the Oestrogen Receptor

8.1 Introduction

Tamoxifen is currently one of the most effective but least toxic drug therapies for ERα positive breast cancers. As discussed in chapter 1, Tamoxifen, an oestrogen antagonist, is a non-steroid ligand that acts as a selective oestrogen receptor modulator (SERM). It functions by competitively inhibiting the interaction of oestrogen (E2) with ERα, by directly binding to the AF-2 transcriptional activation domain receptor. Hence, it blocks the effects of E2 and subsequently inhibits the activity of the receptor. However, resistance to tamoxifen treatment, either at primary treatment (*de novo*), or arising during treatment (acquired), is the cause of significant morbidity and mortality.

The mechanisms driving the development of Tamoxifen resistance are not fully understood; however, there are several hypotheses. ERα can be activated in a ligand-dependent manner, via E2, or in a ligand-independent manner, via signal transduction pathways. Research suggests that activation of the Ras/Raf-1/MAPK pathway contributes to the development of tamoxifen resistance through phosphorylating and activating the ERα. Results from chapter 6 suggested that increased expression of activated Raf-1, pRaf(ser338), and MAPK in patients' tumours was associated with a greater risk of relapsing on Tamoxifen. MAPK directly and indirectly phosphorylates ERα at serine 118 and serine 167, respectively (29;39;197). The interaction between MAPK and ERα is well documented, though it is unclear if it occurs in the cytoplasm or nuclei of cells.

This study aimed to compare the ligand-dependent and ligand-independent phosphorylation and activation of the ERα and since ERα phosphorylation via MAPK seems to be an important factor in the development of Tamoxifen resistance, to ultimately

probe the relationship between MAPK and the ERα. *In vitro* analysis of MCF-7 breast cancer cells was performed to investigate the interactions between MAPK and ER. There were three key elements to this study: time course treatments to compare the ligand-dependent and independent activation of the ERα and immunofluorescence (IF) and subcellular fractionation experiments to monitor the localisation of MAPK and ERα following stimulation with E2, Heregulin (HRG) and MAPK inhibitors.

8.2 Immunofluorescent localisation of pMAPK, ER, pER(ser118) and pER(ser167) in MCF-7 breast cancer cells following treatment with Oestrogen, Heregulin and Felodipine.

To visualise the response and localisation of MAPK and ERα following ligand-dependent and independent activation, an immunofluorescent (IF) study was designed. Cells were exposed to E2, HRG and Felodipine (FEL). FEL is a calcium antagonist that prevents phosphorylated MAPK from translocating into the nucleus. This enabled the localisation of MAPK and ERα to be monitored following ligand-dependent and independent phosphorylation, whilst the presence of FEL addressed whether MAPK interacts with and phosphorylates ERα in the cytoplasm or nuclei of cells. In total, there were 16 treatments over six time points; cells were incubated with 1nM/10nM HRG and E2, both individually and in combination, and in the presence and absence of 30μM FEL, for 5, 15, 30 minutes, and 1, 2 and 3 hours. Table 2.10 lists all the drug treatments given to the MCF-7 cells. The localisation of pMAPK, ERα, pER(ser118) and pER(ser167) was observed. The major focus of this study was on the nuclear localisation of the proteins, as it was easier to monitor any differences in the extent of protein expression in the nuclei rather than the cytoplasm.

8.2.1 Localisation of pMAPK

In untreated MCF-7 cells, pMAPK was predominantly localised to the cytoplasm; almost no nuclear pMAPK was detected. Throughout all treatments, the levels of cytoplasmic pMAPK remained generally high. However, treatment with both HRG and E2 stimulated nuclear translocation of pMAPK. Of the two treatments, HRG was the more effective activator of MAPK. For both treatments, maximum levels of nuclear pMAPK were observed after 5 minutes, though the expression levels were much higher when stimulated with HRG. After 5 minute treatments with both drugs, the levels of nuclear pMAPK dropped dramatically, but were shown to gradually increase again after 1hour (Figures 8.1 & 8.2). Similar trends were observed for the 1nM and 10nM treatments, though as expected the 10nM drugs induced a stronger response. Surprisingly, when both drugs were given in combination, there was a reduction in the levels of nuclear pMAPK, in comparison to the levels observed when the two drugs were given individually. After the 2 and 3 hour treatments, the two drugs seemed to work synergistically to promote nuclear translocation of pMAPK (Figures 8.1 & 8.2). Treatment with FEL prevented the nuclear translocation of pMAPK in MCF-7 cells, even in the presence of HRG or E2 (Figures 8.3-8.5).

The expression levels of pMAPK appeared to fluctuate quite significantly in response to the different treatments. Therefore, as described in section 2.6.4 an IF scoring system was established in an attempt to semi-quantify the levels of pMAPK protein localised to the nuclei. Unfortunately, it was impossible to score the levels of cytoplasmic pMAPK. Scoring a proportion of all treated cells confirmed the results generated from visualising the cells down a fluorescent microscope, but it allowed the results to be

presented in a numerical context. Figures 8.6a, b further highlight the effects, of HRG, E2 and FEL, on the nuclear localisation of pMAPK.

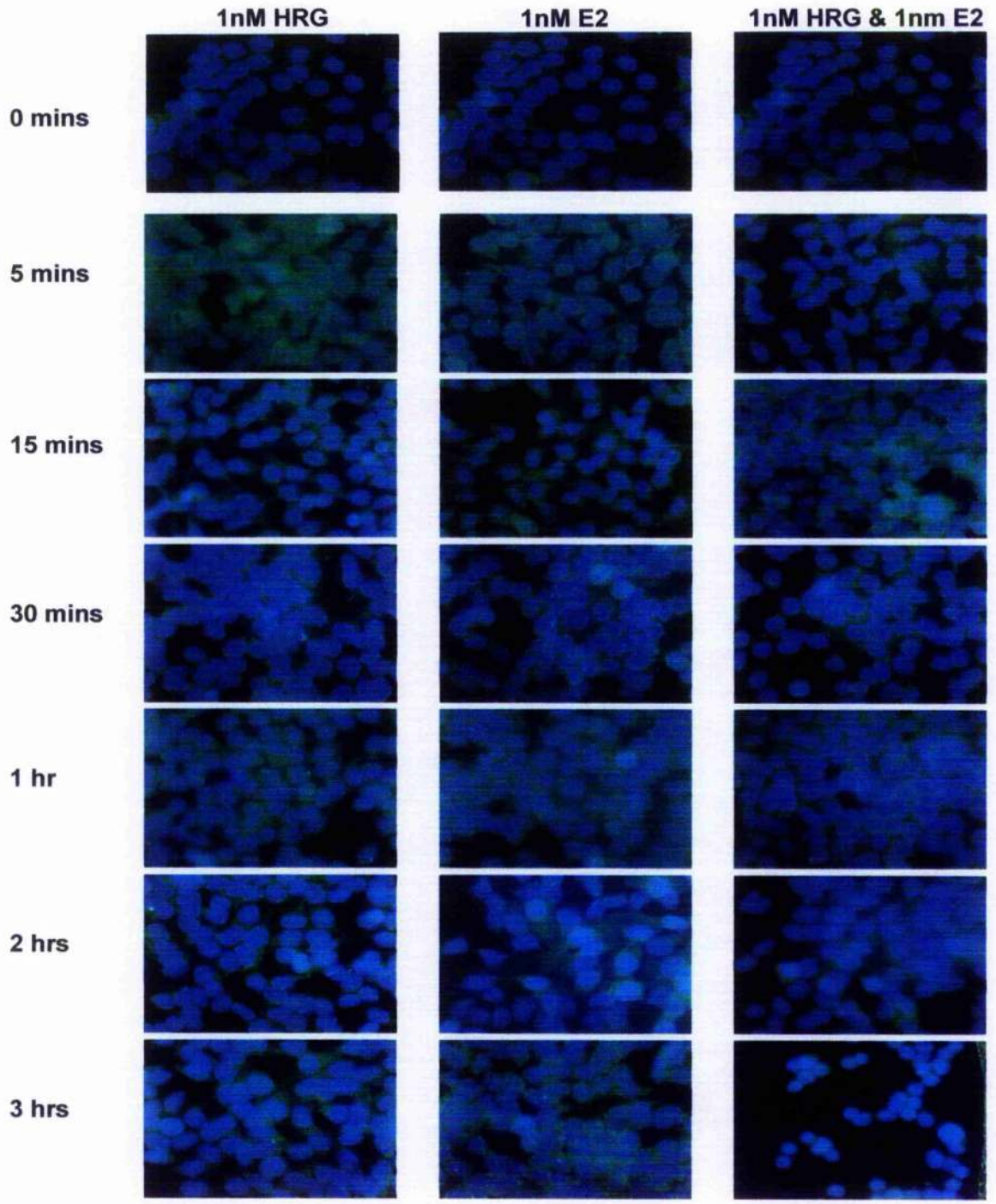

Figure 8.1: pMAPK IF on MCF-7 cells treated with 1nM HRG and 1nM E2

Immunofluorescence of MCF-7 cells stimulated with 1nM HRG and 1nM E2, individually and in combination, for 0, 5, 15, 30 minutes, 1, 2, 3 hours and treated with pMAPK antibody and Fluorescein avidin D (green). pMAPK was localised to both the cytoplasm and nuclei of cells. Nuclei stained with DAPI (blue).

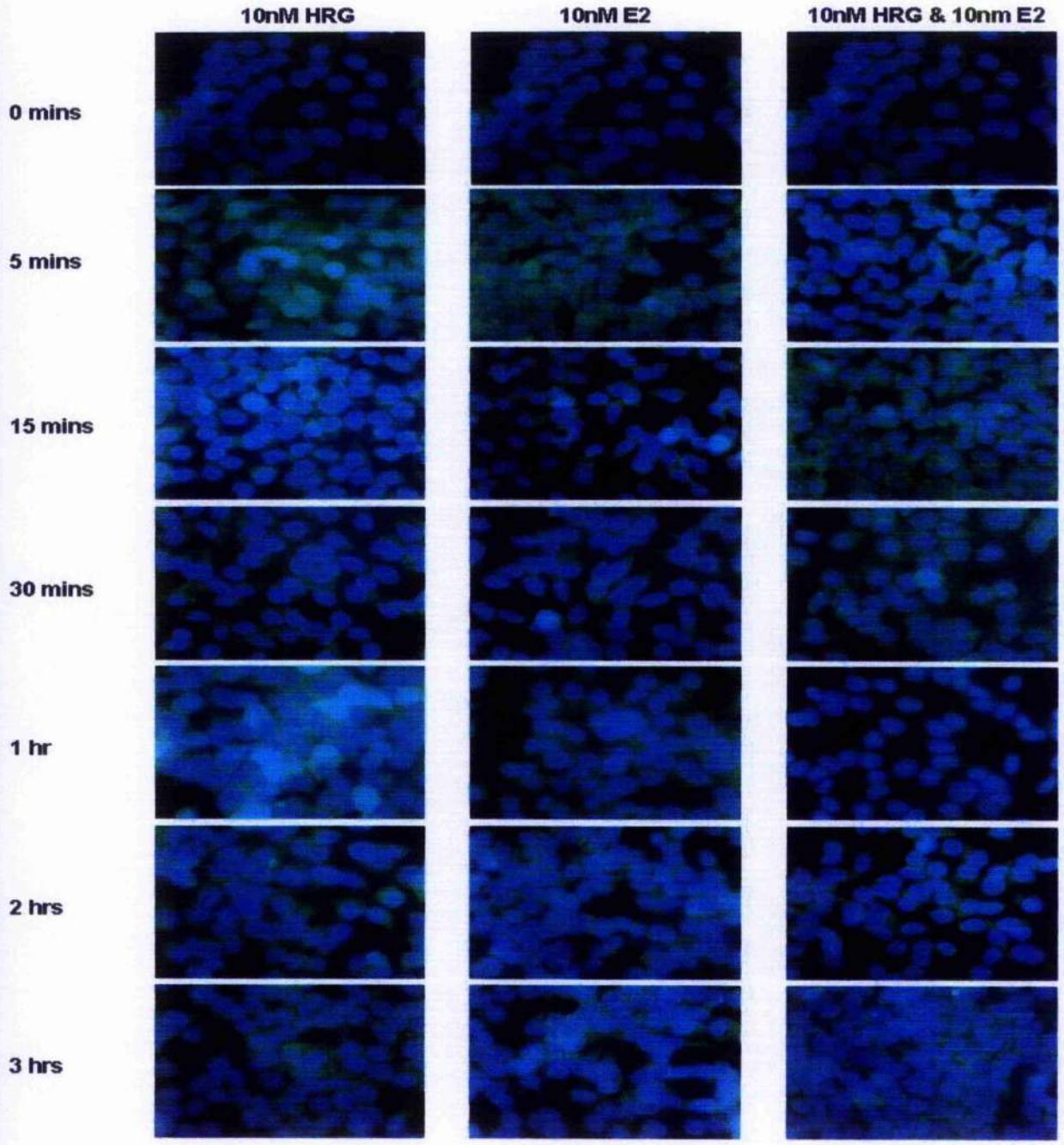

Figure 8.2: pMAPK IF on MCF-7 cells treated with 10nM HRG and 10nM E2

Immunofluorescence of MCF-7 cells stimulated with 10nM HRG and 10nM E2, individually and in combination, for 0, 5, 15, 30 minutes, 1, 2, 3 hours and treated with pMAPK antibody and Fluorescein avidin D (green). pMAPK was localised to both the cytoplasm and nuclei of cells. Nuclei stained with DAPI (blue).

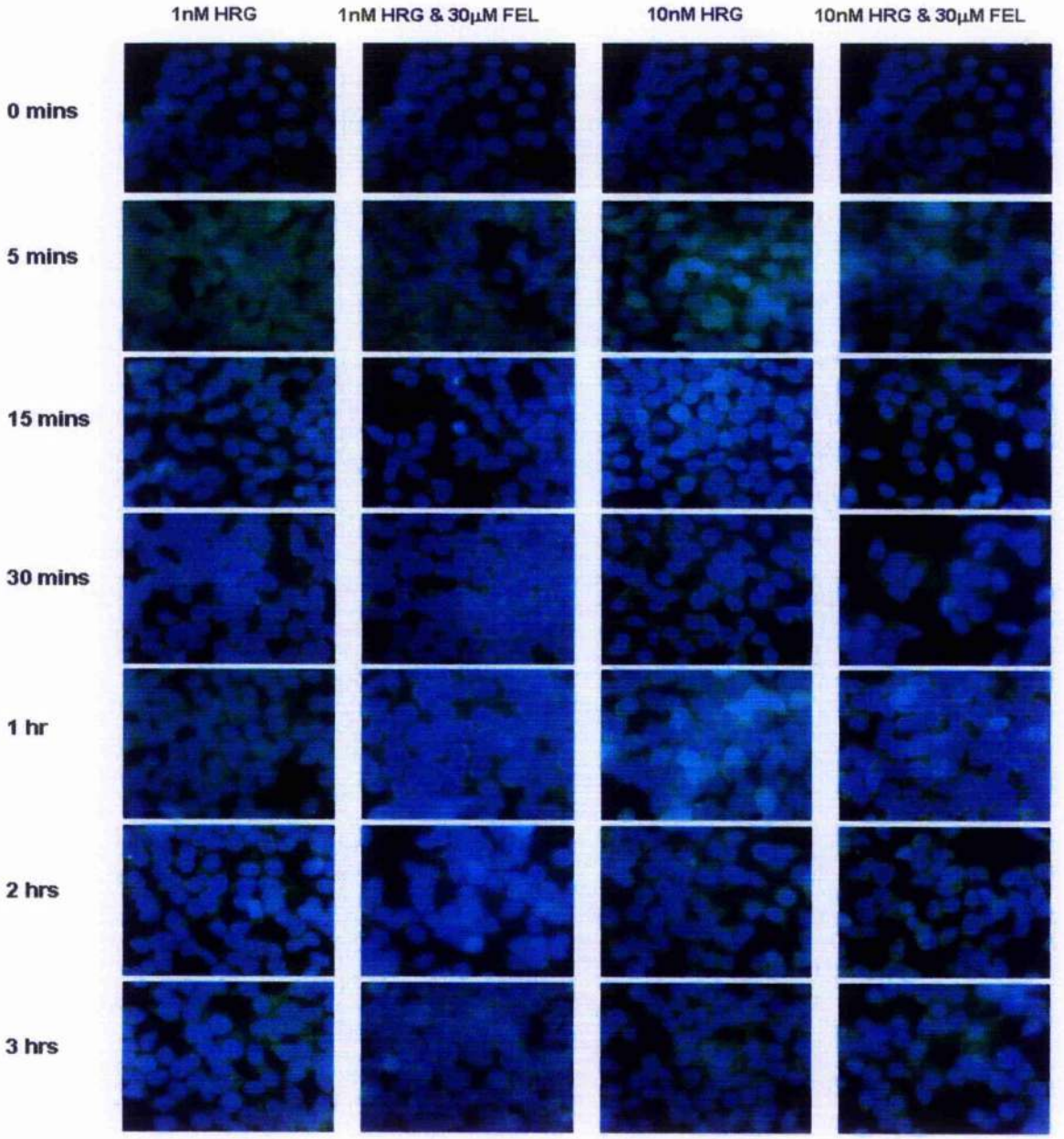

Figure 8.3: pMAPK IF on MCF-7 cells treated with 1nM/10nM HRG and 30mM Felodipine

Immunofluorescence of MCF-7 cells stimulated with 1nM/10nM HRG, in the absence and presence of 30μM Felodipine, for 0, 5, 15, 30 minutes, 1, 2, 3 hours and treated with pMAPK antibody and Fluorescein avidin D (green). pER(ser118) was localised to both the cytoplasm and nuclei of cells. Nuclei stained with DAPI (blue).

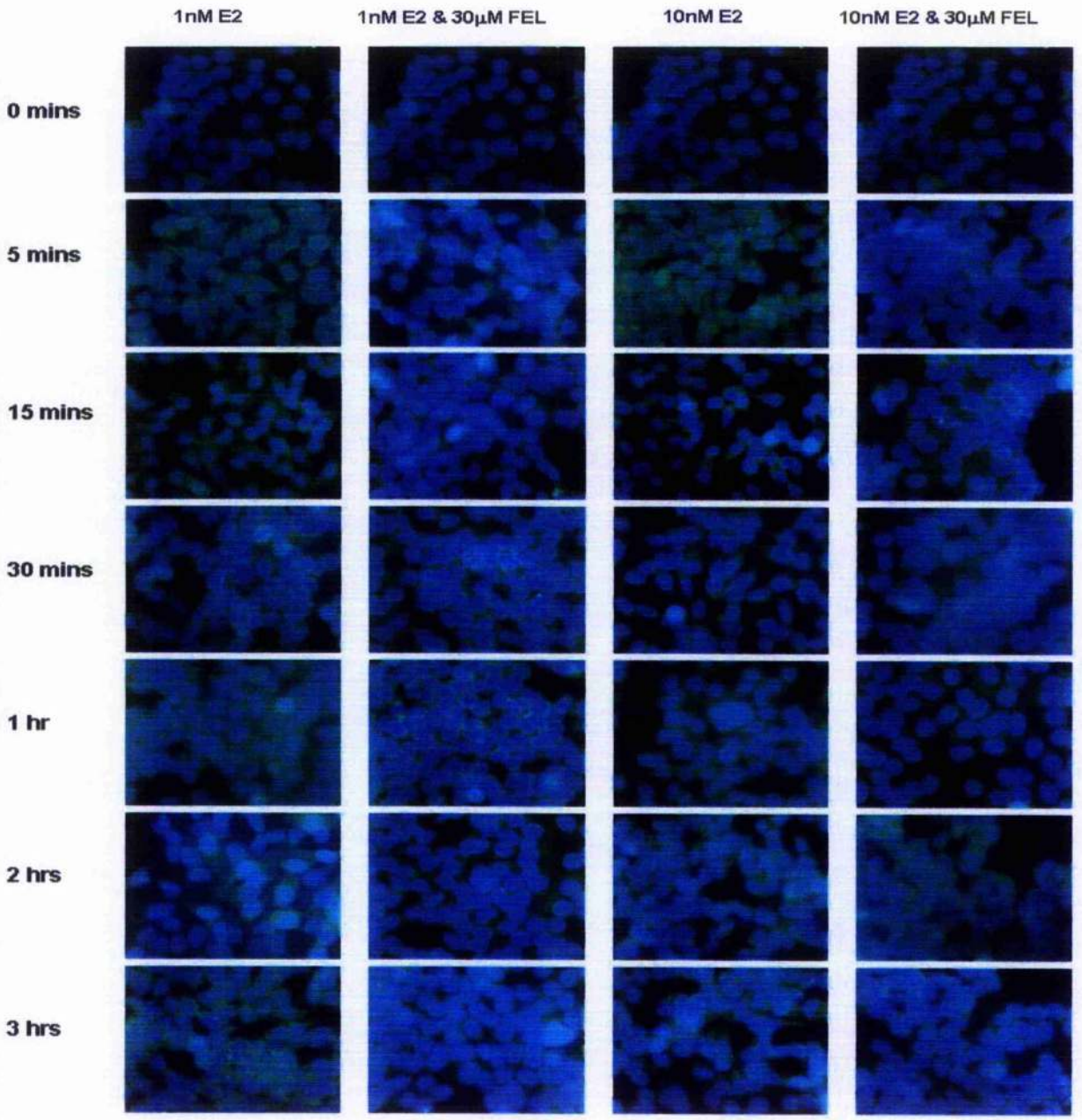

Figure 8.4: pMAPK IF on MCF-7 cells treated with 1nM/10nM E2 and 30mM Felodipine

Immunofluorescence of MCF-7 cells stimulated with 1nM/10nM E2, in the absence and presence of 30μM Felodipine, for 0, 5, 15, 30 minutes, 1, 2, 3 hours and treated with pMAPK antibody and Fluorescein avidin D (green). pMAPK was localised to both the cytoplasm and nuclei of cells. Nuclei stained with DAPI (blue).

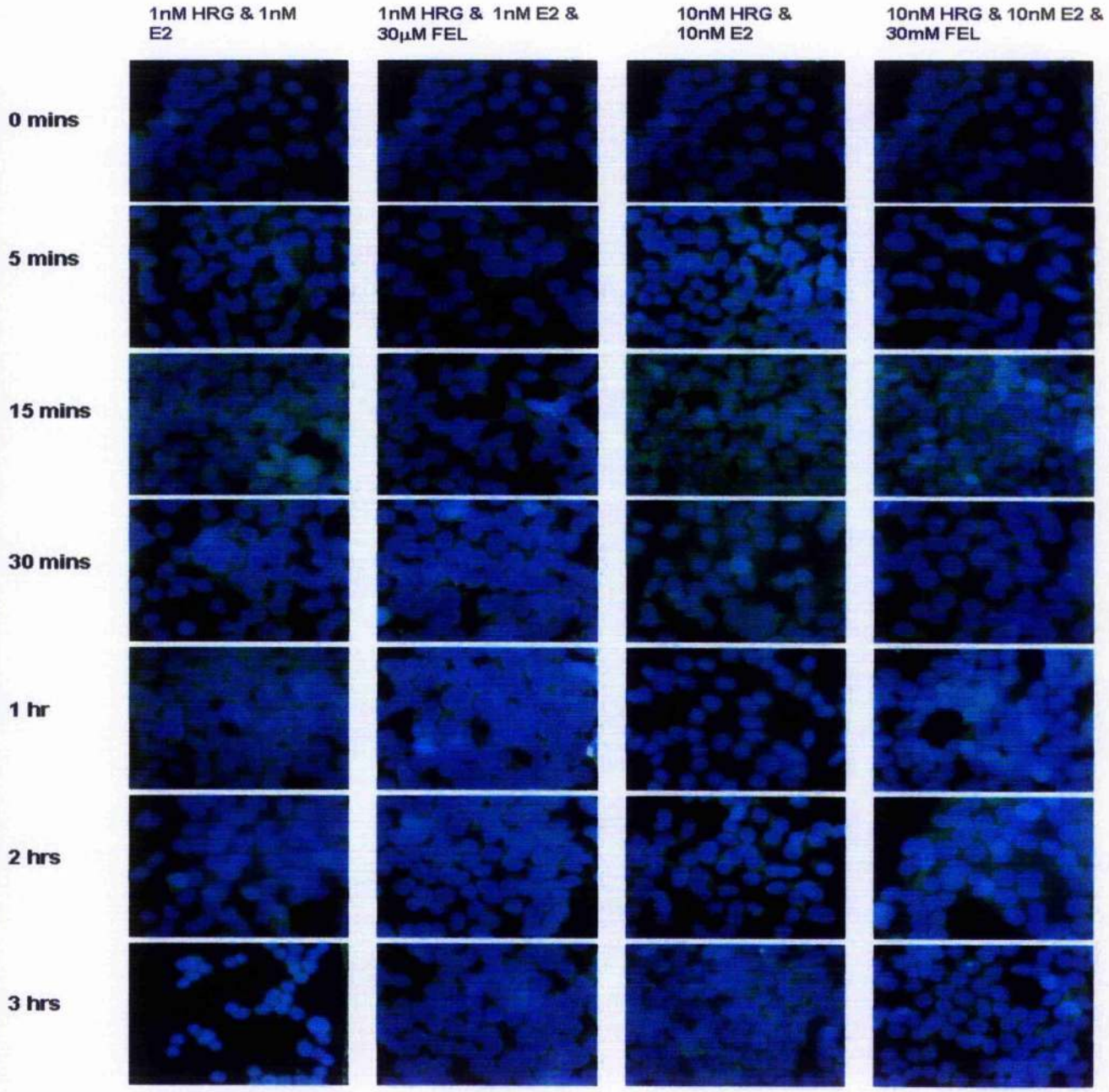

Figure 8.5: pMAPK IF on MCF-7 cells treated with 1nM HRG/E2, 10nM HRG/E2 and 30mM Felodipine

Immunofluorescence of MCF-7 cells stimulated with 1nM HRG/E2 and 10nM HRG/E2, in the absence and presence of 30μM Felodipine, for 0, 5, 15, 30 minutes, 1, 2, 3 hours and treated with pMAPK antibody and Fluorescein avidin D (green). pMAPK was localised to both the cytoplasm and nuclei of cells. Nuclei stained with DAPI (blue).

(a)

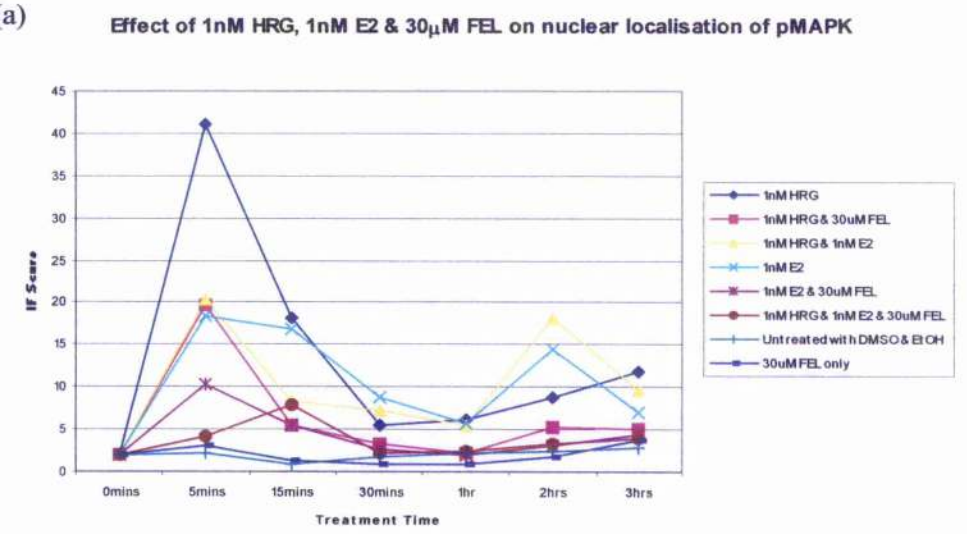

(b)

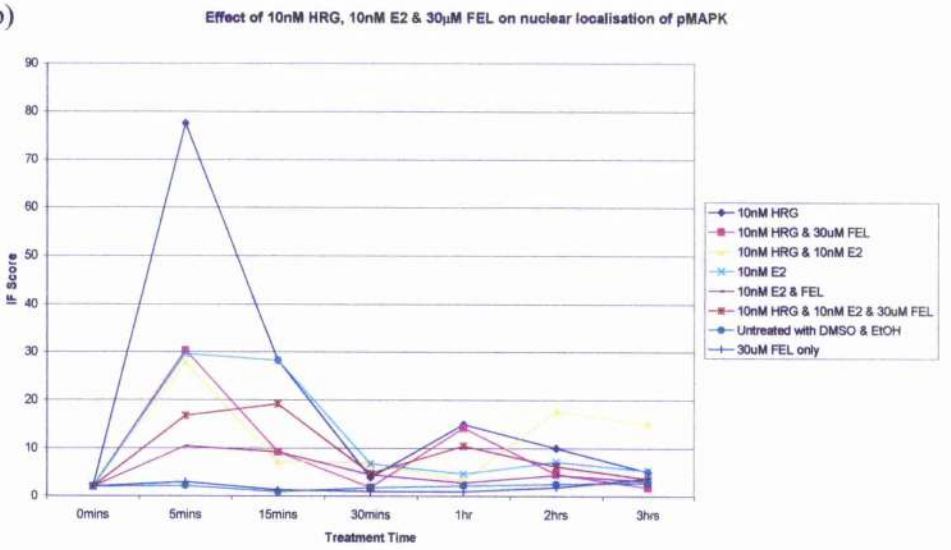

Figure 8.6: Line Graphs of Nuclear Distribution of pMAPK

MCF-7 cells were treated with Heregulin (HRG), Oestrogen (E2) and Felodipine (FEL for 0, 5, 15 30 mins and 1,2 and 3hours, and immunofluorescence performed to detect pMAPK. A proportion of the cells were scored for nuclear expression of pMAPK in order to semi-quantify the effects of the various treatments on pMAPK nuclear localisation. The graphs show the levels of pMAPK expressed in the nuclei during the course of treatments with (a) 1nM HRG, 1nM E2 and 30μM FEL and (b) 10nM HRG, 10nM E2 and 30μM FEL.

8.2.2 Localisation of ER

ER was detected in the cytoplasm and nuclei of untreated MCF-7 cells. The levels of cytoplasmic ERα appeared to remain high throughout the treatments. Additionally, the levels of nuclear ERα did not seem to fluctuate greatly in response to the various treatments (Figure 8.7).

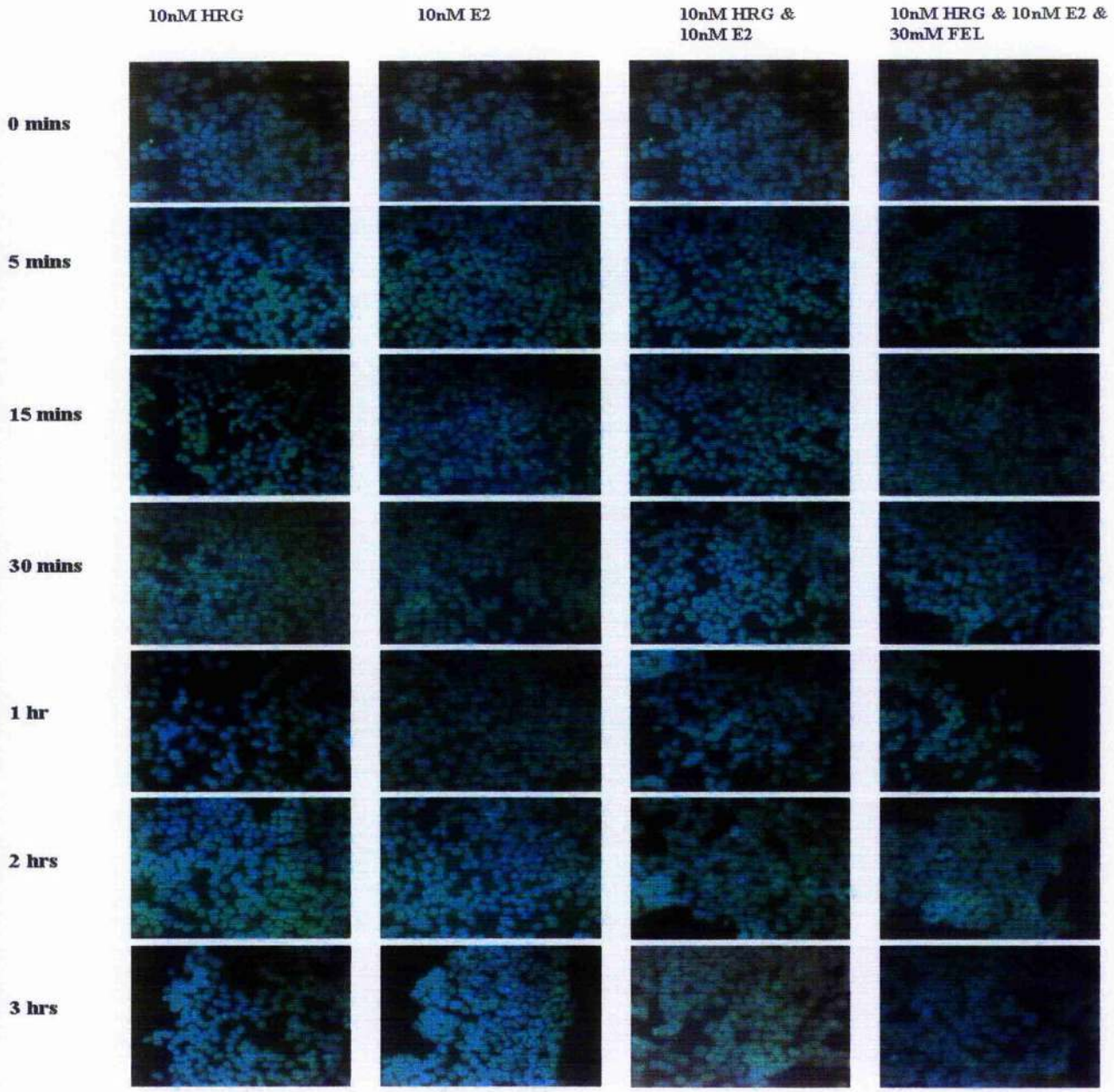

Figure 8.7: ERα IF on MCF-7 cells treated with 10nM HRG, 10nM E2 and 30mM Felodipine

Immunofluorescence of MCF-7 cells, stimulated with 10nM HRG and 10nM E2, singly and in combination, and in the absence and presence of 30μM Felodipine, for 0, 5, 15, 30 minutes, 1, 2, 3 hours. Cells were treated with ERα antibody and Fluorescein avidin D (green). ERa was localised to both the cytoplasm and nuclei of cells. Nuclei stained with DAPI (blue).

8.2.3 Localisation of pER(ser118)

Untreated MCF-7 cells displayed cytoplasmic pER(ser118) but almost no nuclear pER(ser118). The levels of cytoplasmic pER(ser118) in cells appeared to be high, regardless of the treatment. As with pMAPK, nuclear localisation of pER(ser118) varied in response to both the drug used and the incubation time. Therefore, the levels of nuclear pER(ser118) were semi-quantified using the IF scoring system.

Treatment of cells with both 1nM and 10nM E2 induced a rapid influx of pER(ser118) into the nuclei. The maximum level of nuclear pER(ser118) was observed after the 15 minute treatments. A decrease in the expression of nuclear pER(ser118) was witnessed following the longer treatment times, though levels did start to rise again after 3 hours. Conversely, a 5 minute treatment with 1nM and 10nM HRG resulted in a substantial increase in the levels of pER(118) localised to the nuclei. However, the levels were lower than that observed following E2 stimulation. Additionally, there was an immediate depletion in the levels of nuclear pER(ser118), following the 15 and 30 minute treatments. There was almost no nuclear pER(ser118) detectable; however, it was present in the cytoplasm. Nuclear pER(ser118) levels were shown to slightly increase after 2 hours (Figure 8.8 & 8.9).

In cells treated with both E2 and HRG for 5 minutes, nuclear pER(ser118) was detected at relatively high levels although levels were lower than those seen with E2 treatment alone. After 15 and 30 minutes, there was a considerable reduction in expression of nuclear pER(ser118); however, cytoplasmic pER(ser118) remained. The levels remained low until 2 hours, when a second peak of nuclear pER(ser118) expression was observed (Figure 8.8 & 8.9).

Treatment of the cells with FEL produced different results, depending on which drug it was combined with. Its presence did not seem to have a major effect on the E2-dependent phosphorylation and localisation of pER(ser118) (Figure 8.10), whereas when it was given in combination with HRG, a substantial decrease in the localisation of pER(ser118) to the nuclei of MCF-7 cells was observed (Figure 8.11). When cells were treated with all three drugs, the levels of nuclear pER(ser118) were lower than when treated with E2 alone, but were generally higher than those observed when E2 and HRG were given in combination (Figure 8.12). This suggested that the presence of FEL partially overrides the effects of HRG on the ER.

These trends are depicted in both the IF pictures (Figures 8.8-8.12) and in the graphs generated from the IF scores (Figure 8.13).

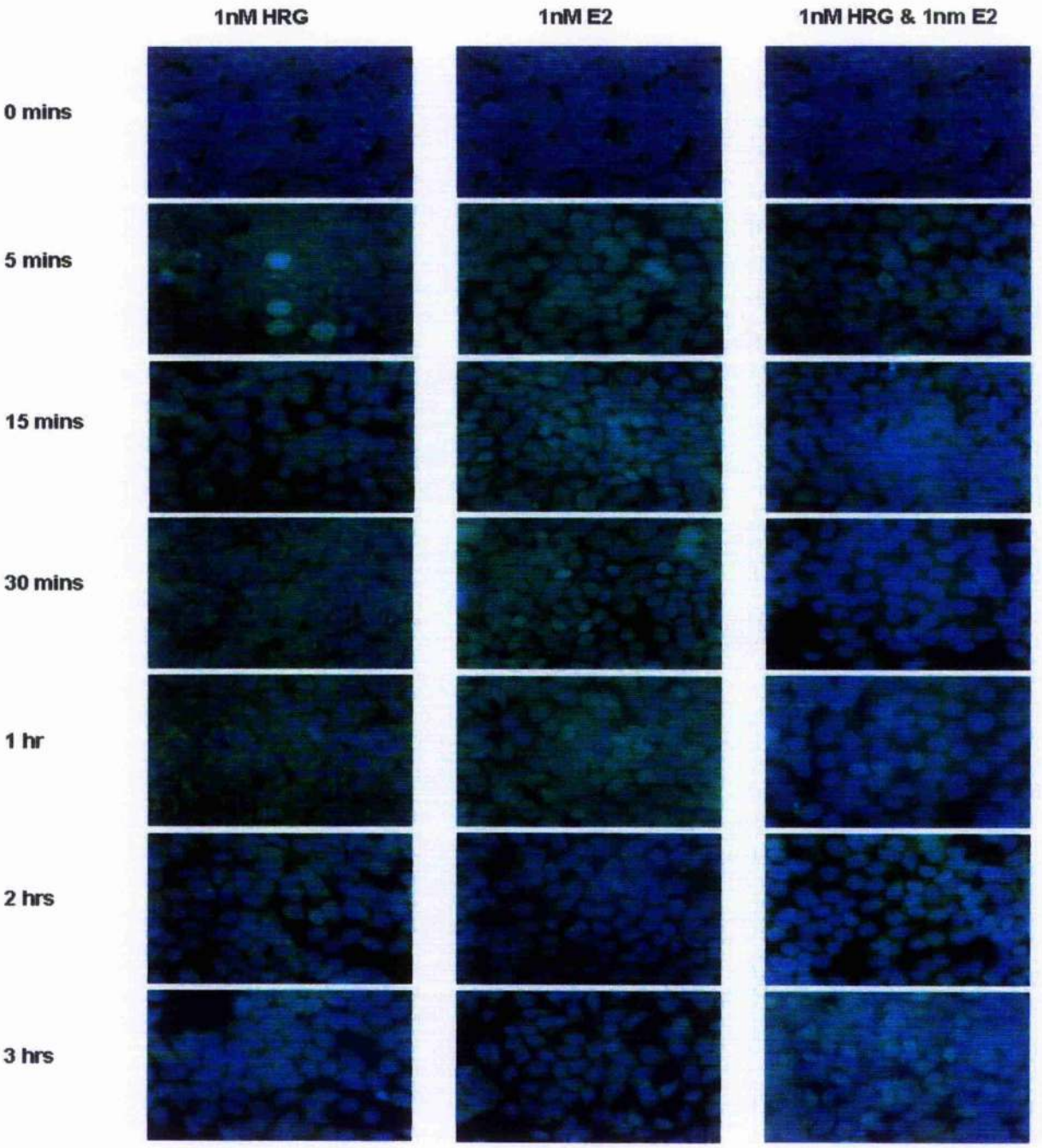

Figure 8.8: pER(ser118) IF on MCF-7 cells treated with 1nM HRG and 1nM E2

Immunofluorescence of MCF-7 cells stimulated with 1nM HRG and 1nM E2, individually and in combination, for 0, 5, 15, 30 minutes, 1, 2, 3 hours and treated with pER(ser118) antibody and Fluorescein avidin D (green). pER(ser118) was localised to both the cytoplasm and nuclei of cells. Nuclei stained with DAPI (blue).

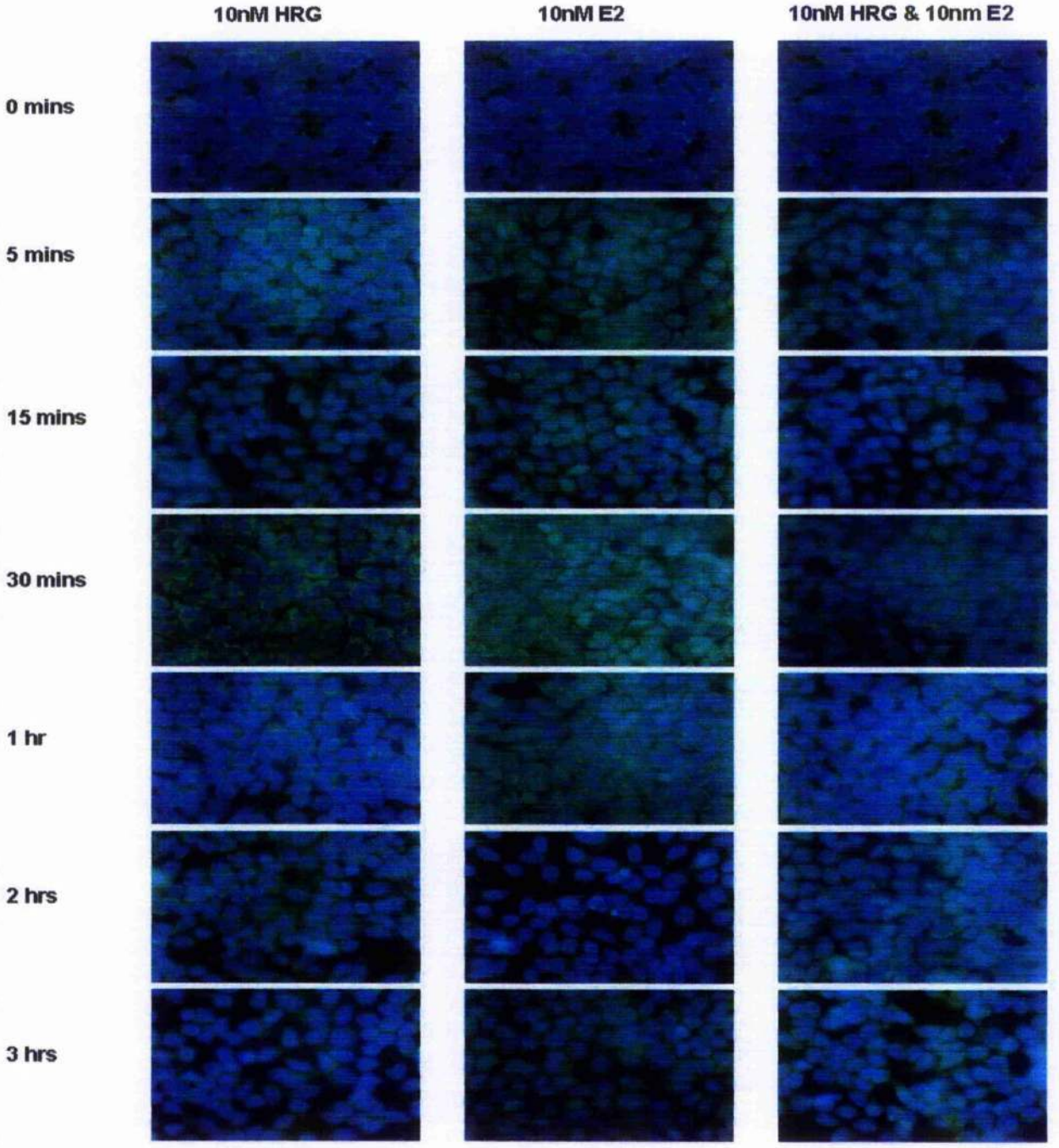

Figure 8.9: pER(ser118) IF on MCF-7 cells treated with 10nM HRG and 10nM E2

Immunofluorescence of MCF-7 cells stimulated with 10nM HRG and 10nM E2, individually and in combination, for 0, 5, 15, 30 minutes, 1, 2, 3 hours and treated with pER(ser118) antibody and Fluorescein avidin D (green). pER(ser118) was localised to both the cytoplasm and nuclei of cells. Nuclei stained with DAPI (blue).

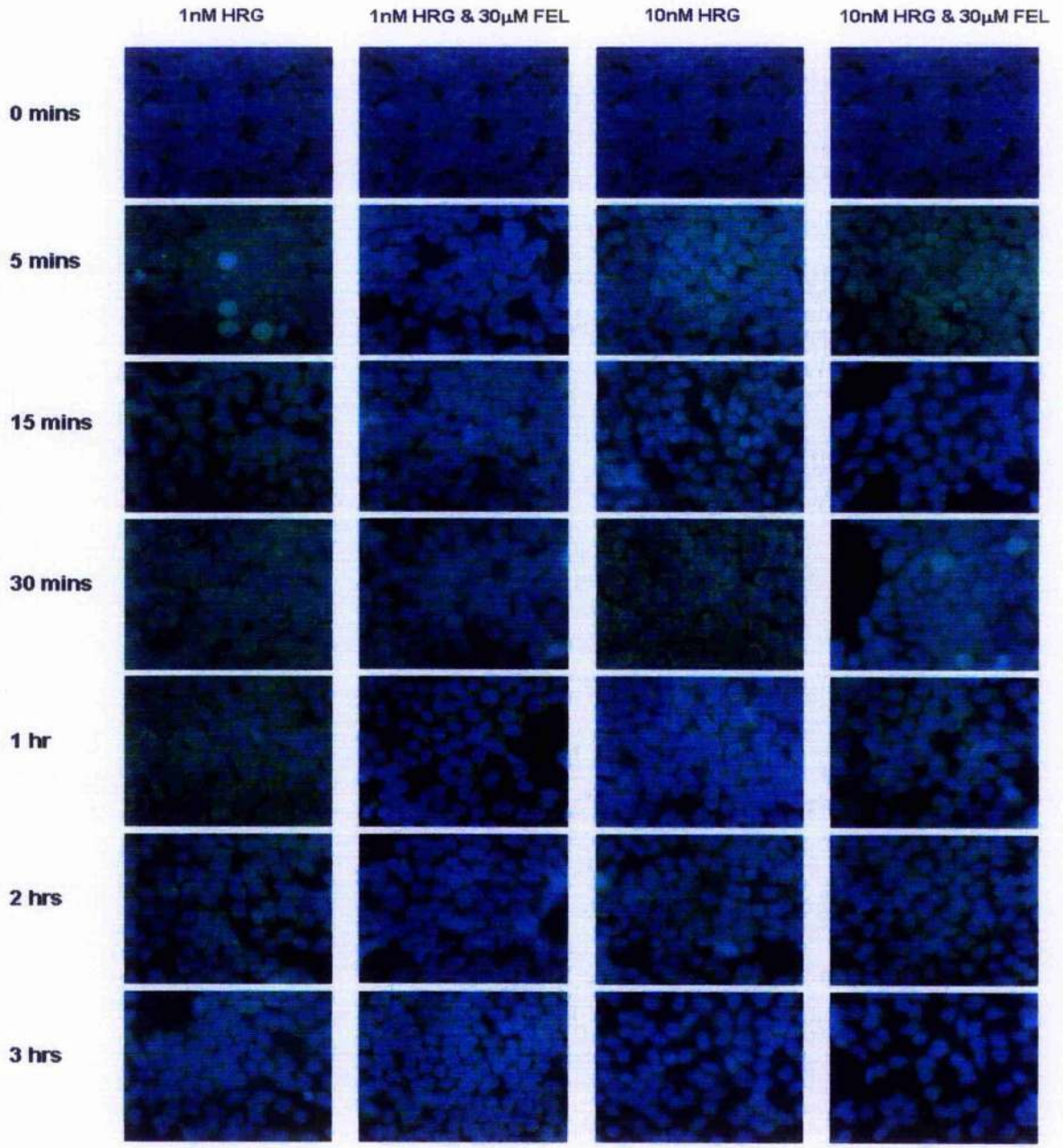

Figure 8.10: pER(ser118) IF on MCF-7 cells treated with 1nM and 10nM HRG and 30mM Felodipine

Immunofluorescence of MCF-7 cells stimulated with 1nM/10nM Heregulin (HRG), in the absence and presence of 30μM Felodipine (FEL), for 0, 5, 15, 30 minutes, 1, 2, 3 hours and treated with pER(ser118) antibody and Fluorescein avidin D (green). pER(ser118) was localised primarily in the cytoplasm of cells. Nuclei stained with DAPI (blue).

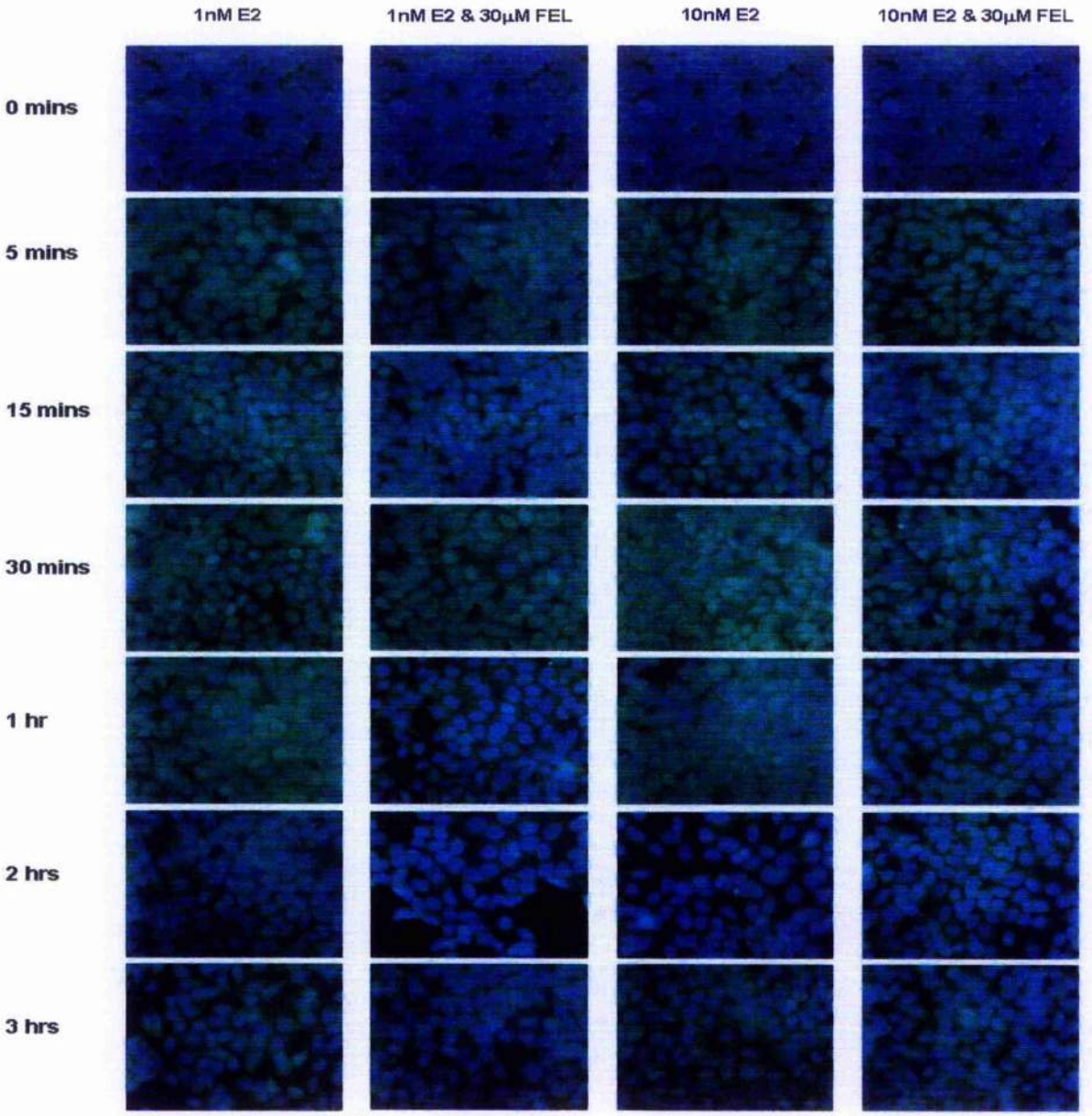

Figure 8.11: pER(ser118) IF on MCF-7 cells treated with 1nM/10nM E2 and 30mM Felodipine

Immunofluorescence of MCF-7 cells stimulated with 1nM/10nM E2, in the absence and presence of 30μM Felodipine, for 0, 5, 15, 30 minutes, 1, 2, 3 hours and treated with pER(ser118) antibody and Fluorescein avidin D (green). pER(ser118) was localised to both the cytoplasm and nuclei of cells. Nuclei stained with DAPI (blue).

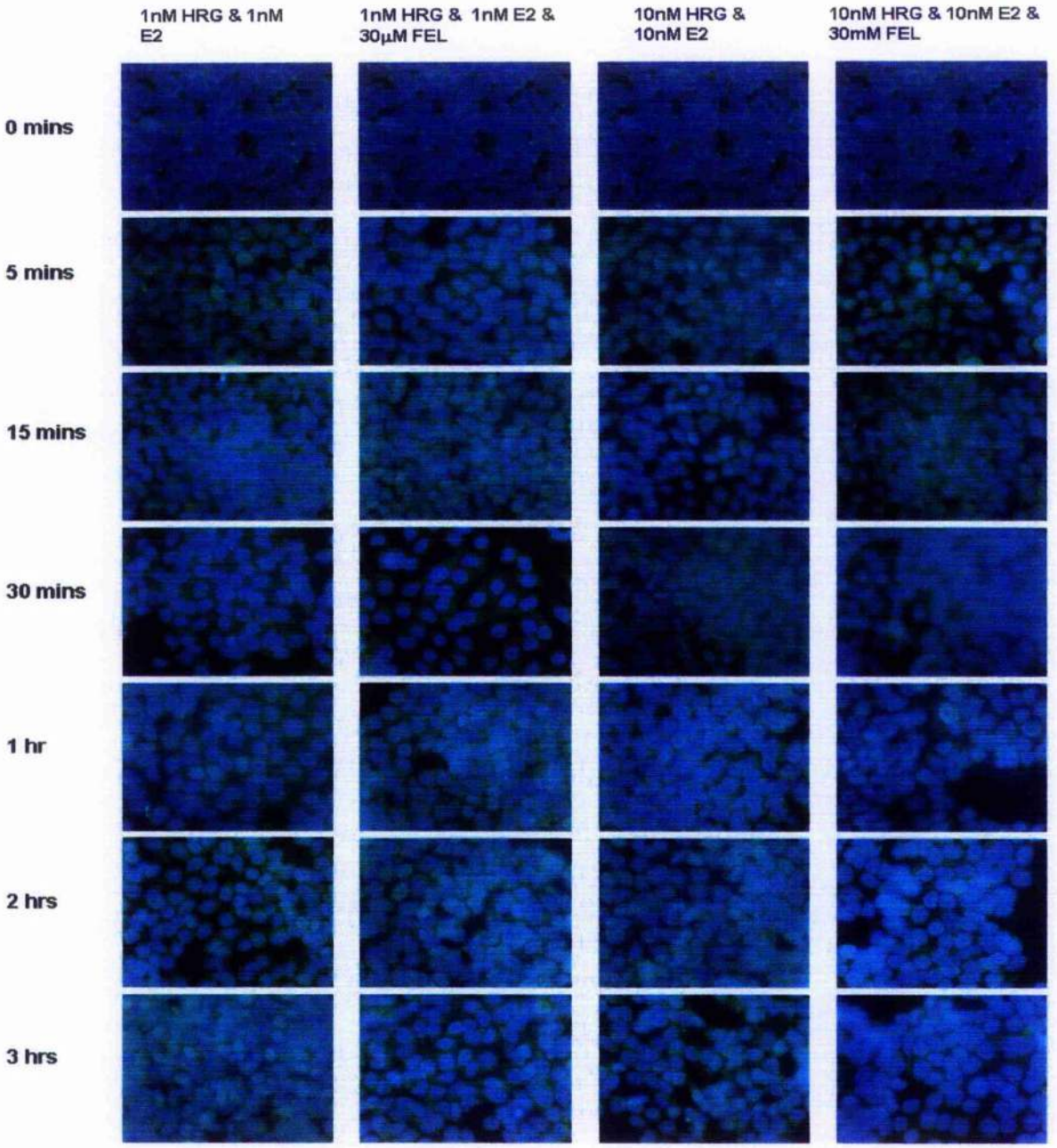

Figure 8.12: pER(ser118) IF on MCF-7 cells treated with 1nM HRG/E2, 10nM HRG/E2 and 30mM Felodipine

Immunofluorescence of MCF-7 cells stimulated with 1nM HRG/E2 and 10nM HRG/E2, in the absence and presence of 30μM Felodipine, for 0, 5, 15, 30 minutes, 1, 2, 3 hours and treated with pER(ser118) antibody and Fluorescein avidin D (green). pER(ser118)MAPK was localised to both the cytoplasm and nuclei of cells. Nuclei stained with DAPI (blue).

(a)

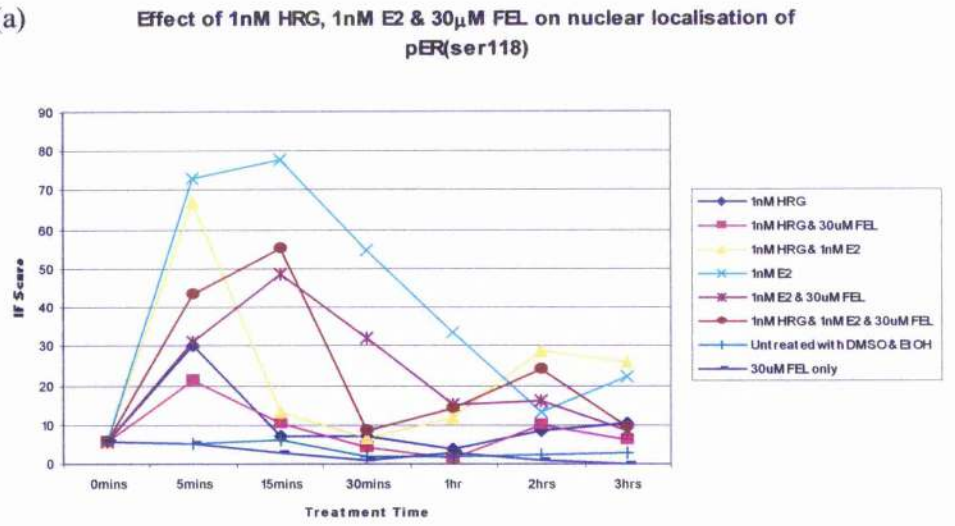

(b)

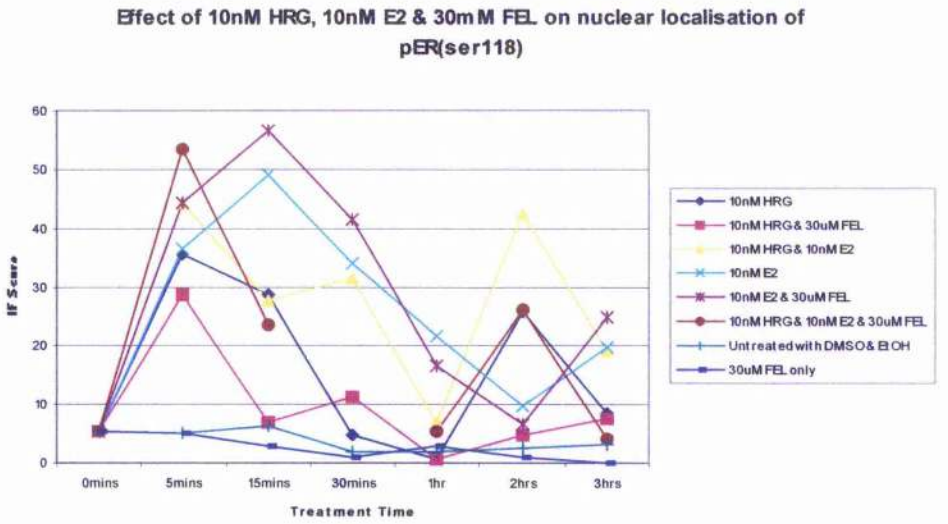

Figure 8.13: Line Graphs of Nuclear Distribution of pER(ser118)

MCF-7 cells were treated with Heregulin (HRG), Oestrogen (E2) and Felodipine (FEL) for 0, 5, 15, 30 mins and 1,2 and 3hours, and immunofluorescence performed to detect pER(ser118). A proportion of the cells were scored for nuclear expression of pER(ser118) in order to semi-quantify the effects of the various treatments on pER(ser118) nuclear localisation. The graphs show the levels of pER(ser118) expressed in the nuclei during the course of treatments with (a) 1nM HRG, 1nM E2 and 30μM FEL and (b) 10nM HRG, 10nM E2 and 30μM FEL.

8.2.4 Localisation of pER(ser167)

Analysis of the localisation of pER(ser167) generated some unexpected results. In the untreated cells, expression of pER(ser167) was constrained to the cytoplasm, as was observed with pER(ser118). However, stimulation with neither E2 nor HRG induced nuclear expression of pER(ser167). At no time point from 5 minutes to 3 hours, with any treatment, was pER(ser167) detected in the nuclei of cells, though it was expressed in the cytoplasm. The absence of nuclear pER(ser167) is highlighted in Figure 8.14, which depicts the localisation of pER(ser167) in MCF-7 cells following a selection of treatments. Interestingly, pER(ser167) may not have localised to the nuclei, but it was expressed at the plasma membrane (Figure 8.15).

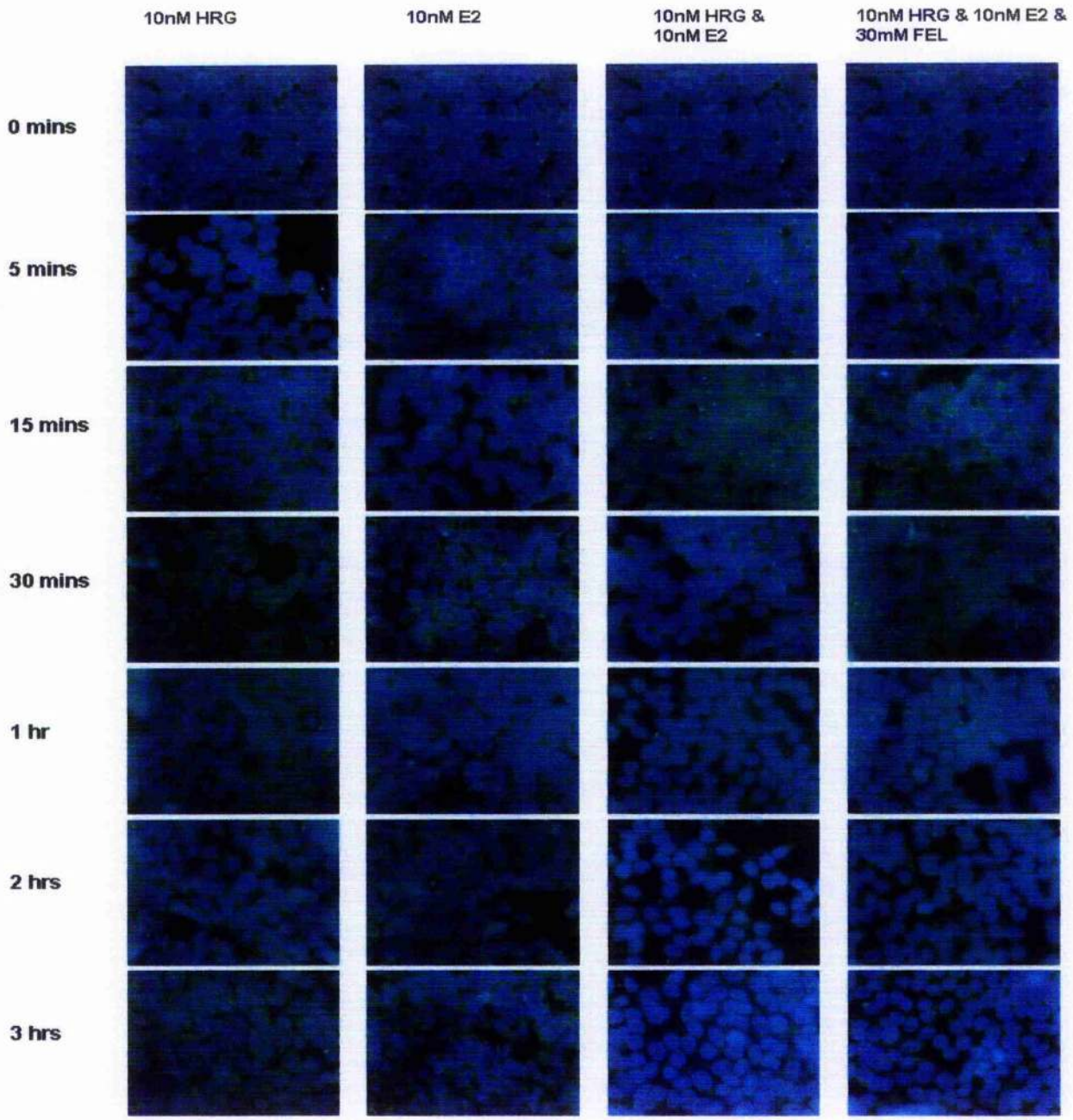

Figure 8.14: pER(ser167) IF on MCF-7 cells treated with 10nM HRG, 10nM E2 and 30mM Felodipine

Immunofluorescence of MCF-7 cells, stimulated with 10nM HRG and 10nM E2, singly and in combination, and in the absence and presence of 30μM Felodipine, for 0, 5, 15, 30 minutes, 1, 2, 3 hours. Cells were treated with pER(ser167) antibody and Fluorescein avidin D (green). pER(ser167) was localised to only the cytoplasm of cells. Nuclei stained with DAPI (blue).

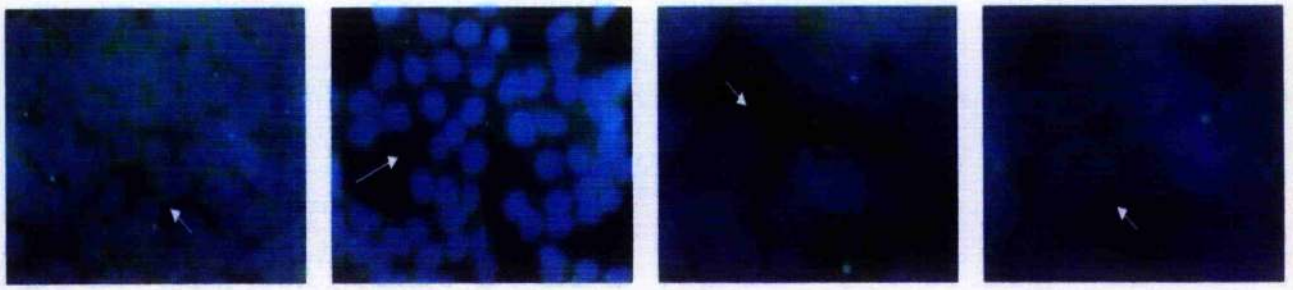

Figure 8.15: Immunofluorescent detection of membranous pER(ser167)

Immunofluorescence of MCF-7 cells stimulated with Heregulin (HRG), Oestrogen (E2) and Felodipine (FEL) and treated with pER(ser167) antibody and Fluorescein Avidin D. pER(ser167) was not detected in the nuclei of cells, but was evident at the plasma membrane, as highlighted by the arrows.

8.3 Investigation of nuclear localisation of pMAPK and pER(ser118) in MCF-7 cells

The interesting results generated from the preliminary IF study, regarding the localisation of pMAPK and pER(ser118), prompted a more thorough investigation of their localisation following stimulation with HRG, E2 and FEL. In this more in depth IF study, it was deemed appropriate to only investigate the 5, 15 and 30 minute treatments, as these were identified as the key time points in the preliminary study. As described in chapter 2, during the course of an IF experiment, each treatment was performed in quadruplicate, and each experiment was performed three times. Therefore, in total, there were 12 sets of treated cells for each condition. Once again, the levels of nuclear pMAPK and pER(ser118) were semi-quantified using the IF scoring method.

8.3.1 Effects of HRG, E2 and FEL on pMAPK and pER(ser118) localisation

The three individual IF experiments produced similar results (Figure 8.16 - 8.19). As in the preliminary study, untreated MCF-7 cells displayed strong levels of cytoplasmic pMAPK and pER(ser118), but almost no expression was detected in the nuclei. After 5 minutes of 1nM/10nM E2 stimulation, there was a rapid influx of pER(ser118) into the nuclei; strong levels were also detected in the cytoplasm. These nuclear levels were maintained throughout the 15 and 30 minute treatments. Likewise, cells treated with 1nM/10nM HRG for 5 minutes presented with nuclear pER(ser118), but at levels much lower than those observed following E2 stimulation. Additionally, there was a major decrease in the levels of nuclear pER(ser118). Following the 15 and 30 minute HRG treatments, there was almost no nuclear pER(ser118) detectable. However, it was still present in the cytoplasm. In cells treated with both E2 and HRG for 5 minutes, nuclear

pER(ser118) was visible; however, levels were comparable with those seen with HRG treatment alone. After 15 and 30 minutes, the levels of nuclear pER(ser118) once again dropped, and pER(ser118) was predominantly expressed in the cytoplasm.

Both HRG and E2 stimulated pMAPK translocation to the nucleus, though HRG was once again shown to be the more effective activator of the two. HRG and E2 were shown to function synergistically; combined treatment of the two drugs increased the nuclear levels of pMAPK in comparison with either treatment alone, especially when given for 15 and 30 minutes.

Felodipine prevented nuclear translocation of pMAPK, following treatment with both HRG and E2, when given individually and in combination. It also reduced the levels of nuclear pER(ser118) following HRG stimulation; however, it seemed to have less effect on the E2 phosphorylation of ER. In cells treated with all three drugs, nuclear levels of pER(ser118) were lower than when cells were treated with E2 alone, but were generally higher than those observed following HRG treatment, alone or in combination with E2.

To ensure that the observed effects on pMAPK and pER(ser118) localisation were due to the activity of the drugs alone and not a consequence of other factors, such as the presence of DMSO and EtOH, several controls were included. These controls are described in chapter 2. Neither the presence of DMSO, nor EtOH, altered the localisation of pMAPK and pER(ser118). Cells were also treated with FEL alone, to determine its effects on protein expression; it too failed to have any effects. These controls are included in the graphs (Figures 8.16 - 8.19), which display the trends of nuclear expression for both pMAPK and pER(ser118), following the various treatments.

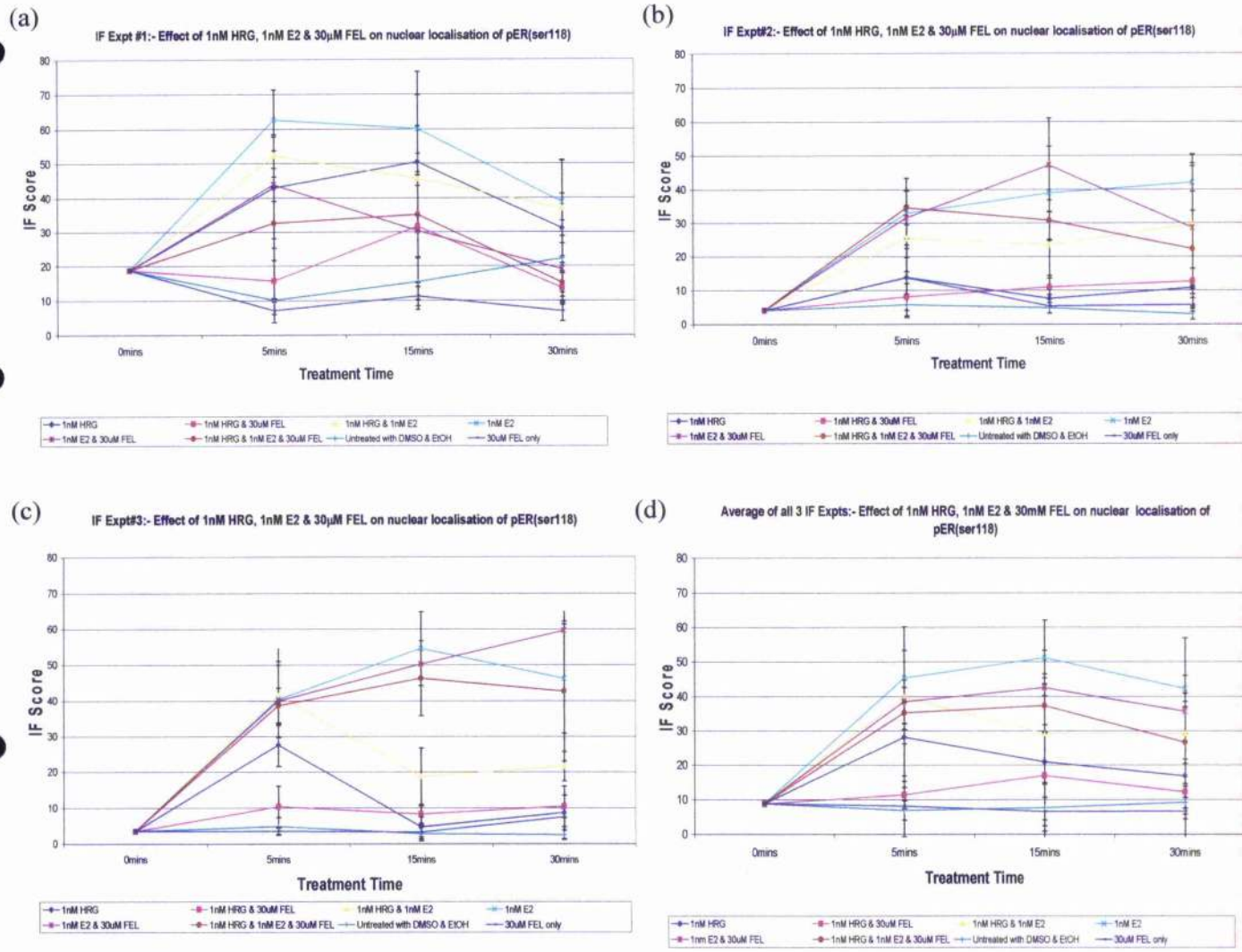

Figure 8.16: Nuclear Distribution of pER(ser118) in MCF-7 cells treated with 1nM HRG, 1nM E2 & 30mM FEL

MCF-7 cells were treated with 1nM Heregulin (HRG), 1nM Oestrogen (E2) and 30μM Felodipine (FEL) for 0, 5, 15 and 30 mins, and immunofluorescence performed to detect pER(ser118). The experiment was performed 3 times, and a proportion of the cells were scored for nuclear expression of pER(ser118). The graphs show the levels of pER(ser118) expressed in the nuclei during the course of treatments for each of the individual experiments (a-c) and the average from all 3 experiments (d).

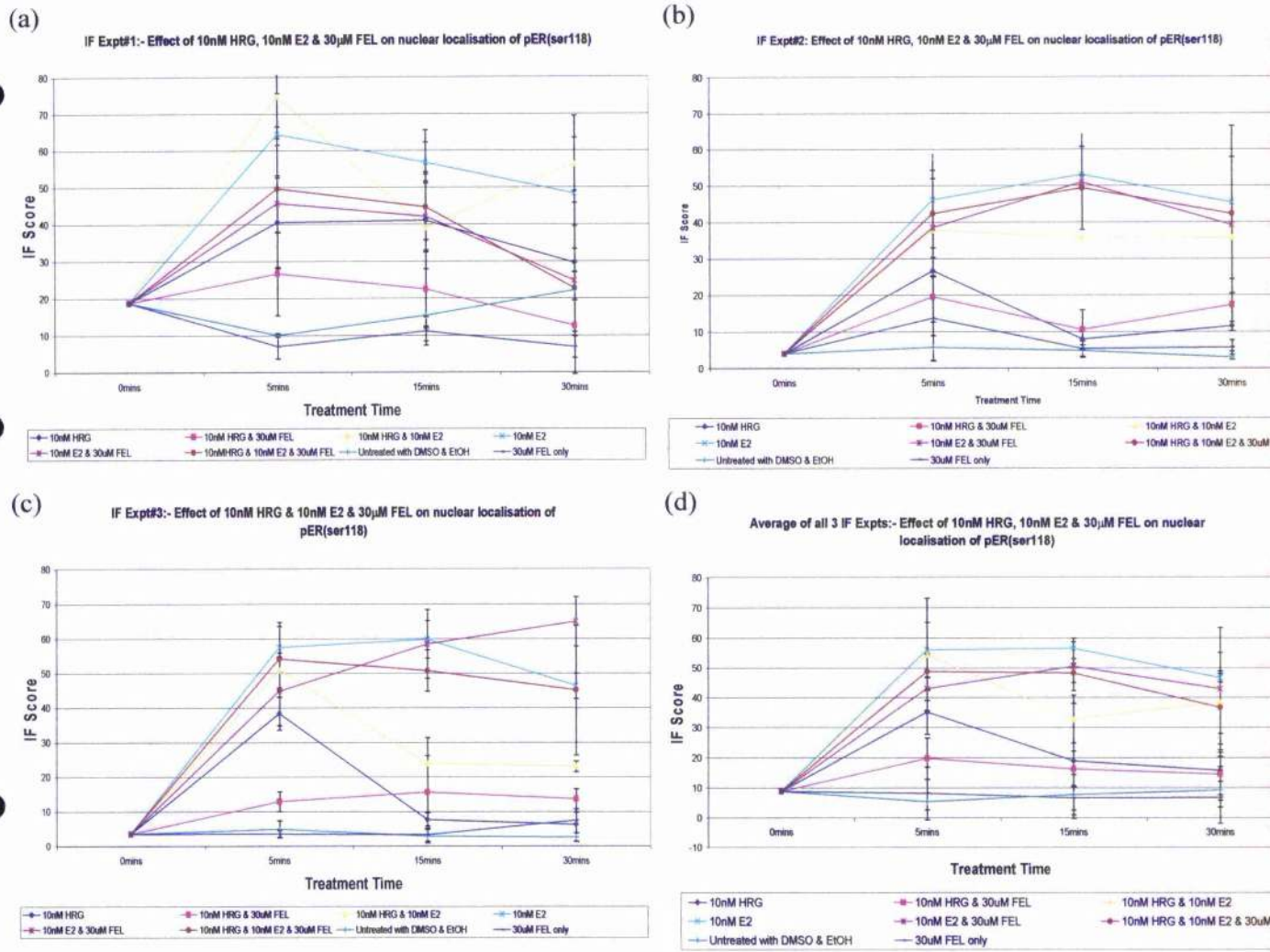

Figure 8.17: Nuclear Distribution of pER(ser118) in MCF-7 cells treated with 10nM HRG, 10nM E2 & 30mM FEL

MCF-7 cells were treated with 10nM Heregulin (HRG), 10nM Oestrogen (E2) and 30μM Felodipine (FEL) for 0, 5, 15 and 30 mins, and immunofluorescence performed to detect pER(ser118). The experiment was performed 3 times, and a proportion of the cells were scored for nuclear expression of pER(ser118). The graphs show the levels of pER(ser118) expressed in the nuclei during the course of treatments for each of the individual experiments (a-c) and the average from all 3 experiments (d).

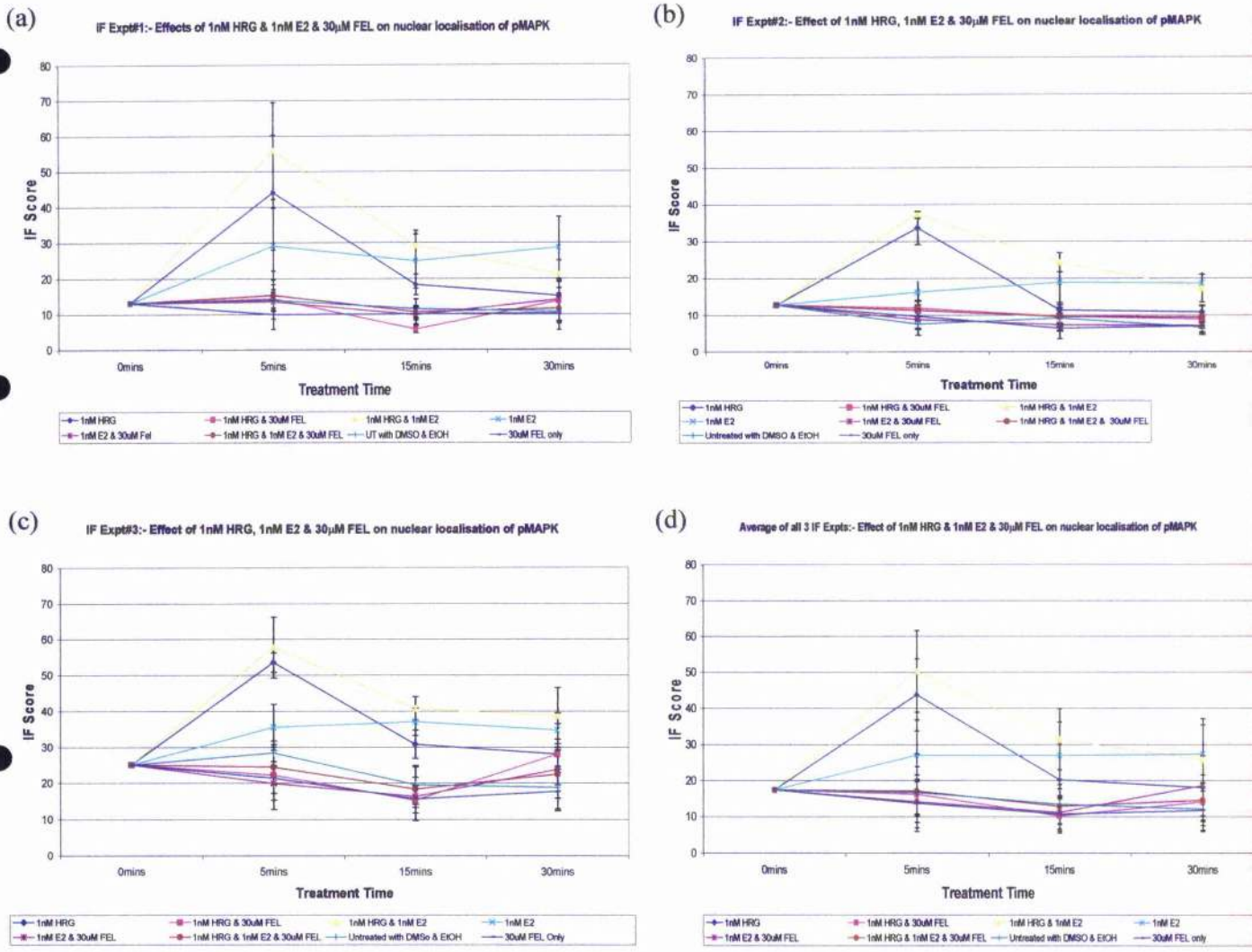

Figure 8.18: Nuclear Distribution of MAPK in MCF-7 cells treated with 1nM HRG, 1nM E2 & 30mM FEL

MCF-7 cells were treated with 1nM Heregulin (HRG), 1nM Oestrogen (E2) and 30μM Felodipine (FEL) for 0, 5, 15 and 30 mins, and immunofluorescence performed to detect pMAPK. The experiment was performed 3 times, and a proportion of the cells were scored for nuclear expression of pMAPK. The graphs show the levels of pMAPK expressed in the nuclei during the course of treatments for each of the individual experiments (a-c) and the average from all 3 experiments (d).

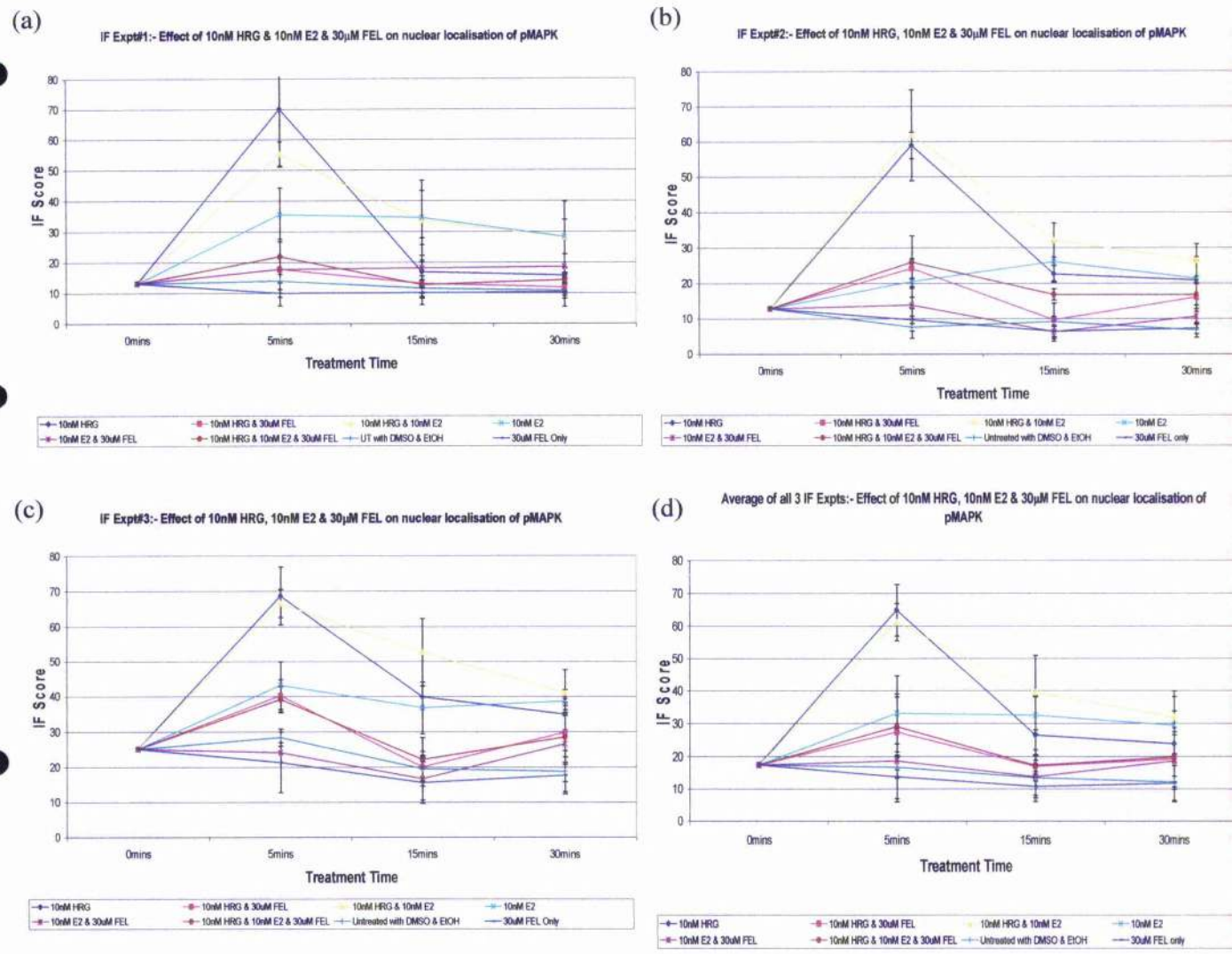

Figure 8.19: Nuclear Distribution of pMAPK in MCF-7 cells treated with 10nM HRG, 10nM E2 & 30mM FEL

MCF-7 cells were treated with 10nM Heregulin (HRG), 10nM Oestrogen (E2) and 30μM Felodipine (FEL) for 0, 5, 15 and 30 mins, and immunofluorescence performed to detect pMAPK. The experiment was performed 3 times, and a proportion of the cells were scored for nuclear expression of pMAPK. The graphs show the levels of pMAPK expressed in the nuclei during the course of treatments for each of the individual experiments (a-c) and the average from all 3 experiments (d).

8.4 Activation of MAPK and ER in MCF-7 breast cancer cells following treatment with Oestrogen and Heregulin

An *in vitro* study was designed to investigate the effects of HRG and E2 on the activation status of MAPK and ER in MCF-7 breast cancer cells. Time course treatments were set up, whereby cells were stimulated with HRG or E2, singly and in combination, for 5, 15 and 30 minutes. Table 2.12 lists the drug treatments. Western blotting was used to monitor the levels of pMAPK and pER (described in sections 2.7 & 2.9)

8.4.1 Activation of MAPK

Treatment of MCF-7 cells, with HRG or E2, stimulated increased expression of pMAPK. (Figure 8.1); However, of the two drugs, HRG proved the most effective activator of MAPK. Maximum activation of MAPK appeared to occur following the 15 minute HRG treatment. Combined treatment of HRG and E2 seemed to induce greater levels of pMAPK, suggesting that these two drugs functioned in an additive or synergistic manner (Figure 8.20).

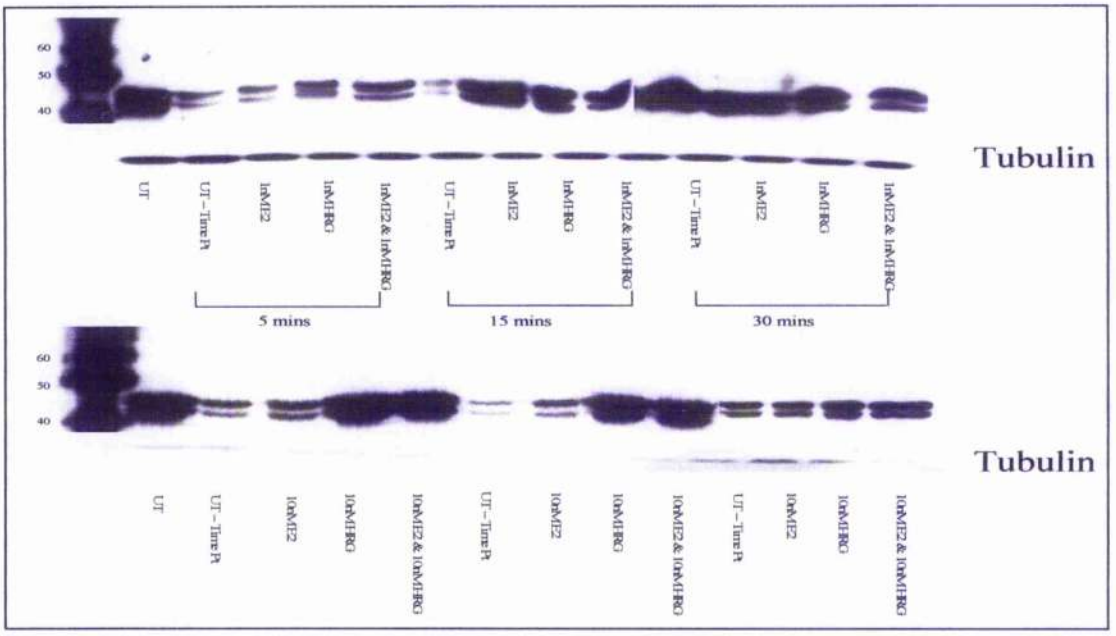

Figure 8.20: Expression levels of pMAPK in MCF-7 cells following time course treatments

MCF-7 cells were stimulated with 1nM/10nM Heregulin (HRG) and Oestrogen (E2), singly and in combination, for 5, 15 and 30 minutes. Western blotting was performed on 25μg cell lysate and samples probed for pMAPK (44/42kDa) expression.
UT= Untreated control without DMSO, EtOH, UT time pt = 5, 15, or 30 minute untreated control with DMSO, ETOH

8.4.2 Activation of ER

- **pER(ser118)**

The pER(ser118) antibody seemed to be batch specific. The batch used for the immunofluorescent studies worked well in western blotting; however, subsequent batches failed to produce similar results. It was, therefore, impossible to obtain western blots for all the samples using pER(ser118).

Treatment of MCF-7 cells with 10nM E2 stimulated phosphorylation of ERα at serine 118. Conversely treatment with HRG did not seem to significantly increase expression levels of pER(ser118). It also appeared in the five and fifteen treatments that

the presence of HRG reduced the levels of E2 stimulated phosphorylation. However, after the 15 minutes, the combined treatment with both E2 and HRG seemed to induce increased expression levels of pER(ser118) (Figure 8.21).

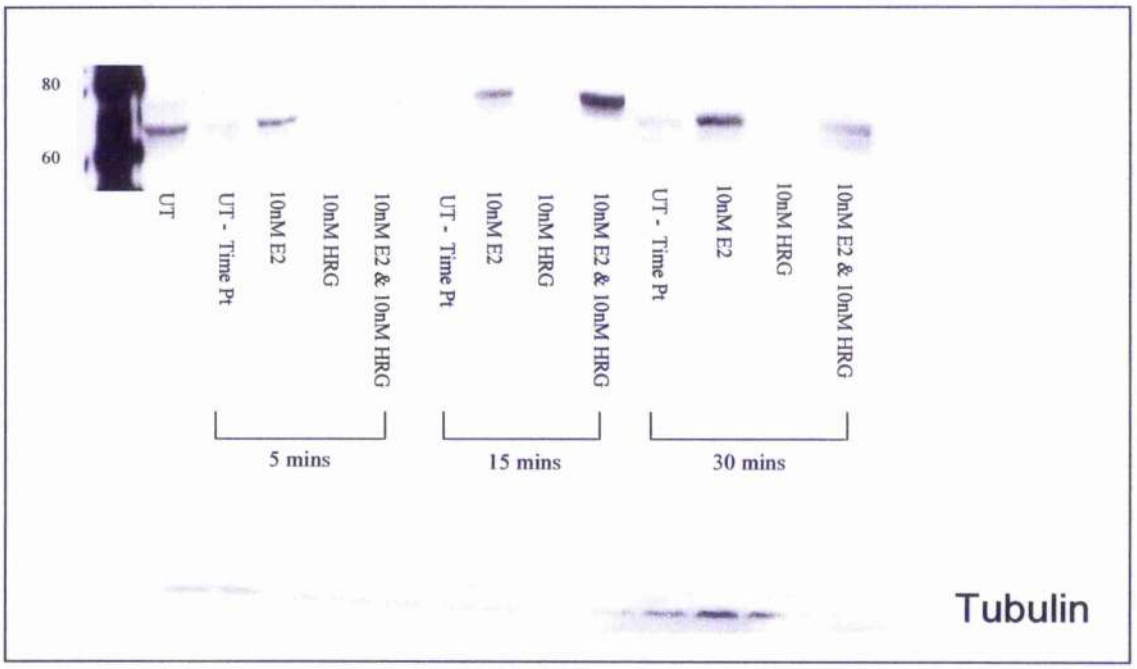

Figure 8.21: Expression levels of pER(ser118) in MCF-7 cells following time course treatments

MCF-7 cells were stimulated with 10nM Heregulin (HRG) and Oestrogen (E2), singly and in combination, for 5, 15 and 30 minutes. Western blotting was performed on 25μg cell lysate and samples probed for pER(ser118) (66kDa) expression. Tubulin was used as a loading control. UT= Untreated control without DMSO, EtOH, UT time pt = 5, 15, or 30 minute untreated control with DMSO, ETOH

- **pER(ser167):** Unfortunately, after completing the immunofluorescent studies, the pER(ser167) antibody was withdrawn from the market, and the replacement antibody proved non-specific. Therefore, it was impossible to measure the levels of pER(ser167) in MCF-7 cells, following the various treatments.

8.5 Investigation of localisation of pMAPK and pER(ser118) in MCF-7 cells using subcellular fractionation

Having investigated the localisation of MAPK and ER in the IF studies, it was deemed appropriate to further probe the distribution of these proteins using a subcellular fractionation approach. The IF study indicated that the major changes in cellular localisation occurred at the 5 and 15 minute time points. Accordingly, subcellular fractionation, generating membrane, cytoplasmic and nuclear fractions, was performed, following 5 and 15 minute stimulations. As in the IF study, MCF-7 cells were treated with 1nM/10nM HRG and E2, singly and in combination, and in the presence and absence of 30mM FEL. Additionally, for the 15 minute treatment, the MEK inhibitor, U0126, which prevents activation of MAPK, was used in combination with HRG and E2. A list of all treatments is provided in Table 2.14 and 2.15. Western blotting was performed on the protein fractions using antibodies specific to pMAPK and pER(ser118). Unfortunately, the localisation of pER(ser167) could not be investigated further, since the antibody was withdrawn from the market, and the replacement antibody was shown to be non-specific in the time course treatment experiments.

8.5.1 Effects of HRG, E2, FEL and U0126 on pMAPK localisation

Subcellular fractionation produced similar results to those from the IF study. Stimulation of MCF-7 cells with HRG and E2 resulted in nuclear expression of pMAPK. As with the IF study, HRG seemed to induce greater nuclear translocation of pMAPK than E2, but both drugs did seem to function synergistically in promoting nuclear expression of pMAPK. Yet again, FEL demonstrated its ability to prevent nuclear translocation of pMAPK following treatment with either HRG or E2. However, it appeared to be less

effective when given in combination with both HRG and E2 (Figure 8.20c,d). Treatment with U0126 inhibited activation of MAPK, even in the presence of HRG or E2.

In comparison, treatment with HRG, E2 or FEL did not seem to induce major changes in the expression of membranous or cytoplasmic pMAPK. pMAPK was detected in both membrane and cytoplasmic fractions, regardless of treatment (Figure 8.22a,b,e,f).

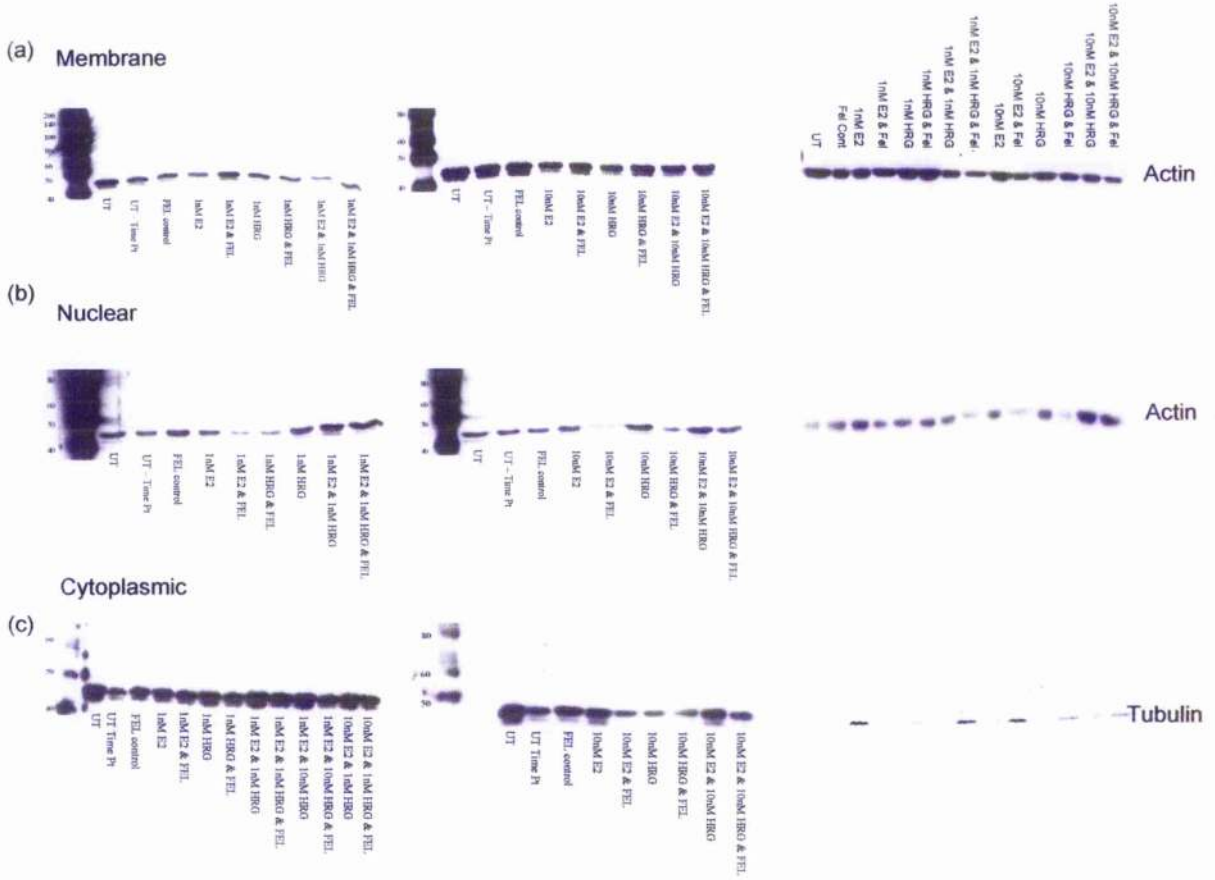

Figure 8.22: Detection of pMAPK in protein fractions following 5 minute treatment with HRG, E2 and FEL

MCF-7 cells were treated with 1/10nM Heregulin (HRG) and Oestrogen (E2), singly and in combination, and in the presence or absence of Felodipine (FEL), for 5 minutes. Subcellular fractionation was then performed, generating membranous, cytoplasmic and nuclear fractions. Western blotting was performed on 25µg of membrane (a), nuclear (b), and cytoplasmic (c) protein fractions and samples probed for pMAPK (44/42kDa) expression. Actin and Tubulin were used as loading controls. UT= Untreated control without DMSO & EtOH, UT time pt = 5 minute untreated control with DMSO & ETOH, FEL control= 30µM Felodipine only

8.5.2 Effects of HRG, E2, FEL and U0126 on pER(ser118)localisation

The results from the IF study meant that the nuclear localisation of pER(ser118) was of particular interest. Unfortunately, due to unforeseen problems with the pER(ser118) antibody, western blots could not be obtained for all the protein fractions. Only the 15 minute nuclear fraction western blot was available for analysis (Figure 8.23). However, the results from this did confirm the findings from the IF study. In the control cells, in particular UT time pt, FEL control & U0126 control, there was almost no pER(ser118) detectable in the nuclei. However, following a 15 minute stimulation with 1nM/10nM E2, there was an obvious increase in the levels of nuclear pER(ser118). In contrast, the levels of nuclear pER(ser118) were much lower following treatment with 1nM/10nM HRG. Levels were comparable with those seen in the UT cells. Furthermore, combined treatment with E2 and HRG did induce some nuclear pER(ser118) expression, but the levels were considerably lower than those evident in cells treated only with E2.

As with the IF study, FEL severely reduced nuclear expression of pER(ser118) following HRG treatment. Likewise, the combined treatment of U0126 and HRG substantially reduced the presence of pER(ser118) in the nuclei of MCF-7 cells. U0126 reduced the levels of pER(ser118) following treatment with 1nM E2, but appeared to have no effect on those stimulated with 10nM E2. Felodipine did appear to reduce the levels of nuclear pER(ser118) following E2 stimulation, but to a lesser extent than observed with HRG. Interestingly, the addition of either FEL or U0126 to cells treated with both E2 and HRG seemed to negate the inhibitory effects of HRG on E2 dependent localisation of pER(ser118). Of the two, U0126 appeared to be the most effective in over riding the effects of HRG and inducing nuclear expression of pER(ser118).

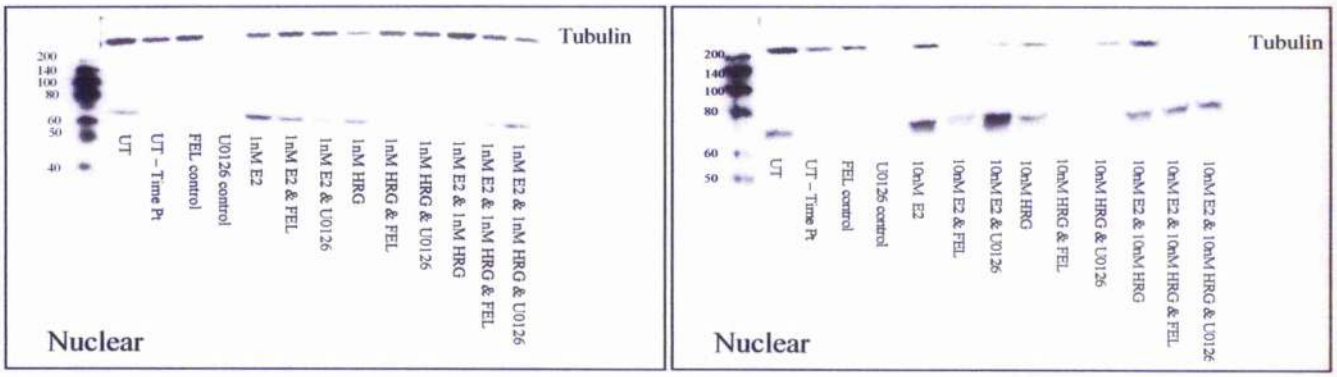

Figure 8.23: Detection of pER(ser118) in nuclear protein fractions following 15 minute treatment with HRG, E2, FEL and U0126

MCF-7 cells were treated with 1/10nM Heregulin (HRG) and Oestrogen (E2), singly and in combination, and in the presence or absence of Felodipine (FEL), for 15 minutes. Subcellular fractionation was then performed. Western blotting was performed on 25μg of nuclear protein fractions and samples probed for pER(ser118) (66kDa) expression. Tubulin was used a loading control. UT= Untreated control without DMSO & EtOH, UT time pt = 15 minute untreated control with DMSO & ETOH, FEL control= 30μM Felodipine only

8.6 Discussion

The relationship between MAPK and ERα is well documented; however, our understanding of the interaction between the two is sparse. It is undisputed that MAPK can activate ERα in a ligand-independent manner, via phosphorylation of serines 118 and 167, but what are the consequences of this ligand-independent activity? Furthermore, it is accepted that there is cross talk between the ERα and the growth factor receptors (RTKs), but to what extent does the ligand-independent activation of ERα differ from that of ligand-dependent activity? The study aimed to investigate the interaction and localisation of MAPK and ERα, and to provide information regarding the ligand-dependent and independent phosphorylation/activation of ERα.

This study not only confirmed previous findings regarding the activation of ERα but also produced several interesting discoveries. Results from the localisation studies indicated that ligand-mediated phosphorylation was associated with rapid but sustained

nuclear localisation of ERα, probably due to E2 binding. In both the IF and subcellular fractionation studies, stimulation of MCF-7 cells with E2, for only 5 minutes, resulted in a considerable increase in the levels of nuclear pER(ser118), when compared to untreated cells. These findings are in keeping with previous studies, which have shown that E2 binding to ERα promotes nuclear translocation of the receptor. Furthermore, there is evidence that E2 stimulation is associated with changes in the intranuclear distribution of ERα, and that these changes occur rapidly (277). It is thought that the alterations in ERα localisation enable it to associate with the nuclear matrix and recruit co-activators, such as AIB1. Hence, this ligand-dependent nuclear localisation is essential for ERα transcriptional activity. However, the original IF study demonstrated that the levels of nuclear pER(ser118) were shown to gradually decrease during the longer incubation times with E2. ERα expression levels are maintained via a balance of synthesis and degradation. Research has suggested that binding of ligands, such as E2, enhances receptor degradation. One study showed a decrease in the levels of nuclear ERα following a two hour treatment with 10nM E2 (278). Therefore, the reduction in nuclear expression of pER(ser118) may be a consequence of agonist mediated ERα degradation.

This study also confirmed that ERα is phosphorylated at serine 118 in a ligand-independent manner, via MAPK(29;39). However, in contrast to E2 stimulation, treatment with HRG induced rapid but transient phosphorylation of ERα. Maximum levels of nuclear pER(ser118) were observed following 5 minute stimulation with HRG, and levels were shown to drop dramatically with longer treatments. These findings are in keeping with other studies which show that ligand-dependent phosphorylation and activation of ERα is sustained, but that ligand-independent activity is short-lived in

comparison (29;279). These noticeable differences between HRG and E2 mediated phosphorylation of ERα support the fact that E2 mediated phosphorylation of serine 118 relies on a kinase other than MAPK. Previous research has indicated that the kinase, CDK7, is necessary for ligand-dependent phosphorylation of serine 118 (29;280;281). Additionally, in this study, prevention of nuclear translocation of pMAPK, using FEL, and inhibition of MAPK activation, using U0126, did not appear to have a major effect on E2 regulated expression of nuclear pER(ser118). This confirmed that MAPK is not the kinase responsible for E2 mediated phosphorylation of the receptor. Conversely, inhibition of MAPK severely impaired the ligand-independent phosphorylation of ERα. In the IF and fractionation studies, treatment with HRG in the presence of FEL reduced expression of nuclear pER(ser118), to almost non-existent levels. The same observations were made following inhibition with U0126 in the 15 minute fractionation experiment. These findings confirmed that MAPK is the kinase responsible for phosphorylating serine 118 in a ligand-independent manner, via activation of the RTKs. However, more interestingly, they implied that phosphorylation and activation of MAPK is not sufficient to promote nuclear expression of pER(ser118). For pER(ser118) to be expressed in the nuclei of cells, pMAPK must also translocate into the nucleus. Other studies have previously shown that MAPK induces nuclear localisation of the ERα; however, they failed to demonstrate that MAPK translocation in to the nucleus was also required (277;282). There are two possible explanations as to why preventing nuclear expression of pMAPK should inhibit pER(ser118) nuclear expression. The first is that pMAPK directly phosphorylates ERα in the nuclei of cells; therefore translocation of MAPK into the nucleus is compulsory. The second is that pMAPK phosphorylates ERα in the

cytoplasm, and that the phosphorylated receptor "piggy backs" into the nucleus with pMAPK. Studies have identified the E2-dependent nuclear localisation signal at amino acids 256-303 (283), but perhaps phosphorylation of ERα at serine 118 and 167 via MAPK is insufficient to promote nuclear translocation. Therefore, ERα is dependent on MAPK to facilitate its transport from the cytoplasm into the nucleus. Perhaps cytoplasmic pMAPK sequesters pER in the cytoplasm. The fact that FEL was shown to lower the levels of nuclear pER(ser118) only slightly, following treatment with E2, possibly suggests that the containment of pMAPK within the cytoplasm commandeered low levels of the activated receptor within the cytoplasm. Having observed that nuclear translocation of pMAPK is essential for the ligand-independent expression of pER(ser118) in the nucleus of cells, the next step is to further elucidate the mechanism by which nuclear pMAPK regulates localisation of pER(Ser118).

Considering that the effects of E2 on ERα were supposedly independent of MAPK, the combined treatment of MCF-7 cells with E2 and HRG produced some very interesting results. One might have expected that, since the two drugs phosphorylated ERα via different mechanisms, that they might function in an additive or synergistic manner to promote nuclear localisation of pER(ser118). Alternatively, one might have predicted that, as the principal ligand for ERα, E2 would be the driving force in regulating the phosphorylation, activation and localisation of the receptor. However, neither of these scenarios proved to be true. Co-stimulation with both E2 and HRG suggested that the two drugs did not co-operate synergistically, but that, in fact, HRG, and not E2, mediated signalling determined the subcellular localisation of ERα. Despite the presence of E2, which translocated ERα to the nucleus in the absence of HRG, in

cells treated with both drugs there was a substantial reduction in nuclear pER(ser118). Unexpectedly, HRG appeared to inhibit E2 mediated effects. This is dissimilar to the findings of another group that suggested that constitutive activation of the growth factor pathways was incompatible with E2 signalling, and that, of the two, E2 effects dominated (220). Conversely, in the IF and fractionation studies, the two drugs appeared to work synergistically to increase the levels of nuclear pMAPK expression. Perhaps, this increased expression of nuclear pMAPK enhanced the activation of ERα by direct phosphorylation, and subsequently resulted in its rapid deactivation, due to degradation, or its relocalisation from the nucleus to the cytoplasm or plasma membrane. Both these possibilities are dependent on the nuclear export of the receptor. To be degraded, ERα is exported from the cytoplasm to the nucleus via CRM1 (284). It is speculated that the interaction between ERα and its co-activator AIB1 is not only crucial for ER-mediated transcription, but is also a key step in the degradation process. Studies have shown that suppression of AIB1 stabilises ERα in the presence of E2 (285). Hence, activation of AIB1 may be an important factor in the degradation of ERα. Activation of the co-activators is dependent on phosphorylation, and besides its ability to directly phosphorylate ERα, MAPK can also phosphorylate and activate AIB1. Perhaps, the elevated levels of pMAPK in the nucleus led to increased phosphorylation and activation of ERα and AIB1, which ultimately resulted in the degradation of the two.

An alternative explanation is that the increased expression of pMAPK caused pER(ser118) to relocalise from the nucleus to either the cytoplasm or membrane. This theory supports the findings of another group, which provided evidence that

overexpression of HER2, and increased activation of MAPK, in breast cancer cells, promoted the translocation of ERα from the nuclei to the cytoplasm (286).

The suggestion that MAPK is a key factor in driving the HRG mediated signalling and inhibiting the E2 dependent effects of ERα is sustained by the results from the IF and fractionation studies, when MCF-7 cells were treated with HRG and E2 in the presence of the inhibitors. Both MAPK inhibitors, particularly U0126, in the 15 minute fractionation experiment, seemed to negate the inhibitory effects of HRG on E2, in terms of nuclear localisation of pER(ser118). Increased levels of nuclear pER(ser118) were evident in the IF and fractionation studies, following treatment with HRG, E2 and the MAPK inhibitors, in comparison to cells only treated with HRG and E2. These results imply that prevention of MAPK activation and translocation to the nucleus permits activated ERα to remain in the nuclei of cells. Hence, activated MAPK must be involved in the export of ERα from the nucleus, though at present the mechanism and function of this is unknown. Additional, *in vitro* studies are required to further enhance our understanding of the relationship between MAPK and ERα.

9. General Discussion

The main aim of this thesis was to investigate the role of the Ras/Raf-1/MAPK pathway in the development and progression of breast cancer, and to determine if it influenced patient outcome and response to treatments targeted against both ERα and proliferating cells. Two of the key functions of the Ras cascade are controlling cell proliferation and altering the phosphorylation and activation status of ERα in a ligand-independent manner. The research presented in this thesis tested the hypothesis that activation of this pathway is an indicator of response to endocrine and cytotoxic therapies.

Tamoxifen, an oestrogen antagonist, is currently the most successful and least toxic drug treatment for the 70-80% of patients diagnosed with ERα positive breast cancer. It competitively inhibits oestrogen binding and favours ERα interactions with co-repressors, subsequently down-regulating ERα mediated gene transcription and inhibiting proliferation (38;107).

The majority of chemotherapeutic agents function most effectively against proliferating tumour cells in growth phase (287). It has been suggested that tumours with low proliferative indices may respond poorly to these therapeutic agents. However, proliferative indices are poor predictors of chemotherapeutic response (288).

Tamoxifen and chemotherapy are key treatments for breast cancer; however, resistance to both therapies is a major problem and is significantly related to patient relapse and death. The exact mechanisms that drive resistance are not completely understood; however, the Ras/Raf-1/MAPK pathway has been implicated in mediating response to both treatments.

Expression of the Ras/Raf-1/MAPK proteins was assessed in breast tumours from three different patient cohorts. The initial pilot study was comprised of a mixture of ERα positive and negative patients, whose treatment included tamoxifen, chemotherapy and radiotherapy. The second group was a cohort of ERα positive patients, all of whom received Tamoxifen treatment for a median of five years (STB Study). The final cohort consisted of patients from the NEAT/BR9601 clinical trial, who randomly received one of two chemotherapeutic regimes: epirubicin followed by CMF, or CMF alone.

The findings from the pilot study suggested that the Ras pathway is in part responsible for mediating patient outcome. Elevated expression of N-Ras in breast tumours was associated with shortened disease-free survival (DFS) and overall survival (OS) time (Figure 3.9). This laid the foundation for the two studies investigating the role of the Ras, Raf-1 and MAPK proteins in influencing response to tamoxifen and chemotherapy. The results of these studies, firstly, suggested that the Ras/Raf-1/MAPK pathway was a functional signalling cascade in clinical breast tumours. Analysis suggested that increased expression of Ras, in particular N-Ras, was associated with increased levels of activated Raf-1, which in turn was linked to activation of MAPK. Additionally, there was an association between pMAPK and inactive Raf-1, pRaf(ser259). This is further evidence of an intact signalling pathway, since several studies have demonstrated that downregulation of Raf-1 is partly dependent on negative feedback following mitogen stimulation. Inhibition of MEK and MAPK signalling preserves Raf-1 in its active conformation (178;181). Secondly, it was implied that increased expression and activation of the Ras cascade predicted for poor outcome on tamoxifen but not chemotherapy.

Initial analysis of the entire STB cohort (303 tamoxifen treated and 99 tamoxifen & chemotherapy treated patients) suggested that N-Ras, pRaf(ser338) and MAPK were all associated with an increased risk of relapsing whilst receiving Tamoxifen. Previous *in vitro* studies have demonstrated that constitutive activation of Ras and Raf-1 in MCF-7 cells induces hormone-independent growth (220), whilst increased expression of MAPK has been shown to be associated with the growth of ERα positive cell lines during adaptation to long-term E2 deprivation and the development of tamoxifen resistance in these cell lines(221;259;289). Clinical studies investigating expression of phosphorylated MAPK have been slightly contradictory. pMAPK has been shown not to be involved in the development of tamoxifen resistance, but has also been associated with both a poor and an improved outcome on tamoxifen (212;213;223;224;226). These findings, in addition to our own, suggested that increased expression and activation of the Ras/Raf-1/MAPK pathway was a contributing factor in the development of tamoxifen resistance. However, additional analysis of only the tamoxifen treated patients demonstrated that, whilst N-Ras and MAPK served to highlight the importance of the Ras pathway in mediating response to tamoxifen, pRaf(ser338) was the key factor in reducing response time to tamoxifen treatment. Increased expression of activated Raf-1 in patients' tumours was also associated with reduced DFS and OS time. Furthermore, pRaf(ser338) expression was shown to be independent of known prognostic markers, namely tumour size, grade and nodal status, in predicting for tamoxifen relapse (Table 6.5). Conversely, in the NEAT study, neither Raf-1 nor MAPK tumour expression was associated with outcome in patients treated with chemotherapy, regardless of whether they received Epirubicin and CMF or CMF alone.

This study is important, not only because it examines multiple components of the MAPK cascade, as opposed to single proteins in clinical breast tumours, but also because it investigates the extent to which expression of these proteins predicts patients' response to different treatments. The observation that the Ras/Raf-1/MAPK pathway mediates response to tamoxifen but not chemotherapy might be slightly unexpected. Since the Raf-1/MAPK pathway regulates cell proliferation, and since chemotherapeutic agents are believed to be more effective in highly proliferating cells, one might have speculated that this pathway would predict for response to chemotherapy. However, previous studies investigating the role of the Raf-1 cascade in mediating response to chemotherapy have been performed in cell lines and have been inconclusive. Several studies have suggested that the Ras/Raf-1/MAPK pathway is linked to response to epirubicin and doxorubicin treatment. *In vitro* Raf-1 (154;227) and MAPK (273) expression is associated with increased proliferation and anthracycline resistance. Yet, increased MAPK activation is also linked to enhanced apoptosis and anthracycline sensitivity (230).

When considering reasons why the Ras pathway might predict for response to tamoxifen but not chemotherapy, it is necessary to take into account the two populations of patients analysed. The STB cohort was treated routinely with Tamoxifen, whilst the NEAT patients were all part of a clinical trial (BR9601) designed to compare the effects of CMF alone against that of sequential Epirubicin followed by CMF. Subsequently, comparison of the STB and NEAT cohorts revealed that the NEAT patients presented with more aggressive tumours: they tended to be larger and of a higher grade. Generally these patients also presented with an increased number of positive lymph nodes in comparison with the STB patients. Furthermore, only 63% of the NEAT patients were

ERα positive. Additionally the percentage of breast cancer recurrences and breast cancer specific deaths was higher in the NEAT cohort, as opposed to the STB cohort (34.9% versus 27.9% and 26.4% versus 18.4% respectively). It was not surprising that the NEAT patients displayed more aggressive tumours than the STB patients, since they had been selected to receive the more severe treatment of chemotherapy. Only 99 patients from the STB cohort received chemotherapy in addition to tamoxifen.

That neither Raf-1 nor MAPK were predictive for outcome in the NEAT patients might be an indicator that these proteins are involved in the early stages of tumourigenesis and cancer progression. Previous research has demonstrated an increase in the levels of active MAPK in approximately 50% of breast tumours, in comparison with their normal breast tissue (213). Additionally, activated MAPK was shown to be associated with lymph node metastases. The levels of active MAPK in lymph node metastases were significantly higher than those in the primary breast tumour (213). Therefore, increased expression of MAPK might be a marker for lymph node metastases and might identify patients who require more aggressive treatments. Perhaps Raf-1 and MAPK tumour expression levels can help identify those patients most likely to benefit from chemotherapy. However, if it is the case that increased expression levels of Raf-1 and MAPK are predictive for more aggressive tumours and poorer outcome, possibly these levels become redundant in predicting for outcome in a group of patients, such as the NEAT cohort, who all generally presented with aggressive tumours and positive lymph nodes. In this cohort no association was observed between Raf-1 or MAPK expression and nodal status, perhaps due to the fact that 86.3% of patients were node positive. Consequently, neither Raf-1 nor MAPK expression levels were significantly

linked with DFS or OS. Conversely, in the less aggressive STB tumours, both nuclear pRaf(ser338) and cytoplasmic MAPK tumour levels were positively correlated with nodal status and associated with an increased risk of relapsing on tamoxifen. Perhaps in the less aggressive tumours, the Ras pathway was still significantly contributing to tumour progression and, therefore, was predictive for patient outcome, whereas the more advanced NEAT tumours were less dependent on the Ras, Raf-1, and MAPK proteins.

In addition to activating the Raf-1/MAPK cascade, Ras also stimulates the apoptotic P13K/AKT pathway. AKT phosphorylates substrates that directly or indirectly regulate apoptosis, such as BAD, caspase 9 and forkhead transcription factors (290-292). Furthermore, Raf-1 has been identified as an AKT target. Activation of AKT can induce inactivation of Raf-1 via phosphorylation of serine 259, subsequently downregulating activity of this proliferative pathway (173). Consequently, it might be that AKT and its downstream factors are more appropriate markers for response to chemotherapy. This has been suggested in several *in vitro* studies (229;276).

However, the theory that tumour expression of Raf-1 and MAPK might help identify patients who would perhaps benefit from chemotherapy was also suggested in the STB study. In the tamoxifen only treated patients, elevated levels of activated Raf-1 in tumours predicted for poor response to tamoxifen, independently of tumour size, grade or nodal status. However, when the 99 tamoxifen and chemotherapy treated patients were included in the analysis, high levels of pRaf(ser338) continued to predict for tamoxifen relapse, but not independently of the known prognostic markers. In the entire cohort, it was MAPK expression that was independently associated with quicker relapse whilst receiving tamoxifen. In the tamoxifen only treated patients, both pRaf(ser338) and

MAPK seemed to regulate early events involved in the development of tamoxifen resistance, whereas in those patients who received both tamoxifen and chemotherapy, the negative effects of pRaf(ser338) seemed to be delayed. This suggests that the additional treatment of chemotherapy, for patients expressing high levels of pRaf(ser338), improved their outcome and delayed the development of tamoxifen resistance. However, the number of patients receiving both treatments in the STB study was relatively small. It was; therefore, appropriate to combine patients from the STB and NEAT cohorts who received both tamoxifen and chemotherapy. In this sub-group of patients neither pRaf(ser338) nor MAPK expression levels were associated with patient outcome. One possible explanation for this is that the addition of chemotherapy reduces the proliferative effects of Raf-1/MAPK. Chemotherapy compensates for the shortened response time to tamoxifen in those patients who express high tumour levels of these proteins, to such an extent that they have a similar prognosis to those who expressed lower levels. However, the results from these analyses should be viewed with some caution, as it was two different groups of patients that were combined for analysis. Ideally, the role of Raf-1 and MAPK should be further investigated in a larger cohort of patients to compare the clinical effects of tamoxifen and chemotherapy, both singly and in combination, to determine if either of these proteins are potential predictive markers for patients who should receive tamoxifen in combination with chemotherapy. Recently the International Clinical Breast Cancer Study Group Trial 13-93, which compared the disease-free survival of lymph node positive, premenopausal women who received adjuvant chemotherapy, followed by either tamoxifen or no further treatment, demonstrated that tamoxifen after adjuvant chemotherapy significantly improved treatment outcome (293).

A recent *in vitro* study has also reported that tamoxifen can modulate the cytotoxicity of anthracyclines, such as epirubicin in breast cancer cell lines (294). The effectiveness of chemotherapeutic agents is often limited by multi-drug resistance (MDR) (295). The mechanisms controlling MDR are not completely understood, although overexpression of P-glycoprotein (P-gp) on the cell membrane is often associated with its development (296). P-gp is an ATP-dependent membrane transporter that functions as an efflux pump for chemotherapeutic agents. P-gp is expressed in 40-50% of breast cancers, with larger tumours more likely to express this protein (297). Following chemotherapy, there is an increase in the percentage of tumours expressing P-gp, from 40-50% to 60-70% (297). Consequently, much research has focused on identifying agents that will down-regulate P-gp mediated chemotherapy resistance. Several studies have recognised that tamoxifen has the potential to modify the effectiveness of therapies, such as epirubicin (294;296). Pretreatment of MCF-7 and NCl-adr breast cancer cells with tamoxifen enhanced the cytoxicity of epirubicin in these cells by 4.3 and 6.5 folds respectively (294). All these findings suggest that the combined treatment of tamoxifen and chemotherapy is an important therapy option, but given the aggressive nature of chemotherapy, only those patients likely to benefit from the additional treatment should be targeted. Further investigation is required to determine if pRaf(ser338) or MAPK might represent possible predictive markers to identify those patients requiring additional treatments to tamoxifen.

Tamoxifen functions by down-regulating ERα activity and transcription of E2-regulated genes, whilst chemotherapy uses cytotoxic drugs to kill proliferating cancer cells, preventing them from multiplying, invading and metastasing. The Ras/Raf-

I/MAPK pathway phosphorylates and activates multiple substrates, such as the pro-proliferative, c-fos (196), and the anti-apoptotic, p90RSK (197); one other key substrate is ERα (39;197;201). The unexpected finding that the Ras/Raf-1/MAPK proteins, in particular Raf-1, are potential predictive markers for survival and response to Tamoxifen, but not chemotherapy, suggests that it is the interaction between this pathway and ERα, and not its ability to regulate cell proliferation, that is fundamental in influencing patient outcome.

ERα contains two activation domains, AF1 and AF2, which regulate transcription. AF2 contains the Ligand Binding Domain (LBD), and its activity requires the binding of E2. AF1 is activated by phosphorylation of several sites, including Serine 118 and Serine 167, which are phosphorylated, following the binding of E2 to AF2. E2 causes a conformational change in ERα, resulting in dimerisation and binding to oestrogen response elements in promoter regions of E2 regulated genes (29;39;40). Co-activators and co-repressors modulate the activity of the ER (67;298-300). However, ERα can also be phosphorylated in a ligand-independent manner (29;39;95;96). This results in activation of the receptor and subsequent transcription of E2-regulated genes and cell proliferation. The ligand-independent phosphorylation of ERα at serine 118 is believed to be a major contributor to the development of tamoxifen resistance.

The discovery that pRaf(ser338) and MAPK expression both correlated with loss of sensitivity to tamoxifen prompted further investigation of the interactions between this pathway and ERα. The relationship between the Ras/Raf-1/MAPK pathway and ERα has been well documented; MAPK directly and indirectly phosphorylates ERα in a ligand-independent manner at serines 118 and 167, which enhances interactions with

coactivators rather than co-repressors, and subsequently increases transcriptional activity of the receptor (39;197;201). It is thought that this plays a key role in the development of tamoxifen resistance, by promoting the agonistic activities of Tamoxifen and tumour growth (69;301). Tamoxifen-resistant cells show increased levels of activated MAPK, phosphorylated ERα and transcription of oestrogen-regulated genes. Tamoxifen promotes, rather than inhibits, growth of these cells (50;222). However, our understanding of the mechanistic nature of the MAPK and ERα interactions is limited. It is accepted that MAPK phosphorylates ERα at serine 118, but what is the subcellular location for this interaction, and does this ligand-independent phosphorylation of ERα induce the same effects as E2 mediated activation?

In vitro studies were designed to probe the ligand-dependent and ligand-independent phosphorylation of ERα, and to investigate the subcellular localisation of the activated receptor. There were several key findings from these studies. The first confirmed previous research that E2 stimulated phosphorylation of ERα at serine 118 and its nuclear translocation, independently of MAPK. CDK7 has previously been identified as the kinase mediating E2 phosphorylation of serine 118 (44). However, MAPK was necessary for the ligand-independent phosphorylation of the receptor. Previous studies have shown that MAPK induced nuclear expression of ERα (277;282); however, they failed to demonstrate that nuclear translocation of pMAPK was required to generate expression of nuclear pER(ser118). Throughout the studies presented here, the nucleus has been identified as a key subcellular location for the Ras pathway. Ras was unexpectedly localised to the nuclei of tumour cells, and was shown to be associated with poor outcome in the pilot study. Nuclear but not cytoplasmic pRaf(ser338) was identified

as a possible predictive marker for tamoxifen relapse, and finally expression of nuclear pMAPK was necessary for expression of nuclear pER(ser118). It is unknown whether the nucleus represents an alternative site for activation of the Ras pathway; however, it would appear that expression of these nuclear proteins is important in cancer development, progression and response to treatment. Further work is obviously required to understand the mechanisms controlling nuclear expression or activation of the Ras cascade.

In undertaking these *in vitro* studies we hoped to increase our understanding of the relationship between the ligand-dependent and independent activation of ERα, as knowledge of this is limited. We had hypothesised that treatment of MCF-7 cells with both HRG and E2 would have an additive effect on the phosphorylation and activation of ER, since they both operate via different mechanisms. However, this proved not to be the case. Surprisingly, co-stimulation with both E2 and HRG suggested that the effects of HRG mediated signalling were dominant over those of E2. These studies produced the novel finding that HRG, as opposed to E2, determined the subcellular localisation of ER in breast cancer cells. Despite the presence of E2, which translocated ER to the nucleus in the absence of HRG, in MCF-7 cells treated with both drugs, there was a substantial reduction in the levels of nuclear pER(ser118). These new and intriguing findings suggest that the ligand-independent phosphorylation of ERα modifies its subcellular localisation, even in the presence of E2, the principal ligand of the receptor. However, as discussed in chapter 8, this is via an unknown mechanism and further *in vitro* work is necessary to determine this.

That the ligand-independent activation of ERα can alter it subcellular location may have important implications for the responsiveness of tumours to endocrine

therapies, such as tamoxifen. Tamoxifen binds to ERα and down-regulates its activity in the nuclei of tumour cells. Previous clinical studies have demonstrated that expression of pER(ser118) and pER(ser167) in the nuclei of breast tumour cells is associated with an improved outcome in patients treated with tamoxifen (226;302;303). It was speculated that phosphorylation of the receptor was indicative of an intact ligand-dependent ERα signalling pathway, and that expression of the phosphorylated receptor in the nuclei of tumour cells represented a predictive marker for response to tamoxifen. Consequently, if ligand-independent activation of ERα can override the ligand-dependent effects and prevent nuclear expression of phosphorylated ERα, this may explain the loss of sensitivity to tamoxifen and poorer outcome associated with activation of the Ras pathway. It has previously been demonstrated that overexpression of HER2 and increased activation of MAPK resulted in the translocation of ERα from the nucleus to the cytoplasm(286). Furthermore, it has been suggested that HER2 mediated tamoxifen resistance is a consequence of its interaction with membranous ER (107).

For a long time, the Ras/Raf-1/MAPK pathway has been considered an attractive target for anticancer therapies. The research presented here, further highlights the importance of these proteins as possible therapeutic targets. Increased expression of these proteins in tumours was associated with the development of tamoxifen resistance and identified those patients who required additional therapies, such as chemotherapy or AIs. As the effectiveness of AIs in treating breast cancer patients, continues to be highlighted, the need to identify patients most suitable for this treatment grows. The results from the STB suggest that pRaf(ser338) might be a potential marker for patients more likely to benefit from AIs, as opposed to Tamoxifen, or a combined treatment of the two.

However, this would need to be investigated further, perhaps in the IES, TEAM or ATAC trial.

N-Ras, pRaf(ser338) and MAPK were all associated with relapse on tamoxifen suggesting that therapies targeted against these proteins might be beneficial in combination with tamoxifen. Combined treatment of Ras/Raf-1/MAPK inhibitors with tamoxifen might potentially delay or reverse tamoxifen resistance. Research has shown that the use of FTIs targeted against Ras, in combination with Tamoxifen, increases the antitumour effect of both drugs (234). Several clinical trials are currently investigating the effects of FTIs in combination with tamoxifen, to determine if the presence of FTIs can delay the development of tamoxifen resistance (304). A recent study of Farnesylthiosalicylic acid (FTS), which inhibits Ras binding to its membrane acceptor sites, revealed that FTS induced apoptosis and inhibited proliferation in wild-type and E2 deprived MCF-7 cells. It is speculated that FTS may be useful in the treatment of patients, in combination with tamoxifen or AIs (305). Since FTIs and FTS impact Ras activation, this would ultimately influence the levels of activated Raf-1 and MAPK. This would be crucial, since in our study it was pRaf(ser338) that was identified as the key target. The importance of Raf-1 in regulating tumour growth was further highlighted by an *in vitro* study that reported that the RTK inhibitor AG 879 inhibits proliferation of breast cancer cells by down-regulating expression of the Raf-1 gene (306). Other treatment options are Raf-1 inhibitors, such as Sorafenib (BAY 43-9006), and MEK inhibitors, such as PD0325901 (242). Clinical trials are currently underway investigating the effectiveness of these treatments in combination with endocrine therapies. Despite our findings that expression levels of neither Raf-1 nor MAPK in patients tumours

significantly altered response to chemotherapy, it is also thought that therapies directed against these proteins, such as MEK inhibitors, would increase the cytotoxicity of chemotherapy agents (242).

The Ras/Raf-1/MAPK pathway controls multiple cellular processes, such as proliferation, differentiation, apoptosis, senescence, migration and invasion, all of which are fundamental in tumour growth. The research presented in this thesis demonstrates that the Ras cascade plays an important role in regulating breast tumourigenesis, in mediating response to Tamoxifen, and in modifying the phosphorylation and activation status of ERα. The activated form of Raf-1 has been identified as a possible predictive marker of tamoxifen response. Furthermore, these studies have highlighted a possible mechanism by which activation of this pathway contributes to the development of tamoxifen resistance. It appeared that that the ligand-independent phosphorylation and activation of ERα was dominant over the ligand-dependent effects, and that it was able to modify the subcellular localisation of the receptor.

It is becoming clear that multiple signal transduction mechanisms are involved in the development of resistance to current breast cancer therapeutic options. The current study highlights, using both *in vivo* and *in vitro* approaches, that the MAPK cascade is associated with development of tamoxifen resistance in a sub cohort of patients. However, reports from the literature also highlight that other cascades, such as PI3K/AKT, which is known to interact with the MAPK pathway, also have a role in the development of resistance. As the number of women diagnosed with breast cancer continues to rise, so too does the need for improved treatment options for these patients. To achieve this, we need to further our understanding of the mechanisms that drive

treatment failure and identify markers that are predictive for response to these treatments. This will ultimately enable clinicians to treat and predict individual patients outcome more effectively.

Reference List

(1) Cancer Research. 2006.
Ref Type: Internet Communication

(2) Breast Cancer Campaign. 2006.
Ref Type: Internet Communication

(3) Kahn P. Coming to grips with genes and risk. Science 1996; 274(5287):496-498.

(4) Nature Special Focus Website. 2006.
Ref Type: Internet Communication

(5) Russo J, Russo IH. Development of the human breast. Maturitas 2004; 49(1):2-15.

(6) Kelly PA, Bachelot A, Kedzia C, Hennighausen L, Ormandy CJ, Kopchick JJ et al. The role of prolactin and growth hormone in mammary gland development. Mol Cell Endocrinol 2002; 197(1-2):127-131.

(7) Sunil R.Lakharu et al. Basic Pathology – An intro to mechanisms of disease . 2006.

(8) Pinder SE, Ellis IO, Elston CW. Prognostic factors in primary breast carcinoma. Journal of Clinical Pathology 1995; 48(11):981-983.

(9) Haybittle J.L., Blamey R.W., Elston C.W., Johnson J., Doyle P.J., Campbell F.C. et al. A Prognostic Index In Primary Breast Cancer. Br J Cancer 1982; 45:361-366.

(10) Early Breast Cancer Trialists' Collaborative Group. Radiotherapy for early breast cancer. The Cochrane Database of Systematic Reviews 2002;(2).

(11) Systemic treatment of early breast cancer by hormonal, cytotoxic, or immune therapy. 133 randomised trials involving 31,000 recurrences and 24,000 deaths among 75,000 women. Early Breast Cancer Trialists' Collaborative Group. Lancet 1992; 339(8785):71-85.

(12) Early Breast Cancer Trialists' Collaborative Group. Multi-agent chemotherapy for early breast cancer. Cochrane Database of Systematic Reviews 2006; 2001(4).

(13) Skeel R.T. Handbook of Cancer Chemotherapy. 6th ed. Lippincott, Williams & Wilkins, 2006.

(14) Lebwohl DE, Canetta R. New developments in chemotherapy of advanced breast cancer. Ann Oncol 1999; 10 Suppl 6:139-146.

(15) Smith G, Henderson IC. New treatments for breast cancer. Semin Oncol 1996; 23(4):506-528.

(16) Ghersi D, Wilcken N, Simes J, Donoghue E. Taxane containing regimens for metastatic breast cancer. Cochrane Database Syst Rev 2005;(2):CD003366.

(17) Harvey JM, Clark GM, Osborne CK, Allred DC. Estrogen receptor status by immunohistochemistry is superior to the ligand-binding assay for predicting response to adjuvant endocrine therapy in breast cancer. J Clin Oncol 1999; 17(5):1474-1481.

(18) Kong EH, Pike ACW, Hubbard RE. Structure and mechanism of the oestrogen receptor. Biochemical Society Transactions 2003; 31:56-59.

(19) Beatson GT. On the treatment of inoperable cases of carcinoma of the mamma; suggestions for a new method of treatment, with illustrative cases. Lancet 1896; ii:104-107.

(20) Jensen EV, Jacobson HI. Basic guides to the mechanism of estrogen action. Recent Prog Horm Res 1962; 18:387-414.

(21) Green S, Walter P, Kumar V, Krust A, Bornert JM, Argos P et al. Human oestrogen receptor cDNA: sequence, expression and homology to v-erb-A. Nature 1986; 320(6058):134-139.

(22) Greene GL, Gilna P, Waterfield M, Baker A, Hort Y, Shine J. Sequence and expression of human estrogen receptor complementary DNA. Science 1986; 231(4742):1150-1154.

(23) Kuiper GG, Enmark E, Pelto-Huikko M, Nilsson S, Gustafsson JA. Cloning of a novel receptor expressed in rat prostate and ovary. Proc Natl Acad Sci U S A 1996; 93(12):5925-5930.

(24) Gosden JR, Middleton PG, Rout D. Localization of the human oestrogen receptor gene to chromosome 6q24----q27 by in situ hybridization. Cytogenet Cell Genet 1986; 43(3-4):218-220.

(25) Enmark E, Pelto-Huikko M, Grandien K, Lagercrantz S, Lagercrantz J, Fried G et al. Human estrogen receptor beta-gene structure, chromosomal localization, and expression pattern. J Clin Endocrinol Metab 1997; 82(12):4258-4265.

(26) Clarke RB, Howell A, Potten CS, Anderson E. Dissociation between steroid receptor expression and cell proliferation in the human breast. Cancer Res 1997; 57(22):4987-4991.

(27) Schmitt FC. Multistep progression from an oestrogen-dependent growth towards an autonomous growth in breast carcinogenesis. Eur J Cancer 1995; 31A(12):2049-2052.

(28) Chung YL, Sheu ML, Yang SC, Lin CH, Yen SH. Resistance to tamoxifen-induced apoptosis is associated with direct interaction between Her2/neu and cell membrane estrogen receptor in breast cancer. Int J Cancer 2002; 97(3):306-312.

(29) Chen D, Washbrook E, Sarwar N, Bates GJ, Pace PE, Thirunuvakkarasu V et al. Phosphorylation of human estrogen receptor α at serine 118 by two distinct signal transduction pathways revealed by phosphorylation specific antisera. Oncogene 2002; 21:4921-4931.

(30) Johnston SRD, Head J, Pancholi S, Detre S, Martin LA, Smith IE et al. Integration of Signal Transduction Inhibitors with Endocrine Therapy: An Approach to Overcoming Hormone Resistance in Breast Cancer. Clin Cancer Res 2003; 9(1):524S-5532.

(31) Enmark E, Gustafsson JA. Oestrogen receptors - an overview. J Intern Med 1999; 246(2):133-138.

(32) Aumais JP, Lee HS, Lin R, White JH. Selective interaction of hsp90 with an estrogen receptor ligand-binding domain containing a point mutation. J Biol Chem 1997; 272(18):12229-12235.

(33) Sommer S, Fuqua SA. Estrogen receptor and breast cancer. Semin Cancer Biol 2001; 11(5):339-352.

(34) Nilsson S, Makela S, Treuter E, Tujague M, Thomsen J, Andersson G et al. Mechanisms of estrogen action. Physiol Rev 2001; 81(4):1535-1565.

(35) Klinge CM. Estrogen receptor interaction with co-activators and co-repressors. Steroids 2000; 65(5):227-251.

(36) Freedman LP. Increasing the complexity of coactivation in nuclear receptor signaling. Cell 1999; 97(1):5-8.

(37) Dobrzycka KM, Townson SM, Jiang S, Oesterreich S. Estrogen receptor corepressors - a role in human breast cancer? Endocr Relat Cancer 2003; 10(4):517-536.

(38) Hall JM, Couse JF, Korach KS. The multifaceted mechanisms of estradiol and estrogen receptor signaling. J Biol Chem 2001; 276(40):36869-36872.

(39) Kato S, Endoh H, Masuhiro Y, Kitamoto T, Uchiyama S, Sasaki H et al. Activation of the estrogen receptor through phosphorylation by mitogen-activated protein kinase. Science 1995; 270(5241):1491-1494.

(40) Ali S, Coombes RC. Endocrine-responsive breast cancer and strategies for combating resistance. Nat Rev Cancer 2002; 2(2):101-112.

(41) Schiff R, Osborne CK. Endocrinology and hormone therapy in breast cancer: new insight into estrogen receptor-alpha function and its implication for endocrine therapy resistance in breast cancer. Breast Cancer Res 2005; 7(5):205-211.

(42) Carroll JS, Liu XS, Brodsky AS, Li W, Meyer CA, Szary AJ et al. Chromosome-wide mapping of estrogen receptor binding reveals long-range regulation requiring the forkhead protein FoxA1. Cell 2005; 122(1):33-43.

(43) Lin CY, Strom A, Vega VB, Kong SL, Yeo AL, Thomsen JS et al. Discovery of estrogen receptor alpha target genes and response elements in breast tumor cells. Genome Biol 2004; 5(9):R66.

(44) Kato S, Masuhiro Y, Watanabe M, Kobayashi Y, Takeyama K, Endoh H et al. Molecular mechanism of a cross-talk between oestrogen and growth factor signalling pathways. Genes To Cells 2000; 5(8):593-601.

(45) Rogatsky I, Trowbridge JM, Garabedian MJ. Potentiation of human estrogen receptor alpha transcriptional activation through phosphorylation of serines 104 and 106 by the cyclin A-CDK2 complex. J Biol Chem 1999; 274(32):22296-22302.

(46) Chen D, Pace PE, Coombes RC, Ali S. Phosphorylation of human estrogen receptor alpha by protein kinase A regulates dimerization. Mol Cell Biol 1999; 19(2):1002-1015.

(47) Weis KE, Ekena K, Thomas JA, Lazennec G, Katzenellenbogen BS. Constitutively active human estrogen receptors containing amino acid substitutions for tyrosine 537 in the receptor protein. Mol Endocrinol 1996; 10(11):1388-1398.

(48) Losel RM, Falkenstein E, Feuring M, Schultz A, Tillmann HC, Rossol-Haseroth K et al. Nongenomic steroid action: controversies, questions, and answers. Physiol Rev 2003; 83(3):965-1016.

(49) Zivadinovic D, Watson CS. Membrane estrogen receptor-alpha levels predict estrogen-induced ERK1/2 activation in MCF-7 cells. Breast Cancer Res 2005; 7(1):R130-R144.

(50) Britton DJ, Hutcheson IR, Knowlden JM, Barrow D, Giles M, McClelland RA et al. Bidirectional cross talk between ERalpha and EGFR signalling pathways regulates tamoxifen-resistant growth. Breast Cancer Res Treat 2006; 96(2):131-146.

(51) Levin ER. Bidirectional signaling between the estrogen receptor and the epidermal growth factor receptor. Mol Endocrinol 2003; 17(3):309-317.

(52) Razandi M, Pedram A, Park ST, Levin ER. Proximal Events in Signaling by Plasma Membrane Estrogen Receptors. J Biol Chem 2003; 278(4):2701.

(53) Pace P, Taylor J, Suntharalingam S, Coombes RC, Ali S. Human estrogen receptor beta binds DNA in a manner similar to and dimerizes with estrogen receptor alpha. J Biol Chem 1997; 272(41):25832-25838.

(54) Paech K, Webb P, Kuiper GG, Nilsson S, Gustafsson J, Kushner PJ et al. Differential ligand activation of estrogen receptors ERalpha and ERbeta at AP1 sites. Science 1997; 277(5331):1508-1510.

(55) Couse JF, Korach KS. Estrogen receptor null mice: what have we learned and where will they lead us? Endocr Rev 1999; 20(3):358-417.

(56) Krege JH, Hodgin JB, Couse JF, Enmark E, Warner M, Mahler JF et al. Generation and reproductive phenotypes of mice lacking estrogen receptor beta. Proc Natl Acad Sci U S A 1998; 95(26):15677-15682.

(57) Dotzlaw H, Leygue E, Watson PH, Murphy LC. Expression of estrogen receptor-beta in human breast tumors. J Clin Endocrinol Metab 1997; 82(7):2371-2374.

(58) Fuqua SA, Schiff R, Parra I, Moore JT, Mohsin SK, Osborne CK et al. Estrogen receptor beta protein in human breast cancer: correlation with clinical tumor parameters. Cancer Res 2003; 63(10):2434-2439.

(59) Speirs V, Parkes AT, Kerin MJ, Walton DS, Carleton PJ, Fox JN et al. Coexpression of estrogen receptor alpha and beta: poor prognostic factors in human breast cancer? Cancer Res 1999; 59(3):525-528.

(60) Hou YF, Yuan ST, Li HC, Wu J, Lu JS, Liu G et al. ERbeta exerts multiple stimulative effects on human breast carcinoma cells. Oncogene 2004; 23(34):5799-5806.

(61) Omoto Y, Inoue S, Ogawa S, Toyama T, Yamashita H, Muramatsu M et al. Clinical value of the wild-type estrogen receptor beta expression in breast cancer. Cancer Lett 2001; 163(2):207-212.

(62) Iwao K, Miyoshi Y, Egawa C, Ikeda N, Noguchi S. Quantitative analysis of estrogen receptor-beta mRNA and its variants in human breast cancers. Int J Cancer 2000; 88(5):733-736.

(63) Jarvinen TA, Pelto-Huikko M, Holli K, Isola J. Estrogen receptor beta is coexpressed with ERalpha and PR and associated with nodal status, grade, and proliferation rate in breast cancer. Am J Pathol 2000; 156(1):29-35.

(64) Klijn JG, Blamey RW, Boccardo F, Tominaga T, Duchateau L, Sylvester R. Combined tamoxifen and luteinizing hormone-releasing hormone (LHRH) agonist versus LHRH agonist alone in premenopausal advanced breast cancer: a meta-analysis of four randomized trials. J Clin Oncol 2001; 19(2):343-353.

(65) Shiau AK, Barstad D, Loria PM, Cheng L, Kushner PJ, Agard DA et al. The structural basis of estrogen receptor/coactivator recognition and the antagonism of this interaction by tamoxifen. Cell 1998; 95(7):927-937.

(66) Cuzick J, Powles T, Veronesi U, Forbes J, Edwards R, Ashley S et al. Overview of the main outcomes in breast-cancer prevention trials. Lancet 2003; 361(9354):296-300.

(67) Schiff R, Massarweh S, Shou J, Osborne CK. Breast cancer endocrine resistance: how growth factor signaling and estrogen receptor coregulators modulate response. Clin Cancer Res 2003; 9(1 Pt 2):447S-454S.

(68) Chung Y, Sheu M, Yang S, Lin C, Yen S. Resistance to tamoxifen-induced apoptosis is associated with direct interaction between Her2/neu and cell membrane estrogen receptor in breast cancer. International Journal of Cancer 2002; 97:306-312.

(69) Kurokawa H, Lenferink AE, Simpson JF, Pisacane PI, Sliwkowski MX, Forbes JT et al. Inhibition of HER2/neu (erbB-2) and mitogen-activated protein kinases enhances tamoxifen action against HER2-overexpressing, tamoxifen-resistant breast cancer cells. Cancer Res 2000; 60(20):5887-5894.

(70) Fawell SE, White R, Hoare S, Sydenham M, Page M, Parker MG. Inhibition of estrogen receptor-DNA binding by the "pure" antiestrogen ICI 164,384 appears to be mediated by impaired receptor dimerization. Proc Natl Acad Sci U S A 1990; 87(17):6883-6887.

(71) Robertson JF. Faslodex (ICI 182, 780), a novel estrogen receptor downregulator--future possibilities in breast cancer. J Steroid Biochem Mol Biol 2001; 79(1-5):209-212.

(72) Brodie AM, Njar VC. Aromatase inhibitors and breast cancer. Semin Oncol 1996; 23(4 Suppl 9):10-20.

(73) Morandi P, Rouzier R, Altundag K, Buzdar AU, Theriault RL, Hortobagyi G. The role of aromatase inhibitors in the adjuvant treatment of breast carcinoma: the M. D. Anderson Cancer Center evidence-based approach. Cancer 2004; 101(7):1482-1489.

(74) Smith IE, Dowsett M. Aromatase inhibitors in breast cancer. N Engl J Med 2003; 348(24):2431-2442.

(75) Eiermann W, Paepke S, Appfelstaedt J, Llombart-Cussac A, Eremin J, Vinholes J et al. Preoperative treatment of postmenopausal breast cancer patients with letrozole: A randomized double-blind multicenter study. Ann Oncol 2001; 12(11):1527-1532.

(76) Ellis MJ, Coop A, Singh B, Tao Y, Llombart-Cussac A, Janicke F et al. Letrozole inhibits tumor proliferation more effectively than tamoxifen independent of HER1/2 expression status. Cancer Res 2003; 63(19):6523-6531.

(77) Baum M, Budzar AU, Cuzick J, Forbes J, Houghton JH, Klijn JG et al. Anastrozole alone or in combination with tamoxifen versus tamoxifen alone for adjuvant treatment of postmenopausal women with early breast cancer: first results of the ATAC randomised trial. Lancet 2002; 359(9324):2131-2139.

(78) Bonneterre J, Buzdar A, Nabholtz JM, Robertson JF, Thurlimann B, von Euler M et al. Anastrozole is superior to tamoxifen as first-line therapy in hormone receptor positive advanced breast carcinoma. Cancer 2001; 92(9):2247-2258.

(79) Elisaf MS, Bairaktari ET, Nicolaides C, Kakaidi B, Tzallas CS, Katsaraki A et al. Effect of letrozole on the lipid profile in postmenopausal women with breast cancer. Eur J Cancer 2001; 37(12):1510-1513.

(80) McEwen BS, Alves SE, Bulloch K, Weiland NG. Ovarian steroids and the brain: implications for cognition and aging. Neurology 1997; 48(5 Suppl 7):S8-15.

(81) Ellis MJ, Coop A, Singh B, Mauriac L, Llombert-Cussac A, Janicke F et al. Letrozole is more effective neoadjuvant endocrine therapy than tamoxifen for ErbB-1- and/or ErbB-2-positive, estrogen receptor-positive primary breast cancer: evidence from a phase III randomized trial. J Clin Oncol 2001; 19(18):3808-3816.

(82) Hopp TA, Fuqua SA. Estrogen receptor variants. J Mammary Gland Biol Neoplasia 1998; 3(1):73-83.

(83) Roodi N, Bailey LR, Kao WY, Verrier CS, Yee CJ, Dupont WD et al. Estrogen receptor gene analysis in estrogen receptor-positive and receptor-negative primary breast cancer. J Natl Cancer Inst 1995; 87(6):446-451.

(84) Speirs V, Malone C, Walton DS, Kerin MJ, Atkin SL. Increased expression of estrogen receptor beta mRNA in tamoxifen-resistant breast cancer patients. Cancer Res 1999; 59(21):5421-5424.

(85) O'Neill PA, Davies MP, Shaaban AM, Innes H, Torevell A, Sibson DR et al. Wild-type oestrogen receptor beta (ERbeta1) mRNA and protein expression in Tamoxifen-treated post-menopausal breast cancers. Br J Cancer 2004; 91(9):1694-1702.

(86) McInerney EM, Weis KE, Sun J, Mosselman S, Katzenellenbogen BS. Transcription activation by the human estrogen receptor subtype beta (ER beta) studied with ER beta and ER alpha receptor chimeras. Endocrinology 1998; 139(11):4513-4522.

(87) Montano MM, Muller V, Trobaugh A, Katzenellenbogen BS. The carboxy-terminal F domain of the human estrogen receptor: role in the transcriptional activity of the receptor and the effectiveness of antiestrogens as estrogen antagonists. Mol Endocrinol 1995; 9(7):814-825.

(88) Mann S, Laucirica R, Carlson N, Younes PS, Ali N, Younes A et al. Estrogen receptor beta expression in invasive breast cancer. Hum Pathol 2001; 32(1):113-118.

(89) Nicholson RI, Hutcheson IR, Britton D, Knowlden JM, Jones HE, Harper ME et al. Growth factor signalling networks in breast cancer and resistance to endocrine agents: new therapeutic strategies. J Steroid Biochem Mol Biol 2005; 93(2-5):257-262.

(90) Anzick SL, Kononen J, Walker RL, Azorsa DO, Tanner MM, Guan XY et al. AIB1, a steroid receptor coactivator amplified in breast and ovarian cancer. Science 1997; 277(5328):965-968.

(91) Smith CL, Nawaz Z, O'Malley BW. Coactivator and corepressor regulation of the agonist/antagonist activity of the mixed antiestrogen, 4-hydroxytamoxifen. Mol Endocrinol 1997; 11(6):657-666.

(92) Takimoto GS, Graham JD, Jackson TA, Tung L, Powell RL, Horwitz LD et al. Tamoxifen resistant breast cancer: coregulators determine the direction of transcription by antagonist-occupied steroid receptors. J Steroid Biochem Mol Biol 1999; 69(1-6):45-50.

(93) Shou J, Massarweh S, Osborne CK, Wakeling AE, Ali S, Weiss H et al. Mechanisms of tamoxifen resistance: increased estrogen receptor-HER2/neu cross-talk in ER/HER2-positive breast cancer. J Natl Cancer Inst 2004; 96(12):926-935.

(94) Bouras T, Southey MC, Venter DJ. Overexpression of the steroid receptor coactivator AIB1 in breast cancer correlates with the absence of estrogen and progesterone receptors and positivity for p53 and HER2/neu. Cancer Res 2001; 61(3):903-907.

(95) Driggers PH, Segars JH. Estrogen action and cytoplasmic signaling pathways. Part II: the role of growth factors and phosphorylation in estrogen signaling. Trends In Endocrinology And Metabolism 2002; 13(10):422-428.

(96) Lannigan DA. Estrogen receptor phosphorylation. Steroids 2003; 68(1):1-9.

(97) Osborne CK, Schiff R. Growth factor receptor cross-talk with estrogen receptor as a mechanism for tamoxifen resistance in breast cancer. Breast 2003; 12(6):362-367.

(98) Kraus MH, Issing W, Miki T, Popescu NC, Aaronson SA. Isolation and characterization of ERBB3, a third member of the ERBB/epidermal growth factor receptor family: evidence for overexpression in a subset of human mammary tumors. Proc Natl Acad Sci U S A 1989; 86(23):9193-9197.

(99) Reese DM, Slamon DJ. HER-2/neu signal transduction in human breast and ovarian cancer. Stem Cells 1997; 15(1):1-8.

(100) Yarden Y, Sliwkowski MX. Untangling the ErbB Signalling Network. Nature Reviews:- Molecular Cell Biology 2001; 2:127-137.

(101) Vojtek AB, Der CJ. Increasing complexity of the Ras signaling pathway. J Biol Chem 1998; 273(32):19925-19928.

(102) de Bono JS, Rowinsky EK. The ErbB receptor family: a therapeutic target for cancer. Trends in Molecular Medicine 2002; 8(4):19-26.

(103) Tovey S, Dunne B, Witton CJ, Forsyth A, Cooke TG, Bartlett JM. Can molecular markers predict when to implement treatment with aromatase inhibitors in invasive breast cancer? Clin Cancer Res 2005; 11(13):4835-4842.

(104) Tovey SM, Witton CJ, Bartlett JM, Stanton PD, Reeves JR, Cooke TG. Outcome and human epidermal growth factor receptor (HER) 1-4 status in invasive breast carcinomas with proliferation indices evaluated by bromodeoxyuridine labelling. Breast Cancer Res 2004; 6(3):R246-R251.

(105) Witton CJ, Reeves JR, Going JJ, Cooke TG, Bartlett JM. Expression of the HER1-4 family of receptor tyrosine kinases in breast cancer. J Pathol 2003; 200(3):290-297.

(106) Normanno N, Campiglio M, De Luca A, Somenzi G, Maiello M, Ciardiello F et al. Cooperative effect of ZD1839(Iressa) in combination with trastuzumab (Herceptin) on human breast cancer cell growth. Annals of Oncology 2002; 13:65-72.

(107) Chung YL, Sheu ML, Yang SC, Lin CH, Yen SH. Resistance to tamoxifen-induced apoptosis is associated with direct interaction between Her2/neu and cell membrane estrogen receptor in breast cancer. Int J Cancer 2002; 97(3):306-312.

(108) Adjei AA. Blocking Oncogenic Ras Signaling for Cancer Therapy. Journal of the National Cancer Institute 2001; 93(14):1062-1074.

(109) Macaluso M, Russo G, Cinti C, Bazan V, Gebbia N, Russo A. Ras family genes: an interesting link between cell cycle and cancer. J Cell Physiol 2002; 192(2):125-130.

(110) Pruitt K, Der CJ. Ras and Rho regulation of the cell cycle and oncogenesis. Cancer Lett 2001; 171(1):1-10.

(111) Barbacid M. ras genes. Annu Rev Biochem 1987; 56:779-827.

(112) Burgering BM, Bos JL. Regulation of Ras-mediated signalling: more than one way to skin a cat. Trends Biochem Sci 1995; 20(1):18-22.

(113) Roskoski R, Jr. Protein prenylation: a pivotal posttranslational process. Biochem Biophys Res Commun 2003; 303(1):1-7.

(114) Dhillon AS, Kolch W. Untying the regulation of the Raf-1 kinase. Archives of Biochemistry and Biophysics 2002; 404:3-9.

(115) Dhillon AS, Meikle S, Yazici Z, Eulitz M, Kolch W. Regulation of Raf-1 activation and signalling by dephosphorylation. EMBO J 2002; 21(1&2):64-71.

(116) Santen RJ, Song RX, McPherson R, Kumar R, Adam L, Jeng MH et al. The role of mitogen-activated protein (MAP) kinase in breast cancer. Journal Of Steroid Biochemistry And Molecular Biology 2002; 80(2):239-256.

(117) Silvius JR. Mechanisms of Ras Protein Targeting in Mammalian Cells. The Journal of Membrane Biology 2002; 190:83-92.

(118) Bos JL. ras oncogenes in human cancer: a review. Cancer Res 1989; 49(17):4682-4689.

(119) Crespo P, Leon J. Ras proteins in the control of the cell cycle and cell differentiation. Cell Mol Life Sci 2000; 57(11):1613-1636.

(120) Lowy DR, Willumsen BM. Function and regulation of ras. Annu Rev Biochem 1993; 62:851-891.

(121) Willumsen BM, Christensen A, Hubbert NL, Papageorge AG, Lowy DR. The p21 *ras* C-terminus is required for transformation and membrane association. Nature 1984; 310(5978):583-586.

(122) Wittinghofer A, Pai EF. The structure of Ras protein: a model for a universal molecular switch. Trends Biochem Sci 1991; 16(10):382-387.

(123) Ma J, Karplus M. Molecular switch in signal transduction: reaction paths of the conformational changes in ras p21. Proc Natl Acad Sci U S A 1997; 94(22):11905-11910.

(124) Polakis P, McCormick F. Structural requirements for the interaction of p21ras with GAP, exchange factors, and its biological effector target. J Biol Chem 1993; 268(13):9157-9160.

(125) Choy E, Chiu VK, Silletti J, Feoktistov M, Morimoto T, Michaelson D et al. Endomembrane trafficking of ras: the CAAX motif targets proteins to the ER and Golgi. Cell 1999; 98(1):69-80.

(126) Magee T, Marshall C. New insights into the interaction of Ras with the plasma membrane. Cell 1999; 98(1):9-12.

(127) Apolloni A, Prior IA, Lindsay M, Parton RG, Hancock JF. H-ras but not K-ras traffics to the plasma membrane through the exocytic pathway. Mol Cell Biol 2000; 20(7):2475-2487.

(128) Prior IA, Hancock JF. Compartmentalization of Ras proteins. J Cell Sci 2001; 114(Pt 9):1603-1608.

(129) Magee AI, Gutierrez L, McKay IA, Marshall CJ, Hall A. Dynamic fatty acylation of p21N-ras. EMBO J 1987; 6(11):3353-3357.

(130) Bivona TG, Philips MR. Ras pathway signaling on endomembranes. Curr Opin Cell Biol 2003; 15(2):136-142.

(131) Hancock JF. Ras proteins: Different signals from different locations. Nature Reviews Molecular Cell Biology 2003; 4(5):373-384.

(132) Yan J, Roy S, Apolloni A, Lane A, Hancock JF. Ras Isoforms Vary in Their Ability to Activate Raf-1 and Phosphoinositide 3-Kinase. J Biol Chem 1998; 273(37):24052-24056.

(133) Voice JK, Klemke RL, Le A, Jackson JH. Four human Ras homologs differ in their abilities to activate Raf-1, induce transformation, and stimulate cell motility. J Biol Chem 1999; 274(24):17164-17170.

(134) McCormick F. Signal transduction. How receptors turn Ras on. Nature 1993; 363(6424):15-16.

(135) Perez-Sala D, Rebollo A. Novel aspects of Ras proteins biology: regulation and implications. Cell Death Differ 1999; 6(8):722-728.

(136) Daly RJ. Take your partners, please--signal diversification by the erbB family of receptor tyrosine kinases. Growth Factors 1999; 16(4):255-263.

(137) Pawson T. Protein modules and signalling networks. Nature 1995; 373(6515):573-580.

(138) Malumbres M, Pellicer A. RAS pathways to cell cycle control and cell transformation. Front Biosci 1998; 3:d887-d912.

(139) Chiu VK, Bivona T, Hach A, Sajous JB, Silletti J, Wiener H et al. Ras signalling on the endoplasmic reticulum and the Golgi. Nat Cell Biol 2002; 4(5):343-350.

(140) Ebinu JO, Bottorff DA, Chan EY, Stang SL, Dunn RJ, Stone JC. RasGRP, a Ras guanyl nucleotide- releasing protein with calcium- and diacylglycerol-binding motifs. Science 1998; 280(5366):1082-1086.

(141) Bivona TG, Perez DC, I, Ahearn IM, Grana TM, Chiu VK, Lockyer PJ et al. Phospholipase Cgamma activates Ras on the Golgi apparatus by means of RasGRP1. Nature 2003; 424(6949):694-698.

(142) Feig LA, Urano T, Cantor S. Evidence for a Ras/Ral signaling cascade. Trends Biochem Sci 1996; 21(11):438-441.

(143) Rak J, Mitsuhashi Y, Bayko L, Filmus J, Shirasawa S, Sasazuki T et al. Mutant ras oncogenes upregulate VEGF/VPF expression: implications for induction and inhibition of tumor angiogenesis. Cancer Res 1995; 55(20):4575-4580.

(144) Downward J. Cell cycle: routine role for Ras. Curr Biol 1997; 7(4):R258-R260.

(145) Malaney S, Daly RJ. The ras signaling pathway in mammary tumorigenesis and metastasis. J Mammary Gland Biol Neoplasia 2001; 6(1):101-113.

(146) Li W, Zhu T, Guan KL. Transformation potential of Ras isoforms correlates with activation of phosphatidylinositol 3-kinase but not ERK. J Biol Chem 2004; 279(36):37398-37406.

(147) Zachos G, Spandidos DA. Expression of *ras* proto-oncogenes: regulation and implications in the development of human tumors. Critical Reviews in Oncology/Hematology 1997; 26:65-75.

(148) Macaluso M, Russo G, Cinti C, Bazan V, Gebbia N, Russo A. Ras family genes: an interesting link between cell cycle and cancer. J Cell Physiol 2002; 192(2):125-130.

(149) Thor A, Ohuchi N, Hand PH, Callahan R, Weeks MO, Theillet C et al. ras gene alterations and enhanced levels of ras p21 expression in a spectrum of benign and malignant human mammary tissues. Lab Invest 1986; 55(6):603-615.

(150) Verbeek BS, Adriaansen-Slot SS, Rijksen G, Vroom TM. Grb2 overexpression in nuclei and cytoplasm of human breast cells: a histochemical and biochemical study of normal and neoplastic mammary tissue specimens. J Pathol 1997; 183(2):195-203.

(151) Miyakis S, Sourvinos G, Spandidos DA. Differential expression and mutation of the ras family genes in human breast cancer. Biochem Biophys Res Commun 1998; 251(2):609-612.

(152) Watson DM, Elton RA, Jack WJ, Dixon JM, Chetty U, Miller WR. The H-ras oncogene product p21 and prognosis in human breast cancer. Breast Cancer Res Treat 1991; 17(3):161-169.

(153) Gohring UJ, Schondorf T, Kiecker VR, Becker M, Kurbacher C, Scharl A. Immunohistochemical detection of H-ras protooncoprotein p21 indicates

favorable prognosis in node-negative breast cancer patients. Tumour Biol 1999; 20(4):173-183.

(154) Weinstein-Oppenheimer CR, Henriquez-Roldan CF, Davis JM, Navolanic PM, Saleh OA, Steelman LS et al. Role of the Raf signal transduction cascade in the in vitro resistance to the anticancer drug doxorubicin. Clin Cancer Res 2001; 7(9):2898-2907.

(155) Rasouli-Nia A, Liu D, Perdue S, Britten RA. High Raf-1 kinase activity protects human tumor cells against paclitaxel-induced cytotoxicity. Clin Cancer Res 1998; 4(5):1111-1116.

(156) Rapp UR, Goldsborough MD, Mark GE, Bonner TI, Groffen J, Reynolds FH, Jr. et al. Structure and biological activity of v-raf, a unique oncogene transduced by a retrovirus. Proc Natl Acad Sci U S A 1983; 80(14):4218-4222.

(157) Bonner TI, Kerby SB, Sutrave P, Gunnell MA, Mark G, Rapp UR. Structure and biological activity of human homologs of the raf/mil oncogene. Mol Cell Biol 1985; 5(6):1400-1407.

(158) Huebner K, ar-Rushdi A, Griffin CA, Isobe M, Kozak C, Emanuel BS et al. Actively transcribed genes in the raf oncogene group, located on the X chromosome in mouse and human. Proc Natl Acad Sci U S A 1986; 83(11):3934-3938.

(159) Ikawa S, Fukui M, Ueyama Y, Tamaoki N, Yamamoto T, Toyoshima K. B-raf, a new member of the raf family, is activated by DNA rearrangement. Mol Cell Biol 1988; 8(6):2651-2654.

(160) Storm SM, Cleveland JL, Rapp UR. Expression of raf family proto-oncogenes in normal mouse tissues. Oncogene 1990; 5(3):345-351.

(161) Kolch W. Meaningful relationships: the regulation of the Ras/Raf/MEK/ERK pathway by protein interactions. Biochem J 2000; 351 Pt 2:289-305.

(162) Hagemann C, Rapp UR. Isotype-specific functions of Raf kinases. Exp Cell Res 1999; 253(1):34-46.

(163) Wiese S, Pei G, Karch C, Troppmair J, Holtmann B, Rapp UR et al. Specific function of B-Raf in mediating survival of embryonic motoneurons and sensory neurons. Nat Neurosci 2001; 4(2):137-142.

(164) Davies H, Bignell GR, Cox C, Stephens P, Edkins S, Clegg S et al. Mutations of the BRAF gene in human cancer. Nature 2002; 417(6892):949-954.

(165) Nassar N, Horn G, Herrmann C, Scherer A, McCormick F, Wittinghofer A. The 2.2 A crystal structure of the Ras-binding domain of the serine/threonine kinase

c-Raf1 in complex with Rap1A and a GTP analogue. Nature 1995; 375(6532):554-560.

(166) Inouye K, Mizutani S, Koide H, Kaziro Y. Formation of the Ras dimer is essential for Raf-1 activation. J Biol Chem 2000; 275(6):3737-3740.

(167) Chong H, Vikis HG, Guan KL. Mechanisms of regulating the Raf kinase family. Cellular Signalling 2003; 15(5):463-469.

(168) Xing H, Kornfeld K, Muslin AJ. The protein kinase KSR interacts with 14-3-3 protein and Raf. Current Biology 1997; 7(5):294-300.

(169) Morrison DK, Heidecker G, Rapp UR, Copeland TD. Identification of the major phosphorylation sites of the Raf-1 kinase. J Biol Chem 1993; 268(23):17309-17316.

(170) Wu J, Dent P, Jelinek T, Wolfman A, Weber MJ, Sturgill TW. Inhibition of the EGF-activated MAP kinase signaling pathway by adenosine 3',5'-monophosphate. Science 1993; 262(5136):1065-1069.

(171) Tzivion G, Luo Z, Avruch J. A dimeric 14-3-3 protein is an essential cofactor for Raf kinase activity. Nature 1998; 394(6688):88-92.

(172) Chong H, Guan KL. Regulation of Raf through Phosphorylation and N Terminus-C Terminus Interaction. J Biol Chem 2003; 278(38):36269-36276.

(173) Zimmermann S, Moelling K. Phosphorylation and regulation of Raf by Akt (protein kinase B). Science 1999; 286(5445):1741-1744.

(174) Dhillon AS, Pollock C, Steen H, Shaw PE, Mischak H, Kolch W. Cyclic AMP-Dependent Kinase Regulates Raf-1 Kinase Mainly by Phosphorylation of Serine 259. Mol Cell Biol 2002; 22(10):3237-3246.

(175) Dumaz N, Marais R. Protein Kinase A Blocks Raf-1 Activity by Stimulating 14-3-3 Binding and Blocking Raf-1 Interaction with Ras. J Biol Chem 2003; 278(32):29819-29823.

(176) Ory S, Zhou M, Conrads TP, Veenstra TD, Morrison DK. Protein phosphatase 2A positively regulates ras signaling by dephosphorylating KSR1 and Raf-1 on critical 14-3-3 binding sites. Current Biology 2003; 13(16):1356-1364.

(177) Wellbrock C, Karasarides M, Marais R. The RAF proteins take centre stage. Nat Rev Mol Cell Biol 2004; 5(11):875-885.

(178) Therrien M, Michaud NR, Rubin GM, Morrison DK. KSR modulates signal propagation within the MAPK cascade. Genes Dev 1996; 10(21):2684-2695.

(179) Roy F, Laberge G, Douziech M, Ferland-McCollough D, Therrien M. KSR is a scaffold required for activation of the ERK/MAPK module. Genes & Development 2002; 16(4):427-438.

(180) Hagan S, Garcia R, Dhillon A, Kolch W. Raf kinase inhibitor protein regulation of raf and MAPK signaling. Methods Enzymol 2005; 407:248-259.

(181) Alessi DR, Cuenda A, Cohen P, Dudley DT, Saltiel AR. PD 098059 is a specific inhibitor of the activation of mitogen-activated protein kinase kinase in vitro and in vivo. J Biol Chem 1995; 270(46):27489-27494.

(182) Dougherty MK, Muller J, Ritt DA, Zhou M, Zhou XZ, Copeland TD et al. Regulation of Raf-1 by direct feedback phosphorylation. Mol Cell 2005; 17(2):215-224.

(183) Jaiswal RK, Moodie SA, Wolfman A, Landreth GE. The mitogen-activated protein kinase cascade is activated by B-Raf in response to nerve growth factor through interaction with p21ras. Mol Cell Biol 1994; 14(10):6944-6953.

(184) Wang S, Ghosh RN, Chellappan SP. Raf-1 Physically Interacts with Rb and Regulates Its Function: a Link between Mitogenic Signaling and Cell Cycle Regulation. Mol Cell Biol 1998; 18(12):7487.

(185) Zhang L, Bewick M, Lafrenie RM. EGFR and ErbB2 differentially regulate Raf-1 translocation and activation. Lab Invest 2002; 82(1):71-78.

(186) Leng Q, Mixson AJ. Small interfering RNA targeting Raf-1 inhibits tumor growth in vitro and in vivo. Cancer Gene Ther 2005; 12(8):682-690.

(187) Scholl FA, Dumesic PA, Khavari PA. Mek1 alters epidermal growth and differentiation. Cancer Res 2004; 64(17):6035-6040.

(188) Sebolt-Leopold JS, Herrera R. Targeting the mitogen-activated protein kinase cascade to treat cancer. Nat Rev Cancer 2004; 4(12):937-947.

(189) Li L, Wysk M, Gonzalez FA, Davis RJ. Genomic loci of human mitogen-activated protein kinases. Oncogene 1994; 9(2):647-649.

(190) Fukuda M, Gotoh I, Adachi M, Gotoh Y, Nishida E. A novel regulatory mechanism in the mitogen-activated protein (MAP) kinase cascade. Role of nuclear export signal of MAP kinase kinase. J Biol Chem 1997; 272(51):32642-32648.

(191) Tanoue T, Adachi M, Moriguchi T, Nishida E. A conserved docking motif in MAP kinases common to substrates, activators and regulators. Nat Cell Biol 2000; 2(2):110-116.

(192) Robinson FL, Whitehurst AW, Raman M, Cobb MH. Identification of novel point mutations in ERK2 that selectively disrupt binding to MEK1. J Biol Chem 2002; 277(17):14844-14852.

(193) Rubinfeld H, Hanoch T, Seger R. Identification of a cytoplasmic-retention sequence in ERK2. J Biol Chem 1999; 274(43):30349-30352.

(194) Santen RJ, Song RX, McPherson R, Kumar R, Adam L, Jeng MH et al. The role of mitogen-activated protein (MAP) kinase in breast cancer. The Journal of Steroid Biochemistry and Molecular Biology 2002; 80(2):239-256.

(195) Khokhlatchev AV, Canagarajah B, Wilsbacher J, Robinson M, Atkinson M, Goldsmith E et al. Phosphorylation of the MAP kinase ERK2 promotes its homodimerization and nuclear translocation. Cell 1998; 93(4):605-615.

(196) Yoon S, Seger R. The extracellular signal-regulated kinase: multiple substrates regulate diverse cellular functions. Growth Factors 2006; 24(1):21-44.

(197) Joel PB, Smith J, Sturgill TW, Fisher TL, Blenis J, Lannigan DA. pp90(rsk1) regulates estrogen receptor-mediated transcription through phosphorylation of Ser-167. Mol Cell Biol 1998; 18(4):1978-1984.

(198) Murphy LO, Smith S, Chen RH, Fingar DC, Blenis J. Molecular interpretation of ERK signal duration by immediate early gene products. Nat Cell Biol 2002; 4(8):556-564.

(199) Traverse S, Seedorf K, Paterson H, Marshall CJ, Cohen P, Ullrich A. EGF triggers neuronal differentiation of PC12 cells that overexpress the EGF receptor. Curr Biol 1994; 4(8):694-701.

(200) Marshall CJ. Specificity of receptor tyrosine kinase signaling: transient versus sustained extracellular signal-regulated kinase activation. Cell 1995; 80(2):179-185.

(201) Bunone G, Briand PA, Miksicek RJ, Picard D. Activation of the unliganded estrogen receptor by EGF involves the MAP kinase pathway and direct phosphorylation. EMBO J 1996; 15(9):2174-2183.

(202) Kurokawa H, Arteaga CL. ErbB (HER) receptors can abrogate antiestrogen action in human breast cancer by multiple signaling mechanisms. Clin Cancer Res 2003; 9(1 Pt 2):511S-515S.

(203) Nicholson RI, Hutcheson IR, Hiscox SE, Knowlden JM, Giles M, Barrow D et al. Growth factor signalling and resistance to selective oestrogen receptor modulators and pure anti-oestrogens: the use of anti-growth factor therapies to treat or delay endocrine resistance in breast cancer. Endocr Relat Cancer 2005; 12(Supplement_1):S29-S36.

(204) Nakopoulou L, Mylona E, Rafailidis P, Alexandrou P, Giannopoulou I, Keramopoulos A. Effect of different ERK2 protein localizations on prognosis of patients with invasive breast carcinoma. APMIS 2005; 113(10):693-701.

(205) Oh AS, Lorant LA, Holloway JN, Miller DL, Kern FG, El Ashry D. Hyperactivation of MAPK induces loss of ERalpha expression in breast cancer cells. Mol Endocrinol 2001; 15(8):1344-1359.

(206) Holloway JN, Murthy S, El Ashry D. A cytoplasmic substrate of mitogen-activated protein kinase is responsible for estrogen receptor-alpha down-regulation in breast cancer cells: the role of nuclear factor-kappaB. Mol Endocrinol 2004; 18(6):1396-1410.

(207) Liu Y, El Ashry D, Chen D, Ding IY, Kern FG. MCF-7 breast cancer cells overexpressing transfected c-erbB-2 have an in vitro growth advantage in estrogen-depleted conditions and reduced estrogen-dependence and tamoxifen-sensitivity in vivo. Breast Cancer Res Treat 1995; 34(2):97-117.

(208) Creighton CJ, Hilger AM, Murthy S, Rae JM, Chinnaiyan AM, El Ashry D. Activation of Mitogen-Activated Protein Kinase in Estrogen Receptor {alpha}-Positive Breast Cancer Cells In vitro Induces an In vivo Molecular Phenotype of Estrogen Receptor {alpha}-Negative Human Breast Tumors. Cancer Res 2006; 66(7):3903-3911.

(209) Krueger JS, Keshamouni VG, Atanaskova N, Reddy KB. Temporal and quantitative regulation of mitogen-activated protein kinase (MAPK) modulates cell motility and invasion. Oncogene 2001; 20(31):4209-4218.

(210) Seddighzadeh M, Zhou JN, Kronenwett U, Shoshan MC, Auer G, Sten-Linder M et al. ERK signalling in metastatic human MDA-MB-231 breast carcinoma cells is adapted to obtain high urokinase expression and rapid cell proliferation. Clin Exp Metastasis 1999; 17(8):649-654.

(211) Ripple MO, Kalmadi S, Eastman A. Inhibition of either phosphatidylinositol 3-kinase/Akt or the mitogen/extracellular-regulated kinase, MEK/ERK, signaling pathways suppress growth of breast cancer cell lines, but MEK/ERK signaling is critical for cell survival. Breast Cancer Res Treat 2005; 93(2):177-188.

(212) Atanaskova N, Keshamouni VG, Krueger JS, Schwartz JA, Miller F, Reddy KB. MAP kinase/estrogen receptor cross-talk enhances estrogen-mediated signaling and tumor growth but does not confer tamoxifen resistance. Oncogene 2002; 21(25):4000-4008.

(213) Adeyinka A, Nui Y, Cherlet T, Snell L, Watson PH, Murphy LC. Activated mitogen-activated protein kinase expression during human breast tumorigenesis and breast cancer progression. Clin Cancer Res 2002; 8(6):1747-1753.

(214) Mueller H, Flury N, Eppenberger-Castori S, Kueng W, David F, Eppenberger U. Potential prognostic value of mitogen-activated protein kinase activity for disease-free survival of primary breast cancer patients. Int J Cancer 2000; 89(4):384-388.

(215) Milde-Langosch K, Bamberger AM, Rieck G, Grund D, Hemminger G, Muller V et al. Expression and prognostic relevance of activated extracellular-regulated kinases (ERK1/2) in breast cancer. Br J Cancer 2005; 92(12):2206-2215.

(216) Font dM, Brown M. AIB1 is a conduit for kinase-mediated growth factor signaling to the estrogen receptor. Mol Cell Biol 2000; 20(14):5041-5047.

(217) Lopez GN, Turck CW, Schaufele F, Stallcup MR, Kushner PJ. Growth factors signal to steroid receptors through mitogen-activated protein kinase regulation of p160 coactivator activity. J Biol Chem 2001; 276(25):22177-22182.

(218) Rowan BG, Weigel NL, O'Malley BW. Phosphorylation of steroid receptor coactivator-1. Identification of the phosphorylation sites and phosphorylation through the mitogen-activated protein kinase pathway. J Biol Chem 2000; 275(6):4475-4483.

(219) Hong SH, Privalsky ML. The SMRT corepressor is regulated by a MEK-1 kinase pathway: inhibition of corepressor function is associated with SMRT phosphorylation and nuclear export. Mol Cell Biol 2000; 20(17):6612-6625.

(220) El Ashry D, Miller DL, Kharbanda S, Lippman ME, Kern FG. Constitutive Raf-1 kinase activity in breast cancer cells induces both estrogen-independent growth and apoptosis. Oncogene 1997; 15(4):423-435.

(221) Rabenoelina F, Semlali A, Duchesne MJ, Freiss G, Pons M, Badia E. Effect of prolonged hydroxytamoxifen treatment of MCF-7 cells on mitogen activated kinase cascade. Int J Cancer 2002; 98(5):698-706.

(222) Nicholson RI, Hutcheson IR, Britton D, Knowlden JM, Jones HE, Harper ME et al. Growth factor signalling networks in breast cancer and resistance to endocrine agents: new therapeutic strategies. The Journal of Steroid Biochemistry and Molecular Biology 2005; 93(2-5):257-262.

(223) Gee JM, Robertson JF, Ellis IO, Nicholson RI. Phosphorylation of ERK1/2 mitogen-activated protein kinase is associated with poor response to anti-hormonal therapy and decreased patient survival in clinical breast cancer. Int J Cancer 2001; 95(4):247-254.

(224) Svensson S, Jirstrom K, Ryden L, Roos G, Emdin S, Ostrowski MC et al. ERK phosphorylation is linked to VEGFR2 expression and Ets-2 phosphorylation in breast cancer and is associated with tamoxifen treatment resistance and small tumours with good prognosis. Oncogene 2005; 24(27):4370-4379.

(225) Gee JM, Robertson JF, Gutteridge E, Ellis IO, Pinder SE, Rubini M et al. Epidermal growth factor receptor/HER2/insulin-like growth factor receptor signalling and oestrogen receptor activity in clinical breast cancer. Endocr Relat Cancer 2005; 12(Supplement_1):S99-111.

(226) Bergqvist J, Elmberger G, Ohd J, Linderholm B, Bjohle J, Hellborg H et al. Activated ERK1/2 and phosphorylated oestrogen receptor alpha are associated with improved breast cancer survival in women treated with tamoxifen. Eur J Cancer 2006; 42(8):1104-1112.

(227) Davis JM, Navolanic PM, Weinstein-Oppenheimer CR, Steelman LS, Hu W, Konopleva M et al. Raf-1 and Bcl-2 induce distinct and common pathways that contribute to breast cancer drug resistance. Clin Cancer Res 2003; 9(3):1161-1170.

(228) Rasouli-Nia A, Liu D, Perdue S, Britten RA. High Raf-1 kinase activity protects human tumor cells against paclitaxel-induced cytotoxicity. Clin Cancer Res 1998; 4(5):1111-1116.

(229) Jin W, Wu L, Liang K, Liu B, Lu Y, Fan Z. Roles of the PI-3K and MEK pathways in Ras-mediated chemoresistance in breast cancer cells. Br J Cancer 2003; 89(1):185-191.

(230) Guise S, Braguer D, Carles G, Delacourte A, Briand C. Hyperphosphorylation of tau is mediated by ERK activation during anticancer drug-induced apoptosis in neuroblastoma cells. J Neurosci Res 2001; 63(3):257-267.

(231) Li T, Sparano JA. Inhibiting Ras signaling in the therapy of breast cancer. Clin Breast Cancer 2003; 3(6):405-416.

(232) Reuther GW, Der CJ. The Ras branch of small GTPases: Ras family members don't fall far from the tree. Curr Opin Cell Biol 2000; 12(2):157-165.

(233) Kelland LR, Smith V, Valenti M, Patterson L, Clarke PA, Detre S et al. Preclinical antitumor activity and pharmacodynamic studies with the farnesyl protein transferase inhibitor R115777 in human breast cancer. Clin Cancer Res 2001; 7(11):3544-3550.

(234) Doisneau-Sixou SF, Cestac P, Faye JC, Favre G, Sutherland RL. Additive effects of tamoxifen and the farnesyl transferase inhibitor FTI-277 on inhibition of MCF-7 breast cancer cell-cycle progression. Int J Cancer 2003; 106(5):789-798.

(235) Wilhelm SM, Carter C, Tang L, Wilkie D, McNabola A, Rong H et al. BAY 43-9006 exhibits broad spectrum oral antitumor activity and targets the RAF/MEK/ERK pathway and receptor tyrosine kinases involved in tumor progression and angiogenesis. Cancer Res 2004; 64(19):7099-7109.

(236) Wan PT, Garnett MJ, Roe SM, Lee S, Niculescu-Duvaz D, Good VM et al. Mechanism of activation of the RAF-ERK signaling pathway by oncogenic mutations of B-RAF. Cell 2004; 116(6):855-867.

(237) Dudley DT, Pang L, Decker SJ, Bridges AJ, Saltiel AR. A synthetic inhibitor of the mitogen-activated protein kinase cascade. Proc Natl Acad Sci U S A 1995; 92(17):7686-7689.

(238) Favata MF, Horiuchi KY, Manos EJ, Daulerio AJ, Stradley DA, Feeser WS et al. Identification of a novel inhibitor of mitogen-activated protein kinase kinase. J Biol Chem 1998; 273(29):18623-18632.

(239) Hoshino R, Tanimura S, Watanabe K, Kataoka T, Kohno M. Blockade of the extracellular signal-regulated kinase pathway induces marked G1 cell cycle arrest and apoptosis in tumor cells in which the pathway is constitutively activated: up-regulation of p27(Kip1). J Biol Chem 2001; 276(4):2686-2692.

(240) Sebolt-Leopold JS, Dudley DT, Herrera R, Van Becelaere K, Wiland A, Gowan RC et al. Blockade of the MAP kinase pathway suppresses growth of colon tumors in vivo. Nat Med 1999; 5(7):810-816.

(241) Ohren JF, Chen H, Pavlovsky A, Whitehead C, Zhang E, Kuffa P et al. Structures of human MAP kinase kinase 1 (MEK1) and MEK2 describe novel noncompetitive kinase inhibition. Nat Struct Mol Biol 2004; 11(12):1192-1197.

(242) Kohno M, Pouyssegur J. Targeting the ERK signaling pathway in cancer therapy. Ann Med 2006; 38(3):200-211.

(243) Navolanic PM, Lee JT, McCubrey JA. Docetaxel cytotoxicity is enhanced by inhibition of the Raf/MEK/ERK signal transduction pathway. Cancer Biol Ther 2003; 2(6):677-678.

(244) McCarty KS, Jr., Miller LS, Cox EB, Konrath J, McCarty KS, Sr. Estrogen receptor analyses. Correlation of biochemical and immunohistochemical methods using monoclonal antireceptor antibodies. Arch Pathol Lab Med 1985; 109(8):716-721.

(245) Kirkegaard T, Edwards J, Tovey S, McGlynn LM, Krishna SN, Mukherjee R et al. Observer variation in immunohistochemical analysis of protein expression, time for a change? Histopathology 2006; 48(7):787-794.

(246) Chiu VK, Bivona T, Hach A, Sajous JB, Silletti J, Wiener H et al. Ras signalling on the endoplasmic reticulum and the Golgi. Nature Cell Biology 2002; 4(5):343-350.

(247) Wurzer G, Mosgoeller W, Chabicovsky M, Cerni C, Wesierska-Gadek J. Nuclear ras: Unexpected subcellular distribution of oncogenic forms. Journal Of Cellular Biochemistry 2001;1-11.

(248) Guil S, de La Glesia N, Fernandez-Larrea J, Cifuentes D, Ferrer JC, Guinovart JJ et al. Alternative splicing of the human proto-oncogene c-H-ras renders a new Ras family protein that trafficks to cytoplasm and nucleus. Cancer Res 2003; 63(17):5178-5187.

(249) Clark GJ, Der CJ. Aberrant function of the Ras signal transduction pathway in human breast cancer. Breast Cancer Res Treat 1995; 35(1):133-144.

(250) Miyakis S, Sourvinos G, Spandidos DA. Differential expression and mutation of the ras family genes in human breast cancer. Biochem Biophys Res Commun 1998; 251(2):609-612.

(251) Voice JK, Klemke RL, Le A, Jackson JH. Four Human Ras Homologs Differ in Their Abilities to Activate Raf-1, Induce Transformation, and Stimulate Cell Motility. The Journal of Biological Chemistry 1999; 274(24):17164-17170.

(252) Ehrhardt A, David MD, Ehrhardt GRA, Schrader JW. Distinct mechanisms determine the patterns of differential activation of H-Ras, N-Ras, K-Ras 4B, and M-Ras by receptors for growth factors or antigen. Mol Cell Biol 2004; 24(14):6311-6323.

(253) Mukherjee R, Bartlett JMS, Krishna NS, Underwood MA, Edwards J. Raf-1 expression may influence progression to androgen insensitive prostate cancer. Prostate 2005; 64(1):101-107.

(254) Di Fiore PP. Signal transduction - Life on Mars, cellularly speaking. Nature 2003; 424(6949):624-625.

(255) Bind E, Kleyner Y, Skowronska-Krawczyk D, Bien E, Dynlacht BD, Sanchez I. A novel mechanism for mitogen-activated protein kinase localization. Mol Biol Cell 2004; 15(10):4457-4466.

(256) Pryde JG. A group of integral membrane proteins of the rat liver Golgi contains a conserved protein of 100 kDa. J Cell Sci 1994; 107 (Pt 12):3425-3436.

(257) Nizak C, Monier S, del Nery E, Moutel S, Goud B, Perez F. Recombinant antibodies to the small GTPase Rab6 as conformation sensors. Science 2003; 300(5621):984-987.

(258) Humphries DE, Sullivan BM, Aleixo MD, Stow JL. Localization of human heparan glucosaminyl N-deacetylase/N-sulphotransferase to the trans-Golgi network. Biochem J 1997; 325 (Pt 2):351-357.

(259) Nicholson RI, Hutcheson IR, Hiscox SE, Knowlden JM, Giles M, Barrow D et al. Growth factor signalling and resistance to selective oestrogen receptor modulators and pure anti-oestrogens: the use of anti-growth factor therapies to treat or delay endocrine resistance in breast cancer. Endocr Relat Cancer 2005; 12 Suppl 1:S29-S36.

(260) Liu X, Yan S, Zhou TH, Terada Y, Erikson RL. The MAP kinase pathway is required for entry into mitosis and cell survival. Oncogene 2004; 23(3):763-776.

(261) Mercer K, Giblett S, Oakden A, Brown J, Marais R, Pritchard C. A-Raf and Raf-1 work together to influence transient ERK phosphorylation and G1/S cell cycle progression. Oncogene 2005; 24(33):5207-5217.

(262) Marais R, Light Y, Paterson HF, Mason CS, Marshall CJ. Differential regulation of Raf-1, A-Raf, and B-Raf by oncogenic ras and tyrosine kinases. J Biol Chem 1997; 272(7):4378-4383.

(263) Papin C, Denouel A, Calothy G, Eychene A. Identification of signalling proteins interacting with B-Raf in the yeast two-hybrid system. Oncogene 1996; 12(10):2213-2221.

(264) Ehrenreiter K, Piazzolla D, Velamoor V, Sobczak I, Small JV, Takeda J et al. Raf-1 regulates Rho signaling and cell migration. J Cell Biol 2005; 168(6):955-964.

(265) Dasgupta P, Sun J, Wang S, Fusaro G, Betts V, Padmanabhan J et al. Disruption of the Rb--Raf-1 interaction inhibits tumor growth and angiogenesis. Mol Cell Biol 2004; 24(21):9527-9541.

(266) Varma H, Conrad SE. Reversal of an antiestrogen-mediated cell cycle arrest of MCF-7 cells by viral tumor antigens requires the retinoblastoma protein-binding domain. Oncogene 2000; 19(41):4746-4753.

(267) Hurd C, Khattree N, Dinda S, Alban P, Moudgil VK. Regulation of tumor suppressor proteins, p53 and retinoblastoma, by estrogen and antiestrogens in breast cancer cells. Oncogene 1997; 15(8):991-995.

(268) Yeh S, Miyamoto H, Nishimura K, Kang H, Ludlow J, Hsiao P et al. Retinoblastoma, a tumor suppressor, is a coactivator for the androgen receptor in human prostate cancer DU145 cells. Biochem Biophys Res Commun 1998; 248(2):361-367.

(269) Adegbola O, Pasternack GR. A pp32-retinoblastoma protein complex modulates androgen receptor-mediated transcription and associates with components of the splicing machinery. Biochem Biophys Res Commun 2005; 334(2):702-708.

(270) Berstein LM, Zheng H, Yue W, Wang JP, Lykkesfeldt AE, Naftolin F et al. New approaches to the understanding of tamoxifen action and resistance. Endocr Relat Cancer 2003; 10(2):267-277.

(271) Lee M, Koh WS, Han SS. Down-regulation of Raf-1 kinase is associated with paclitaxel resistance in human breast cancer MCF-7/Adr cells. Cancer Lett 2003; 193(1):57-64.

(272) Coombes RC, Hall E, Gibson LJ, Paridaens R, Jassem J, Delozier T et al. A randomized trial of exemestane after two to three years of tamoxifen therapy in postmenopausal women with primary breast cancer. N Engl J Med 2004; 350(11):1081-1092.

(273) Zhao Y, You H, Yang Y, Wei L, Zhang X, Yao L et al. Distinctive regulation and function of PI 3K/Akt and MAPKs in doxorubicin-induced apoptosis of human lung adenocarcinoma cells. J Cell Biochem 2004; 91(3):621-632.

(274) Small GW, Somasundaram S, Moore DT, Shi YY, Orlowski RZ. Repression of Mitogen-Activated Protein Kinase (MAPK) Phosphatase-1 by Anthracyclines Contributes to Their Antiapoptotic Activation of p44/42-MAPK. J Pharmacol Exp Ther 2003; 307(3):861-869.

(275) Lee JT, Jr., Steelman LS, McCubrey JA. Modulation of Raf/MEK/ERK kinase activity does not affect the chemoresistance profile of advanced prostate cancer cells. Int J Oncol 2005; 26(6):1637-1644.

(276) Tsurutani J, West KA, Sayyah J, Gills JJ, Dennis PA. Inhibition of the phosphatidylinositol 3-kinase/Akt/mammalian target of rapamycin pathway but not the MEK/ERK pathway attenuates laminin-mediated small cell lung cancer cellular survival and resistance to imatinib mesylate or chemotherapy. Cancer Res 2005; 65(18):8423-8432.

(277) Takahashi T, Ohmichi M, Kawagoe J, Ohshima C, Doshida M, Ohta T et al. Growth factors change nuclear distribution of estrogen receptor-alpha via mitogen-activated protein kinase or phosphatidylinositol 3-kinase cascade in a human breast cancer cell line. Endocrinology 2005; 146(9):4082-4089.

(278) Nonclercq D, Journe F, Body JJ, Leclercq G, Laurent G. Ligand-independent and agonist-mediated degradation of estrogen receptor-alpha in breast carcinoma cells: evidence for distinct degradative pathways. Mol Cell Endocrinol 2004; 227(1-2):53-65.

(279) Joel PB, Traish AM, Lannigan DA. Estradiol and phorbol ester cause phosphorylation of serine 118 in the human estrogen receptor. Mol Endocrinol 1995; 9(8):1041-1052.

(280) Joel PB, Traish AM, Lannigan DA. Estradiol-induced Phosphorylation of Serine 118áin the Estrogen Receptor Is Independent of p42/p44 Mitogen-activated Protein Kinase. J Biol Chem 1998; 273(21):13317-13323.

(281) Ito S, Takeyama K, Yamamoto A, Sawatsubashi S, Shirode Y, Kouzmenko A et al. In vivo potentiation of human oestrogen receptor alpha by Cdk7-mediated phosphorylation. Genes Cells 2004; 9(10):983-992.

(282) Lu Q, Ebling H, Mittler J, Baur WE, Karas RH. MAP kinase mediates growth factor-induced nuclear translocation of estrogen receptor [alpha]. Febs Letters 2002; 516(1-3):1-8.

(283) Picard D, Kumar V, Chambon P, Yamamoto KR. Signal transduction by steroid hormones: nuclear localization is differentially regulated in estrogen and glucocorticoid receptors. Cell Regul 1990; 1(3):291-299.

(284) Maruvada P, Baumann CT, Hager GL, Yen PM. Dynamic shuttling and intranuclear mobility of nuclear hormone receptors. J Biol Chem 2003; 278(14):12425-12432.

(285) Shao W, Keeton EK, McDonnell DP, Brown M. Coactivator AIB1 links estrogen receptor transcriptional activity and stability. Proc Natl Acad Sci U S A 2004; 101(32):11599-11604.

(286) Yang Z, Barnes CJ, Kumar R. Human epidermal growth factor receptor 2 status modulates subcellular localization of and interaction with estrogen receptor alpha in breast cancer cells. Clin Cancer Res 2004; 10(11):3621-3628.

(287) Amadori D, Volpi A, Maltoni R, Nanni O, Amaducci L, Amadori A et al. Cell proliferation as a predictor of response to chemotherapy in metastatic breast cancer: a prospective study. Breast Cancer Res Treat 1997; 43(1):7-14.

(288) Rees M, Stahl M, Klump B, Willers R, Gabbert HE, Sarbia M. The prognostic significance of proliferative activity, apoptosis and expression of DNA topoisomerase II alpha in multimodally-treated oesophageal squamous cell carcinoma. Anticancer Res 2001; 21(5):3637-3642.

(289) Martin LA, Farmer I, Johnston SRD, Ali S, Marshall C, Dowsett M. Enhanced Estrogen Receptor (ER) {alpha}, ERBB2, and MAPK Signal Transduction Pathways Operate during the Adaptation of MCF-7 Cells to Long Term Estrogen Deprivation. J Biol Chem 2003; 278(33):30458-30468.

(290) Datta SR, Dudek H, Tao X, Masters S, Fu H, Gotoh Y et al. Akt phosphorylation of BAD couples survival signals to the cell-intrinsic death machinery. Cell 1997; 91(2):231-241.

(291) Cardone MH, Roy N, Stennicke HR, Salvesen GS, Franke TF, Stanbridge E et al. Regulation of cell death protease caspase-9 by phosphorylation. Science 1998; 282(5392):1318-1321.

(292) Brunet A, Bonni A, Zigmond MJ, Lin MZ, Juo P, Hu LS et al. Akt promotes cell survival by phosphorylating and inhibiting a Forkhead transcription factor. Cell 1999; 96(6):857-868.

(293) Colleoni M, Gelber S, Goldhirsch A, Aebi S, Castiglione-Gertsch M, Price KN et al. Tamoxifen after adjuvant chemotherapy for premenopausal women with

lymph node-positive breast cancer: International Breast Cancer Study Group Trial 13-93. J Clin Oncol 2006; 24(9):1332-1341.

(294) Azab SS, El Demerdash E, Abdel-Naim AB, Youssef E, El Sharkawy N, Osman AM. Modulation of epirubicin cytotoxicity by tamoxifen in human breast cancer cell lines. Biochem Pharmacol 2005; 70(5):725-732.

(295) Moscow JA, Cowan KH. Multidrug resistance. J Natl Cancer Inst 1988; 80(1):14-20.

(296) Saeki T, Tsuruo T, Sato W, Nishikawsa K. Drug resistance in chemotherapy for breast cancer. Cancer Chemother Pharmacol 2005; 56 Suppl 1:84-89.

(297) Leonessa F, Clarke R. ATP binding cassette transporters and drug resistance in breast cancer. Endocr Relat Cancer 2003; 10(1):43-73.

(298) Osborne CK, Bardou V, Hopp TA, Chamness GC, Hilsenbeck SG, Fuqua SA et al. Role of the estrogen receptor coactivator AIB1 (SRC-3) and HER-2/neu in tamoxifen resistance in breast cancer. J Natl Cancer Inst 2003; 95(5):353-361.

(299) Martini PG, Katzenellenbogen BS. Modulation of estrogen receptor activity by selective coregulators. J Steroid Biochem Mol Biol 2003; 85(2-5):117-122.

(300) Tamrazi A, Carlson KE, Rodriguez AL, Katzenellenbogen JA. Coactivator proteins as determinants of estrogen receptor structure and function: spectroscopic evidence for a novel coactivator-stabilized receptor conformation. Mol Endocrinol 2005; 19(6):1516-1528.

(301) Osborne CK, Shou J, Massarweh S, Schiff R. Crosstalk between Estrogen Receptor and Growth Factor Receptor Pathways as a Cause for Endocrine Therapy Resistance in Breast Cancer. Clin Cancer Res 2005; 11(2):865s-8870.

(302) Murphy LC, Niu Y, Snell L, Watson P. Phospho-serine-118 estrogen receptor-alpha expression is associated with better disease outcome in women treated with tamoxifen. Clin Cancer Res 2004; 10(17):5902-5906.

(303) Yamashita H, Nishio M, Kobayashi S, Ando Y, Sugiura H, Zhang Z et al. Phosphorylation of estrogen receptor alpha serine 167 is predictive of response to endocrine therapy and increases postrelapse survival in metastatic breast cancer. Breast Cancer Res 2005; 7(5):R753-R764.

(304) Head J, Johnston S. New targets for therapy in breast cancer: Farnesyltransferase inhibitors. Breast Cancer Res 2004; 6(6):262-268.

(305) Santen RJ, Lynch AR, Neal LR, McPherson RA, Yue W. Farnesylthiosalicylic acid: inhibition of proliferation and enhancement of apoptosis of hormone-dependent breast cancer cells. Anticancer Drugs 2006; 17(1):33-40.

(306) Larsson LI. Novel actions of tyrphostin AG 879: inhibition of RAF-1 and HER-2 expression combined with strong antitumoral effects on breast cancer cells. Cell Mol Life Sci 2004; 61(19-20):2624-2631.

Appendix 1

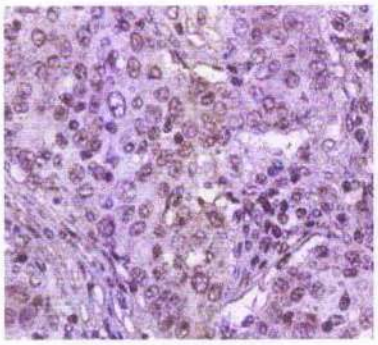

Negative Cytoplasm (0+)
Weak Cytoplasm (1+)

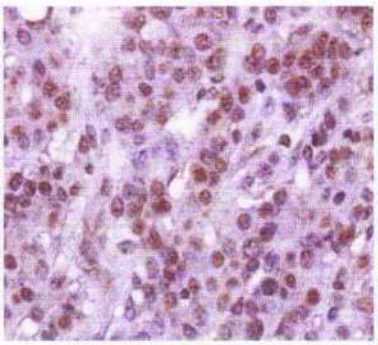

Weak Cytoplasm (1+)

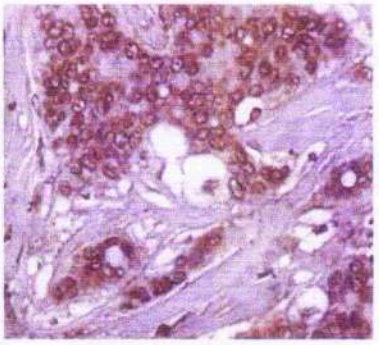

Weak Cytoplasm (1+)
Moderate Cytoplasm (2+)

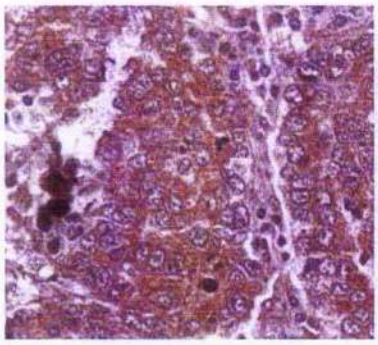

Moderate Cytoplasm (2+)
Strong Cytoplasm (3+)

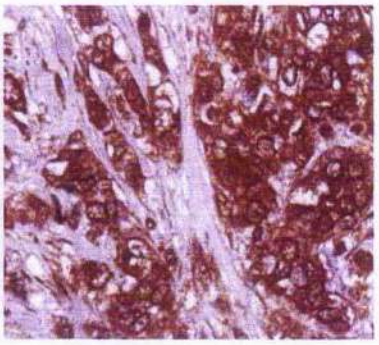

Strong Cytoplasm (3+)

Following immunohistochemistry all tumours were scored for cytoplasmic and nuclear staining, using a semi-quantitative weighted histoscore method. The intensity of staining was categorised as negative (0), weak (1), moderate (2) and strong (3) and the percentage of tumour cells within each category estimated. The above figures highlight the different intensities of cytoplasmic staining.

Appendix 2

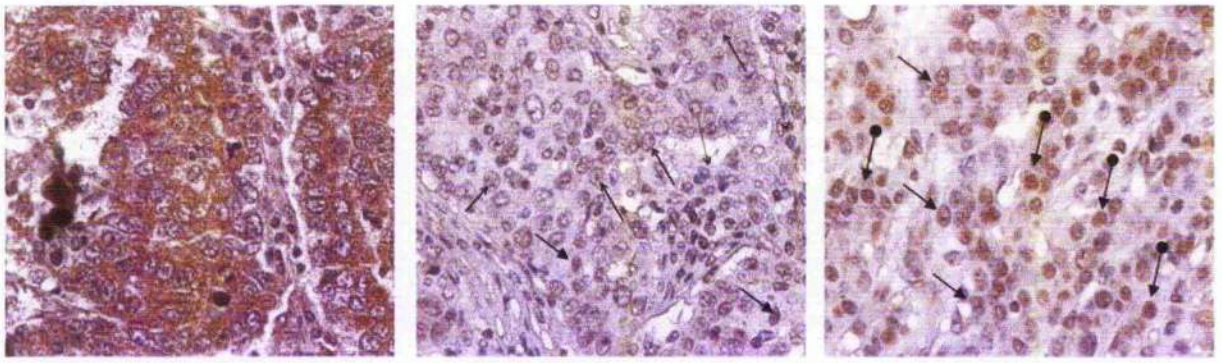

Negative Nuclei (0+)

Negative Nuclei (0+)
Weak Nuclei (1+)
Moderate Nuclei (2+)

Moderate Nuclei (2+)
Strong Nuclei (3+)

Following immunohistochemistry all tumours were scored for cytoplasmic and nuclear staining, using a semi-quantitative weighted histoscore method. The intensity of staining was categorised as negative (0), weak (1), moderate (2) and strong (3) and the percentage of tumour cells within each category estimated. The above figures highlight the different intensities of nuclear staining.

Appendix 3

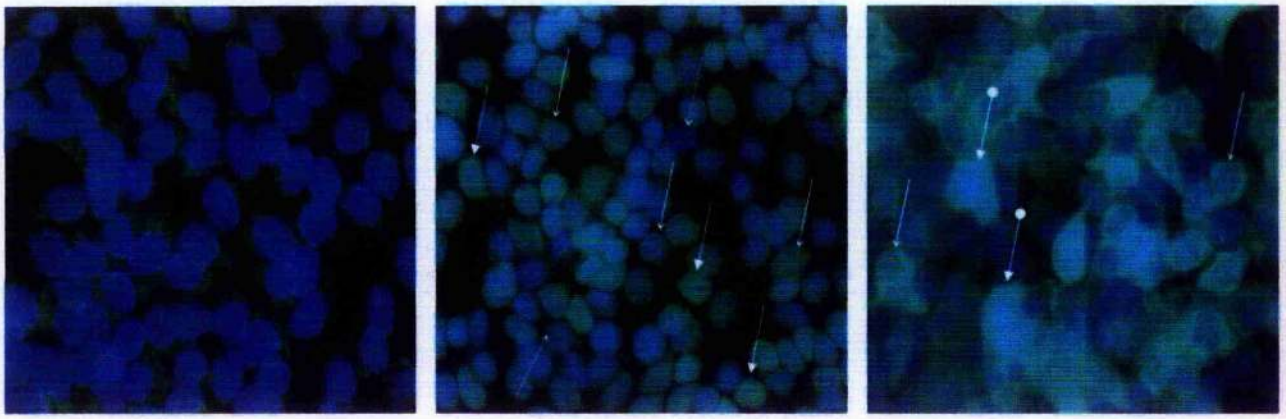

Negative Nuclei (0+)

Negative Nuclei (0+)
Weak Nuclei (1+)
Moderate Nuclei (2+)

Weak Nuclei (2+)
Strong Nuclei (3+)

In order to semi-quantify the levels of fluorescent protein detected, a scoring method similar to that of the histoscore was devised. Only protein expressed within the nuclei was scored using this method. As with the histoscores, the intensity of nuclear staining was categorised as negative (0), weak/speckled (1), moderate (2) and strong (3). The above figures highlight the intensity of nuclear fluorescent staining.

Appendix 4

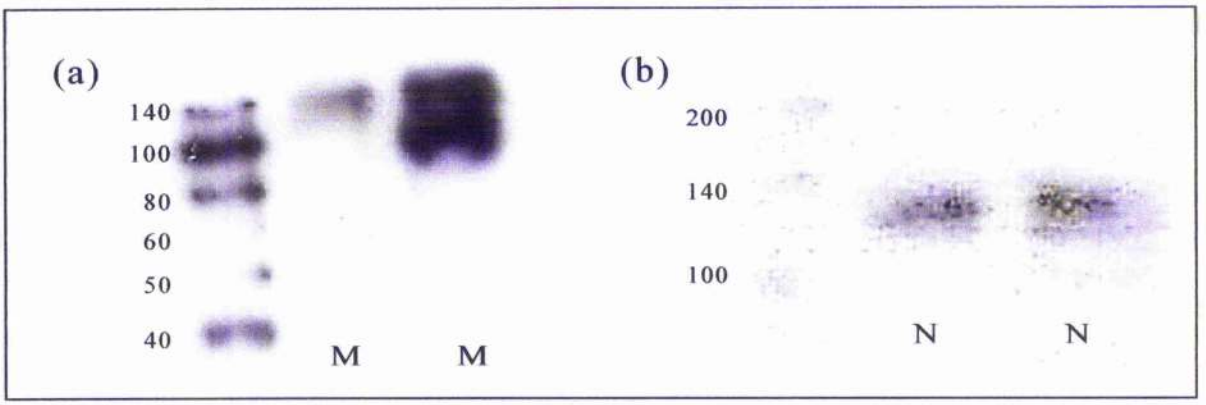

Subcellular markers were used to ensure that the protein fractions generated from the fractionation experiments were specific for their subcellular location. (a) The membrane marker was a Sodium Potassium ATPase (112kDa, 150kDa) and was detected only in the membrane fractions (M). (b) The nuclear marker was Retinoblastoma (105kDa) and was detected only in the nuclear fraction (N).

Appendix 5

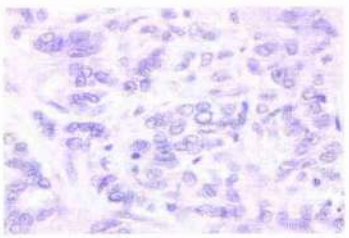

Pan-Ras

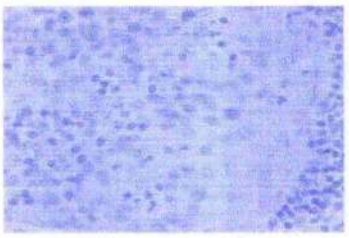

Ras Ab-1

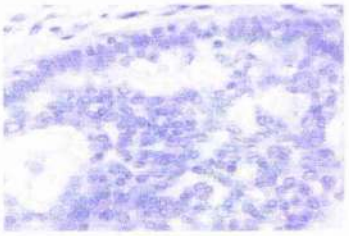

H-Ras

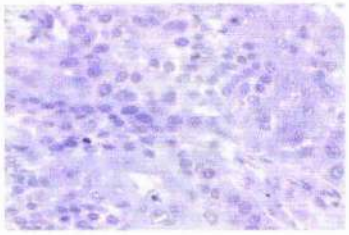

N-Ras

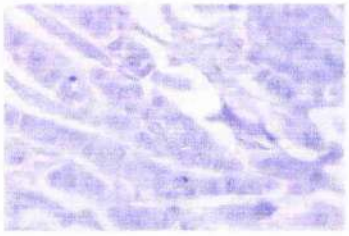

K-Ras

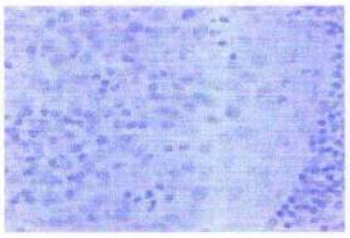

Raf-1

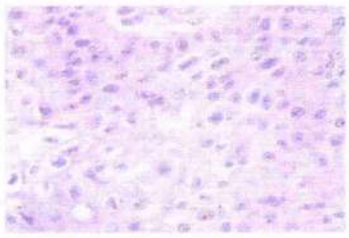

Phospho-Raf(ser338)

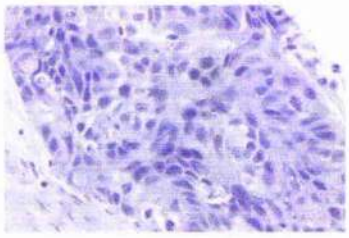

Phospho-Raf(ser259)

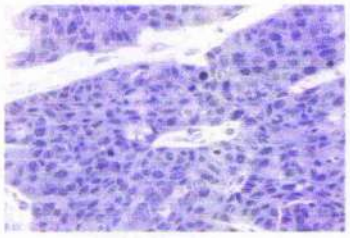

p44/42 MAPK

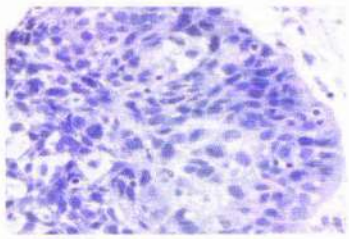

Phospho-p44/42 MAPK

Negative controls were included in each IHC run. The above figures represent the negative controls for each antibody used.